UNIVERSITY OF ALBERTA

CAVEOLIN-1 KNOCKOUT ALTERS NEURAL AND MYOGENIC FUNCTION IN MOUSE SMALL INTESTINE

BY

AHMED EL-YAZBI ©

A thesis submitted to the Faculty of Graduate Studies and Research in partial fulfillment of the requirements for the degree of **Doctor of Philosophy.**

DEPARTMENT OF PHARMACOLOGY

EDMONTON, ALBERTA

Spring 2008

Library and
Archives Canada

Published Heritage
Branch

395 Wellington Street
Ottawa ON K1A 0N4
Canada

Bibliothèque et
Archives Canada

Direction du
Patrimoine de l'édition

395, rue Wellington
Ottawa ON K1A 0N4
Canada

Your file Votre référence
ISBN: 978-0-494-45422-0
Our file Notre référence
ISBN: 978-0-494-45422-0

NOTICE:
The author has granted a non-exclusive license allowing Library and Archives Canada to reproduce, publish, archive, preserve, conserve, communicate to the public by telecommunication or on the Internet, loan, distribute and sell theses worldwide, for commercial or non-commercial purposes, in microform, paper, electronic and/or any other formats.

The author retains copyright ownership and moral rights in this thesis. Neither the thesis nor substantial extracts from it may be printed or otherwise reproduced without the author's permission.

AVIS:
L'auteur a accordé une licence non exclusive permettant à la Bibliothèque et Archives Canada de reproduire, publier, archiver, sauvegarder, conserver, transmettre au public par télécommunication ou par l'Internet, prêter, distribuer et vendre des thèses partout dans le monde, à des fins commerciales ou autres, sur support microforme, papier, électronique et/ou autres formats.

L'auteur conserve la propriété du droit d'auteur et des droits moraux qui protège cette thèse. Ni la thèse ni des extraits substantiels de celle-ci ne doivent être imprimés ou autrement reproduits sans son autorisation.

In compliance with the Canadian Privacy Act some supporting forms may have been removed from this thesis.

While these forms may be included in the document page count, their removal does not represent any loss of content from the thesis.

Conformément à la loi canadienne sur la protection de la vie privée, quelques formulaires secondaires ont été enlevés de cette thèse.

Bien que ces formulaires aient inclus dans la pagination, il n'y aura aucun contenu manquant.

Canada

ABSTRACT

Intracellular signal transduction involves multiple interactions between signaling molecules. For efficient signal transduction, signaling components are spatially organized into complexes by scaffolding proteins. Among these is caveolin-1, identified in 1998 as the structural protein component of the plasma membrane caveolae. These are flask-shaped invaginations that were later shown to be enriched in a number of signaling proteins whose function is regulated by caveolin-1. The roles of caveolin-1 in the regulation of signaling pathways that control small intestinal motility are currently unknown. In this thesis, I used caveolin-1 knockout mice to elucidate the role of caveolin-1 in the regulation of some signaling pathways in mouse small intestine.

First, I examined how the nitric oxide-mediated relaxation changed in caveolin-1 knockout mouse small intestine. This tissue showed reduced relaxation to endogenous and exogenous nitric oxide. I showed that this reduction was due to an increased activity of phosphodiesterase 5, which metabolizes cGMP, a mediator of nitric oxide effects.

Another pathway leading to intestinal smooth muscle relaxation was also affected by caveolin-1 loss. cAMP-dependent relaxation downstream of β-adrenoceptor stimulation was reduced in caveolin-1 knockout mice compared to their wild type controls. I showed that this reduction was likely due to the redistribution of the downstream mediator of cAMP relaxation, protein kinase A, away from its downstream targets.

Furthermore, wild type mice expressed a splice variant of neuronal nitric oxide synthase in small intestinal smooth muscle. This was activated in response to calcium entry into smooth muscle cells to produce nitric oxide that counteracted the contraction.

The caveolin-1 knockout tissues lacked this splice variant and the effect it exerts on smooth muscle contraction.

Finally, I found that calcium extrusion from intestinal smooth muscle through the plasma membrane calcium ATPase isoform 4 was reduced in caveolin-1 knockout mice. This was probably due to the loss of the close association between the plasma membrane and the sarcoplasmic reticulum at the caveolae domains. To conclude, my observations suggest that the alteration in the examined functions due to the loss of caveolin-1 is likely a result of the loss of organization of key signaling molecules closely related to caveolae.

TO

Nour, Mariam, Mom, and Dad

ACKNOWLEDGEMENTS

I would like to express my deepest gratitude to my Supervisor Dr. Edwin E. Daniel for his outstanding supervision, enlightening guidance, motivation, and above all patience during my Ph.D. years. Although I greatly appreciate his pivotal efforts in introducing me to the smooth muscle research field, I appreciate even more his remarkable manners and superior communication and social skills that I hope to be able to adopt in treating my students and other people one day. Equally I would like to extend my most sincere appreciation to my Co-supervisor Dr. Richard Schulz for his close follow-up and supervision, continuous support, and positive challenge. I specifically acknowledge his valuable advice in experimental design in addition to his tireless and selfless efforts in editing and formatting my Ph.D. thesis.

I also thank Drs. Peter E. Light and Peter A. Smith of my supervisory committee for their experienced and insightful guidance along the course of my Ph.D. training.

Many thanks are due to Geoffrey Boddy who showed me how to perform the functional experiments done in this thesis. My heartfelt appreciation goes to Woo Jung Cho for his help with immunohistochemistry and electron microscopy. His accuracy and his meticulous techniques were always a guarantee for the success of our experiments. I am also indebted to Jolanta Sawicka who introduced me to Western blotting and immunoprecipitation. Her mother-like kindness and care alleviated a lot of the beginner's frustration.

In addition, I would like to thank my friends and colleagues from Dr. Schulz lab for the friendly work environment they offered. I specifically acknowledge the help of Jonathan Cena and Ava Chow on various occasions.

My gratitude also goes to Drs. Simonetta Sipione, Elena Posse de Chaves, and Andrew Holt for their valuable scientific advice. Special thanks are due to Judy Deuel, Dr. Wendy Gati, and Dr. Susan Dunn for their continuous help with administrative details during my Ph.D. program.

I thank the Department of Pharmacology at the University of Alberta, the Killam Trusts foundation, and the Alberta Heritage Foundation for Medical Research for supporting me financially.

Finally, I thank my parents Drs. Fawzy A. El-Yazbi and Rawya El-Fadly, who formed and shaped my character and imagination and pushed me to where I am today. I always knew that they were around to help and that I had a safe resort to turn to. My sincere gratitude goes to my wife Mariam Ibrahim for her support and patience during the long days and nights we have gone through together. I also thank my little girl Nour who had to put up with an exhausted father for so many days.

May Allah, all mighty, reward all of you.

TABLE OF CONTENTS

CHAPTER I INTRODUCTION 1

1.1 Regulation of gastrointestinal motility 2

- 1.1.1 A simplified overview of the structure of the GIT wall
- 1.1.2 The neuronal circuits of the enteric nervous system
- 1.1.3 Myogenic (muscle-dependent) motility patterns
- 1.1.4 Nerve-dependent motility patterns
- 1.1.5 The relationship between the slow wave myogenic activity and enteric neural input
- 1.1.6 The relationship between contraction of the CM and LM layers

1.2 Caveolae and caveolin proteins 22

- 1.2.1 History
- 1.2.2 Caveolae
- 1.2.3 Caveolin proteins
- 1.2.4 Caveolae formation
- 1.2.5 Caveolins and signal transduction
- 1.2.6 Caveolin knockout mice

1.3 Signal transduction pathways leading to smooth muscle relaxation in mouse small intestine 40

- 1.3.1 Overview of the regulation of smooth muscle contraction
- 1.3.2 NO and cGMP pathway
- 1.3.3 Apamin-sensitive mediators: ATP and pituitary adenylate cyclise-activating peptide
- 1.3.4 cAMP-dependent relaxation
- 1.3.5 Regulation of contractile tone by NO produced in smooth muscle cells

1.4 Caveolin-1 and intestinal function: hypotheses and objectives 49

1.4.1 A guide to the development of the hypothesis
1.4.2 Hypotheses

1.5 References 55

CHAPTER II METHODS 77

2.1 Animals 78

2.2 Functional experiments on intact tissue preparations 79

2.3 Electron microscopy 86

2.4 Immunohistochemistry 87

2.5 Western blotting 91

2.6 References 96

CHAPTER III NEUROTRANSMITTERS INVOLVED IN NERVE-MEDIATED RELAXATION IN BALB/C MOUSE SMALL INTESTINE 98

3.1 Introduction 99

3.2 Materials and methods 100

3.3 Results 102

3.4 Discussion 117

3.5 References 124

CHAPTER IV CAVEOLIN-1 KNOCKOUT ALTERS THE RESPONSE TO NO IN MOUSE SMALL INTESTINE 129

4.1 Introduction 130

4.2 Materials and methods 131

4.3 Results 134

4.4 Discussion 161

4.5 References 166

CHAPTER V CAVEOLIN-1 KNOCKOUT ALTERS β-ADRENOCEPTOR FUNCTION IN MOUSE

SMALL INTESTINE 172

5.1 Introduction 173
5.2 Materials and methods 175
5.3 Results 179
5.4 Discussion 201
5.5 References 209

CHAPTER VI LOSS OF SMOOTH MUSCLE NITRIC OXIDE SYNTHASE FUNCTION IN CAVEOLIN-1 KNOCKOUT MOUSE SMALL INTESTINE 214

6.1 Introduction 215
6.2 Materials and methods 216
6.3 Results 221
6.4 Discussion 237
6.5 References 244

CHAPTER VII CALCIUM EXTRUSION BY PLASMA MEMBRANE CALCIUM PUMP IS IMPAIRED IN CAVEOLIN-1 KNOCKOUT MOUSE SMALL INTESTINE 248

7.1 Introduction 249
7.2 Materials and methods 251
7.3 Results 255
7.4 Discussion 265
7.5 References 272

CHAPTER VIII GENERAL DISCUSSION, LIMITATIONS, AND FUTURE DIRECTION S 277

8.1 General discussion 278
8.2 Limitations 282
8.3 Future directions 287
8.4 References 291

LIST OF TABLES

Table 5.1 Antibodies and normal sera used in Chapter V 178

Table 6.1 Antibodies and normal sera used in Chapter VI 219

LIST OF FIGURES

Figure 1.1 Different layers comprising the GIT wall. 5

Figure 1.2 Arrangement of neurons in the enteric nervous system in myenteric and submucosal plexuses. 10

Figure 1.3 Spontaneous rhythmic contractions of longitudinal and circular muscle layers. 12

Figure 1.4 Polarized peristaltic reflex in preparations with intact and severed myenteric plexus. 18

Figure 1.5 Electron micrograph showing the characteristic flask shape of caveolae in the plasma membrane of an adipocyte. 24

Figure 1.6 Aligned sequences of human caveolin-1, 2, and 3. 29

Figure 1.7 Caveolae formation. 34

Figure 1.8 Binding of calcium and calmodulin is necessary for the alignment of the two NOS domains and electron flow. 44

Figure 2.1 Mounting CM and LM preparations on electrode holders. 81

Figure 2.2 Measurement of the amplitude of contraction of muscle preparations. 84

Figure 2.3 Expression of flotillin and actin in different membrane fractions. 94

Figure 3.1 Spontaneous pacing frequency after block of muscarinic and adrenergic mediators in mouse small intestine. 103

Figure 3.2 Maximum inhibitory responses of the mouse small intestinal tissue segments to electric field stimulation in the presence of atropine (10^{-7} M), prazosin (10^{-6} M), and timolol (10^{-6} M). 106

Figure 3.3 Effects of agents blocking neurotransmitter action on EFS-induced relaxation in the presence of atropine (10^{-7} M), prazosin (10^{-6} M), and timolol (10^{-6} M) in LM and CM. 108

Figure 3.4 Effects of ODQ (1 μM) on the EFS-evoked relaxation in presence of atropine (10^{-7} M), prazosin (10^{-6} M), and timolol (10^{-6} M) in LM and CM. 111

Figure 3.5 Effect of ODQ (1 μM) on VIP (0.33 μM)-induced relaxation in CM of mouse small intestine. 113

Figure 3.6 Effects of ODQ (1 μM) and apamin (1 μM) on the inhibitory response to SNP (100 μM) in LM and CM. 115

Figure 3.7 Effect of apamin (1 μM) on the inhibitory response to 8-br cGMP (100 μM) in LM and CM. 118

Figure 4.1 Electron microscope images of LM and CM of cav$1^{+/+}$ and cav$1^{-/-}$ small intestine. 135

Figure 4.2 Cryosections from cav$1^{+/+}$ and cav$1^{-/-}$ small intestine stained for caveolin-1, caveolin-3, and doubly stained for caveolin-1 and soluble guanylate cyclase. 138

Figure 4.3 Myenteric ganglia in whole mount preparations from cav$1^{+/+}$ and cav$1^{-/-}$ stained for vimentin. 141

Figure 4.4 Myenteric ganglia in whole mount preparations from cav1$^{+/+}$ and cav1$^{-/-}$ stained for HuC/D protein and nNOS. 143

Figure 4.5 Frequency of the spontaneously-paced contractions in CM of cav1$^{+/+}$ and cav1$^{-/-}$ small intestine. 146

Figure 4.6 Effect of LNNA (100 μM) on EFS-induced relaxation in the presence of atropine (10^{-7} M), prazosin (10^{-6} M), and timolol (10^{-6} M) in LM and CM of cav1$^{+/+}$ and cav1$^{-/-}$ small intestine. 148

Figure 4.7 Relaxation due to SNP (100 μM) in LM and CM of cav1$^{+/+}$ and cav1$^{-/-}$ and the effects of ODQ (1 μM) and apamin (1 μM) on this relaxation. 151

Figure 4.8 Effect of PDE5 inhibitor II (1 μM) on LNNA (100 μM) blockade of EFS-evoked relaxation and SNP (100 μM)-produced relaxation in cav1$^{+/+}$ and cav1$^{-/-}$ LM. 154

Figure 4.9 Effect of apamin (1 μM) on EFS-induced relaxation in LM and CM of cav1$^{+/+}$ and cav1$^{-/-}$ small intestine. 156

Figure 4.10 Expression of PDE5 in caveolae/lipid raft-enriched membrane fractions and whole tissue homogenates from cav1$^{+/+}$ and cav1$^{-/-}$ small intestine. 159

Figure 5.1 Double immunohistochemical staining of caveolin-1 and β-adrenoceptors in cryosections from cav1$^{+/+}$ and cav1$^{-/-}$ small intestine. 180

Figure 5.2 Double immunohistochemical staining for caveolin-1 and catalytic sub-unit of PKA in cryosections from cav1$^{+/+}$ and cav1$^{-/-}$ small intestine. 183

Figure 5.3 Tonic amplitude following CCh (1, 3, and 10 µM) addition to cav1$^{+/+}$ and cav1$^{-/-}$ LM preparations. 185

Figure 5.4 Concentration-response curves of (-)-isoprenaline in small intestinal tissue segments from cav1$^{+/+}$ and cav1$^{-/-}$ mice contracted with 1 µM CCh. 188

Figure 5.5 Effect of selective β-adrenoceptor antagonists (0.1 µM) on the (-)-isoprenaline-induced relaxation in small intestinal tissue segments from cav1$^{+/+}$ and cav1$^{-/-}$ mice contracted with 1 µM CCh. 190

Figure 5.6 Effect of timolol (1 µM) on the (-)-isoprenaline-induced relaxation in cav1$^{+/+}$ and cav1$^{-/-}$ intestinal tissue segments contracted with 1 µM CCh. 193

Figure 5.7 Concentration-response curves of BRL37344 in small intestinal tissue segments from cav1$^{+/+}$ and cav1$^{-/-}$ mice contracted with 1 µM CCh. 195

Figure 5.8 Effect of the PKA inhibitor, H-89 (1 µM), on the (-)-isoprenaline-induced relaxation in small intestinal tissue segments from cav1$^{+/+}$ and cav1$^{-/-}$ mice contracted with 1 µM CCh. 197

Figure 5.9 PKA inhibitor H-89 (0.5 μM) reduces the forskolin (1 μM)- and di-bu cAMP (100 μM)-induced relaxation in small intestinal tissue segments from cav1$^{+/+}$ but not from cav1$^{-/-}$ mice. 199

Figure 5.10 Expression of caveolin-1 and PKA catalytic subunit in the lipid raft-rich membrane fraction and the heavy (non-raft) membrane fractions in cav1$^{+/+}$and cav1$^{-/-}$mice small intestinal tissue. 202

Figure 6.1 Cryosections and whole mount preparations of cav1$^{+/+}$ and cav1$^{-/-}$ mice small intestine immunostained for caveolin-1 and nNOS. 223

Figure 6.2 Representative blot of nNOS immunoprecipitated from BALB/c mouse small intestinal homogenate with anti-caveolin-1 antibody. 225

Figure 6.3 Effect of LNNA (100 μM) on contractile tone of BALB/c, cav1$^{+/+}$, and cav1$^{-/-}$ intestinal tissue preparations following depolarization by KCl (60 mM). 228

Figure 6.4 Effect of caveolae disruption by cholesterol depletion on the immunoreactivities of caveolin-1 and nNOS in smooth muscle cell membrane and the response to LNNA (100 μM) following tissue depolarization by KCl (60 mM) in BALB/c mouse small intestine. 230

Figure 6.5 Increase in contractile tone by LNNA (100 μM) following different agents affecting intracellular calcium in BALB/c mouse intestinal tissue. 233

Figure 6.6 Effects of different agents acting on the signal transduction mechanisms downstream of NO on BALB/c intestinal tissue following depolarization by KCl (60 mM). 235

Figure 6.7 Hypothesized role of smooth muscle nNOS in the regulation of contraction induced by depolarization. 242

Figure 7.1 Immunohistochemical staining of caveolin-1 and PMCA in cryosections from mouse small intestine and bovine tracheal smooth muscle. 256

Figure 7.2 Distribution of PMCA4 in lipid raft-rich membrane fractions of mouse small intestinal smooth muscle and raft and non-raft membrane fractions from bovine tracheal smooth muscle. 258

Figure 7.3 Response of small intestinal segments from cav1$^{+/+}$ and cav1$^{-/-}$ to CCh (1, 3, and 10 μM). 261

Figure 7.4 Effect of caloxin 1C2 (5 μM) on tissue response to 10 μM CCh in cav1$^{+/+}$ and cav1$^{-/-}$ small intestinal tissue. 263

Figure 7.5 Effect of caloxin 1C2 (5 μM) on the response to 0.1 μM CCh in bovine tracheal smooth muscle. 266

LIST OF PUBLICATIONS

Full-length peer reviewed papers:

Published:

1. Omar AG, Sharabi FM, Daabees TT, El-Mallah AI, and El-Yazbi A. Comparative functional antagonistic potencies of tamsulosin and terazosin at α_1-adrenoceptors *in vitro*. *J Egypt Soc Pharm Exp Ther* 26: 569-587, 2005.
2. El-Yazbi AF, Cho WJ, Boddy G, and Daniel EE. Caveolin-1 gene knock out impairs nitrergic function in mouse small intestine. *Br J Pharmacol* 145: 1017-1026, 2005.
3. El-Yazbi AF, Cho WJ, Boddy G, Schulz R, and Daniel EE. Impact of Caveolin-1 knockout on NANC relaxation in circular muscle of the mouse small intestine compared with longitudinal muscle. *Am J Physiol 290*: G394-G403, 2006.
4. El-Yazbi AF, Schulz R, Cho WJ, and Daniel EE. Caveolin-1 knockout alters β-adrenoceptors function in mouse small intestine. *Am J Physiol* 291: G1020-G1030, 2006.
5. Daniel EE, El-Yazbi A, and Cho WJ. Caveolae and Calcium Handling, a Review and a Hypothesis J *Cell Mol Med* 10: 529-544, 2006.
6. El-Yazbi AF, Schulz R, and Daniel EE. Different inhibitory control of circular and longitudinal smooth muscle layers of mouse small intestine. *Auton Neurosci* 131: 36-44, 2007.
7. Daniel EE, El-Yazbi AF, Mannarino M, Galante G, Boddy G, Livergant J, and Oskouei TE. Do gap junctions play a role in nerve transmission as well as pacing in mouse intestine? *Am J Physiol* 292: G734-G745, 2007.

8. Chow AK, Cena J, El-Yazbi AF, Crawford BD, Holt A, Cho WJ, Daniel EE, and Schulz, R. Caveolin-1 inhibits matrix metalloproteinase-2 activity in the heart. *J Mol Cell Cardiol* 42: 896-901, 2007.

Under Review:

1. El-Yazbi AF, Cho WJ, Cena J, Schulz R, and Daniel EE. Smooth muscle nitric oxide synthase, colocalized with caveolin-1, modulates depolarization-induced contraction in mouse small intestine. *Am J Physiol Gastrointest and Liver Physiol*, under review.
2. El-Yazbi AF, Cho WJ, Pande J, Schulz R, Grover AK, and Daniel EE. Caveolin-1 knockout alters calcium extrusion by PMCA in mouse small intestine. *J Cell Mol Med*, under review.
3. Sommer B, Montaño LM, Bazan-Perkins B, El-Yazbi AF, Cho WJ, and Daniel EE. Caveolae disruption impairs serotoninergic ($5\text{-}HT_{2A}$) and histaminergic (H_1) in bovine airway smooth muscle: Role of Rho-kinase signalling. *J Cell Mol Med*, under review.

Peer reviewed abstracts:

1. Daniel EE, El-Yazbi AF, and Boddy G. Role of sequestered extracellular calcium in ICC pacing of intestine. *Neurogastroenterol Motil* 17: 611, 2006.
2. El-Yazbi AF, Cho WJ, and Daniel EE. Caveolin-1 knock-out affects NANC inhibitory mediators differently in circular vs. longitudinal muscle layers of the mouse small intestine. *Neurogastroenterol Motil* 17: 611, 2006.
3. El-Yazbi AF, Boddy G, Schulz R, and Daniel EE. Differential response to nitric oxide donors in circular vs. longitudinal muscles of wild type and caveolin-1 knock out

mouse small intestine. *Neurogastroenterol Motil* 17: 611, 2006.

4. Omar AG, Sharabi FM, Daabees TT, El-Mallah AI, and El-Yazbi AF. Comparative functional antagonistic potencies of tamsulosin and terazosin at alpha1-adrenoceptors *in vitro. 47th Annual Conference of the Egyptian Society of Pharmacology and Experimental Therapeutics*, Helwan, Egpyt, September 2005.
5. El-Yazbi AF, Cho WJ, Schulz R and Daniel EE. Caveolin-1 knockout alters β-adrenoceptor function in mouse small intestine. *FASEB J* 20: A248, 2006.
6. Chow AK, Cena J, El-Yazbi AF, Holt A, Daniel EE, and Schulz R. Caveolin-1 inhibits matrix metalloproteinase-2 activity in the heart. *Canadian Cardiovascular Society Congress*, Vancouver BC, October, 2006.
7. El-Yazbi AF, Sommer B, Bazan-Perkins B, Cho WJ, Montano LM, and Daniel EE. H_1- and 5-HT_{2A}-receptor-mediated contraction of bovine tracheal smooth muscle requires intact caveolae and occurs through the activation of Rho-dependent Kinase. *Pharmacology and Therapeutics Conference*, Banff, March 2007.
8. El-Yazbi AF, Cho WJ, Cena J, Schulz R, Daniel EE. Smooth muscle nNOS, co-localized with caveolin-1, modulates depolarization-induced contraction in mouse small intestine. *FASEB J* 21: A808, 2007.

ABBREVIATIONS

ANOVA	analysis of variance
ATP	adenosine triphosphate
8-br cGMP	8-bromoguanosine-3':5'-cyclic monophosphate
cAMP	cyclic adenosine monophosphate
$Cav1^{-/-}$	caveolin-1 knockout mice
$Cav1^{+/+}$	wild type controls for $cav1^{-/-}$ mice
CCh	carbachol
cGMP	cyclic guanosine monophosphate
CM	circular muscle
CRC	concentration-response curve
Di-bu cAMP	N^6,2'-O-dibutyryladenosine 3':5'-cyclic monophosphate
EFS	electric field stimulation
EGTA	ethylene glycol bis(2-aminoethyl ether)-N,N,N,N-tetraacetic acid
eNOS	endothelial nitric oxide synthase
GIT	gastrointestinal tract
HRP	horseradish peroxidise
ICC	interstitial cells of Cajal
iNOS	inducible nitric oxide synthase
IP_3	inositol triphosphate
LM	longitudinal muscle
LNNA	N^{ω}-nitro-L-arginine
Me-β-CDX	methyl-β-cyclodextrin

nNOS	neuronal nitric oxide synthase
NO	nitric oxide
ODQ	1H-(1,2,4)oxadiazolo(4,3-a)quinazoline-1-one
PDE	phosphodiesterase
PKA	cAMP-dependent protein kinase
PKG	cGMP-dependent protein kinase
PMCA	plasma membrane calcium ATPase
SERCA	sarco/endoplasmic reticulum calcium ATPase
SNP	sodium nitroprusside
TTX	tetrodotoxin
VIP	vasoactive intestinal peptide

PHARMACOLOGICAL AGENTS

Apamin	SK3 channel blocker
Atropine	Muscarinic receptor antagonist
BRL37344	Selective β_3-adrenoceptor agonist
Caloxin 1C2	Selective PMCA4 inhibitor
CGP20712A	Selective β_1-adrenoceptor antagonist
ω-conotoxin	N-type calcium channel blocker
Cyclopiazonic acid	SERCA pump inhibitor
Forskolin	Direct adenylate cyclase activator
H-89	PKA inhibitor
Iberiotoxin	BK channel blocker
ICI118551	Selective β_2-adrenoceptor antagonist
LNNA	Nitric oxide synthase inhibitor
Nicardipine	L-type calcium channel blocker
ODQ	Soluble guanylate cyclise inhibitor
Prazosin	α-adrenoceptor antagonist
SR59230A	Selective β_3-adrenoceptor antagonist
TTX	Voltage-gated sodium channel blocker
Timolol	Non-selective β-adrenoceptor antagonist

CHAPTER I

INTRODUCTION

1.1 Regulation of gastrointestinal motility

The gastrointestinal tract (GIT) is a complex multi-organ system with tissues that differ structurally and functionally. The interactions among neuronal, muscular, immune, and glandular tissues allow the GIT to perform its main physiological functions. These include digestion and absorption of ingested food in addition to protection against the ingested microbes and finally the expulsion of the undigested residues[1]. Movements of the GIT provide for the mixing of the ingested food with the digestive secretion, the propulsion of the nutrients to be digested together with the undigested remains along the length of the alimentary canal, and also for the determination of the length of time available for digestion and absorption in each of the GIT sections[1]. The mixing and propulsive movements of the GIT are generated by an interaction between an intricate network of neurons located within the wall of the alimentary canal, termed the enteric nervous system, and an intrinsic pace-maker system distinct from the neuronal tissue and inherent to the contractile tissue[2]. In the following sections I will describe the structure of the wall of the GIT and the components of GIT movement in more detail with more focus on the small intestine.

1.1.1 A simplified overview of the structure of the GIT wall[3]:

The GIT is a hollow tubular structure that has varying diameters along its length. However, it has much the same basic structural organization in the different regions with 4 distinct layers forming the wall of the alimentary canal from the lumen outwards:

- the *mucosa*, formed of specialized epithelial cells (exocrine and endocrine secretory cells) covering a layer of connective tissue (*lamina propria*) and smooth muscle (*muscularis mucosae*),
- the *submucosa*, formed of dense connective tissue,
- the *muscularis externa*, formed of two layers of smooth muscle, circular muscle (CM) running along the diameter of the tube, and longitudinal muscle (LM) running along the length of the tube, and
- the *serosa*, formed of simple squamous epithelium and small amounts of underlying connective tissue.

These different tissue layers provide the structural and functional basis for the GIT physiology. The epithelial layer in the *mucosa*, through tight junctions among individual cells, forms a barrier that separates the GIT lumen from the internal body environment. Epithelial cells secrete the constituents of the digestive juices in addition to hormones and other antimicrobial components. Absorption of nutrients takes place across the epithelium and into the connective tissue region in the *lamina propria* that is rich in blood vessels and lymphatics. The *lamina propria* also acts as an immune barrier consisting of diffuse lymphatic tissue, lymph nodules, and macrophages. This barrier protects the body against pathogens and other antigens that might be ingested with food. The *muscularis mucosae* offers mucosal movement that is independent of the movement of the whole intestinal wall. The *submucosa* layer contains the larger blood vessels and lymphatics that send branches to the mucosa layer in addition to neuronal tissue that regulates motility and secretion. The mixing and propulsive movement necessary for the digestion and absorption of luminal content in addition to expulsion of the undigested residues is brought about by the contraction of the *muscularis externa* layers. Finally, the *serosa* layer binds the GIT components to the mesentery and the lining of the abdominal wall.

In addition to the previously mentioned layers, a large amount of neural tissue is contained within the wall of the digestive tract arranged in two ganglionated plexuses, the myenteric plexus and the submucosal plexus(es)[4]. The myenteric plexus lies between the CM and LM layers of the *muscularis externa* and extends the full length of the GIT from the esophagus to the rectum. The submucosal plexus extends along the small intestine and colon. At least 17 types of intrinsic neurons are found in both plexuses constituting the enteric nervous system[5] that regulates the different motility and secretion functions of the GIT. The neuron types involved in the regulation of the GIT motility will be discussed in more detail in the next section. Fig 1.1 depicts the different layers of the GIT wall.

1.1.2 The neuronal circuits of the enteric nervous system:

The movement and secretory functions of the GIT are controlled by the intrinsic enteric nervous system that can function even in absence of extrinsic neuronal influence[2]. Neurons in the enteric nervous system are generally classified as motor neurons, interneurons, and intrinsic primary afferent neurons[5].

Fig 1.1 Different layers comprising the GIT wall from the luminal side (below) to the serosal side (above). (From Furness. The enteric nervous system. p.2. Blackwell Publishing, Massachusetts, 2006)

Fig 1.1

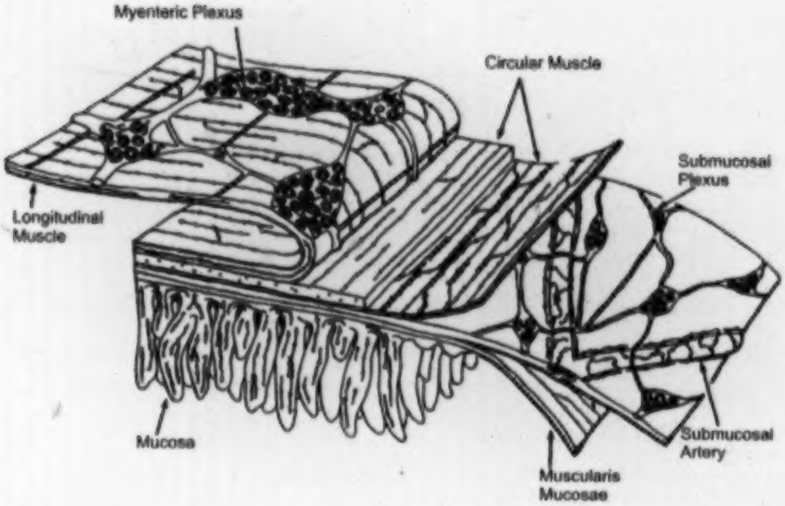
Myenteric Plexus
Circular Muscle
Submucosal Plexus
Longitudinal Muscle
Mucosa
Muscularis Mucosae
Submucosal Artery

1.1.2.1 Motor neurons:

These neurons innervate the circular and longitudinal muscle layers in addition to the glandular epithelium (secretomotor neurons). The CM and LM layers are independently dually innervated by excitatory and inhibitory neurons, whose cell bodies are in the myenteric plexus in the GIT wall[5]. These neurons can be activated by the appropriate electrical stimuli applied across or around the gut wall[5]. The main class of excitatory neurons release acetylcholine in addition to tachykinins that are released at higher frequencies of stimulation[6]. M_2 and M_3 receptors are the main muscarinic receptors of the gastrointestinal muscle[7]. NK_1 and NK_2 receptors mediate the excitatory transmission by tachykinins[7]. Excitatory motor neurons project to the muscle cells adjacent to their cell bodies and a short distance in the oral direction[8]. Similar to excitatory neurons, inhibitory neurons have more than one transmitter. These include nitric oxide (NO), adenosine triphosphate (ATP), vasoactive intestinal peptide (VIP), and pituitary adenylate cyclase-activating peptide. Of these, NO is implicated as the primary transmitter[9]. Inhibitory motor neurons project to muscle cells either adjacent to or lying anal to their cell bodies[10]. It is now generally accepted that the effects of excitatory and inhibitory neurons on smooth muscle are relayed at least in part via the intramuscular interstitial cells of Cajal (ICC) – see below.

A third type of motor neurons innervates the mucosa to stimulate glandular secretion and vasodilatation to increase the supply of water and electrolytes to the exocrine tissue[5]. These are called secretomotor or secretomotor/vasodilator neurons and their cell bodies are mainly present in the sub-mucosal plexus. These neurons produce acetylcholine and VIP.

1.1.2.2 Interneurons:

Structural studies show the existence of neurons with cell bodies lying in the myenteric ganglia and projecting into other ganglia lying oral or anal[2]. These are interneurons which are either ascending or descending. The transmission in the ascending interneuron pathway, which relays into excitatory motor neurons, is mainly cholinergic occurring via nicotinic receptors[11]. In contrast, the descending interneuron pathway, which relays into inhibitory motor neurons, is resistant to nicotinic antagonists[12]. The main neurotransmitter in this pathway is thought to be ATP acting on P_2-purinergic receptors[13].

1.1.2.3 Intrinsic primary afferent neurons:

These are sensory neurons with endings in the mucosa that initiate reflexes in the intestine in response to mechanical, chemical, and stretch stimuli[5]. They are the first type of neurons to be activated during the digestive process in the intrinsic nerve circuits[2] and are responsible for the maintenance of intestinal reflexes in isolated tissues in which extrinsic nerves had been cut and sufficient time was allowed for their endings to degenerate[14]. These neurons possess mechanosensitive ion channels that allow them to respond to mechanical distortion in their processes by firing action potentials[15]. They can also respond to chemicals such as inorganic acids, short chain fatty acids and glucose[16,17,18]. Upon the distortion of the mucosa or change in the chemical environment, enteroendocrine cells can release mediators, primarily serotonin, to activate the intrinsic primary afferent neurons and trigger a reflex response[17,19]. Fig 1.2 depicts the arrangement of the neurons of the enteric nervous system.

1.1.3 Myogenic (muscle-dependent) motility patterns:

Gastrointestinal smooth muscle shows regular rhythmic contractions that persist in isolated tissues and thus are not initiated by circulating mediators and are not suppressed by atropine, suggesting that they are not driven by the excitatory neurons[20]. These rhythmic contractions also persist following ganglion blockade[21] and inhibition of nerve activity by tetrodotoxin[22], indicating that they are independent of neuronal activity (Fig 1.3). The rhythmic contractions are driven by slow waves of depolarization in smooth muscle, which coincide with and initiate these contractions[23]. In some GIT smooth muscles action potentials superimpose on these depolarizing waves leading to contraction[24]. Although these slow electrical waves were shown to be non-neural in origin[25], single smooth muscle cells from the GIT do not spontaneously produce rhythmic depolarizing waves[26], indicating that these waves are characteristic to the full thickness of the tissue rather than an automatic property inherent to single smooth muscle cells. A variety of experiments showed that the slow waves are generated at the outer surface of the circular muscle layer of stomach and intestine[27], which corresponds to the location of the ICC. Strips of muscle from the small intestine showed slow waves only in preparations with ICC but not in others where the ICC had been removed[28].

Fig 1.2 Arrangement of neurons in the enteric nervous system in myenteric (MP) and submucosal (SM) plexuses. 1 & 2, excitatory motor neurons to longitudinal muscle (LM) and circular muscle (CM), respectively; 3, ascending interneuron; 4, intrinsic primary afferent neuron with cell body in the MP; 5, descending interneuron; 6 & 7, inhibitory motor neuron to LM and CM respectiviely; 8, intrinsic primary afferent neuron with cell body in the submucosal plexus; 9, 10 & 11, secretomotor neurons supplying the mucosa (Muc); 12, secretomotor vasodilator neuron; and 13, enterendocrine cell that secretes mediators that activate the intrinsic primary afferent neuron. (Adapted from Furness. The enteric nervous system. p.30. Blackwell Publishing, Massachusetts, 2006)

Note: the designation of interneurons as ascending and descending is in the sense of their direction towards the oral side (ascending) and the anal side (descending).

Fig 1.2

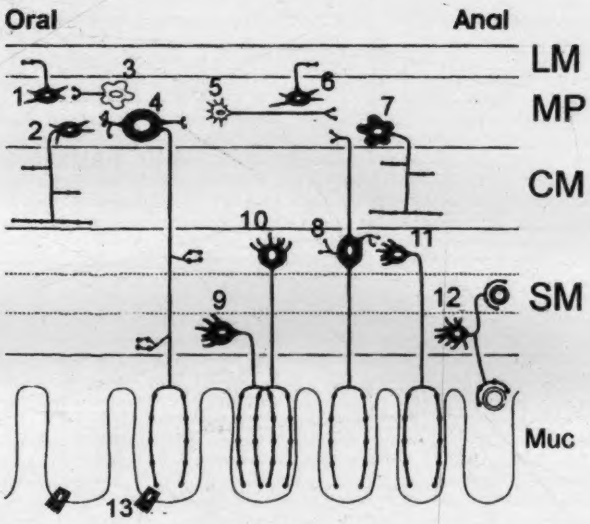
Oral
Anal
LM
MP
CM
SM
Muc
1
2
3
4
5
6
7
8
9
10
11
12
13

Fig 1.3 Spontaneous rhythmic contractions of longitudinal (LM) and circular (CM) muscle layers. Contractions were recorded from isolated intact tissue segments of mouse small intestine in presence of tetrodotoxin (1 µM) to block the nerve activity. The dotted line represent the passive basal tone of the tissue. (Adapted from Daniel *et al.* A new model of pacing in mouse small intestine. *Am J Physiol* 286: G253-G262, 2004)

Fig 1.3

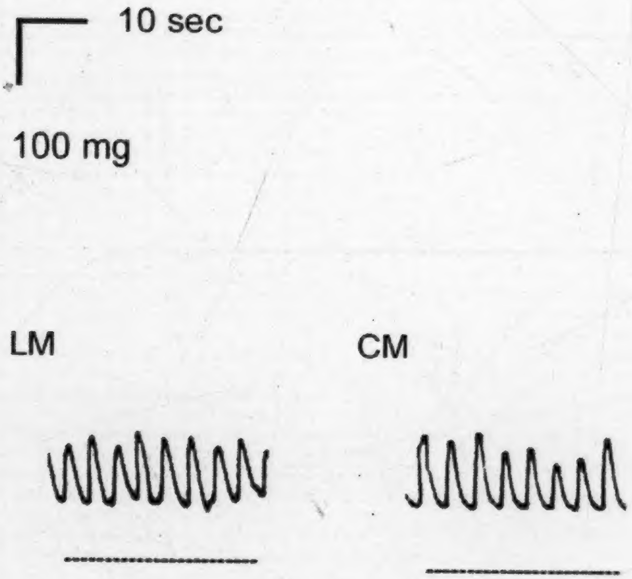

ICC were first identified histologically by Cajal and others in the 1890s by the use of methylene blue and silver staining[29]. Cajal decribed these cells as neuron-like cells which were present between nerve fibres and smooth muscle cells[30]. However, later on, ultrastructural examination showed that ICC are not neurons since they do not contain neurotransmitter vesicles, do not possess axons, and cytoplasmic components of their cell bodies do not resemble those of neurons[31,32]. ICC can now be recognized by the expression of the receptor tyrosine kinase *ckit*[33] that is necessary for their development. ICC of the myenteric plexus and smooth muscle cells have a common precursor since smooth muscle cell markers, *e.g.* heavy chain of smooth muscle myosin, are co-expressed with *kit* during the development of the GIT[34] and *in vivo* blockade of *kit* with antibodies causes the ICC to transdifferentiate into smooth muscle cells[35].

ICC are generally regarded as the pacemakers of the nerve-independent rhythmic contractions of the GIT[36]. However, not all the ICC that can be found in different tissue layers in the GIT are primary pacemaker cells. Three main groups are important for the regulation of GIT motility, namely ICC in the myenteric plexus, ICC in the CM layer (intramuscular ICC), and ICC in the deep muscular plexus[37]. In mouse GIT, the importance of myenteric plexus ICC as pacemakers was shown with the development of the W/W^{v} mutant mice which lack the myenteric plexus ICC and do not produce slow waves of depolarization detected upon recording from intestinal smooth muscle of control mice[38,39]. They also do not show rhythmic contractions in the CM layer in experiments with isolated muscle strips[38,39].

In addition to the initiation of the slow depolarization waves, ICC also propagate and conduct these waves through a continuous network and are then passively spread to the surrounding smooth muscle cells along the length of the GIT[40]. The frequency of rhythmic contractions is not the same along the length of the intestine, but rather there is a decrease in the pacing frequency in local regions towards distal parts[36,39]. However, because the consecutive regions are electrically coupled, the occurrence of slow waves in one region triggers the adjacent regions to follow with the higher frequency in the proximal areas, driving the lower frequency in the more distal parts[41]. This pattern continues until the difference between the driving frequency and the intrinsic frequency of the region is too large for the distal region to follow. At this point a region of irregular activity is created at which the frequency of pacing falls off to a new plateau[41]. Distal to this point, regular pacing activity at a lower frequency is established and the pattern continues until another frequency plateau is reached, followed by a frequency drop[41].

Furthermore, ICC, especially the intramuscular ICC and ICC of the deep muscular plexus, are thought to act as mediators of neuronal signals. ICC interpose between nerve axons and smooth muscle cells in a position that allows them to receive the neuronal input and relay it to the smooth muscle cells[36]. Specialized junctional areas exist between the motor neuron varicosities and the intramuscular ICC[42] which possess receptors for a variety of neurotransmitters and circulating hormones[43]. The post-junctional responses induced by the neurotransmitters in the ICC are thought to be conducted to the surrounding smooth muscle cells via gap junctions[43]. In the absence of ICC both the nitrergic[44] and the cholinergic[45] components of the post-junctional response are lost or markedly reduced, becoming dependent on mediator diffusion form nerve endings.

1.1.4 Nerve-dependent motility patterns:

In this section I will describe the nerve-dependent events that take place in the motility of the small intestine. The patterns of small intestinal motility in humans and carnivores, that take food intermittently, differ in the unfed (fasted or between meals) and fed (following a meal) states[37].

1.1.4.1 Motility in the fasted state: Migrating myoelectric complexes:

The fasted state in humans and carnivores is characterized by the occurrence of migrating myoelectric complexes which are recurring regional intense contractile activity that starts at the lower esophageal sphincter and slowly traverses the stomach and the full length of the small intestine[46]. On the other hand, in herbivores and ruminants migrating myoelectric complexes happen at all times which may be related to a continuous release of stored food material from the stomach(s) of these animals to the intestine[47]. In humans and carnivores the recurrent activity that occurs during the unfed state is divided into four phases: Phase I, quiescent phase; Phase II, an irregular activity phase; Phase III, intense regular contractions; and Phase IV, a brief cycle of irregular activity at the end of Phase III[48]. This pattern of movement is solely dependent on the activity of the enteric nervous system where the local blockade of the enteric neurons with tetrodotoxin[49] or systemic administration of atropine or hexamethonium[50] blocked the contractile phase of these complexes. Even complete extrinsic denervation of the small intestine did not block the initiation or progress of migrating myoelectric complexes[51]. On the other hand, the mechanism of initiation of this pattern of movement is still unexplained. A role for the gastric hormone, motilin, was suggested in the initiation of the migrating myoelectric complexes in humans[52] and dogs[53]. The physiological function of the migrating myoelectric complexes is the removal of the epithelial cells shed from the intestinal mucosa together with any remaining secretions and undigested food from the small intestine[54].

1.1.4.2 Motility in the fed state: Segmental movement:

Following feeding in humans and carnivores the pattern of activity is converted first into a continuous irregular contractile activity that pushes intestinal contents both orally and anally[55]. Following the relaxation of the contracted area, the contents return to their original position. This contractile movement that segment the intestinal content (and hence the name segmental movement) serves to mix the chyme with the digestive juices and expose it to the absorptive surface of the mucosa[37].

1.1.4.3 Peristalsis:

Once mixing of the intestinal content has occurred, the peristaltic reflex begins. It is the simplest type of intestinal movement that reflects the requirement for the integrative activity of the enteric nervous system neurons. This reflex consists of a polarized contraction of the CM oral to the food bolus (stimulus) and a relaxation on the anal side[56] (Fig 1.4). The peristaltic reflex can be evoked by the stimulation of

Fig 1.4 Polarized peristaltic reflex in preparations with intact (A) and severed (B) myenteric plexus. The neuronal reflex conducts through the myenteric plexus to cause contraction on the oral side and relaxation on the anal side of the stimulus. The time interval where the stimulus was given is indicated on the line below the tracings. (From Furness. The enteric nervous system. P.86. Blackwell Publishing, Massachusetts, 2006)

Fig 1.4

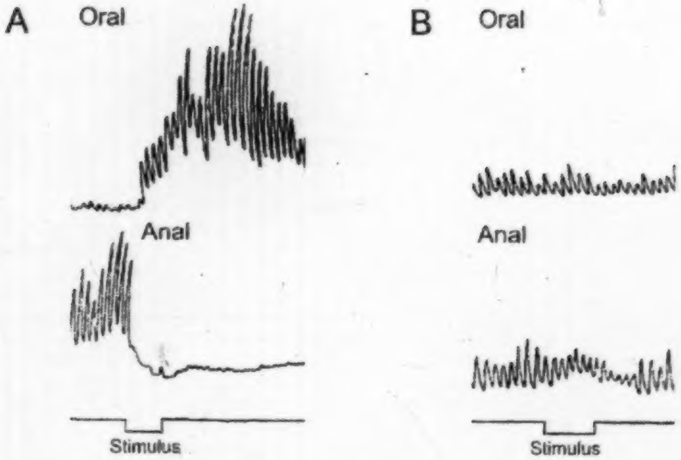

isolated tissue segments *in vitro*[57] and *in vivo* by mechanical or chemical stimuli[58,59] after all connections with the central nervous system are cut[56] indicating that they are independent of extrinsic neuronal input. The simplest description of the neuronal circuit involved is that the intrinsic primary afferent neurons in the enteric nervous system pick up the mechanical or chemical signals and relay them to ascending and descending interneurons which in turn impinge onto excitatory and inhibitory motor neurons, respectively, leading to contraction on the oral side of the stimulus and relaxation on the anal side[37]. The dependence of this reflex on the enteric ganglia in the myenteric plexus can be demonstrated by the loss of the response in the muscle after the myenteric plexus had been severed between the points of stimulus and response[60] (Fig 1.4). *In vivo* a combination of mucosal movement, changes in the intraluminal chemical environment, and slight distension on the intestinal wall stimulates clusters of rhythmic contractions that travel from the oral side to the anal side for variable distances at a speed of about 2 cm/min[37].

1.1.5 The relationship between the slow wave myogenic activity and enteric neural input:

Physiologically significant contractions secondary to slow wave activity only occur if the slow waves are of amplitude sufficient to generate enough depolarization either during the slow wave or during action potentials initiated by the slow wave in smooth muscle cells[61] to activate L-type calcium channels. In tissues where action potentials are initiated, contractions are graded according to the number of action potentials produced[61]. Thus the activity of the enteric excitatory motor neurons brings the slow waves to threshold for peristaltic contractions[62]. As mentioned earlier, there is a gradient in the frequency of occurrence of spontaneous slow waves and contractions along the intestine[36,39]. This leads to the regions of lower intrinsic frequencies being driven by regions of higher frequencies[63], thus the slow waves will be conducted from the oral to the anal side. Therefore, when slow waves are brought to threshold by nerve activity they function to push the intestinal content to the anal direction[37]. On the other hand, the large increase in intestinal contractile activity observed when the synthesis of NO is blocked[41,64] provides some evidence that the inhibitory motor neurons could also be continuously active, providing an inhibitory tone in the intact intestine.

1.1.6 The relationship between contraction of the CM and LM layers:

Contractile phases of peristalsis, segmental movement, and migrating myoelectric complexes involve contraction and shortening of the CM so as to occlude the lumen. This occlusion is counteracted by the simultaneous contraction of the LM layer which leads to the shortening of the intestinal segment length and reduction of the occlusion[37]. Slow waves[28] and propulsive contractions[56] occur simultaneously in both regions. In addition, calcium transients recorded from both layers show that they are excited at the same time[65]. Thus, the instances in which recordings show that one muscle layer elongates while the other contracts[66,67] can be explained on the basis that a sufficiently strong contraction of one layer can overcome the contraction of the other layer and force it to elongate.

1.2 Caveolae and caveolin proteins

1.2.1 History:

The first description of caveolae was based on their morphological appearance during the examination of the ultrastructure of the cell. They were first described in 1953 by George Palade as morphologically distinct plasma membrane invaginations in electron micrographs of endothelial cells[68]. However, the term *caveolae* or *caveolae intracellulare* was coined in 1955 by Eichi Yamada to reflect their little cave-like appearence[69]. For the following 40 years, the literature regarding caveolae remained limited mainly due to the lack of any biochemical marker to allow their isolation and study[70]. It was not until 1989 when caveolin, the signature protein of caveolae, was identified as a 21-22 kD tyrosine phosphorylated substrate in chick fibroblasts[71]. Three years later, caveolin was identified as a protein component of the caveolae membrane[72].

Since that time, the field of caveolae/caveolin research has grown exponentially with caveolae being implicated in many cellular and tissue functions including, but not limited to, endocytotic processes, cholesterol and lipid homeostasis, signal transduction, and tumor suppression[73]. The physiological functions of caveolae and caveolins vary greatly in different cells or tissues. While endocytotic and vasoregulatory functions predominate in the vasculature, roles related to the maintenance of structural integrity are important in the musculature[73]. The identification of the functions of caveolae/caveolins in different cell and tissue types has been extended and clarified by the availability of caveolin-deficient mouse models. A caveolin-1 knockout mouse model was used in this thesis to investigate the effects of the absence of caveolin-1 on some aspects of GIT motility.

1.2.2 Caveolae:

1.2.2.1 Morphology:

In electron micrographs, caveolae appear as "smooth" 60-80 nm flask-shaped invaginations of the plasma membrane that have no obvious coat[74], as opposed to the other coated vesicles *e.g.* clathrin-coated pits. The stomatal diaphragm, a characteristic structural feature at the neck of caveolae, appears in some tissues[75]. However, caveolae can appear in other shapes as vesicles detached from the plasma membrane. They can appear as grape-like clusters (common in developing skeletal muscle), rosettes (in adipocytes), and fused detached vesicles/tubules (endothelial cells)[73]. Fig 1.5 shows the classical shape of caveolae.

1.2.2.2 Tissue distribution:

Caveolae are found in the plasma membrane of most cell types with different abundances. Cell types which have a high abundance of caveolae include adipocytes[76], endothelial cells[68], smooth muscle cells[77], and skeletal muscle cells[78].

Fig 1.5 Electron micrograph showing the characteristic flask shape of caveolae in the plasma membrane of an adipocyte. (From Parton RG and Simons K. The multiple faces of caveolae. *Nat Rev Mol Cell Biol* 8: 185-194, 2007)

Fig 1.5

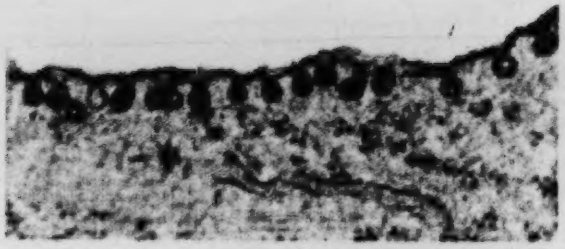

On the other hand, some cell types are devoid of caveolae invaginations in their plasma membrane *e.g.* lymphocytes[79] and central nervous system neurons[80]. The difference in the abundance of caveolae expression in different cell and tissue types is postulated to be related to the proposed function of caveolae in each of the cell types[73].

1.2.2.3 Biochemical properties:

Research in recent years changed the traditional view of the plasma membrane as a fluid mosaic[81]. In that model, membrane proteins are regarded as islands floating freely in the membrane lipid bilayer. The lipids are assumed to exist in a "liquid-disordered" or a "liquid-crystalline" state in which they can undergo rapid lateral diffusion. Currently, however, the plasma membrane is thought to contain discrete "liquid-ordered" domains in which the lipid movement is more restricted. These domains have relatively thicker and more rigid bilayers due to the coalescence of cholesterol and sphingolipids (glycosphingolipids and sphingomyelins)[82]. These assemblies were given the name "lipid rafts". Certain proteins accumulate in lipid rafts preferentially and can be even used as markers for their detection including floatilin and glycosylphosphatidylinositol-anchored proteins[82]. Membrane domains with caveolae have the same membrane lipid structure as the lipid rafts but also contain the marker protein, caveolin-1 and thus are considered to be a subset of lipid rafts[82].

The characteristic lipid composition of lipid rafts and caveolae provides unique properties for these membrane domains. These allow for their separation and purification from other cellular and plasma membrane components. These properties include: a reduced density compared to the other non-lipid raft plasma membrane domains and resistance to solubilization by mild non-ionic detergents such as Triton X-100 at 4°C[73]. Based on these properties, simple biochemical methods, *e.g.* sucrose density gradient fractionation, can be used to separate lipid raft/ caveolae domains from non-lipid raft membrane fractions and cytosolic proteins.

1.2.3. Caveolin proteins:

The discovery of caveolin-1, the first member of this family, was achieved through the work of a number of investigators from different research fields. While looking for tyrosine-phosphorylated substrates in Rous sarcoma virus transformed fibroblasts, Glenny came across a 22 kD protein whose phosphorylation is strongly correlated with the transformation[71]. Immunohistochemical staining with antibodies raised against this protein revealed a punctuate distribution pattern along the plasma membrane similar to that observed for the flask-shaped caveolae[72]. Ultrastructural examination showed that caveolae are formed of series of concentric striations that stained with antibodies raised against this protein, which was then termed caveolin due its close association with caveolae[72].

Following the identification of the first caveolin protein family member, caveolin-1, two additional related proteins were identified. Caveolin-2 was discovered and cloned upon the examination of proteins in caveolae-enriched adipocyte membranes[83]. The third member, caveolin-3, was discovered by cDNA library screening for caveolin-1 homologous genes[84]. A stretch of amino acids "FEDVIAEP" is conserved in all 3 caveolins in the majority of the species examined and is referred to as the "caveolin signature motif"[73]. Caveolin-1 and 2 have α and β-isoforms, the latter being a smaller truncated isoform resulting from an alternative translational start site[85]. A high degree of sequence identity is seen between caveolin-1 and 3 while caveolin-2 is the most divergent (Fig 1.6). In the following sub-sections, I will discuss each of the three caveolin proteins in more detail.

1.2.3.1 Caveolin-1:

Caveolin-1 is most abundantly expressed in terminally differentiated cells *e.g.* epithelial and endothelial cells, adipocytes, fibroblasts, and smooth muscle cells[73]. Caveolin-1 is integrally associated with the plasma membrane, a property indicated by its resistance to extraction by sodium carbonate[86]. The overall structure and membrane association of caveolin-1 are unusual. Both the N and C termini of caveolin-1 are cytoplasmic since antibodies raised against them can bind caveolin-1 only when the cells are permeabilized with a detergent[87], the membrane-associated caveolin-1 remains sensitive to proteolysis[88], and cell-surface biotinylation shows no labeling of caveolin-1[89]. Thus caveolin-1 inserts as a hair pin loop into the plasma membrane. The membrane spanning domain is composed of a hydrophobic amino acid region (residues 102-134)[73]. However, the membrane spanning domain is not sufficient for membrane attachment, which is instead dependent on two regions in the

Fig 1.6 Aligned sequences of human caveolin-1, 2, and 3. Identical residues are highlighted in red. The membrane-spanning region is highlighted in green, the oligomerization domain is highlighted in blue, and the scaffolding domain is indicated by the hatched blue bar. (From Razani *et al.* Caveolae: from cell biology to animal physiology. *Pharmacol Rev* 54: 431-467, 2202)

Fig 1.6

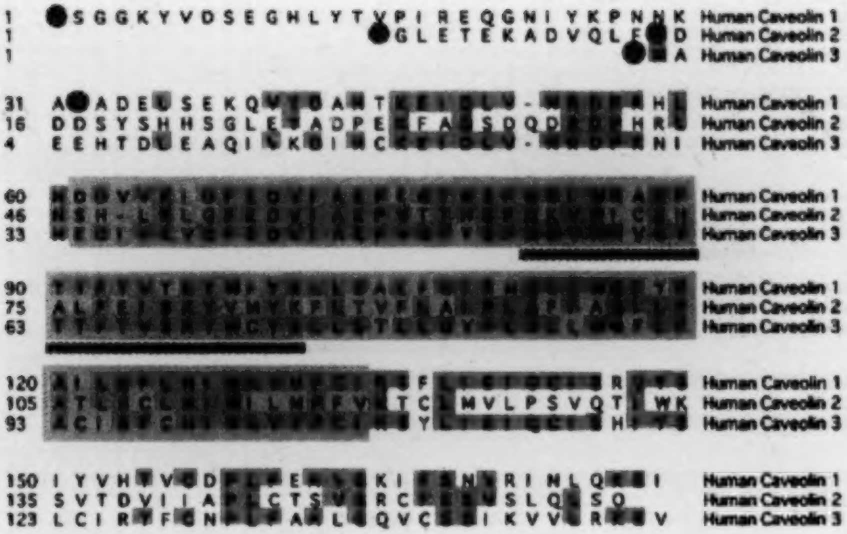
Human Caveolin 1
Human Caveolin 2
Human Caveolin 3

N and C termini of caveolin-1 – the N-terminal membrane attachment domain (residues 82-101) that directs caveolin-1 specifically to caveolar membranes and the C-terminal membrane attachment domain (residues 135-150)[90]. The interaction of caveolin-1 with the membrane is stabilized by palmitoylation at 3 cysteine residues (C133, C143, and C156)[91].

Caveolin-1 molecule contains a 41 amino acid region (oligomerization domain, residues 61-101) that mediates the formation of caveolin-1 homooligomers (14-16 molecules) in the endoplasmic reticulum[89]. Upon transport through the Golgi apparatus, the oligomers increase in size by interacting with one another through contacts between the N-terminal and the C-terminal regions in a side-by-side packing scheme, thereby forming a caveolar coat[92] that is a high molecular weight complex (350-400 kD)[89]. Caveolin-1 can also form a stable heterooligomeric complex with caveolin-2 by the interaction between the respective membrane- spanning domains[93]. However, caveolin-1 alone is sufficient to trigger caveolae formation[94] that is not affected by the absence of caveolin-2[95].

A 20 amino acid domain in the cytosolic N-terminal region of caveolin-1 (residues 82-101) has been shown to bind to and modulate the function of a number of signaling molecules[73]. This region is called the caveolin scaffolding domain. The importance of caveolin-1 and specifically this domain in the regulation of signal transduction pathways will be discussed in detail in a later section.

1.2.3.2 Caveolin-2:

Caveolin-2 is expressed in all cell types expressing caveolin-1[96]. It may function as an accessory protein to caveolin-1 since its intracellular transport requires the presence of caveolin-1 and, unlike caveolin-1 and 3, it lacks the capacity to form caveolae on its own and has no effective scaffolding domain[93,96,97]. In absence of caveolin-1, caveolin-2 is retained intracellularly at the level of the Golgi apparatus where it undergoes proteasomal degradation[97].

1.2.3.3 Caveolin-3:

Caveolin-3 expression is specific to all types of muscle cells (cardiac, skeletal, and smooth muscle)[98]. Owing to the close sequence similarity to caveolin-1 (Fig. 1.6), caveolin-3 is thought to have similar structural properties. Caveolin-3 undergoes homooligomerization *in vivo* and *in vitro* to form 350-400 kD complexes that can trigger caveolae formation[98]. However, unlike caveolin-1, caveolin-3 cannot form heterooligomers with caveolin-2[93]. Caveolin-3 also has a scaffolding domain similar to that of caveolin-1, which is similarly involved in protein-protein interactions[99]. Caveolin-3 was shown to interact with β-dystrophin, an important component of the plasmalemmal dystroglycan complex that links the cytoskeleton to the extracellular matrix[98] and is lacking in models of Duchene muscle dystrophy that also show caveolin-3 upregulation[70]. In addition, caveolin-3 abnormalities are linked with other skeletal muscle pathologies as Limb Girdle Muscle Dystrophy is associated with mutations in the membrane spanning region and the scaffolding domain of caveolin-3 leading to reduction of plasmalemmal caveolin-3 and caveolae[70].

1.2.4 Caveolae formation:

Caveolae formation is dependent on the availability of two factors: cholesterol and caveolin-1 and/or 3. Following treatment of endothelial cells with cholesterol binding agents e.g. nystatin, filipin, and cyclodextrin, caveolae are ablated[72,100] and the striations seen in electron micrographs corresponding to the caveolin oligomers are dissociated from the membrane[72]. Moreover, the absolute cellular levels of cholesterol are required to be above a certain threshold value before caveolae formation starts[100]. Caveolin binds very strongly to the lipid raft membrane components cholesterol and sphingolipids[101,102]. As mentioned previously, caveolin-1 has the ability to organize into large complexes by associating with other caveolin molecules through the C-terminus[89]. This local high concentration of lipids bound to the meshwork of caveolin protein complexes is thought to elicit the bending of the plasma membrane to form the invagination characteristic of caveolae[73]. An alternative hypothesis explains the formation of caveolae on the basis of an interaction between caveolin recruited to the lipid rafts and cytoskeletal proteins as actin and tubulin[103]. Caveolin interacts with tubulin directly and with actin through filamin or through the dystroglycan complex. Interaction with these cytoskeletal components pulls the plasma membrane region where caveolin-1 is present to form the characteristic invagination of the caveolae (personal communication). Fig 1.7 depicts the formation of caveolae from lipid rafts.

Fig 1.7 Caveolae formation. A caveola is formed by the insertion of caveolin complexes formed from the interaction of a large number of caveolin molecules in the plasma membrane at lipid raft domains rich in cholesterol and sphingolipids. (From Razani *et al.* Caveolae: from cell biology to animal physiology. *Pharmacol Rev* 54: 431-467, 2002)

Fig 1.7

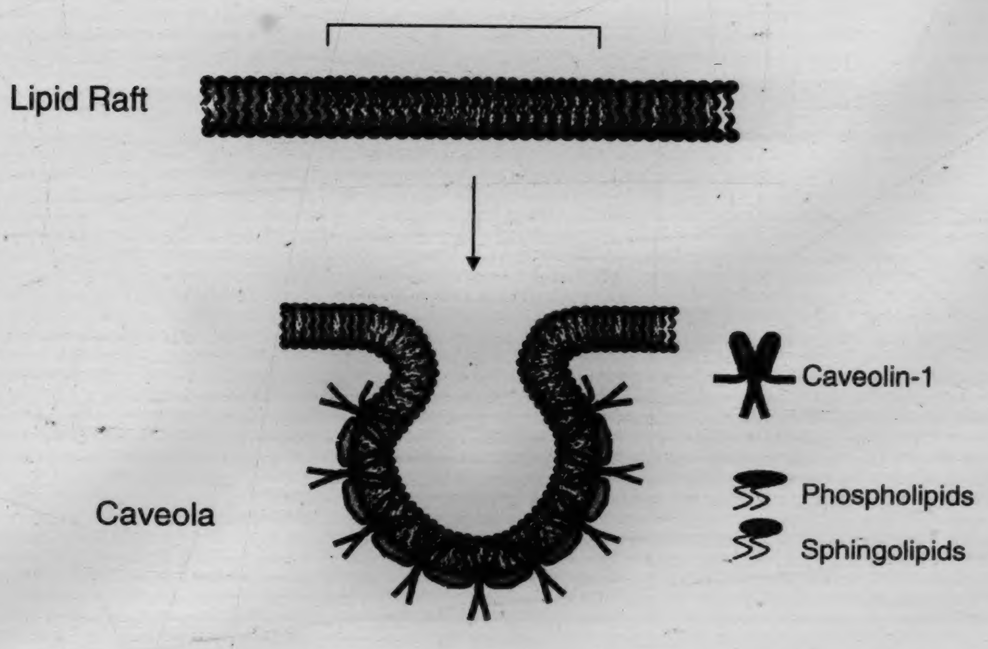
Lipid Raft
Caveola
Caveolin-1
Phospholipids
Sphingolipids

1.2.5 Caveolins and signal transduction:

The examination of the protein content of purified caveolae showed that a large majority of the co-segregated proteins were signal transduction molecules[104, 105]. This led the investigators at that time to the hypothesis that caveolae serve as platforms for the concentration and aggregation of signaling molecules allowing cross-talk between signaling pathways[105]. So far, a wide array of proteins has been shown to preferentially localize in caveolae. Among those are G protein coupled receptors such as β-adrenoceptors[106], bradykinin B_2 receptors[107], and M_2 acetylcholine receptor[108], the α subunit of heterotrimeric G proteins[109], insulin receptor[110], plasma membrane calcium pump[111], membrane-type 1 matrix metalloproteinase[112], matrix metalloproteinase 2[113], non-receptor tyrosine kinases such as Src and Fyn[104], non-receptor serine/threonine kinases such as cAMP-dependent protein kinase (PKA)[114], MEK and ERK[115], eNOS[116], and H-Ras[117]. Although not an absolute necessity, some of the proteins that are well-characterized residents of caveolae seem to be targeted there by having one or more lipid modifications[109,116].

Moreover, caveolae are not passive aggregates of signaling molecules, but rather play a functional role in the regulation and modification of the activity of these signaling molecules. Caveolin-1 acts as a scaffolding protein that binds to and modulates, usually inhibiting, the activity of caveolae-localized signaling molecules through the caveolin scaffolding domain mentioned earlier (residues 82-101)[99, 118, 119]. The caveolin scaffolding domain is capable of binding to a wide host of signaling molecules via interaction with a caveolin-binding motif on the target protein containing at least three aromatic residues[118]. The proposed structure of the caveolin-binding motif is ΦXΦXXXXΦ, ΦXXXXΦXXΦ, or ΦXΦXXXXΦXXΦ, where Φ is an aromatic residue (phenylalanine, tyrosine, or tryptophan) and X is any amino acid[120]. With a few exceptions, the interaction with the caveolin scaffolding domain leads to inhibition of the signaling molecule[73].

As mentioned earlier, caveolin-3 has a structure highly homologous to caveolin-1, whereas caveolin-2 has a more divergent sequence. Caveolin-3 also contains a scaffolding domain analogous to caveolin-1 and is thought to be able to act as a scaffolding protein when expressed in the absence of caveolin-1[73]. Caveolin-2, on the other hand has not so far been shown to modulate any signaling pathway. The functions of each of the three caveolin proteins were elaborated by the availability of mouse knockout models for each. I will present a brief overview of the phenotypes of these knockouts in the next section.

1.2.6 Caveolin knockout mice:

Mice models lacking each of the three caveolin proteins were generated by recombination techniques deleting the corresponding genes. Caveolin-1 knockout mice were generated in 2001 by the deletion of exons 1 and 2 in the caveolin-1 gene[121]. Similarly caveolin-2 knockouts were developed in 2002[95] and caveolin-3 knockouts in 2001[122]. All three mouse models are viable and fertile and do not show any overt phenotype. However, the most striking observation in these models was the total loss of caveolae in tissues expressing caveolin-1 or -3 in the respective knockout model providing more support for the pivotal role of caveolin-1 and -3 in caveolae formation. In this thesis, I used a caveolin-1 knockout mouse model to study the role of caveolin-1 in the regulation of signaling events controlling small intestinal motility.

1.2.6.1 Caveolin-1 Knockout mice:

Caveolin-1 knockout mice lack any morphologically identifiable caveolae in tissues expressing caveolin-1[121]. However, they also lack the expression of caveolin-2 in the cell membrane and the residual amounts remaining become trapped in the Golgi apparatus[70]. Caveolin-1 knockout mice show a reduced life span that is related to hypertrophic cardiomyopathy and pulmonary dysfunction developing with age[70,73,123]. These conditions also render the caveolin-1 knockout mice exercise intolerant. As mentioned previously, caveolae are important in endocytosis and transport across the endothelial layer, however, caveolin-1 knockout mice still maintain a form of transport across the endothelium that is rather due to disrupted tight junctions between the endothelial cells and poor attachment to the basement membrane[124]. Caveolin-1 knockout mice also show a number of metabolic derangements including insulin resistance and post-prandial hyperinsulinemia, high serum triglyceride levels, atrophic adipose tissue, and resistance to diet-induced obesity[73]. Defective urogential function has been reported in these mice with a high basal tone of urinary bladder, reduced carbachol and KCl-induced bladder contraction, and a high incidence of calcium calculi[70]. However, because caveolin-2 is lacking in the caveolin-1 knockout plasma membrane the argument that some of these defects might be due to the loss of caveolin-2 might become reasonable. However, the development of caveolin-2 knockout mice ruled out a role of caveolin-2 in many of these defects.

1.5.6.2 Caveolin-2 knockout mice:

Caveolin-2 knockout mice show normal caveolae expression in all tissues[95]. They appear normal in terms of their cardiovascular functions, lipid profile, and body weight[70,95]. The only defect in common with caveolin-1 knockout mice is the pulmonary dysfunction resulting from alveolar hypercellularity[95]. Thus the pulmonary defects appearing in the caveolin-1 knockout mice are more likely due to the lack of caveolin-2 in the plasma membrane of endothelial cells and pneumocytes in the alveoli.

1.5.6.3 Caveolin-3 knockout mice:

Caveolin-3 knockout mice lack caveolae only in striated muscle tissue[122]. Skeletal muscle in caveolin-3 knockout mice shows a number of abnormalities including disorganized T-tubules and exclusion of the dystroglycan complex from lipid rafts[122]. Caveolin-3 mice show several skeletal muscle disorders consistent with moderate dystrophy with degeneration of the diaphragm and the soleus muscles starting at thirty weeks of age[70]. These mice also develop hypertrophic cardiomyopathy with dilation of the heart and reduced fractional shortening by four months of age[125].

1.5.6.4 Caveolin-1 and -3 double knockouts:

Caveolin-1 and -3 double knockout mice were generated by interbreeding caveolin-1 and caveolin-3 knockout mice[70]. Although these mice lack caveolae in all of their tissues, they are viable and fertile. Since the expression of caveolin-2 in the plasma membrane requires caveolin-1, these mice lack all three caveolin proteins. They develop severe cardiomyopathy with left ventricular hypertrophy and dilation by two months of age[70]. Cardiac myocytes from these animals show severe signs of hypertrophy and degeneration, and microscopically, the heart shows signs of inflammation and perivascular fibrosis[70].

1.3 Signal transduction pathways leading to smooth muscle relaxation in mouse small intestine

1.3.1. Overview of the regulation of smooth muscle contraction:

The smooth muscle cells of the GIT possess properties that distinguish them from other visceral or vascular smooth muscle. Apart from the smooth muscle of the proximal stomach and sphincters, which possess sustained active tone, GIT smooth muscle cells develop spontaneous active tone on which rhythmic contractions occur[126]. These rhythmic contractions are driven by the slow depolarization waves initiated by the previously mentioned ICC. The depolarization waves leads to opening of L-type calcium channels, calcium entry and contraction. Activation of the receptors on smooth muscle surface by neurotransmitters released from excitatory motor neurons (acetylcholine and tachykinins) results in a further increase in intracellular calcium levels by entry or release from intracellular stores and finally more contraction[127]. Smooth muscle contraction is brought about by the intracellular event of myosin light chain phosphorylation[127]. The contraction is either spontaneously terminated by the ending or desensitization of the process producing the contractile signal and the consequent dephosphorylation of myosin light chain or counteracted by the effects of relaxing neurotransmitters and/or processes[127]. This causes the level of intracellular calcium to decrease by the actions of the plasma membrane calcium pump and the sarco/endoplasmic reticulum calcium pump (SERCA) regulated by phospholamban leading finally to the reduction of myosin light chain phosphorylation[127]. In this section, I will focus on reviewing the mediators and the mechanisms of the processes leading to smooth muscle relaxation in the small intestine. As mentioned previously, the neurotransmitter released upon the activation of the inhibitory motor neurons in the GIT include: NO, ATP, pituitary adenylate cyclase-activating peptide, and VIP. In addition, another mechanism, which involves the activation of the NO synthase enzyme expressed in smooth muscle and was found to be involved in regulating and counteracting smooth muscle contraction, will also be discussed.

1.3.2 NO and cGMP pathway:

1.3.2.1 NO production:

Our laboratory was among the first to demonstrate that NO is an inhibitory neurotransmitter in the GIT[128]. Since this early work, it has become acceptable that NO is the main inhibitory neurotransmitter in the different regions of the GIT[129]. NO is produced from inhibitory motor neurons in the GIT by the action of neuronal nitric oxide synthase (nNOS)[129]. Two other NOS isoforms perform different functions in the body, endothelial NOS (eNOS) and inducible NOS (iNOS). NOS enzymes act on the substrates, L-arginine and molecular oxygen converting them it to L-citrulline and NO in a several step reaction that requires the transfer of 5 electrons[130]. NOS enzymes are composed of two domains, the C-terminal reductase and the N-terminal oxygenase domains[131]. The C-terminal reductase domain contains flavin adenine dinucleotide and flavin mononucleotine and binds the reduced form of the co-factor nicotinamide adenine dinucleotide phosphate, whereas the N-terminal oxygenase domain contains a heme group and binds the substrate L-arginine[131]. A hinge region between the reductase and the oxygenase domains contains the calcium/calmodulin binding site[131]. The electrons are transferred from the reduced nicotinamide adenine dinucleotide phosphate, which is an obligate two electron donor, to the flavin co-factors in the reductase domain. These in turn transfer the electrons necessary for the oxygenation of L-arginine one at a time to the heme moiety of the oxygenase domain[131]. However, for the electron flow to occur, the two NOS domains require to be aligned in a certain structure. This alignment is thought to be brought about by binding of calcium and calmodulin, which explains the dependence of eNOS and nNOS on calcium and calmodulin binding for NO production (Fig 1.8). In contrast iNOS, which is permanently bound to calmodulin, is continuously active[131]. In enteric neurons, the calcium necessary for the activation of nNOS to produce NO is brought into the cell by the depolarization signal that activates presynaptic N-type calcium channels[129]. The NO synthesizing activity of NOS can be inhibited by N^{ω}-substituted derivatives of L-arginine *e.g.* N^{ω}-nitro-L-arginine and N^{ω}-methyl-L-arginine[132].

1.3.2.2 Mechanism of NO-induced relaxation in GIT smooth muscle:

In many smooth muscles NO produces relaxation mainly by acting on soluble guanylate cyclase[133]. In GIT smooth muscle, NO produces relaxation not only by soluble guanylate cyclase activation but also by producing membrane hyperpolarization[134]. The membrane hyperpolarization is thought to be brought about by the activation of Ca^{2+}-activated K^+ channels[128]. Three mechanisms of action are proposed for the NO-mediated smooth muscle relaxation in the GIT. The first is through the activation of soluble guanylate cyclase and the production of cyclic guanosine monophosphate (cGMP). This produces relaxation by the reduction of the intracellular calcium concentration[129]. This could possibly be brought about by the activation of cGMP-dependent protein kinase (PKG) and the phosphorylation and modification of activity of several calcium handling proteins. These processes include the inhibition of L-type calcium channels and inositol triphosphate receptor (IP_3) receptors and the activation of the SERCA pump[127], in addition to the reduction of IP_3

Fig. 1.8 Binding of calcium and calmodulin is necessary for the alignment of the two NOS domains and electron flow. (From Griffith and Stuehr. *Annu Rev Physiol* 57: 707-736, 1995)

Fig 1.8

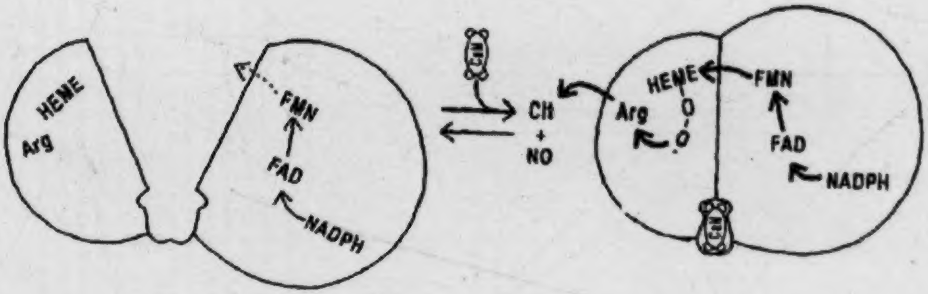
HEME
Arg
FMN
FAD
NADPH
CaM
Cit
+
NO
HEME
Arg
O
O
FMN
FAD
NADPH
CaM

production by stimulatory phosphorylation of RGS proteins that terminate the Gq signal[135]. The second proposed mechanism is via a cGMP-dependent activation of Ca^{2+}-activated K^+ channels and membrane hyperpolarization[129] which could also occur through the activation of PKG followed by the phosphorylation and activation of K^+ channels[127]. The third mechanism is through cGMP-independent effects of NO. NO was reported to activate Ca^{2+}-activated K^+ channels and produce hyperpolarization independent of cGMP production[136]. NO can also activate SERCA pump independent of cGMP[137]. However, it must be noted that the mechanisms of action of nitrergic nerve stimulation-mediated relaxation differ in different species and different regions of the GIT studied[129].

1.3.2.3 Termination of the NO signal:

NO is well known to be a free radical with high diffusion capacity and a limited half-life in a bioassay setting[138]. In addition to that, the generated signal leading to smooth muscle relaxation is regulated and terminated by the action of phosphodiesterase (PDE) enzymes that metabolize cGMP into the inactive GMP. 11 different gene families encoding PDEs have been identified[139]. More than one type of PDEs are usually expressed in the same tissue. In general, cGMP breakdown in smooth muscle cells is mediated by PDE1 and PDE5[140]. Under low basal calcium levels, as assumed during smooth muscle relaxation, PDE5 performs almost all cGMP breakdown in the cell, whereas PDE1 is activated at conditions of higher calcium. Thus PDE5 can be considered as the main regulator of cGMP/PKG signaling pathway[140]. Three isoforms of PDE5A have been identified, PDE5A1, PDE5A2, and PDE5A3. Of those PDE5A1 is the most predominant and is known as cGMP-binding, cGMP-specific PDE[140]. The activity of PDE5 is increased by its phosphorylation by PKG[141] and also by cGMP binding to a site other than the catalytic site on PDE5 which was shown to increase its activity[142].

1.3.3 Apamin-sensitive mediators: ATP and pituitary adenylate cyclase-activating peptide:

Apamin is a bee venom-derived toxin that blocks a small conductance Ca^{2+}-activated K^+ channel (SK_3 channel) that is activated downstream of inhibitory mediators in the GIT[143]. ATP and pituitary adenylate cyclase-activating peptide are among the inhibitory mediators in the GIT. They are reported to produce relaxation by hyperpolarizing the smooth muscle cell membrane following the activation of SK_3 channels[144,145]. The evidence regarding the signal transduction downstream of pituitary adenylate cyclase-activating peptide in mouse small intestine is rather limited. One study showed that pituitary adenylate cyclase-activating peptide induces SK_3 channel activation by producing localized calcium sparks. These are produced by the action of IP_3 produced by phospholipase C on IP_3 receptors[145]. On the other hand, the research work on ATP as a neurotransmitter in mouse small intestine is sparser. ATP is thought to bring about relaxation in mouse small intestine by acting on P_{2Y} receptors[147].

1.3.4 cAMP-dependent relaxation:

VIP is among the mediators released by the inhibitory motor neurons in the GIT. It is postulated to act on the $VPAC_2$ receptor in GIT smooth muscle[148]. This receptor is coupled to G_s and adenylate cyclase and its activation leads to an increased cAMP production and PKA activation[127]. Some of the myenteric neurons in mouse small intestine express VIP[149] and VIP was partially implicated in the nerve-mediated relaxation of the jejunum of the ICR mouse[150]. In addition, cAMP production and PKA activation in intestinal smooth muscle cells can be evoked downstream of β-adrenoceptors[151]. Activation of PKA leads to smooth muscle relaxation by acting on several possible targets including the inositol triphosphate receptor, plasma membrane calcium pump, myosin light chain kinase, phospholamban regulating the SERCA pump activity[152], and ATP-dependent K^+ channels[153]. In addition, in higher concentrations cAMP can activate PKG and lead to relaxation via this pathway[154].

1.3.5 Regulation of contractile tone by NO produced in smooth muscle cells:

Our laboratory showed that a splice variant of nNOS is expressed in the canine lower esophageal sphincter smooth muscle[155]. This enzyme is activated by an increase in intracellular calcium levels to produce NO that regulates the sphincter tone by opening Ca^{2+}-activated K^+ channels and providing membrane hyperpolarization[156]. This is thought to be a feed-back regulatory mechanism to control the tone of the sphincter in response to the constitutive calcium entry through L-type calcium channels.

Smooth muscle NOS was also shown to play an important role in the regulation of vascular tone[157]. Contractions in response to KCl in vascular smooth muscle were increased when nNOS was inhibited or knocked out. In addition, nNOS in smooth muscle was shown to interact with another membrane protein, the plasma membrane calcium pump in the regulation of vascular tone[157]. Removal of calcium by the plasma membrane calcium pump decreased the capacity of nNOS in vascular smooth muscle to produce NO that counteracted the contraction due to KCl.

1.4 Caveolin-1 and intestinal function: Hypotheses and objectives

1.4.1 A guide to the development of the hypothesis:

In this thesis, my main goal is to address the role of caveolin-1 and caveolae in the regulation of small intestine motility. The presence of caveolae in small intestinal smooth muscle and ICC has been documented by electron microscopy in mouse small intestine since the early 1980s[158]. However, despite the rich literature showing the regulatory roles of caveolin-1 in other visceral and vascular smooth muscle (reviewed in[159]), at the time I started this thesis project, the role of caveolin-1 in the regulation of the different signals and events affecting GIT smooth muscle contraction and/or relaxation had not been examined. One study used cultured smooth muscle cells isolated from rabbit intestine to demonstrate the role of caveolin-1 in desensitizing G proteins[160], however the implications of the findings on muscle movement were not studied. Apart from this study, two papers from our laboratory considered a possible role for caveolin-1 in regulating smooth muscle signaling in mouse intestine. The first examined the effects of disruption of caveolae by plasma membrane cholesterol depletion on the spontaneous pacing activity of mouse small intestine[161] while the other looked at the key signaling proteins that are associated with caveolin-1 in the plasma membrane of mouse small intestinal smooth muscle cells[162]. The former paper showed that caveolae disruption reduced the frequency of paced contractions indicating a possible role for caveolae and caveolin-1 in the regulation of GIT motility. On the other hand, the second paper clearly showed that caveolin-1 is co-localized with a number of signaling molecules in the smooth muscle cells and ICC in mouse small intestine including sodium calcium exchanger 1, nNOS, plasma membrane calcium pump, and partially with L-type calcium channels. These results indicated that caveolin-1 in small intestinal smooth muscle and ICC could play an important role in regulating the signaling events regulating smooth muscle contraction/relaxation and hence GIT movement.

1.4.2 Hypotheses:

Since caveolin-1 is involved in the regulation of multiple signal transduction pathways, we expect that the absence of caveolin-1 (in tissues from caveolin-1 knockout mice) will alter the functional responses to physiological or pharmacological stimuli presumed to act via these pathways. We elected to study the effect of caveolin-1 knockout on some of the pathways leading to smooth muscle relaxation in mouse small intestine, in addition to a possible role for caveolin-1 in regulating calcium handling in smooth muscle cells.

1. The neurotransmitters involved in nerve-mediated relaxation in mouse small intestine differ in CM and LM.

NO is considered the main neurotransmitter mediating relaxation in the GIT[9]. Moreover, in C57BL/6 mice inhibition of NO synthesis abolished nerve-mediated relaxation[163]. However, there could be regional and strain differences in the identity and the mechanism of action of the nerve mediators involved in intestinal relaxation in the mouse[150]. In addition, the inhibitory mediators or their mechanisms of action might differ between the CM and LM layers as they were shown to differ in other aspects[39]. Thus, I will first evaluate the contributions of the different neurotransmitters in the nerve-mediated smooth muscle relaxation and the control of basal frequency of paced contractions in the intestine of the control mouse strain (Balb/C) that we use.

The frequency of paced contractions will differ in CM and LM tissue preparations and will be affected differently by the blockade of different neurotransmitters.

The relaxation response to electric field stimulation in presence of muscarinic and adrenergic blocking agents will be affected differently by the blockade of the different neurotransmitters in LM vs. CM tissue preparations.

CM and LM tissue preparations will respond differently to exogenous NO donors.

2. Caveolin-1 knockout will alter the response to NO in mouse small intestine.

Caveolin-1 is involved in the signal transduction pathways in different cell types and caveolae form signal transduction platforms for the organization of the molecular response to the different signals[73]. In a mouse model of muscle dystrophy where part of a protein complex known to interact with caveolin was disrupted, the relaxation response to exogenous and andogenous NO was impaired in the small intestine[164]. Therefore, I hypothesize that the relaxation response to the main inhibitory mediator, NO, will be altered in the small intestine of caveolin-1 knockout mice.

The relaxation response to electric field stimulation will be altered in tissue preparations from caveolin-1 knockout mice and will not be affected similarly by NOS inhibition in tissues from control and knockout mice.

The response of tissue preparations from caveolin-1 knockout mice to exogenous NO donors or cGMP analogues will be reduced compared to control tissues.

The effect of the inhibition of the activity of guanylate cyclase or PDE5, both affecting the signaling pathway downstream of NO, on the response to electric field stimulation will be altered in tissue preparations from caveolin-1 knockout mice.

The expression and distribution of the different signaling proteins in the NO pathway will be altered in caveolin-1 knockout intestinal tissue compared to control tissue.

3. Caveolin-1 knockout will alter the relaxation response to β-adrenoceptor stimulation.

In other tissues caveolin-1 was shown to interact directly with and modulate the function of some adenylate cyclase isoforms[108] and PKA[114]. Therefore, I hypothesize that caveolin-1 knockout will affect the cAMP-dependent relaxation response. I used the stimulation of β-adrenoceptors as a model for intestinal smooth muscle relaxation that is mediated by cAMP since their expression[165] and coupling to cAMP production[151] is well-documented in the GIT.

The relaxation response to β-adrenoceptor stimulation will be altered in caveolin-1 knockout tissue preparations compared to control tissue.

The relaxation response to exogenous cAMP analogues or activation of adenylate cyclase will be altered in caveolin-1 knockout tissue preparations compared to control tissue.

The expression and distribution of PKA will differ in caveolin-1 knockout mouse small intestinal tissue compared to control tissue.

4. The function of smooth muscle NOS will be altered in caveolin-1 knockout mice.

Caveolin-1 is co-localized with a splice variant of nNOS in wild type mouse small intestine smooth muscle and ICC[162]. This splice variant was shown to control the developed tone of contraction in canine lower esophageal sphincter[156]. I hypothesize that this splice variant is also involved in the regulation of contraction in mouse small intestine and that its expression and/or distribution and its function will be altered in absence of caveolin-1.

5. Caveolin-1 knockout will alter calcium extrusion from the cell by the plasma membrane calcium pump.

Caveolin-1 is co-localized with several calcium handling proteins in mouse small intestine among which is the plasma membrane calcium pump[162,166]. Caveolae and caveolin-1 are thought to play a role in calcium recycling between the cytosol and extracellular medium in smooth muscle cells[166]. Therefore, I hypothesize that the function of the plasma membrane calcium pump will be altered by caveolin-1 knockout.

The expression and distribution of plasma membrane calcium pump will be altered in tissues from caveolin-1 knockout mice.

The function of plasma membrane calcium pump, as assessed by using a selective inhibitor in removing cytosolic calcium after treatment with carbachol, will be reduced in caveolin-1 knockout tissue preparations.

1.5 References

1. Barrett KE. Gastrointestinal Physiology. Lange Medical Books/McGraw-Hill, Medical Pub. Division, New York, 2006.
2. Kunze WAA and Furness JB. The enteric nervous system and regulation of intestinal motility. *Annu Rev Physiol* 61: 117-142, 1999.
3. Ross MH, Romrell LJ, and Kaye GI. Histology a Text and Atlas, 3rd ed. Williams & Wilkins, Baltimore, Maryland, 1995.
4. Furness JB, Bornstein JC, Kunze WAA, and Clerc N. The enteric nervous system and its extrinsic connections. In: Yamada T, Alpers DH, Laine L, Owyang C, and Powell DW (Eds.) Textbook of Gastroenterology, Lipincott Williams & Wilkins, Philadelphia, PA, pp. 11-35, 1999.
5. Furness JB. Types of neurons in the enteric nervous system. *J Auton Nerv Syst* 81: 87-96, 2000.
6. Holzer P. Ascending enteric reflex: multiple neurotransmitter systems and interactions. *Am J Physiol* 256: 540-545, 1989.
7. Lecci A, Santicioli P, and Maggi CA. Pharmacology of transmission to gastrointestinal muscle. *Curr Opin Pharm* 2: 630-641, 2002.
8. Gabella G. Innervation of the intestinal muscular coat. *J Neurocytol* 1: 341-362, 1972.
9. Stark ME and Szurszewski JH. Role of nitric oxide in gastrointestinal and hepatic function and disease. *Gastroenterology* 103: 1928-1949, 1992.

10. Brookes SJH, Steele PA, and Costa M. Identification and immunohistochemistry of cholinergic and noncholinergic circular muscle motor neurons in the guinea-pig small intestine. *Neuroscience* 42: 863-878, 1991.

11. Tonini M and Costa M. A pharmacological analysis of neuronal circuitry involved in distention-evoked enteric excitatory reflex. *Neuroscience* 38: 787-795, 1990.

12. Johnsoson PJ, Bornstein JC, Yuan SY, and Furness JB. Analysis of contribution of acetylcholine and tachykinins to neuro-neuronal transmission in motility reflexes in guinea-pig ileum. *Br J Pharmacol* 118: 973-983, 1996.

13. Lepard KJ, Messori E, and Galligan JJ. Purinergic fast excitatory post synaptic potential in myenteric neurons of guinea-pig: distribution and pharmacology. *Gastroenterology* 113: 1522-1534, 1997.

14. Furness JB, Johnson PJ, Pompolo S, and Bornstein JC. Evidence that enteric motility reflexes can be initiated through entirely intrinsic mechanisms in the guinea-pig small intestine. *Neurogastroenterol Motil* 7: 89-96, 1995.

15. Kunze WAA, Furness JB, Bertrand PP, and Bornstein JC. Intracellular recording from the myenteric neurons of the guinea-pig ileum that respond to stretch. *J Physiol* 506: 827-842, 1998.

16. Kunze WAA, Bornstein JC, and Furness JB. Identification of sensory nerve cells in a peripheral organ, the intestine of a mammal. *Neuroscience* 66: 1-4, 1995.

17. Bertrand PP, Kunze WAA, Bornstein JC, Furness JB, and Smith ML. Analysis of the responses of myenteric neurons in the small intestine to chemical stimulation of the mucosa. *Am J Physiol* 273: G422-G435, 1997.

18. Kirchgessner AL, Liu MT, and Gershon MD. *In situ* identification and visualization of neurons that mediate enteric and enteropancreatic reflexes. *J Comp Neurol* 371: 270-286, 1996.

19. Pan H and Gershon MD. Activation of intrinsic afferent pathways in submucosal ganglia of the guinea pig small intestine. *J Neurosci* 20: 3295-3309, 2000.

20. Magnus R. Versuche am überlebenden Dünndarm von Säugethieren. I. Miltheilung. *Pflüger's Arch Ges Physiol* 102: 123-151, 1904.

21. Thomas JE and Kuntz A. A study of gastro-intestinal motility in relation to the enteric nervous system. *Am J Physiol* 76: 606-626, 1926.

22. Liu J, Prosser CL, and Job DD. Ionic dependence of slow waves and spikes in intestinal muscle. *Am J Physiol* 217: 1542-1547, 1969.

23. Alvarez WC and Mahoney LJ. Action currents in stomach and intestine. *Am J Physiol* 58: 476-493, 1922.

24. El-Sharkawy TY, Morgan KG, and Szurszewski JH. Intracellular activity of canine and human gastric smooth muscle. *J Physiol* 279: 291-307, 1978.

25. Connor JA, Kreulen D, Prosser CL, and Wiegel R. Interaction between longitudinal and circular muscle in intestine of cat. *J Physiol* 273: 665-689, 1997.

26. Farrugia G. Ionic conductances in gastrointestinal smooth muscles and interstitial cells of Cajal. *Annu Rev Physiol* 61: 45-84, 1999.

27. Taylor GS, Daniel GS, and Tomita T. origin and mechanism of intestinal slow waves. Proceedings of the fifth international symposium of the gastrointestinal motility. Herentals, Belgium: Typoff, 102-106, 1976.

28. Suzuki N, Prosser CL, and Dahms V. Boundary cells between longitudinal and circular layers: essential for electrical slow waves in cat intestine. *Am J Physiol* 250: G287-G294, 1986.

29. Cajal SRY. Note sobre el plexo de Auerbach de los batracios. *Trab Lab Histol Fac Med Barc* 1: 23-28, 1892.

30. Cajal SRY. Histologie du système nerveux de l'homme et des vertebras. Maloine, Paris, 1911.

31. Richardson KC. Electronmicroscopic observations on Auerbach's plexus in the rabbit, with special reference to the problem of smooth muscle innervation. *Am J Anat* 103: 99-135, 1958.

32. Taxi J. Sur la structure de travées de plexus d'Auerbach: confrontation des données fournies par le microscope ordinaire et par le microscope electroniques. *Ann Sci Nat Zool Biol Anim* 12 : 571-593, 1959.

33. Maeda H, Yamagat A, Nishikawa S, Yoshinaga K, Kobayashi S, Nishi K, and Nishikawa SI. Requirement of *c-kit* for the development of interstitial pacemaker system. *Development* 116: 369-375, 1992.

34. Klüppel M, Huizinga JD, Maysz J, and Bernstein A. Developmental origin and kit-dependence of the interstitial cells of Cajal in the mammalian small intestine. *Dev Dyn* 211: 60-71, 1998.

35. Torihashi S, Nishi K, Tokutomi Y, Nishi T, Ward S, and Sanders KM. Blockade of kit signaling produces trans differentiation of interstitial cells of Cajal into a smooth muscle phenotype. *Gastroenterology* 117: 140-148, 1999.

36. Sanders KM. A case for the interstitial cells of Cajal as pacemakers and mediators of neurotransmission in the gastrointestinal tract. *Gastroenterology* 111: 492-515, 1996.

37. Furness JB. The enteric nervous system. Blackwell Publishing Inc., Malden, MA, 2006.

38. Malysz J, Thuneberg L, Mikkelsen HB, and Huizinga JD. Action potential generation in the small intestine of the W mutant mice that lack the interstitial cells of Cajal. *Am J Physiol* 271: G387-G399, 1996.

39. Daniel EE, Boddy G, Bong A, and Cho WJ. A new model of pacing in the mouse intestine. *Am J Physiol* 286: G253-G262, 2004.

40. Horowitz B, Ward SM, and Sanders KM. Cellular and molecular basis for electrical rhythmicity in gastrointestinal muscles. *Annu Rev Physiol* 61: 19-43, 1999.

41. Diamant NE, and Bortoff A. Nature of the intestinal slow-wave frequency gradient. *Am J Physiol* 216: 301-307, 1969.

42. Daniel EE and Posey-Daniel V. Neuromuscular structures in opossum esophagus: role of interstitial cells of Cajal. *Am J Physiol* 246: G305–G315, 1984.

43. Ward SM and Sanders KM. Involvement of the intramuscular interstitial cells of Cajal in neuroeffector transmission in the gastrointestinal tract. *J Physiol* 576: 675-682, 2006.

44. Burns AJ, Lomax AEJ, Torihashi S, Sanders KM, and Ward SM. Interstitial cells of Cajal mediate inhibitory neurotransmission in the stomach. *Proc Natl Acad Sci U S A* 93: 12008–12013, 1996.

45. Ward SM, Beckett EAH, Wang X-Y, Baker F, Khoyi M, and Sanders KM. Interstitial cells of Cajal mediate cholinergic neurotransmission from enteric motor neurons. *J Neurosci* 20: 1393–1403, 2000.

46. Szurszewski JH. A migrating electric complex of the canine small intestine. *Am J Physiol* 217: 1757-1763, 1969.

47. Ruckebusch Y and Pairet M. origin and characterization of migrating myoelectric complexes in rabbits. *Dig Dis Sci* 30: 742-746, 1985.

48. Carlson GM, Bedi BS, Code CF. Mechanism of propagation of intestinal interdigestive myoelectric complex. *Am J Physiol* 222: 1027-1030, 1972.

49. Sarna S, Stoddard C, Belbeck L, and McWade D. Intrinsic nervous control of migrating myoelectric complexes. *Am J Physiol* 241: G16-G23, 1981.

50. El-Sharkawy TY, Markus H, and Diamant NE. Neural control of the intestinal migrating myoelectric complex. A pharmacological analysis. *Can J Physiol Pharmacol* 60: 794-804, 1982.

51. Aeberhard PF, Magnenat LD, and Zimmerman WA. Nervous control of migrating myoelectric complex of the small bowel. *Am J Physiol* 238: G102-G108, 1980.

52. Bormans V, Peeters TL, Janssens J, Pearce D, Vanderweerd M, and Vantrappen G. In man, only activity fronts that originate in the stomach correlate with motilin peaks. *Scand J Gastroenterol* 22: 781-784,1987.

53. Lee KY, Chang TM, and Chey YK. Effect of rabbit antimotilin serum on myoelectric activity and plasma motilin concentration in fasting dog. *Am J Physiol* 245: 547-553, 1983.

54. Hasler WL. Motility of the small intestine and colon. In: Yamada T (ed.), Textbook of Gastroenterology, 4th edition, Lippincott Williams & Wilkins, Philadelphia, PA, pp. 220-247, 2003.

55. Ehrlin H-J, Schemann M, and Siegle M-L. Motor patterns of the small intestine determined by closely spaced extraluminal transducers and videofluoroscopy. *Am J Physiol* 253: G259-G267, 1987.

56. Bayliss WM and Starling EH. The movements and innervation of the small intestine. *J Physiol* 24: 99-143, 1899.

57. Mall F. A study of the intestinal contraction. *Johns Hopkins Hosp Rep* 1: 37-75, 1896.

58. Hukuhara T and Miyake T. The intrinsic reflexes in the colon. *Jpn J Physiol* 9: 49-55, 1959.

59. Smith TK and Furness JB. Reflex changes in circular muscle activity elicited by stroking the mucosa: an electrophysiological analysis in the isolated guinea-pig ileum. *J Auton Nerv Syst* 25: 205-218, 1988.

60. Hukuhara T, Yamagami M, and Nakayama S. On the intestinal intrinsic reflexes. *Jpn J Physiol* 8: 9-20, 1958.

61. Hara Y, Kubota M, and Szurszewski JH. Electrophysiology of smooth muscle of the small intestine of some mammals. *J Physiol* 372: 501-520, 1986.

62. Reinke DA, Rosenbaum AH, and Bennett DR. Patterns of dog gastrointestinal contractile activity monitored *in vivo* with extraluminal force transducers. *Am J Dig Dis* 12: 113-141, 1967.

63. Bogeski G, Lean NP, Kitchener PD, Timar-Peregrin A, Sanger GJ, Shafton AD, and Furness JB. Analysis of factors that determine the compliance of rat jejunum to distension *in vivo*. *Neurogastroenterol Motil* 15: 417-425, 2003.

64. Ferens DM, Chang EC, Bogeski G, Shafton AD, Kitchener PD, and Furness JB. Motor patterns and propulsion in the rat intestine *in vivo* recorded by spatio-temporal maps. *Neurogastroenterol Motil* 17: 710-717, 2005.

65. Stevens RJ, Publicover NG, and Smith TK. Propagation and neural regulation of calcium waves in longitudinal and circular muscle layers of guinea pig small intestine. *Gastroenterology* 118: 892-904, 2000.

66. Sarna SK. Gastrointestinal longitudinal muscle contractions. *Am J Physiol* 265 : G156-G164, 1993.

67. Grider JR. Reciprocal activity of longitudinal and circular muscle during intestinal peristaltic reflex. *Am J Physiol* 284: G768-G775, 2003.

68. Palade GE. Fine structure of blood capillaries. *J Appl Physiol* 24: 1424-1436, 1953.

69. Yamada E. The fine structure of the gall bladder epithelium of the mouse. *J Biophys Biochem Cytol* 1: 445-458, 1955.

70. Hnasko R and Lisanti MP. The biology of caveolae: lessons from caeolin knockout mice and implications for human disease. *Mol Interv* 3: 445-464, 2003.

71. Glenny JR. Tyrosine phosphorylation of a 22 kDa protein is correlated with transformation by Rous sarcoma virus. *J Biol Chem* 264: 20163-20166, 1989.

72. Rothberg KG, Heus[illegible] JE, Donzell WC, Ying YS, Glenny JR, and Anderson RGW. Caveolin, a protein component of caveolae membrane coats. *Cell* 68: 673-682, 1992.

73. Razani B, Woodman SE, and Lisanti MP. Caveolae: from cell biology to animal physiology. *Pharmacol Rev* 54: 431-467, 2002.

74. Stan RV. Structure of caveolae. *Biochem Biophys Acta* 1746: 334-348, 2005.

75. Stan RV, Tkachenko E, and Niesman IR. PV1 is a key structural component for the formation of the stomatal and fenestral diaphragms. *Mol boil Cell* 15: 3615-3630, 2004.

76. Napolitano LM. The differentiation of white adipose cells. An electron microscope study. *J Cell Biol* 18: 663-679, 1963.

77. Gabella G. Quantitative morphological study of smooth muscle cells of guinea-pig taenia coli. *Cell Tissue Res* 170: 161-186, 1976.

78. Mobley BA and Eisenberg BR. Sizes of components in frog skeletal muscle measured by methods of stereology. *J Gen Physiol* 66:31-45, 1975.

79. Fra AM, Williamson E, Simons K, and Parton RG. Detergent-insoluble glycolipid microdomains in lymphocytes in absence of caveolae. *J Biol Chem* 269: 30745-30748, 1994.

80. Cameron PL, Ruffin JW, Bolag R, Rasmussen H, and Cameron RS. Identification of caveolin and caveolin-related proteins in the brain. *J Neurosci* 17: 9520-9535, 1997.

81. Singer SJ and Nicolson GL. The fluid mosaic model of the structure of cell membranes. *Science* 175: 720-731, 1972.

82. Simons K and Toomre D. Lipid rafts and signal transduction. *Nat Rev Mol Cell Biol* 1: 31-39, 2000.

83. Scherer PE, Okamoto T, Chun M, Nishimoto I, Lodish HF, and Lisanti MP. Identification, sequence, and expression of caveolin-2 define a caveolain gene family. *Proc Natl Acad Sci USA* 93: 131-135, 1996.

84. Way M and Parton R. M-caveolin a muscle-specific caveolin-related protein. *FEBS Lett* 376: 108-112, 1995.

85. Scherer PE, Tang Z-L, Chun MC, Sargiacomo M, Lodish HF, and Lisanti MP. Caveolin isoforms differ in their N-terminal protein sequence and subcellular distribution: Identification and epitope mapping of an isoform specific antibody probe. *J Biol Chem* 270: 16395-16401, 1995.

86. Kurzchalia T, Dupree P, Parton RG, Kellner K, Virta H, Lehnert M, and Simons K. VIP 21, a 21-kD membrane protein is an integral component of

trans-Golgi-network-derived transport vesicles. *J Cell Biol* 118: 1003-1014, 1992.

87. Dupree P, Parton RG, Raposo G, Kurzchalia TV, and Simons K. Caveolae and sorting of the trans-Golgi network of epithelial cells. *EMBO J* 12: 1597-1605, 1993.

88. Monier S, Parton RG, Vogel F, Behlke J, Henske A, and Kurzchalia T. VIP21-caveolin, a membrane protein constituent of the caveolar coat, oligomerizes *in vivo* and *in vitro*. *Mol Biol Cell* 6: 911-927, 1995.

89. Sargiacomo M, Scherer PE, Tang Z-L, Kubler E, Song KS, Sanders MC, and Lisanti MP. Oligomeric structure of caveolin: implications for caveolae membrane organization. *Proc Natl Acad Sci USA* 92: 9407-9411, 1995.

90. Schlegel A and Lisanti MP. A molecular dissection of caveolin-1 membrane attachment and oligomerization. Two separate regions of the caveolin-1 C-terminal domain mediate membrane binding and oligomer/oligomer interactions *in vivo*. *J Biol Chem* 275: 21605-21617, 2000.

91. Monier S, Dietzen DJ, Hastings WR, Lublin DM, and Kurzchalia TV. Oligomerization of VIP21-caveolin *in vitro* is stabilized by long chain fatty acylation or cholesterol. *FEBS Lett* 388: 143-149, 1996.

92. Song KS, Tang Z, Li S, and Lisanti MP. Mutational analysis of the properties of caveolin-1. A novel role for the C-terminal domain in mediating homo-typic caveolin-caveolin interactions. *J Biol Chem* 272: 4398-4403, 1997.

93. Das K, Lewis RY, Scherer PE, and Lisanti MP. The membrane spanning domains of caveolins-1 and -2 mediate the formation of caveolin hetero-oligomers. *J Biol Chem* 274: 18721-18728, 1999.

94. Fra AM, Williamson E, Simons K, and Parton RG. De novo formation of caveolae in lymphocytes by expression of VIP21-caveolin. *Proc Ntl Acad Sci USA* 92: 8655-8659, 1995.

95. Razani B, Wang XB, Engelman JA, Battista M, Lagaud G, Zhang XL, Kneitz B, Hou H, Christ GJ, Edelmann W, and Lisanti MP. Caveolin-2-deficient mice show evidence of severe pulmonary dysfunction without disruption of caveolae. *Mol Cell Biol* 22: 2329-2344, 2002.

96. Scherer PE, Lewis RY, Volonte D, Engelman JA, Galbiati F, Couet J, Kohtz DS, vanDonselaar E, Peters P, and Lisanti MP. Cell-type and tissue-specific expression of caveolin-2. *J Biol Chem* 272: 29337-29346, 1997.

97. Krajewska WM and Maslowska R. Caveolins: structure and function in signal transduction. *Cell Mol Biol Lett* 9: 195-220, 2004.

98. Tang Z-L, Scherer PE, Okamoto T, Song K, Chu C, Kohtz DS, Nishimoto I, Lodish HF, and Lisanti MP. Molecular cloning of caveolin-3, a novel member of the caveolin gene family expressed predominantly in muscle. *J Biol Chem* 271: 2255-2261, 1996.

99. Okamoto T, Schlegel A, Scherer PE, and Lisanti MP. Caveolins, a family of scaffolding proteins for organizing "pre-assembled signaling complexes" at the plasma membrane. *J Biol Chem* 273: 5419-5422, 1998.

100. Hailstones D, Sleer LS, Parton RG, and Stanley KK. Regulation of caveolin and caveolae by cholesterol in MDCK cells. *J Lipid Res* 39: 369-379, 1998.

101. Murata M, Peranen J, Schreiner R, Weiland F, Kurzchalia T, and Simons K. VIP21/caveolin is a cholesterol-binding protein. *Proc Natl Acad Sci USA* 92: 10339-10343, 1995.

102. Thiele C, Hannah MJ, Fahrenholz F, and Huttner WB. Cholesterol binds to synaptophysin and is required for biogenesis of synaptic vesicles. *Nat Cell Biol* 2: 42-49, 2000.

103. Head BP, Patel H, Roth DM, Murray F, Swaney JS, Niesman IR, Farquhar MG, Insel PA. Microtubules and actin microfilaments regulate lipid rafts/caveolae localization of adenylyl cyclase signaling components. *J Biol Chem* 281: 26391-26399, 2006.

104. Sargiacomo M, Sudol M, Tang Z-L, and Lisanti MP. Signal transducing molecules and GPI-linked proteins form a caveolin- rich insoluble complex in MDCK cells. *J Cell Biol* 122: 789-807, 1993.

105. Lisanti MP, Scherer PE, Vidugiriene J, Tang Z-L, Hermanoski-Vosatka A, Tu Y-H, Cook RF, and Sargiacomo M. Characterization of caveolin-rich membrane domains isolated from an endothelial-rich source: Implications for human disease. *J Cell Biol* 126: 111-126, 1994.

106. Schwencke C, Okumura S, Yamamoto M, Geng YJ, and Ishikawa Y. Colocalization of beta-adrenergic receptors and caveolin within the plasma membrane. *J Cell Biochem* 75: 64-72, 1999.

107. Haasemann M, Cartaud J, Muller-Esterl W, and Dunia I. Agonist-induced redistribution of bradykinin B2 receptor in caveolae. *J Cell Sci* 111: 917-928, 1998.

108. Rybin VO, Xu X, Lisanti MP, and Steinberg SF. Differential targeting of beta-adrenergic receptor subtypes and adenylyl cyclase to cardiomyocyte caveolae. A mechanism to functionally regulate the cAMP signaling pathway. *J Biol Chem* 275: 41447-41457, 2000.

109. Li S, Couet J, and Lisanti MP. Src tyrosine kinases, G alpha subunits and H-Ras share a common membrane-anchored scaffolding protein, caveolin. Caveolin binding negatively regulates the auto-activation of Src tyrosine kinases. *J Biol Chem* 271: 29182-29190, 1996.

110. Yamamoto M, Toya Y, Schwencke C, Lisanti MP, Myers M, and Ishikawa Y. Caveolin is an activator of insulin receptor signaling. *J Biol Chem* 273: 26962-26968, 1998.

111. Darby PJ, Kwan CY, and Daniel EE. Caveolae from canine airway smooth muscle contain the necessary components for a role in Ca(2+) handling. *Am J Physiol Lung Cell Mol Physiol* 279: L1226-L1235, 2000.

112. Annabi B, Lachambre M, Bousquet-Gagnon N, Page M, Gingras D, and Beliveau R. Localization of membrane-type 1 matrix metalloproteinase in caveolae membrane domains. *Biochem J* 353: 547-553, 2001.

113. Chow AK, Cena J, El-Yazbi AF, Crawford BD, Holt A, Cho WJ, Daniel EE, and Schulz R. Caveolin-1 inhibits matrix metalloproteinase-2 activity in the heart. *J Mol Cell Cardiol* 42:896-901, 2007.

114. Razani B, Rubin CS, and Lisanti MP. Regulation of cAMP-mediated signal transduction via interaction of caveolins with the catalytic subunit of protein kinase A. *J Biol Chem* 274: 26353-26360, 1999.

115. Engelman JA, Chu C, Lin A, Jo H, Ikezu T, Okamoto T, Kohtz DS, and Lisanti MP. Caveolin-mediated regulation of signaling along the p42/44 MAP kinase cascade *in vivo*. A role for the caveolin-scaffolding domain. *FEBS Lett* 428: 205-211, 1998.

116. Feron O, Belhassen L, Kobzik L, Smith TW, Kelly RA, and Michel T. Endothelial nitric oxide synthase targeting to caveolae. Specific interactions with caveolin isoforms in cardiac myocytes and endothelial cells. *J Biol Chem* 271: 22810-22814, 1996.

117. Roy S, Luetterforst R, Harding A, Apolloni A, Etheridge M, Stang E, Rolls B, Hancock JF, and Parton RG. Dominant-negative caveolin inhibits H-Ras function by disrupting cholesterol-rich plasma membrane domains. *Nat Cell Biol* 1: 98-105, 1999.

118. Li S, Okamoto T, Chun M, Sargiacomo M, Casanova JE, Hansen SH, Nishimoto I, and Lisanti MP. Evidence for a regulated interaction between hetero-trimeric G proteins and caveolin. *J Biol Chem* 270: 15693-15701, 1995.

119. Engelman JA, Zhang XL, Galbiati F, Volonte D, Sotgia F, Pestell RG, Minetti C, Scherer PE, Okamoto T, and Lisanti MP. Molecular genetics of the caveolin gene family: implications for human cancers, diabetes, Alzheimer's disease and muscular dystrophy. *Am J Hum Genetics* 63: 1578-1587, 1998.

120. Couet J, Li S, Okamoto T, Ikezu T, and Lisanti MP. Identification of peptide and protein ligands for the caveolin-scaffolding domain. Implications for the interaction of caveolin with caveolae-associated proteins. *J Biol Chem* 272: 6525-6533, 1997.

121. Razani B, Engelman JA, Wang XB, Schubert W, Zhang XL, Marks CB, Macaluso F, Russell RG, Li M, Pestell RG, Di Vizi D, Hou H Jr., Kneitz B, Lagaud G, Christ GJ, Edelmann W, and Lisanti MP. Caveolin-1 null mice are viable, but show evidence of hyper-proliferative and vascular abnormalities. *J Biol Chem* 276: 38121-38138, 2001.

122. Galbiati F, Engelman JA, Volonte D, Zhang XL, Minetti C, Li M, Hou H, Kneitz B, Edelmann W and Lisanti MP. Caveolin-3 null mice show a loss of caveolae, changes in the microdomain distribution of the dystrophin-glycoprotein complex and T- tubule abnormalities. *J Biol Chem* 276: 21425-21433, 2001.

123. Cohen AW, Park DS, Woodman SE, Williams TM, Chandra M, Shirani J, Pereira dS, Kitsis RN, Russell RG, Weiss LM, Tang B, Jelicks LA, Factor SM, Shtutin V, Tanowitz HB, and Lisanti MP. Caveolin-1 null mice develop cardiac hypertrophy with hyperactivation of p42/44 MAP kinase in cardiac fibroblasts. *Am J Physiol* 284, C457–C474, 2003.

124. Schubert W, Frank PG, Woodman SE, Hyogo H, Cohen DE, Chow CW, and Lisanti MP. Microvascular hyperpermeability in caveolin-1 -/- knock-out mice. Treatment with a specific nitric-oxide synthase inhibitor, L-NAME, restores

normal microvascular permeability in Cav-1 null mice. *J Biol Chem* 277, 40091–40098, 2002.

125. Woodman SE, Park DS, Cohen AW, Cheung MW, Chandra M, Shirani J, Tang B, Jelicks LA, Kitsis RN, Christ GJ, Factor SM, Tanowitz HB, and Lisanti MP. Caveolin-3 knock-out mice develop a progressive cardiomyopathy and show hyperactivation of the p42/44 MAPK cascade. *J Biol Chem* 277, 38988–38997, 2002.

126. Makhlouf GM. Smooth muscle of the gut. In: Yamada T (ed.). Textbook of Gastroenterology, 4th edition, Lippincott Williams & Wilkins, Philadelphia, PA, pp. 92-116, 2003.

127. Murthy KS. Signaling for contraction and relaxation in smooth muscle of the gut. *Annu Rev Physiol* 68: 345-374, 2006.

128. Christinck F, Jury J, Cayabyab F, and Daniel EE. Nitric oxide may be the final mediator of nonadrenergic, noncholinergic inhibitory junction potentials in the gut. *Can J Physiol Pharmacol* 69: 1448-1458, 1991.

129. Toda N and Herman AG. Gastrointestinal functional regulated by nitrergic efferent nerves. *Pharmacol Rev* 57: 315-338, 2005.

130. Bredt DS. Endogenous nitric oxide synthesis: biological functions and pathophysiology. *Free Radic Res* 31: 577-596, 1999.

131. Griffith OW and Stuehr DJ. Nitric oxide synthases: properties and catalytic mechanisms. *Annu Rev Physiol* 77: 707-736, 1995.

132. Moncada S, Palmer RM, and Higgs EA. Nitric oxide: physiology, pathophysiology, and pharmacology. *Pharmacol Rev* 43: 109-142, 1991.

133. Waldman SA and Murad F. Cyclic GMP synthesis and function. *Pharmacol Rev* 39: 163-196, 1987.

134. Thornbury KD, Ward SM, Dalziel HH, Carl A, Westfall DP, and Sanders KM. Nitric oxide and nitrosocysteine mimic nonadrenergic, noncholinergic hyperpolarization in canine proximal colon. *Am J Physiol* 261: G553-G557, 1991.

135. Murthy KS, Severi C, Grider JR, and Makhlouf GM. Inhibition of inositol 1,4,5-triphosphate (IP_3) production and IP_3-dependent Ca^{2+} mobilization by cyclic nucleotides in isolated gastric muscle cells. *Am J Physiol* 264: G967-G974, 1993.

136. Bolotina VM, Najibi S, Palacino JJ, Pogamo PJ, and Cohen RA. Nitric oxide directly activates calcium-dependent potassium channels in vascular smooth muscle. *Nature* 368: 850-853, 1994.

137. Adachi T, Weisbrod RM, Pimentel DR, Ying J, Sharov VS, Schöneich C, and Cohen RA. S-Glutathiolation by peroxynitrite activates SERCA during arterial relaxation by nitric oxide. *Nat Med* 10: 1200-1207, 2004.

138. Ignarro LJ. Endothelium-derived nitric oxide: Actions and properties. *FASEB J* 3: 31-36, 1989.

139. Beavo JA and Brunton LL. Cyclc nucleotide research: still expanding after half a century. *Nat Rev Mol Cell Biol* 3: 710-718, 2002.

140. Rybalkin SD, Yan C, Bornfeldt KE, and Beavo JA. Cyclic GMP phosphodiesterases and regulation of smooth muscle function. *Circ Res* 93: 280-291, 2003.

141. Murthy KS. Activation of PDE5 and inhibition of guanylyl cyclase by cGMP-dependent protein kinase in smooth muscle. *Biochem J* 360: 199-208, 2001.

142. Rybalkin SD, Rybalkina IG, Schimizu-Albergine M, Tang X-B, and Beavo JA. PDE5 is converted into an activated state upon cGMP binding to the GAFA domain. *EMBO J* 22: 469-478, 2003.

143. Maas AJ and Den Hertog A. The effect of apamin on the smooth muscle cells of guinea-pig taenia coli. *Eur J Pharmacol* 58: 151-156, 1979.

144. Ohno N, Xue L, Yamamoto Y, and Suzuki H. Properties of the inhibitory junction potentials in smooth muscle of the guinea pig gastric fundus. *Br J Pharmacol* 117: 974-978, 1996.

145. Pluja L, Fernandez E, and Jiminez M. Electrical and mechanical effects of vasoactive intestinal peptide and pituitary adenylate cyclase-activating peptide in the rat colon involve different mechanisms. *Eur J Pharmacol* 389: 217-224, 2000.

146. Zizzo MG, Mule F, and Serio R. Mechanisms underlying the inhibitory effects induced by pituitary adenylate cyclase-activating peptide in mouse ileum. *Eur J Pharmacol* 521: 133-138, 2005.

147. De Man JG, De Winter BY, Seerden TC, De Schepper HU, Herman AG, and Pelckmans AG. Functional evidence that ATP or a related purine is an inhibitory NANC neurotransmitter in the mouse jejunum: a study on the identity of P2X and P2Y purinoceptors involved. *Br J Pharmacol* 140: 1108-1116, 2003.

148. Murthy KS, Jin J-G, Grider JR, and Makhlouf GM. Characterization of PACAP receptors and signaling pathways in rabbit gastric muscle cells. *Am J Physiol* 272: G1391-G1399, 1997.

149. Sang Q and Young HM. Chemical coding of neurons in the myenteric plexus and external muscle of the small and large intestine of the mouse. *Cell Tissue Res* 284: 39-53, 1996.

150. Satoh Y, Takeuchi T, Yamazaki Y, Okishio Y, Nishio H, Takatsuji K, and Hata F. Mediators of nonadrenergic, noncholinergic relaxation in the longitudinal muscle of the intestine of the ICR mice. *J Smooth Muscle Res* 35: 65-75, 1999.

151. Koike K, Horinouchi T, and Takayanagi I. Possible mechanisms of beta-adrenoceptor-mediated relaxation induced by noradrenaline in guinea pig taenia caecum. *Eur J Pharmacol* 279: 159-163, 1995.

152. Viard P, Macrez N, Mironneau C, and Mironneau J. Involvement of both G protein αs and βγ subunits in β-adrenergic stimulation of vascular L-type Ca^{2+}-channels. *Br J Pharmacol* 132: 669-676, 2001.

153. Kravtsov GM, Hwang IS, and Tang F. The inhibitory effect of adrenomedullin in rat ileum: cross-talk with beta 3-adrenoceptor in the serotonin-induced muscle contraction. *J Pharmacol Exp Ther* 308: 241-248, 2003.

154. Francis SH and Corbin JD. Cyclic nucleotide-dependent protein kinases: intracellular receptors for cAMP and cGMP actions. *Crit Rev Clin Lab Sci* 36: 275-328, 1999.

7

155. Salapatek AM, Wang YF, Mao YK, Lam A, and Daniel EE. Myogenic nitric oxide synthase activity in canine lower oesophageal sphincter: morphological and functional evidence. *Br J Pharmacol* 123: 1055-1064, 1998.

156. Salapatek AM, Wang YF, Mao YK, Mori M, and Daniel EE. Myogenic NOS in canine lower esophageal sphincter: enzyme activation, substrate recycling, and product actions. *Am J Physiol* 274: C1145-C1157, 1998.

157. Schuh K, Quaschning T, Knauer S, Hu K, Kocak S, Roethlein N, and Nyses L. Regulation of vascular tone in animals overexpressing the sarcolemmal calcium pump. *J Biol Chem* 278: 41246-41252.

158. Rumessen JJ, Thuneberg L, and Mikkelsen HB. Plexus muscularis profundus and associated interstitial cells. II. Ultrastructural studies of mouse small intestine. *Anta Rec* 203: 129-146, 1982.

159. Bergdahl A and Sward K. Caveolae associated signaling in smooth muscle. *Can J Physiol Pharmacol* 82: 289-299, 2004.

160. Murthy KS and Makhlouf GM. Heterologous desensitization mediated by G protein-specific binding to caveolin. *J Biol Chem* 275: 30211-30219, 2000.

161. Daniel EE, Bodie G, Mannarino M, Boddy G, and Cho WJ. Changes in membrane cholesterol affect caveolin-1 localization and ICC pacing in mouse jejunum. *Am J Physiol* 287: G202-G210, 2004.

162. Cho WJ and Daniel EE. Proteins of the interstitial cells of Cajal and intestinal smooth muscle, colocalized with caveolin-1. *Am J Physiol* 288: G571-G585, 2005.

163. Ueno T, Duenes JA, Zarroug AE, and Sarr MG. Nitrergic mechanisms mediating inhibitory control of longitudinal smooth muscle contraction in mouse small intestine. *J Gastrointest Surg* 8: 831-841, 2004.

164. Zizzo MG, Mule F, and Serio R. Duodenal contractile activity in dystrophic (mdx) mice: reduction of nitric oxide influence. *Neurogastroenterol Motil* 15: 559-565, 2003.

165. Hutchinson DS, Evans BA, and Summers RJ. Beta(1)-adrenoceptors compensate for beta(3)-adrenoceptors in ileum from beta(3)-adrenoceptor knock-out mice. *Br J Pharmacol* 132: 433-442, 2001.

166. Daniel EE, El-Yazbi A, and Cho WJ. Caveolae and calcium handling, a review and a hypothesis. *J Cell Mol Med* 10: 529-544, 2006.

CHAPTER II

METHODS

The methods that were common to all chapters are described in this section. Methods that were only unique to a certain study are mentioned in the corresponding chapter. These experiments were conducted according a laboratory animal protocol that conforms with the Guide to the Care and Use of Experimental Animals published by the Canadian Council on Animal Care (revised 1993) and approved by our institutional Animal Care and Use Committee.

2.1 Animals:

6-8 week old male mice were used for the studies in this thesis project. Three strains of mice were used. BALB/c mice were used as reference wild type mouse strain (Jackson Laboratories, Bar Harbor, MN). A breeding pair for caveolin-1 knockout mice (Stock Cav <tm 1M 1S>/J, cav1$^{-/-}$) was obtained from Jackson Laboratories and bred in the University of Alberta Health Sciences Laboratory Animal Services facility. The offspring were regularly tested for the expression of caveolin-1 using immunohistochemistry and Western blotting. The third strain, B6 129SF2/J (cav1$^{+/+}$), was obtained from Jackson Laboratories and used as a control to correct for strain variations when comparing cav1$^{-/-}$ to wild type mice. Cav1$^{+/+}$ are second generation hybrids of B6 and 129S mouse strains, the two strains that make up the genetic background of cav1$^{-/-}$ mice. The adult animals bought from Jackson Laboratories together with the cav1$^{-/-}$ offspring after weaning were housed in a conventional animal housing facility under standard temperature, humidity, and light cycle conditions. On the morning of the day of experiment, the required number of animals was brought into the laboratory. Animals were sacrificed by cervical dislocation prior to any experimental manipulations.

2.2 Functional experiments on intact tissue preparations:

2.2.1 Tissue isolation and setup:

After opening the abdominal wall, the gastrointestinal tract, starting from the stomach to the rectum, was removed from the mouse and immediately placed into a beaker of Krebs-Ringer solution containing (in mM): NaCl (115.5), $NaHCO_3$ (21.9), D-glucose (11.1), KCl (4.6), $MgSO_4$ (1.16), $NaHPO_4$ (1.16), and $CaCl_2$ (2.5), at room temperature (21-22°C), and equilibrated with carbogen (95% O_2 and 5% CO_2). In a dissection dish filled with Krebs-Ringer solution and continuously bubbled with carbogen, small intestinal tissue was isolated and cut into approximately 0.5 cm segements for CM preparations and 1-1.5 cm segments for LM preparations. In case of LM, the intestinal content, if any, was pushed out by gently rubbing the segments with dissection forceps. Details of tissue setup were described previously[1]. To study the contraction of CM, the open side of a thin metal triangle was slid through the lumen of the tissue segment. The triangle was then hooked together so that its base passed axially through the lumen of the tissue segment. A stainless steel rod attached to the bottom of the electrode holder was also inserted to pass axially into the lumen of the tissue segment parallel to and beneath the base of the metal triangle. Silk suture thread, attached to the apex of the triangle opposite to the tissue, was tied to an isometric force displacement transducer (Grass FT-03, Astro-Med Inc., West

Warwick, RI). Two thin platinum rods, situated on both sides of and parallel to the tissue, were used for the electrical stimulation of the tissue. To study the contraction of LM, the tissue was placed between two platinum concentric electrodes and tied to a hook at the bottom of the electrode holder with suture thread. The top of the tissue was also tied with suture thread and attached to the isometric force displacement transducer. The CM and LM preparations are depicted in Fig 2.1. The muscle preparations were placed in jacketed tissue baths filled with 10 ml Krebs-Ringer solution, continuously bubbled throughout the experiment with carbogen, and maintained at a temperature of 37°C by a thermostatically controlled water stream flowing through the glass jacket. The tension on the tissue was increased or decreased slowly until the tension that produced the maximum phasic activity was reached (about 0.5 g). Tissue contractile activities were recorded on a Grass Model 7D Polygraph (Astro-Med Inc., West Warwick, RI).

2.2.2 Experimental Protocols:

Prior to any experimental procedures the tissues were equilibrated for at least 20 min. In experiments where blockade of muscarinic and adrenoceptors was required, the corresponding blockers were added at the beginning of the equilibration period and incubated with the tissue for the full length of the experiment. Following the equilibration period, the tissue preparations were either treated with different agents or subjected to electric field stimulation (EFS) using a Grass Model S88 electrical stimulator (Astro-Med Inc., West Warwick, RI). Different frequencies of electric

Fig 2.1 Mounting CM and LM preparations on electrode holders. a. A CM preparation mounted on an electrode holder and a thin metal triangle attached to the force displacement transducer. Two platinum electrodes on both sides of the tissue are used for the electrical stimulation. b. A LM preparation mounted on an electrode holder and passing through two concentric platinum electrodes.

Fig 2.1

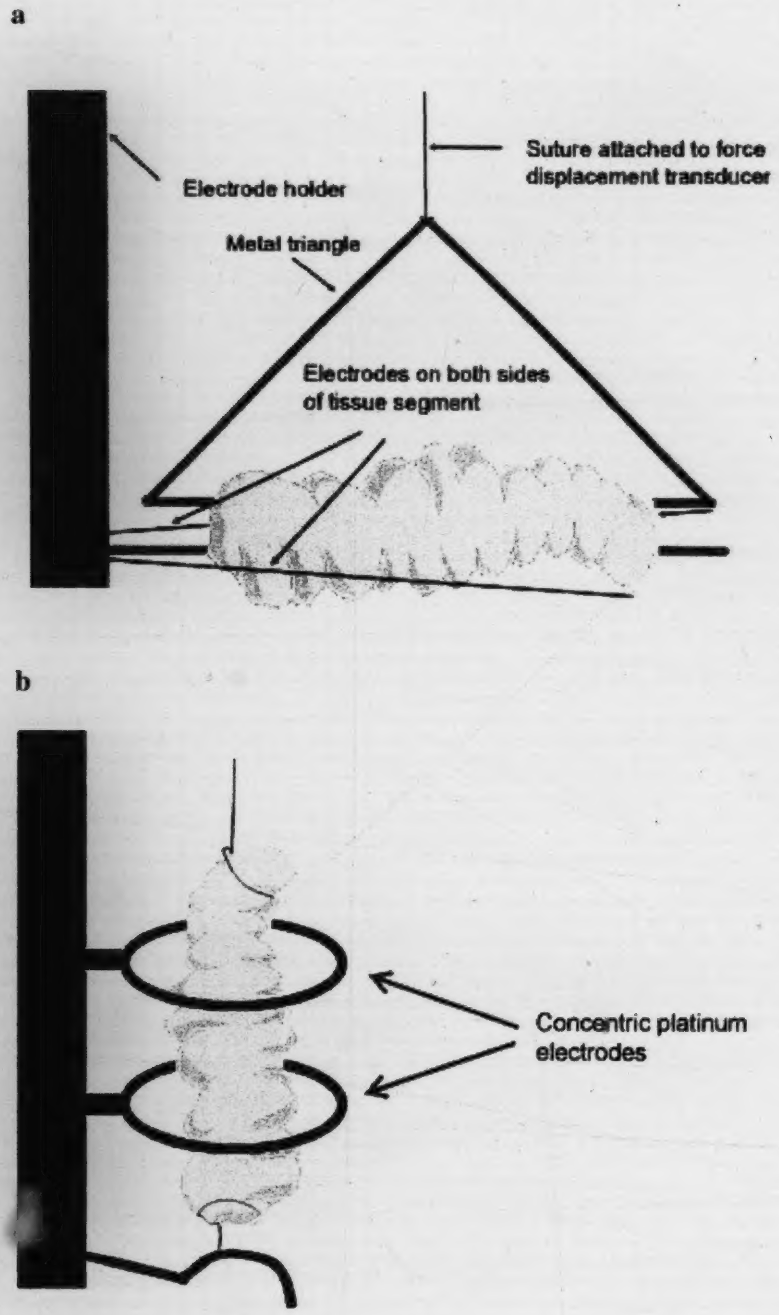
a
Electrode holder
Suture attached to force displacement transducer
Metal triangle
Electrodes on both sides of tissue segment
b
Concentric platinum electrodes

stimulation were used in different experiments. Generally, to study the effects of enteric nerve stimulation a cycle of four trains of different frequencies was used: 1, 3, 10, and 30 Hz. In some experiments, a single stimulation of 5 Hz frequency was used to test the activity of the enteric nerves. A single train consisted of electrical stimulation lasting for 10 s using square pulses (50 mV and 0.5 ms duration). At the end of each experiment, all tissues were washed twice with 10 ml Ca^{2+}-free Krebs-Ringer solution with 1.0 mM ethylene glycol bis(2-aminoethyl ether)-N,N,N,N-tetraacetic acid (EGTA) to relax the tissues to basal passive tension and to abolish spontaneous contractions.

2.2.3 Data analysis:

The basal passive tension, which is the lowest tension recorded from a tissue after incubation in calcium-free Krebs-Ringer solution, was used as the zero reference point for measurement of the spontaneous or evoked changes in tone or amplitude of phasic contractions. The tone was defined as the difference between the lowest points reached during the tissue phasic activity and the level of the basal passive tension. It is also the difference between the basal passive tension and the level of the tissue tension under conditions in which the phasic activity was suppressed. On the other hand, the amplitude of phasic contractions was measured as the difference between the basal passive tension and the crest of the phasic contraction. The amplitude of phasic contractions used in the present studies is actually a mean of amplitudes of at

Fig 2.2 Measurement of the amplitude of contraction of muscle preparations. The tone (tonic amplitude) or the amplitude of phasic contractions (phasic amplitude) were measured with reference to the basal passive tone brought about by incubation of the tissue in calcium-free Krebs-Ringer solution containing 1 mM EGTA.

Fig 2.2

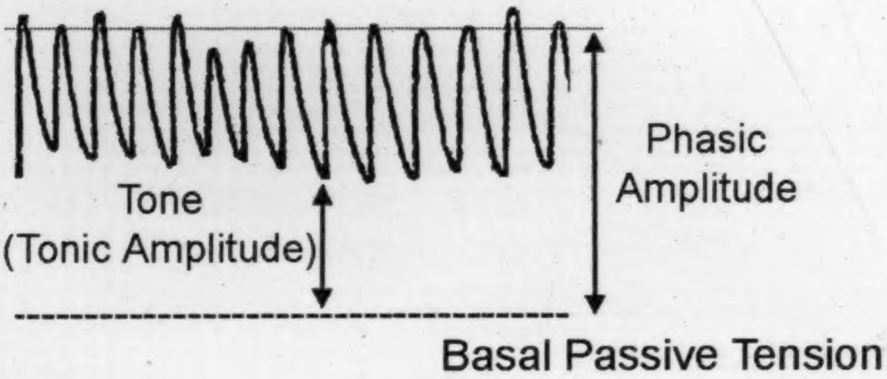
Phasic
Amplitude
Tone
(Tonic Amplitude)
Basal Passive Tension

least 15 individual consecutive contractions. Fig 2.2 depicts the measured values of tone and phasic amplitude. All the measured values were normalized to regions of control activity selected according to the experimental protocol within the same muscle preparations. In all of the studies the value of control activity was expressed in absolute terms (mg tension) and compared statistically between the different mouse strains to ensure that there was no basal difference to affect the interpretation of the normalized results. The frequency of the spontaneously-paced contractions was determined by counting the number of contractions over a period of at least 20 seconds.

2.2.4 Statistical analysis:

The obtained results were expressed as mean±SEM. The values were compared statistically using GraphPad Instat® software with the appropriate of the following tests: paired *t*-test, unpaired *t*-test, analysis of variance (ANOVA) followed by the Bonferroni *post hoc* test, and repeated measures ANOVA followed by the Bonferroni *post hoc* test. A P value < 0.05 was considered to be significant. The n values mentioned represent the number of animals from which tissues were obtained for the experiments.

2.3 Electron microscopy:

Freshly isolated mouse small intestinal tissue was fixed as described previously[2]. The segments were fixed with a mixture of 2.5% glutaraldehyde and 4%

paraformaldehyde in 0.075 M sodium cacodylate buffer (pH 7.4) (Marivac Inc, Montreal, QC) containing 3% sucrose and 1 mM $CaCl_2 \cdot 2H_2O$ for 2 hr at 4°C. The tissue was washed in 0.075 M sodium cacodylate buffer overnight at 4°C. The tissue was then dissected to prepare 1.0 x 4.0 mm segments and muscular layers were separated from mucosal layers. The tissue was stained *en bloc* in saturated (1%) uranyl acetate (Marivac Inc, Montreal, QC) in 70% ethanol for 1 hr at room temperature, post-fixed in 1% OsO_4 (Marivac Inc, Montreal, QC) in 0.05 M sodium cacodylate buffer (pH 7.4) for 2 hr at 4°C, dehydrated in graded solutions of ethanol (50%, 70%, 80%, 90%, 95%, and 100%) and then absolute propylenoxide, and embedded in TAAB 812 resin (Marivac Inc, Montreal, QC). Ultra-thin sections were cut, mounted on 100 or 300-mesh grids coated with 0.25% formvar solution in ethylene dichloride (Electron Microscopy Sciences, Hatfield, PA), and stained with 13% uranyl acetate in 50% ethanol and lead citrate. The grids were examined using a Philips 410 electron microscope equipped with a charge-coupled device camera (MegView III) at 80 kV.

2.4 Immunohistochemistry:

2.4.1 Tissue preparation:

The gastrointestinal tract was obtained from the mice as described under functional experiements and put into ice-cold oxygenated (95% O_2 and 5% CO_2) Krebs–Ringer solution. The small intestinal tissue was prepared for both cryosection and whole mount preparation. For cryosections, the small intestine was opened along the mesenteric border, pinned to a petri-dish lined with Sylgard silicon rubber, and fixed with 4% paraformaldehyde in 0.1 M sodium phosphate buffer for 4 hr. The fixed tissue was rinsed with 0.1 M phosphate buffer eight times each hour and cryoprotected with 30% sucrose in 0.1 M phosphate buffer overnight at 4°C. The cryoprotected tissue was trimmed and put into peel-a-way disposable embedding molds filled with Tissue-Tek® O.C.T. compound (Sakura Finetek Inc., Torrance, CA) in order to obtain optimal sections. The embedding molds were frozen for 1 hr at -28°C, peeled, and trimmed for cryosection. 6 μm cryosections were obtained by a cryostat (Leitz 1720 digital cryostat, Germany) and attached to a glass slide coated with 1.5% 3-aminopropyltriethoxysilane (Sigma, St. Louis, MO) in acetone. The cryosections were dried for 30 min at room temperature.

For whole mount preparation, the small intestine was also opened along the mesenteric border, stretched to about 200% of original size, pinned on a petri-dish lined with Sygard silicon rubber, and fixed with 4% paraformaldehyde in 0.1 M phosphate buffer for 4 hr at room temperature. The fixed tissue was rinsed with 0.1 M phosphate buffer eight times each hour, cleared with dimethylsulfoxide three times every 10 min, and re-rinsed in phosphate-buffered saline three times every 15 min at room temperature. The tissue was trimmed to 1.0 x 1.5 cm (circular muscle dimension x longitudinal muscle dimension). In trimmed tissue, muscle layers (circular and longitudinal muscle layers) were separated from the mucosal and submucosal layers. To obtain myenteric plexus attached to the longitudinal muscle layer, muscle fibers of the circular muscle layer were peeled away using tweezers under a dissection microscope.

2.4.2 Immunolabeling of cyrosections:

The dried cryosections were rinsed with 0.3% Triton-X 100 (VWR International, Edmonton, AB) in phosphate-buffered saline twice every 5 min to facilitate penetration of primary antibody and remove O.C.T. compound, followed by rinsing with phosphate-buffered saline once for 5 min. To reduce non-specific binding to proteins, 10% normal serum (from the host where the corresponding secondary antibody was raised) in phosphate-buffered saline was applied on the cryosection for 30 min at room temperature. One or more primary antibodies were mixed together in 1% serum in phosphate-buffered saline and incubated with the cryosections for 16 to 17 hr. The cryosections were rinsed with 0.3% Triton-X 100 in phosphate-buffered saline twice every 5 min, followed by a wash with phosphate-buffered saline once for 5 min. Fluorophore-conjugated secondary antibodies (1:20-1:40 Cy3- and 1:25-1:50 Alexa Fluor® 488-conjugated) were mixed together in 1% serum in phosphate-buffered saline and incubated with the cryosections for 1.5 hr. The cryosections were rinsed with 0.3% Triton-X 100 in phosphate-buffered saline twice every 5 min, followed by a wash with phosphate-buffered saline once for 5 min. Incubation procedures were performed at room temperature. To determine the specificity of immunolabeling, primary antibody was omitted, or when the antigen was available, it was incubated (at fivefold higher concentration) overnight with the primary antibody to saturate it prior to its application to the cryosection.

2.4.3 *Immunolabeling of whole mount preparations:*

The myenteric plexus attached to the longitudinal muscle preparations were put into a 24-tissue well plate and rinsed with 0.5% Triton-X 100 in phosphate-buffered saline for 1 hr. 10% normal serum (of the secondary antibody host) in 0.5% Triton-X 100 in phosphate-buffered saline was applied on the preparations for 1 hr at room temperature. Primary antibodies were mixed together in 1% serum in phosphate-buffered saline and incubated with the whole mount preparations for 64 to 65 hr. The preparations were rinsed with 0.5% Triton-X 100 in phosphate-buffered saline three times every 15 min. Fluorophore-conjugated secondary antibodies were mixed together in 1% serum in phosphate-buffered saline and incubated with the whole mount preparations for 3 hr. The preparations were rinsed with 0.5% Triton-X 100 in phosphate-buffered saline twice every 15 min followed by a wash with phosphate-buffered saline once for 15 min. Incubation procedures were performed at 4°C. To determine specificity of the immunolabeling, primary antibody was omitted, or when the antigen was available, it was incubated (at fivefold higher concentration) with the primary antibody at 4°C for 64 to 65 hr.

2.4.4 *Confocal laser scanning microscopy:*

The immunolabeled cryosections and whole mount preparations were examined by confocal laser scanning microscope (CLSM 1500, Zeiss, Germany) and saved as digital files by LSM 5 Image software. The images immunolabeled with Cy3-conjugated secondary antibodies were captured by helium/neon laser (excitation wavelength 543 nm laser line) with long path 590 filter, and images immunolabeled with FITC- or Alexa488-conjugated secondary antibodies were taken by Argon laser (excitation wavelength 488 nm laser line) with a band path 500–530 nm filter. The resolution of all images obtained from the confocal microscope was originally 512 x 512 pixels. In the obtained cryosection images mucosa and submucosa were digitally eliminated, and the muscularis was extracted. In the images of whole mount preparation longitudinal muscle layer was digitally eliminated and the myenteric ganglia and plexus were extracted. All final images were enhanced by brightness, contrast, and the gamma tool of LSM 5 image and edited by Adobe PhotoShop Version 7.0.

2.5 Western blotting:

2.5.1 Sample preparation:

Full-length mouse small intestine was obtained and kept in ice-cold oxygenated (95% O_2 and 5% CO_2) Krebs-Ringer solution. The tissue was cleaned from any adhering mesenteric blood vessels and connective tissues. The intestine was opened on the mesenteric border and the mucosa was removed by scraping with a scalpel blade. The remaining smooth muscle tissue was immediately frozen in liquid nitrogen and stored at -80°C until used. On the day of the experiment, frozen tissues were crushed in a mortar under liquid nitrogen and the produced fine powder was used for homogenization. When the whole tissue homogenate was required for blotting, the frozen powdered tissue was homogenized in 50 mM Tris buffer (pH 7.4) (1 mg tissue : 3 µl buffer) containing 3.1 mM sucrose, 1 mM dithiothreitol, 0.1% Triton X-100 and

1:1000 protease inhibitor cocktail (Sigma, Oakville, ON). The tissue was homogenized on ice with a polytron homogenizer (Pro 200, Diamed Lab Supplies Inc., Mississauga, ON) using three 20 s strokes separated by 1 min cooling periods on ice. Following homogenization, the crude homogenate was centrifuged at 12,000 *g* for 5 min to remove large debris. And the supernatant was used for Western blotting.

In experiments where purified membrane fractions were required, membrane fractions were prepared using a detergent-free method as previously described[3,4]. Frozen intestinal tissues from single mice or pooled tissues were crushed in a mortar under liquid nitrogen. The produced fine powder was homogenized on ice in 150 mM Na_2CO_3 (1 mg tissue: 2 µl solution) containing 1:1000 protease inhibitor cocktail using the Polytron homogenizer. Three 20 s strokes separated by 1 min cooling periods were used. 1 ml of the produced homogenate was mixed with 3 ml 60% sucrose solution in a centrifuge tube to reach a final concentration of 45%. Discontinuous gradients were prepared by overlaying 3 ml of 35% sucrose and 3 ml of 5% sucrose. Samples were subjected to ultra-centrifugation (Beckman L8-M Ultracentrifuge, Beckman Coulter Inc., Fullerton, CA) at 200,000 *g* for 18 hr at 4°C. Lipid raft-enriched (buoyant) fractions were collected from the light-dispersing layer at the interface of the 5% and 35% sucrose layers while heavy (non-raft) membrane fractions were collected from the lower half of the 45% sucrose layer. The purity of the separated fractions was assessed by Western blotting of certain protein markers as will be mentioned later. The protein concentration in the samples was determined by bicinchoninic acid assay[5] using bovine serum albumin as a standard.

2.5.2 Immunoblotting:

Sample aliquots diluted to contain equal amount of proteins were blotted as previously described[6]. Following electrophoresis, proteins were wet transferred to a polyvinylidene difluoride membrane (Bio-Rad Laboratories, Hercules, CA) using Towbin's transfer buffer. The membranes were blocked using 5% skim milk in Tris-buffered saline for 2 hr at room temperature, incubated with primary antibody in 5% skim milk for 2 hr at room temperature, or overnight at 4°C. Horseraddish peroxidase (HRP)-conjugated secondary antibody was incubated with the membranes for 1 hr at room temperature and proteins were visualized using an ECL™ Plus chemiluminiscence kit (GE Healthcare, Piscataway, NJ).

2.5.3 Assessment of membrane fraction purity:

As mentioned in the Introduction the main biochemical marker for the caveolae/lipid raft domains of the plasma membrane is caveolin-1. Blotting for caveolin-1 showed its enrichment in the buoyant fractions isolated from wild type mouse small intestinal tissue. However, it was naturally lacking in the corresponding fractions isolated from cav1$^{-/-}$ tissues. The identity of the buoyant fractions isolated from cav1$^{-/-}$ tissues was confirmed using another marker protein, flotillin, which associates with lipid rafts independent of caveolin[7]. The purity of the buoyant fractions was determined by the exclusion of actin[8] and β-adaptin[9]. Fig 2.3 shows representative blots of flotillin and actin in different membrane fractions.

Fig 2.3 Expression of flotillin and actin in different membrane fractions. a. Buoyant fraction from cav1$^{+/+}$ small intestine. b. Buoyant fraction from cav1$^{-/-}$ small intestine. c. Heavy fraction from cav1$^{+/+}$ small intestine. d. Heavy fraction from cav1$^{-/-}$ small intestine.

Fig 2.3

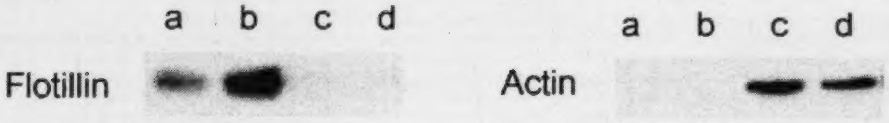
a b c d
Flotillin
a b c d
Actin

2.6 References

1. Daniel EE, Boddy G, Bong A, and Cho WJ. A new model of pacing in the mouse intestine. *Am J Physiol* 286: G253-G262, 2004.
2. Daniel EE, Bodie G, Mannarino M, Boddy G, and Cho WJ. Changes in membrane cholesterol affect caveolin-1 localization and ICC pacing in mouse jejunum. *Am J Physiol* 287: G202-G210, 2004.
3. Yang B, Oo TN, and Rizzo V. Lipid rafts mediate H2O2 prosurvival effects in cultured endothelial cells. *FASEB J* 20: 1501-1503, 2006.
4. Ostrom RS, Liu X, Head BP, Gregorian C, Seasholtz TM, and Insel PA. Localization of adenylyl cyclase isoforms and G protein-coupled receptors in vascular smooth muscle cells: expression in caveolin-rich and noncaveolin domains. *Mol Pharmacol* 62: 983-992, 2002.
5. Smith PK, Krohn RI, Hermanson GT, Mallia AK, Gartner FH, Provenzano MD, Fujimoto EK, Goeke NM, Olson BJ, and Klenk DC. Measurement of protein using bicinchoninic acid. *Anal Biochem* 150: 76-85, 1985.
6. Leon H, Atkinson LL, Sawicka J, Strynadka K, Lopaschuk GD, and Schulz R. Pyruvate prevents cardiac dysfunction and AMP-activated protein kinase activation by hydrogen peroxide in rat hearts. *Can J Physiol Pharmacol* 82: 409-416, 2004.
7. Rajendran L, Le Lay S, and Illges H. Raft association and lipid droplet targeting of flotillins are independent of caveolin. *Biol Chem* 388: 307-314, 2007.
8. Schnitzer JE, Oh P, Jacobson BS, and Dvorak AM. Caveolae from luminal plasmalemma of rat lung endothelium: microdomains enriched in caveolin,

Ca(2+)-ATPase, and inositol trisphosphate receptor. *Proc Natl Acad Sci USA* 92: 1759-1763, 1995.

9. Absi M, Burnham MP, Weston AH, Harno E, Rogers M, and Edwards G. Effects of methyl beta-cyclodextrin on EDHF responses in pig and rat arteries; association between SK(Ca) channels and caveolin-rich domains. *Br J Pharmacol* 151: 332-340, 2007.

CHAPTER III

NEUROTRANSMITTERS INVOLVED IN NERVE-MEDIATED RELAXATION IN BALB/C MOUSE SMALL INTESTINE

A version of this chapter has been published. El-Yazbi, AF, Schulz R, and Daniel EE. Differential inhibitory control of circular and longitudinal smooth muscle layers of Balb/C mouse small intestine. *Auton Neurosci* 131: 36-44, 2007.

3.1 Introduction:

The mixing and propulsive movements of the small intestine are controlled by interactions between the enteric nervous system and an inherent pacemaker system[1]. Enteric neurons control reflex and integrative activities that do not require neuronal influences from extrinsic sources[2]. This intrinsic neuronal control is exerted through dual innervation with excitatory and inhibitory nerve fibres extending from cell bodies present in the myenteric plexus[1]. These excitatory and inhibitory effects are, at least in part, relayed to the smooth muscles via ICC[3,4]. Excitatory neurons extend proximally[5] and release acetylcholine and tachykinins[6,7], whereas, the inhibitory neurons extend distally[8]. These inhibitory nerves mediate relaxation of the GIT smooth muscles.

The descending inhibitory neurons play a major role in the different physiological intestinal motor patterns. Enteric inhibitory neurons involved in descending inhibition release several neurotransmitters including NO[9], ATP[10,11], VIP[12], pituitary adenylate cyclase activating peptide[13], and carbon monoxide[14]. These neurotransmitters often relax smooth muscles by evoking inhibitory junction potentials[15,16], resulting from the opening of potassium and/or closing of chloride channels[15,17]. However, whether a given transmitter acts on both LM and CM layers using the same mechanism of action is uncertain. LM and CM usually contract and relax simultaneously[18,19] and receive synchronous excitatory and inhibitory inputs[20] during the peristaltic reflex. Yet whether the different putative neurotransmitters have identical roles or mechanisms of action in the two layers has not been determined.

Previous research in our laboratory showed that CM and LM layers of mouse small intestine differ in their functional activities in terms of the paced contractions driven by the ICC and responses to some pharmacological agents, such as forskolin or cyclopiazonic acid[21,22]. In other species, different relative roles of NO have been suggested between intestinal LM and CM[23]. These variations could affect the regulation of peristaltic movement in the mouse small intestine. In the present study, we examined the role of NO, apamin-sensitive mediators, and VIP in smooth muscle relaxation in the CM layer, their mechanisms of action, and their relative importance in comparison to the LM layer of the mouse small intestine.

3.2 Materials and Methods:

3.2.1 Preparation of the tissue:

Tissues from 6-8 week old male BALB/c mice were isolated and set up to record the contractile activity of CM and LM as described in Chapter II.

3.2.2 Experimental Protocols:

To study the responses to intrinsic inhibitory mediators, the tissues were equilibrated in the organ bath with a combination of atropine (10^{-7} M), timolol (10^{-6} M), and prazosin (10^{-6} M) for 20 min. In some experiments, EFS was carried out at 1, 3, 10, and 30 Hz, with a 10 min interval between consecutive trains. The LM segments were subjected to a cycle of EFS at the four frequencies following the equilibration period. Afterwards, either the NOS inhibitor, N^{ω}-nitro-L-arginine (LNNA, 100 μM), or the soluble guanylyl cyclase inhibitor, 1H-(1,2,4)oxadiazolo(4,3-a)quinazoline-1-one (ODQ, 1 μM), was added and incubated with the tissue for 20 min followed by another cycle of electric field stimulation. The inhibitory effects of EFS were compared before and after the addition. In other experiments, the inhibitory effects of sodium nitroprusside (SNP, 100 μM), VIP (0.33 μM) and 8-bromoguanosine-3':5'-cyclic monophosphate (8-br cGMP, 100 μM) were studied by adding SNP, VIP, or 8-br cGMP immediately after the equilibration period. Some tissue segments were pre-treated by ODQ (1 μM) or apamin (1 μM) at the beginning of the equilibration period. SNP, 8-br cGMP, and VIP were added in a single concentration (in the higher sub-maximal range-based on preliminary experiments) to produce a clear consistent effect that was lacking with lower doses whose repetition resulted in a reduced response. Experiments on CM segments were done following the same protocols used in LM with the exception of the experiments done to study the effects of different agents on EFS. In these experiments, the effects on EFS responses of LNNA (100 μM), the SK_3-channel blocker apamin (1 μM), ODQ (1 μM), or a combination of LNNA and apamin were studied. These agents were added at the beginning of the equilibration period followed by EFS at the four frequencies. The results were compared to time controls run side by side. We used an unpaired experimental design in the case of CM since their responses to EFS were not fully reproducible upon repeated stimulation in pilot experiments.

3.2.3 Data Analysis:

The frequency of paced contractions and the amplitudes of phasic contractions were determined and statistical analysis was done as described in Chapter II.

3.2.4 Materials:

Atropine sulphate, timolol (as maleate salt), prazosin hydrochloride, ODQ, apamin, LNNA, SNP, 8-br cGMP, and VIP were purchased from Sigma (Oakville, ON, Canada). Dimethyl sulfoxide and EGTA were purchased from Caledon Laboratories (Georgetown, ON, Canada). Apart from apamin and ODQ, double distilled water was used to dissolve the drugs used in experiments in this study. Apamin was dissolved in 0.05 M acetic acid, while a stock solution of ODQ was prepared in dimethyl sulfoxide. Fresh dilutions were prepared on the day of the experiment by tenfold dilution of the stock solution with double distilled water. Neither dimethyl sulfoxide nor 0.05 M acetic acid affected the functional activity of the tissue in the amounts equivalent to that of the maximum drug concentrations used (1 µl in 10 ml bath and 10 µl in 10 ml bath, respectively).

3.3 Results:

3.3.1 Spontaneous contractile activity:

Mouse small intestinal segments set up to record CM or LM activity showed uniformly paced spontaneous rhythmic contractions. The frequency of pacing was measured at the end of the equilibration period in tissue segments obtained from the mid-jejunum to avoid errors resulting from the gradient of decreasing pacing frequency reported along the mouse intestine[21]. The frequency of spontaneous pacing was higher in LM than in CM (Fig 3.1a). However, LNNA (100 µM) and ODQ (1 µM) increased the pacing frequency in CM layer (Fig 3.1b). In LM, pacing frequency was unaffected by these agents (Fig 3.1b).

Fig 3.1 Spontaneous pacing frequency after block of muscarinic and adrenergic mediators in mouse small intestine. a. The frequency of pacing in longitudinal muscle (*n*=8) layer of mouse small intestine was higher than in circular muscle (*n*=17). b. The frequency of pacing in circular muscle was increased by 100 µM LNNA and 1 µM ODQ. (*n* values: 8 and 12). c. The frequency of pacing in longitudinal muscle was affected by neither 100 µM LNNA nor 1 µM ODQ (*n* values: 6 and 8, respectively). Statistically significant differences were measured by *t*-test for a and ANOVA followed by Bonferroni test for b and c, and are denoted by $^*P<0.05$ and $^{***}P<0.001$.

Fig 3.1

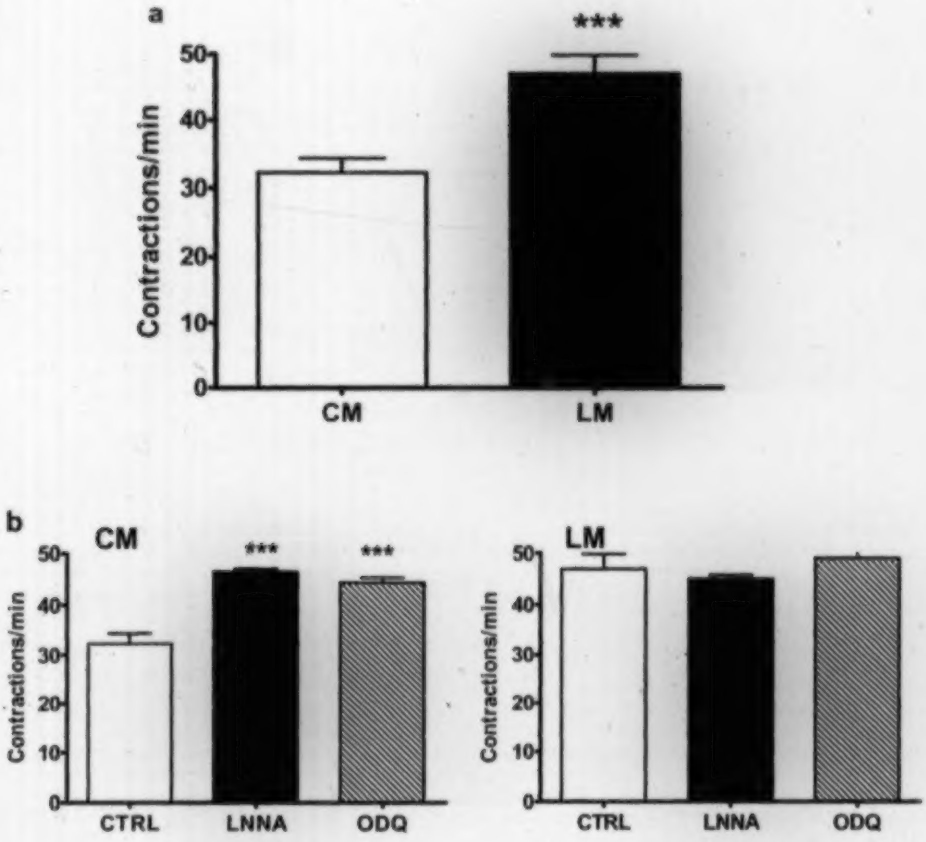
a
***
Contractions/min
0
10
20
30
40
50
CM
LM
b
CM
***
***
Contractions/min
0
10
20
30
40
50
CTRL
LNNA
ODQ
LM
Contractions/min
0
10
20
30
40
50
CTRL
LNNA
ODQ

3.3.2 Response to EFS:

LM and CM preparations responded to EFS by relaxation after inhibition of cholinergic and adrenergic responses. CM relaxation lasted for as long as the stimulus continued in most experiments, while in LM, EFS produced a brief relaxation followed by contraction (Fig 3.2a). The relaxation due to EFS in CM was followed by a rebound contraction, or an "off-effect" after the stimulus ended. The "off-effect" was more marked at higher frequencies of stimulation and appeared as an increase in the amplitude of phasic contractions without an increase in the frequency of pacing. For CM, the greatest relaxation was obtained at 3 Hz EFS (Fig 3.2b). In LM, the greatest relaxation occurred at 10 Hz.

3.3.3 Effects of agents blocking the action of neurotransmitters in LM and CM:

Inhibition of nitric oxide synthase (NOS) activity with 100 μM LNNA abolished the EFS-evoked relaxation in LM at all frequencies (Fig 3.3a). On the contrary, LNNA did not produce a significant reduction of the extent of EFS-evoked relaxation in CM (Fig 3.3a). In addition, blockade of SK_3-channels which mediate the effects of ATP and PACAP by 1 μM apamin did not affect the extent of the EFS-evoked relaxation in CM (Fig 3.3b). However, a combination of LNNA and apamin at the same concentrations used previously, significantly reduced the extent of EFS-induced relaxation of CM. Nevertheless, a residual inhibition of at least 25% persisted at all stimulation frequencies (Fig 3.3c).

Fig 3.2 Maximum inhibitory responses of the mouse small intestinal tissue segments to electric field stimulation in the presence of atropine (10^{-7} M), prazosin (10^{-6} M), and timolol (10^{-6} M). a. Representative tracings of the typical longitudinal muscle (LM) and circular muscle (CM) responses to EFS at a frequency of 10 Hz. b. The extent of inhibition in response to EFS at different stimulation frequencies in CM (*n*=10) and LM (*n*=7). The extent of EFS-induced responses is represented as the % inhibition of amplitude of phasic contractions.

Fig 3.2

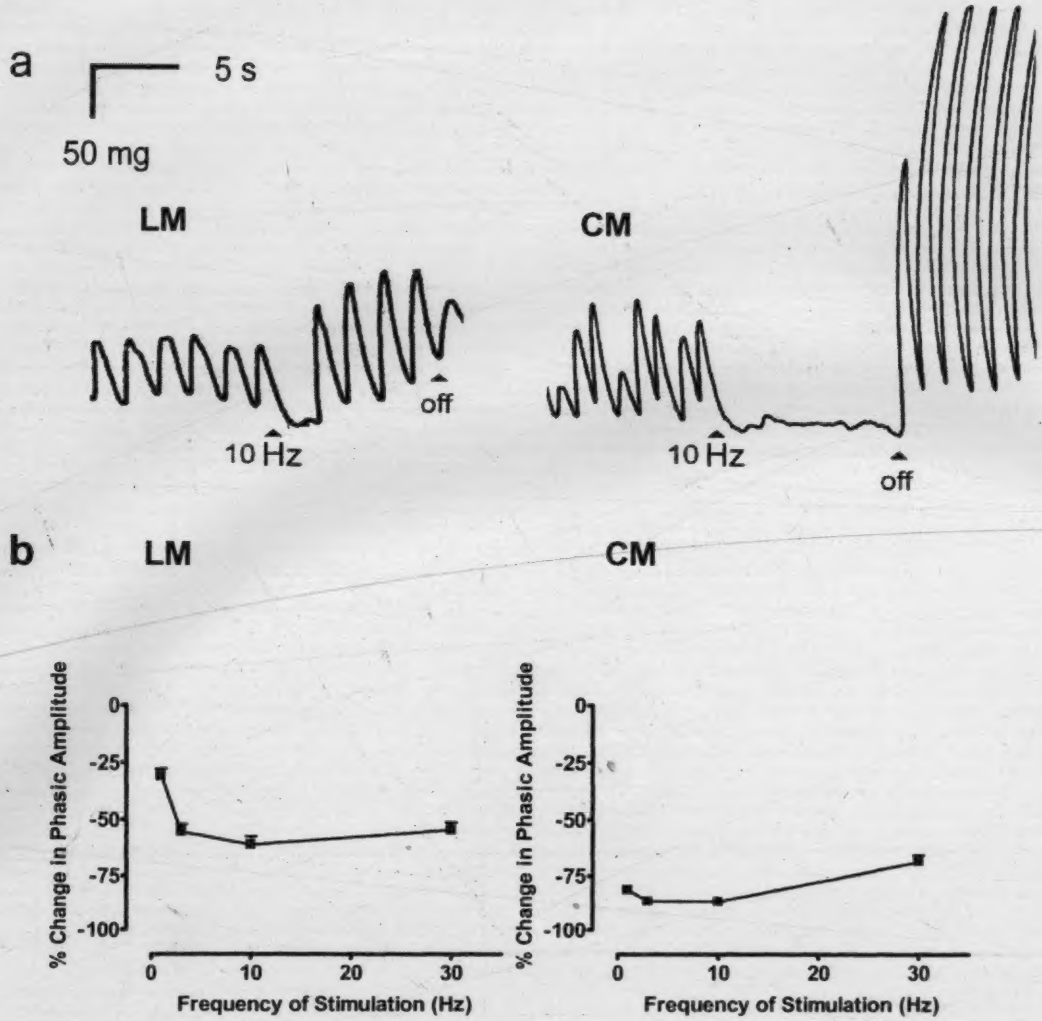
a
5 s
50 mg
LM
CM
10 Hz
off
10 Hz
off
b
LM
CM
% Change in Phasic Amplitude
0
-25
-50
-75
-100
0
10
20
30
Frequency of Stimulation (Hz)
% Change in Phasic Amplitude
0
-25
-50
-75
-100
0
10
20
30
Frequency of Stimulation (Hz)

Fig 3.3 Effects of agents blocking neurotransmitter action on EFS-induced relaxation in the presence of atropine (10^{-7} M), prazosin (10^{-6} M), and timolol (10^{-6} M) in LM (a) and CM (b, c, d). The effects on EFS-evoked relaxation in LM are shown before and after the addition of LNNA, while in CM comparisons are made with time controls. a. LNNA (100 µM) nearly abolished the relaxation in LM. b. LNNA (100 µM) did not show a significant reduction of the relaxation in CM. c. Apamin (1 µM) did not have any effect on the relaxation in CM. d. A combination of LNNA (100 µM) and apamin (1 µM) reduced the relaxation at all frequencies in CM. *n* values were 7 for LM, and for CM, 10 for control, and 6 for LNNA-, apamin- and the combination-treated tissues. Statistically significant differences were measured by ANOVA followed by the Bonferroni test and are denoted by $^{*}P<0.05$ and $^{***}P<0.001$.

Fig 3.3

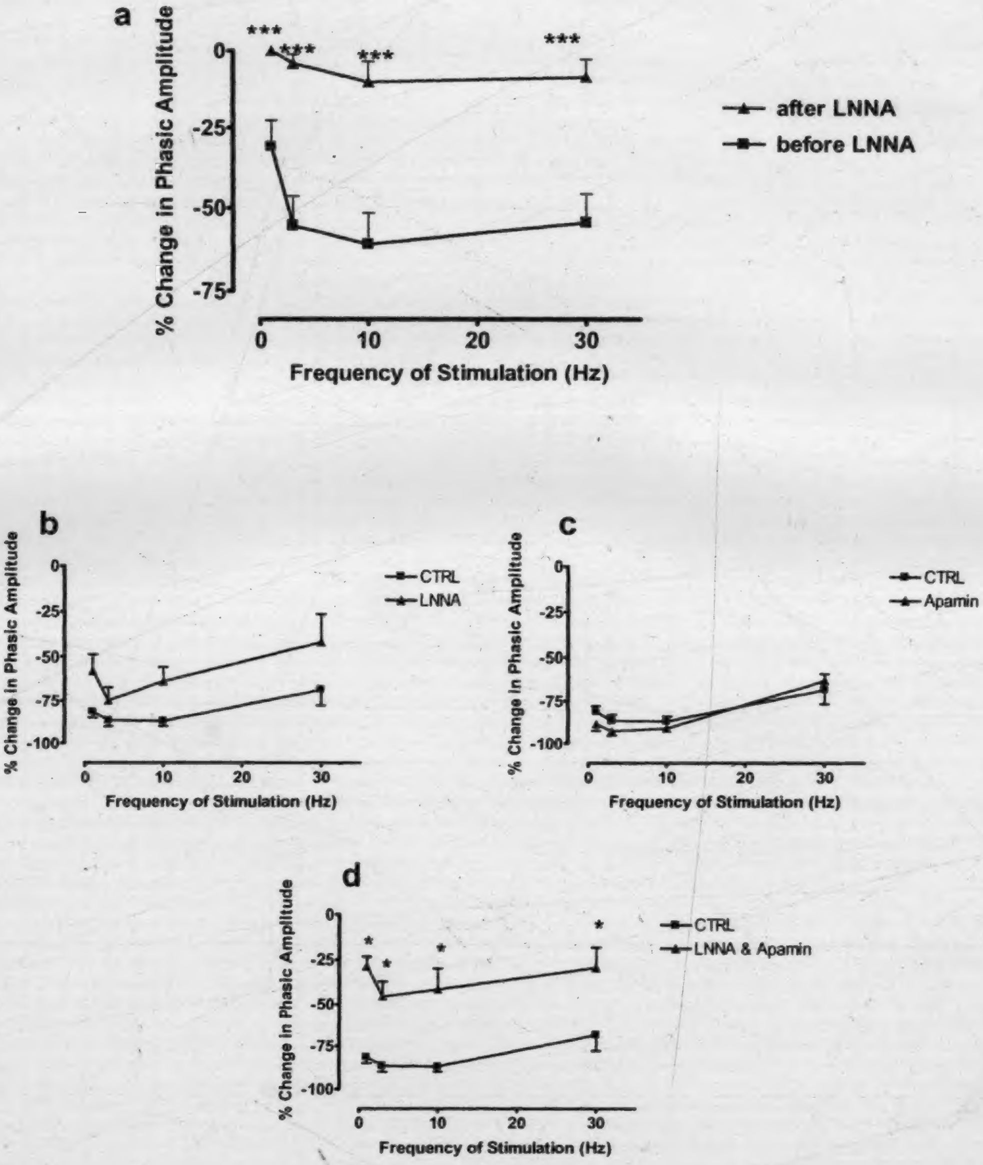
a
% Change in Phasic Amplitude
0
-25
-50
-75
***
***
***
***
0
10
20
30
Frequency of Stimulation (Hz)
after LNNA
before LNNA
b
% Change in Phasic Amplitude
0
-25
-50
-75
-100
0
10
20
30
Frequency of Stimulation (Hz)
CTRL
LNNA
c
% Change in Phasic Amplitude
0
-25
-50
-75
-100
0
10
20
30
Frequency of Stimulation (Hz)
CTRL
Apamin
d
% Change in Phasic Amplitude
0
-25
-50
-75
-100
*
*
*
*
0
10
20
30
Frequency of Stimulation (Hz)
CTRL
LNNA & Apamin

3.3.4 Effects of ODQ on EFS in CM and LM:

In LM, the soluble guanylate cyclase inhibitor ODQ (1μM) nearly abolished the relaxation at all stimulation frequencies similar to LNNA (Fig 3.4a). On the other hand, in CM the same concentration of ODQ had no significant effect at lower stimulation frequencies (similar to LNNA), yet starting at 10 Hz, the EFS-evoked relaxation in CM was significantly reduced and was almost abolished at 30 Hz (Fig 3.4b).

3.3.5 The effect of VIP in CM and LM:

We examined a possible role of VIP in CM and LM relaxation. Addition of 0.33 μM VIP produced an inhibition of the amplitude of the spontaneous contractile activity in CM preparations. This inhibition was reduced in side-by-side tissue segments pretreated with 1 μM ODQ (Fig 3.5). Under our experimental conditions, this concentration of VIP did not produce relaxation in LM.

3.3.6 Effects of ODQ and apamin on relaxation due to SNP in CM and LM:

Addition of the NO donor SNP (100 μM) produced a reduction in the amplitudes and frequencies of contraction of both CM and LM. In LM, either ODQ (1 μM) or apamin (1 μM) nearly abolished the inhibitory response to SNP (Fig 3.6a). On the other hand, ODQ(1 μM) only reduced but did not abolish the relaxation due to SNP in CM, while apamin (1 μM) had no effect on the SNP-induced relaxation (Fig 3.6b). A combination of ODQ and apamin at the previously mentioned concentration reduced the SNP-induced relaxation in CM in a manner similar to that with ODQ alone (data not shown).

Fig 3.4 Effects of ODQ (1 μM) on the EFS-evoked relaxation in presence of atropine (10^{-7} M), prazosin (10^{-6} M), and timolol (10^{-6} M) in LM and CM. In LM the response to EFS is compared before and after the addition of ODQ, while in CM comparisons are made with time controls. a. ODQ abolished the EFS-induced relaxation at all stimulation frequencies in LM (*n*=6). b. The effect of ODQ (1 μM) in CM (*n*=9 for control, and 6 for ODQ-treated tissues). At lower stimulation frequencies, ODQ had no significant effect. At higher frequencies, ODQ caused a more marked reduction in the extent of EFS-induced relaxation. Statistically significance was determined by ANOVA followed by Bonferroni test and is denoted by ****P*<0.001.

Fig 3.4

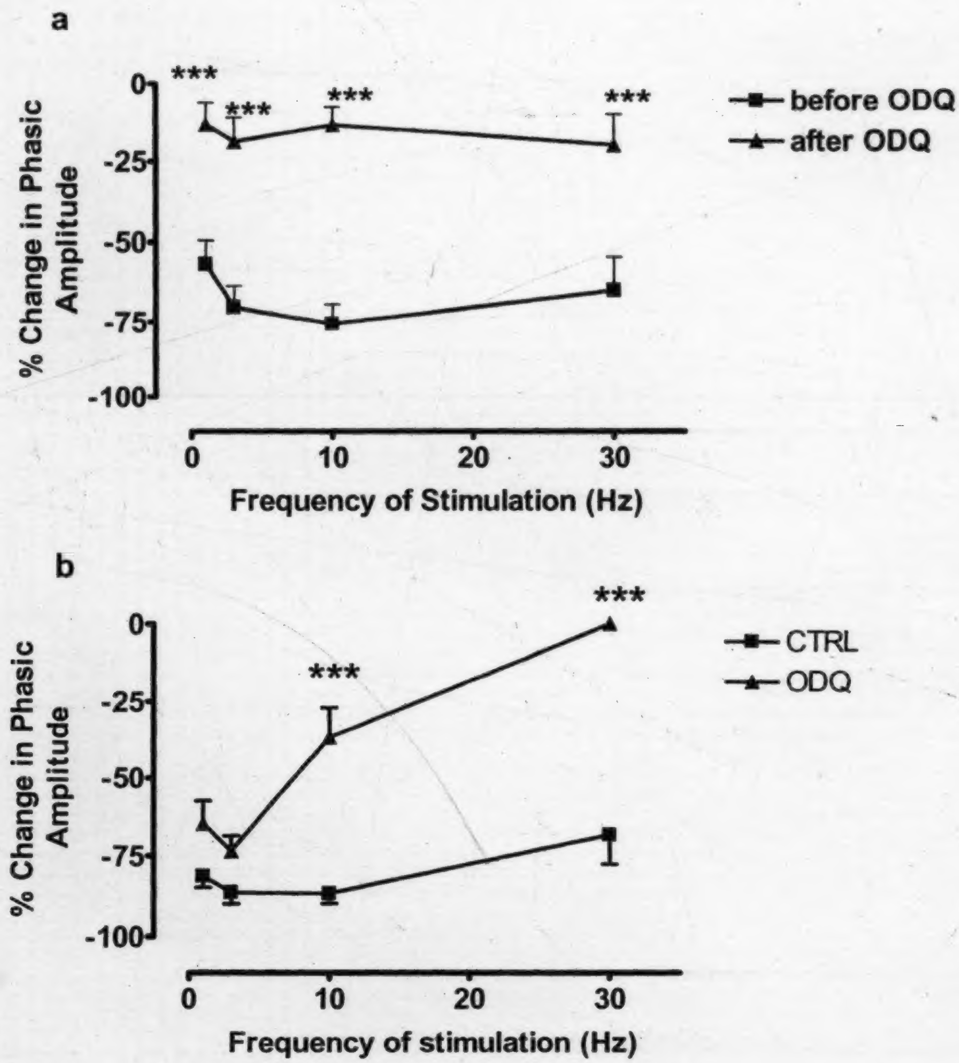
a
% Change in Phasic Amplitude
0
-25
-50
-75
-100
***
***
***
***
before ODQ
after ODQ
0
10
20
30
Frequency of Stimulation (Hz)
b
% Change in Phasic Amplitude
0
-25
-50
-75
-100
***
***
CTRL
ODQ
0
10
20
30
Frequency of stimulation (Hz)

Fig 3.5 Effect of ODQ (1 μM) on VIP (0.33 μM)-induced relaxation in CM of mouse small intestine. The extent of inhibition is represented as the % inhibition of the amplitude. 0.33 μM VIP induced a relaxation of CM that was reduced by 1 μM ODQ. The results shown are mean±SEM of six experiments. Statistical significance was measured by *t*-test (***P*<0.01).

Fig 3.5

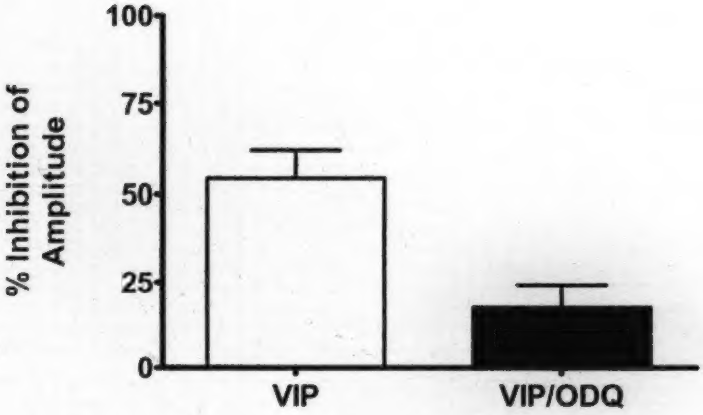

Fig 3.6 Effects of ODQ (1 μM) and apamin (1 μM) on the inhibitory response to SNP (100 μM) in LM and CM. The extent of inhibition is represented as the % inhibition of the amplitude. The values shown are mean±SEM of six experiments. a. In LM ODQ and apamin, independently, abolished the SNP-induced inhibition. b. In CM only ODQ, but not apamin, reduced the SNP-induced relaxation. Statistical significance was tested by ANOVA followed by Bonferroni test and is denoted by $^{**}P<0.01$ and $^{***}P<0.001$.

Fig 3.6

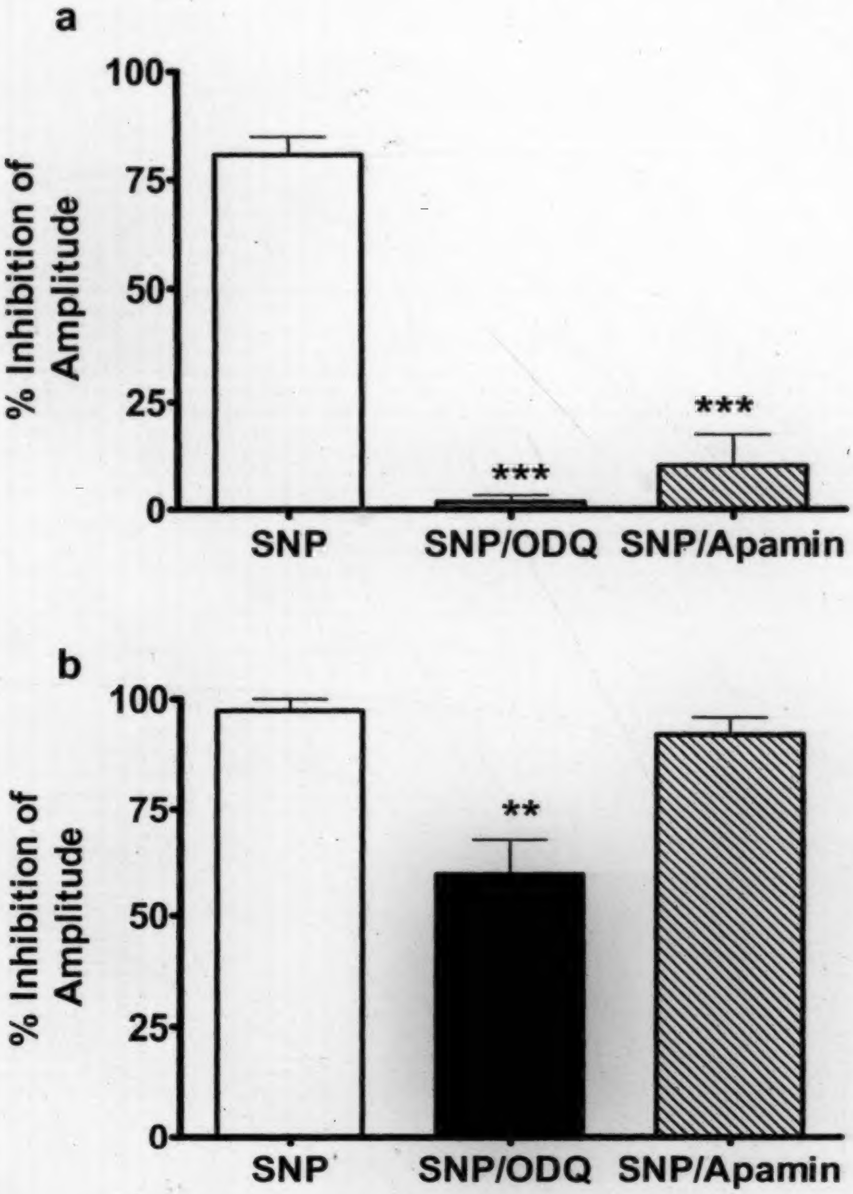
a
% Inhibition of Amplitude
100
75
50
25
0
***
***
SNP
SNP/ODQ
SNP/Apamin
b
% Inhibition of Amplitude
100
75
50
25
0
**
SNP
SNP/ODQ
SNP/Apamin

3.3.7 Effects of apamin on 8-br cGMP-induced relaxation in CM and LM:

The effects of apamin on the relaxation due to 8-br cGMP, a cell-membrane permeable analogue of cGMP, were studied. To allow 8-br cGMP to permeate the tissue, the responses were measured 5 min after its addition. 100 μM 8-br cGMP produced a reduction in the amplitude of contraction of both CM and LM segments. Pretreatment with apamin (1 μM) reduced the extent of 8-br cGMP-induced relaxation in LM but not in CM (Fig 3.7).

3.4 Discussion:

Here we examined and compared the contributions of different intrinsic inhibitory neurotransmitters to the functional activity of the CM and LM layers of the small intestine of BALB/c mouse, a strain commonly used in research. One clear difference in the function of these inhibitory mediators is the presence of a basal inhibitory tone in the spontaneous pacing activity of CM, but not LM. In this study, similar to our previous reports when the sympathetic and cholinergic transmitter actions were not blocked[21], we found that spontaneous pacing in the LM layer is faster than in CM, but was regular in both layers. Previously we also showed that block of nerves with tetrodotoxin eliminated the difference[21]. The spontaneous contractile movement of the CM and LM layers of the small intestine is driven by slow depolarization waves generated from the interstitial cells of Cajal in the myenteric plexus[24]. When measured in other species, the frequency of slow waves was found to be similar in CM and LM[25,26]. However, we previously raised the possibility of a difference in the pacemaker sites for LM and CM where we showed

Fig 3.7 Effect of apamin (1 μM) on the inhibitory response to 8-br cGMP (100 μM) in LM and CM. The extent of inhibition is represented as the % inhibition of the amplitude. The values shown are mean±SEM of six experiments. Apamin reduced the inhibitions due to 8-br cGMP in LM (a) but not in CM (b). Statistical significance was measured by *t*-test, ****P*<0.001.

Fig 3.7

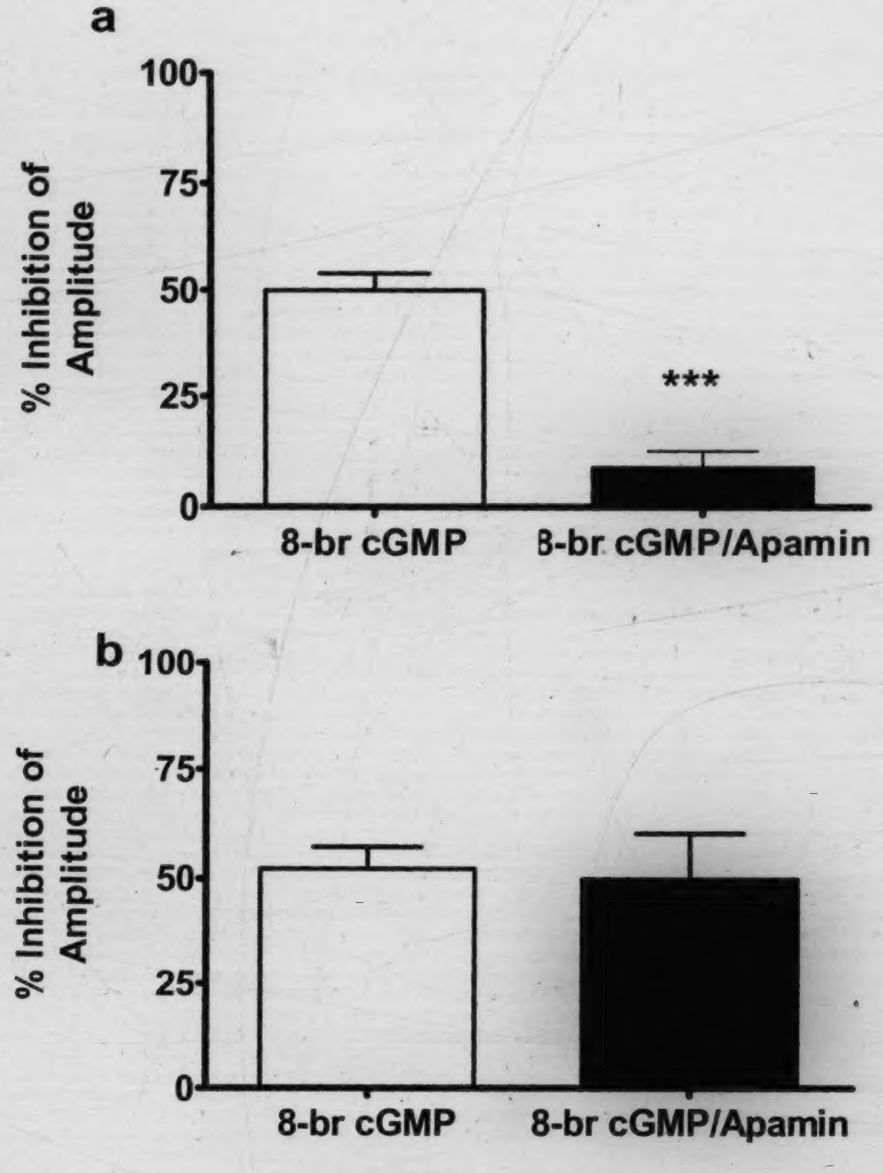
a
100
75
50
25
0
% Inhibition of Amplitude
***
8-br cGMP
8-br cGMP/Apamin
b
100
75
50
25
0
% Inhibition of Amplitude
8-br cGMP
8-br cGMP/Apamin

that the W/W^v mice, which lack the interstitial cells of Cajal in the myenteric plexus, had robust pacing only in LM but not in CM[27]. Our present experiments provide further evidence that the properties of pacing in the LM are different from CM. The addition of LNNA or ODQ increased the frequency of pacing in CM but not LM. These results suggest that only CM pacing is affected by an inhibitory tone exerted by the intrinsic inhibitory neurons.

Furthermore, the evoked inhibitory neuronal activities in CM and LM also differed. Although both LM and CM responded to EFS at different frequencies by initial relaxation, the relaxation continued only in CM, while in LM the relaxation was followed by contraction. This contraction in the LM, after block of muscarinic receptors, was previously shown to involve tachykinins[28]. In addition, only in CM was EFS followed by a rebound contraction or an "off-effect" especially at higher frequencies. The "off-effect" has been reported to result from the activation of chloride[29] and/or non-specific cation conductance[30] reset during the hyperpolarization induced by the EFS-released inhibitory mediators[31]. In LM, the "off-effect" was either masked by the contractile phase of the EFS-evoked response or lacking due to rapid reversal of the hyperpolarization by an excitatory mediator released in the later stages of EFS. The different configurations of the inhibitory responses in the CM and LM might indicate that the inhibitory mediators acting on either layer or the tissue response to them may differ.

In mouse small intestine, inhibitory motor neurons labeled for NOS and VIP were shown in the myenteric plexus and nerve terminals were found in CM but were not examined in LM[32]. A recent study[33] showed that the EFS- evoked relaxation in LM of mouse small intestine is mainly nitrergic. Under our experimental conditions, the EFS-evoked relaxation in LM was totally blocked by inhibition of NOS. We further showed that NO in LM acts mainly by the activation of soluble guanylate cyclase and the production of cGMP since ODQ abolished the EFS-induced relaxation in a manner similar to LNNA. However, in CM LNNA did not have a significant effect on the relaxation to EFS indicating that EFS-evoked relaxation in CM is less dependent on NO than in LM. In contrast to LM, the effect of ODQ on EFS-evoked relaxation in CM differed from that of LNNA. ODQ reduced the extent of EFS-evoked relaxation at higher frequencies and almost abolished it at the highest stimulation frequency, indicating that soluble guanylate cyclase may be activated by a mediator other than NO in CM of mouse small intestine.

Moreover, the addition of apamin did not affect the extent of EFS-evoked relaxation in CM. However, the combination of LNNA and apamin reduced the extent of EFS-evoked relaxation at all frequencies indicating that NO, ATP, and possibly pituitary adenylate cyclase-activating peptide, acting together, may play a role in the EFS-evoked relaxation in CM. A persistent fraction (>25%) of the EFS-evoked relaxation remained after treatment with the combination of LNNA and apamin in CM. These results, together with the effect of ODQ, indicate that there is a third type of neurotransmitter which acts with NO and apamin-sensitive mediators to produce full relaxation in BALB/c mouse CM.

VIP is considered to be an important inhibitory neurotransmitter in the enteric nervous system[34,35]. It was detected in mouse small intestinal nerves[32] and was reported to be responsible for LNNA resistant relaxation in the gastrointestinal tract[36]. Exogenous VIP produced relaxation of CM that was blocked by ODQ. This supports the possible involvement of VIP in the CM relaxation since the persistent relaxation which was blocked neither by LNNA nor apamin, was blocked by ODQ, as was the relaxation to exogenously added VIP. However, the guanylate cyclase-dependence of the residual relaxation in CM might reflect a role for carbon monoxide, another possible inhibitory mediator in the gut[14]. A possible role of carbon monoxide in mouse small intestine has yet to be established. In LM, the concentration of VIP used in CM (and up to twice as much higher concentration) did not elicit any appreciable relaxation, excluding a major role for VIP in the endogenous NANC relaxation of LM in mouse small intestine.

In addition to the effect of endogenous inhibitory mediators, we examined the differences in the response to the NO donor SNP, in CM and LM. Although the response to NO donors is not always the same as endogenous NO and is highly dependent on the chemical entity of the agent used[37], they help elucidate the intracellular processes involved in physiological responses. In LM both ODQ and apamin totally and almost equally abolished the relaxation due to SNP indicating that they most probably act on sequential steps in the signal transduction pathway downstream of the NO-like moiety released by SNP. To confirm this hypothesis, we examined the effect of apamin on 8-br cGMP, the membrane permeable analogue of cGMP. The prevention of the 8-br cGMP-mediated relaxation in LM by apamin indicated that the relaxation due to SNP proceeded by activating soluble guanylate cyclase to produce cGMP, which in turn acted on the small conductance calcium-activated potassium channel blocked by apamin[38], to produce relaxation. This was not the case in CM. ODQ reduced but did not abolish the relaxation to SNP, while apamin had no effect on either SNP or 8-br cGMP-mediated relaxation. These results indicate that there is a potential for variation in the mechanism of action of the same mediator between CM and LM layers of the mouse small intestine and that the same chemical signal can be transduced differently to the same end effect in both layers.

Taken together, our results suggest that there are differences in the inhibitory neurotransmitter profiles acting on the LM and CM layers of the mouse small intestine as examined in the BALB/c mouse with NO accounting for almost all the EFS-evoked inhibition in LM but not in CM. In addition, there is likely a difference in the mechanisms of action of the response to the same neurotransmitter indicating a possible difference in signal transduction mechanism between the two muscle layers.

3.5 References

1. Kunze WAA and Furness JB. The enteric nervous system and regulation of intestinal motility. *Annu Rev Physiol* 61: 117-142, 1999.
2. Furness JB. Types of neurons in the enteric nervous system. *J Auton Nerv Sys*. 81: 87-96, 2000.
3. Huizinga J, Berezin I, Daniel EE, and Chow E. Inhibitory innervation of colo-nic smooth muscle cells and interstitial cells of Cajal. *Can J Physiol Pharmacol* 68: 447-454, 1990.
4. Burns A, Lomax AEJ, Torihashi S, Sanders KM, Ward SM. Interstitial cells of Cajal mediate inhibitory neurotransmission in the stomach. *Proc Natl Acad Sci USA* 93: 12008-12013, 1996.
5. Gabella G. Innervation of the intestinal muscular coat. *J Neurocytol* 1: 341-362, 1972.
6. Holzer P. Ascending enteric reflex: multiple neurotransmitter systems and interactions. *Am J Physiol* 256: 540-545, 1989.
7. Costa M, Brookes SJH, Steele PA, Gibbins I, Burcher E, and Kandiah CJ. Neurochemical classification of myenteric neurons in guinea-pig ileum. *Neuroscience* 75: 949-967, 1996.
8. Brookes SJH, Steele PA, and Costa M. Identification and immunohistochemistry of cicular muscle motor neurons in guinea-pig small intestine. *Neuroscience* 42: 863-878, 1991.

9. Bult H, Boeckxstaens GE, Pelckmans PA, Jordaens FH, Van Maercke YM, and Herman AG. Nitric oxide as an inhibitory non adrenergic non cholinergic neurotransmitter. *Nature* 290: 581-582, 1990.

10. Burnstock G, Campbell G, Satchell D, and Smythe A. Evidence that adenosine triphosphate or a related nucleotide is the transmitter substance released by non-adrenergic inhibitory neurons in the gut. *Br J Pharmacol* 40: 668-688, 1970.

11. Xue L, Farrugia G, Sarr MG, and Szuszewski JH. ATP is a mediator of the fast inhibitory junction potential in human jejunal circular smooth muscles. *Am J Physiol* 276: G1373-G1376, 1999.

12. Goyal RK and Rattan RS. VIP as a possible neurotransmitter in the non-cholinergic non-adrenergic inhibitory neurons. *Nature* 288: 378-380, 1980.

13. Schworer H, Katsoulis H, Creutzfeldt W, and Schmidt WE. Pituitary adenylate cyclase activiating peptide, a novel VIP-like gut-brain paptide, relaxes guinea-pig taenia caeci via apamin-sensitive potassium channels. *Naunyn Schmiedebergs Arch Pharmacol* 346: 511-514, 1992.

14. Rattan RS and Chakder S. Inhibitory effects of CO on internal anal sphincter: heme-oxygenase inhibitor inhibits NANC relaxation. *Am J Physiol* 265: G799-G804, 1993.

15. Sanders KM. Post-junctional electrical mechanisms of neurotransmission. *Gut* 47: 23-25, 2000.

16. Jury J, Boev K, and Daniel EE. Nitric oxide mediates outward potassium currents in opposum esophageal circular smooth muscle. *Am J Physiol* 270: G932-G938, 1996.

17. Crist JR, He XD, and Goyal RK. Chloride-mediated junction potentials in circular muscles of guinea-pig ileum. *Am J Physiol* 261: G742-G751, 1991.

18. Spencer N, Walsh M, and Smith TK. Does the guinea-pig ileum obey the 'law of the intestine'? *J Physiol* 517: 889-898, 1999.

19. Smith TK and Robertson WJ. Synchronous movement of the longitudinal and circular muscle during peristalsis in the isolated guinea-pig distal colon. *J Physiol* 506: 563-567, 1998.

20. Spencer NJ and Smith TK. Simultaneous intracellular recordings from longitudinal and circular muscles during the peristaltic reflex in guinea-pig distal colon. *J Physiol* 533: 787-799, 2001.

21. Daniel EE, Boddy G, Bong A, and Cho WJ. A new model of pacing in the mouse intestine. *Am J Physiol* 286: G253-G262, 2004.

22. Boddy G, Bong A, Cho WJ, and Daniel EE. ICC pacing mechanisms in intact mouse intestine differ from those in cultured or dissected tissue. *Am J Physiol* 286: G653-G662, 2004.

23. Spencer NJ, Hening GW, and Smith TK. Stretch activated neuronal pathways to longitudinal and circular muscle in guinea-pig distal colon. *Am J Physiol* 284: G231-G241, 2003.

24. Sanders KM. A case for interstitial cells of Cajal as pacemakers and media-tors of neurotransmission in the gastrointestinal tract. *Gastroenterology* 111: 492-515, 1996.

25. Cheung DW and Daniel EE. Comparative study of smooth muscle layers of rabbit duodenum. *J Physiol* 309: 13-27, 1980.

26. Hara Y, Kubota M, and Szurszewski JH. Electrophysiology of smooth muscles of the small intestine of some mammals. *J Physiol* 372: 501-520, 1986.

27. Boddy G and Daniel EE. Role of L-type Ca^{2+} channels in intestinal pacing in wild-type and W/W^{v} mice. *Am J Physiol* 288: G439-G446, 2005.

28. Zizzo MG, Mulé F, and Serio R. Tachkinergic neurotransmission is enhanced from duodenum from dystrophic (mdx) mice. *Br J Pharmacol* 145: 334-341, 2005.

29. Crist JR, He XD, and Goyal RK. Chloride mediated inhibitory junction potentials in opossum esophageal circular smooth muscle. *Am J Physiol* 261: G752-G792, 1991.

30. Inoue R. Effects of external Cd^{2+} and other divalent cations on carbachol-activated non-selective cation channels in guinea-pig ileum. *J Physiol* 442: 447-463, 1991.

31. Baker SA, Mutafova-Yambolieva V, Monaghan K, Horowitz B, Sanders KM, and Koh SD. Mechanism of active repolarization of inhibitory junction potential in murine colon. *Am J Physiol* 285: G813-G821, 2003.

32. Sang Q and Young HM. Chemical coding of neurons in the myenteric plexus and external muscle of small and large intestine of the mouse. *Cell Tissue Res* 284: 39-53, 1996.

33. Ueno T, Duenes JA, Zaroug AE, and Sarr MG. Nitrergic mechanisms mediating inhibitory control of longitudinal smooth muscle contraction in mouse small intestine. *J Gastrointest Surg* 8: 831-841, 2004.

34. Bryant MG, Polak MM, Modlin I, Bloom SR, Albuquerque RH, and Pearse AG. Possible dual role for vasoactive intestinal peptide as gastrointestinal hormone and neurotransmitter substance. *Lancet*. 1: 991-993, 1976.

35. Lundberg JM. Pharmacology of co-transmission in the autonomic nervous system: integrative aspects on amines, neuropeptides, adenosine triphosphate, aminoacids, and nitric oxide. *Pharmacol Rev* 48: 113-178, 1996.

36. Takashi T and Owyang C. Vagal control of nitric oxide and vasoactive intesti-nal peptide release in the regulation of gastric relaxation in rat. *J Physiol* 484: 481-492, 1995.

37. Tanovic A, Jiminez M, Fernandez E. Actions of NO donors and endo-genous nitrergic transmission on longitudinal muscle of rat ileum: mechanisms involved. *Life Sci* 69: 1143-1154, 2001.

38. Matsuda NM, Miller SM, Sha L, Farrugia G, and Szuszewski JH. Mediators of non adrenergic non cholinergic neurotransmission in porcine jejunum. *Neurogastroenterol Motil* 16: 605-611, 2004.

CHAPTER IV

CAVEOLIN-1 KNOCKOUT ALTERS THE RESPONSE TO NO IN MOUSE SMALL INTESTINE

Versions of this chapter have been published. El-Yazbi AF, Cho WJ, Boddy G and Daniel EE. Caveolin-1 gene knockout impairs nitrergic function in mouse small intestine. *Br J Pharmacol* 145: 1017-1026, 2005, and El-Yazbi AF, Cho WJ, Boddy G, Schulz R, and Daniel EE. Impact of caveolin-1 knockout on NANC relaxation in circular muscles of the mouse small intestine compared with the longitudinal muscles. *Am J Physiol* 290: 394-403, 2006.

4.1 Introduction:

Inhibitory motor neurons of the myenteric plexus play an important role in the control of gut motility. They mediate most of the inhibitory responses in the GIT and control many physiological reflexes *e.g.* relaxation of the lower esophageal sphincter after swallowing, receptive relaxation of the proximal stomach during eating, and descending inhibition in response to distention[1]. The main inhibitory neurotransmitter in the gut is NO[2], in addition to ATP[3,4], VIP[5], pituitary adenylate cyclase activating peptide[6], and carbon monoxide[7].

In the small intestine, smooth muscle relaxation is often achieved by evoking inhibitory junction potentials[8,9,10]. These result from a direct or an indirect activation of potassium (K^+) and/or chloride (Cl^-) channels[9,11]. Several intracellular mediators *e.g.* cGMP, cAMP, and intracellular calcium, have been reported to be involved in the indirect effect of the inhibitory neurotransmitters on K^+ and Cl^- channels[12,13,14]. Signaling proteins that are involved in the production and regulation of these mediators such as heterotrimeric G proteins, protein kinase C isoforms, and NOS isoforms have been reported to bind to caveolin-1[15,16,17,18]. Accordingly, caveolin(s) may play a role in regulating inhibitory responses to neurotransmitters via the control of the function or formation of the aforementioned intracellular mediators.

In mouse intestine, studies in our laboratory have shown that the disruption of caveolae and caveolin-1 in smooth muscles and ICC with methyl-β-cyclodextrin reduced pacing frequencies and inhibited paced contractions[19]. This suggests the importance of caveolin-1 and caveolae in the control of mouse gut motility. In addition, *mdx* mice that lack dystrophin- a membrane complex closely associated with caveolin[20], showed defective responses to endogenous and exogenous NO[21]. Thus we hypothesize that the absence of caveolin-1 will affect the response to NO in mouse small intestine, where NO is involved as an inhibitory neurotransmitter in all regions of the gut[22,23].

4.2 Materials and methods:

4.2.1 Functional studies:

Tissues from cav1$^{+/+}$ and cav1$^{-/-}$ were set up to record CM and LM contractile activity as described in Chapter II. The effects of the different pharmacological agents used were studied similar to the protocol described in Chapter III. Data analysis and statistics were done as described in Chapter II.

4.2.2 Electron microscopy:

Electron microscopy was done as described in Chapter II.

4.2.3 Immunohistochemical studies:

Cryosections and whole mount preparations were prepared as described in Chapter II. Cryosections were stained with mouse anti-caveolin-1 and mouse anti-caveolin-3 as primary antibodies at a concentration of 1:100. Rabbit anti-subunit α_2 of soluble guanylate cyclase (1:100) was used with mouse anti-caveolin-1 for double staining of cryosections. Cy3 conjugated donkey anti-mouse IgG and Alexa 488-conjugated goat anti-rabbit were used as secondary antibodies. Whole mount preparations were either double immunostained with rabbit anti-nNOS with NH_2-terminal epitope (1:100) and mouse anti-HuC/D (1:200) or single stained with rabbit anti-vimentin (used undiluted). Cy3 conjugated donkey anti-mouse IgG and Alexa Fluor® 488-conjugated goat anti-rabbit IgG were used as secondary antibodies. Confocal imaging was done as described in Chapter II.

4.2.4 Western blotting:

Sample preparation, membrane fractionation and immunoblotting were performed as described in Chapter II. Mouse anti-caveolin-1 (1:1000), rabbit anti-PDE5 (1:500, in some experiments saturated with tenfold higher concentration of antigenic peptide), and rabbit anti-subunit α_2 of soluble guanylate cyclase (1:500) were used as primary antibodies. HRP-conjugated goat anti-mouse IgG (1:4000) and HRP-conjugated goat anti-rabbit IgG (1:4000) were used as secondary antibodies. Quantification of the blots was done by measuring the band density using ImageJ software and determining the ratio to actin as a loading control in case of whole tissue homogenate. Rabbit anti-actin was used as a primary antibody (1:500) for that purpose.

4.2.5 Measurement of PDE5 activity:

The total PDE activity in $cav1^{+/+}$ and $cav1^{-/-}$ intestinal tissue homogenates was measured using a method adapted (*A Holt-personal communication*) from a previously described procedure[24]. Tissue homogenates were prepared as described in Chapter II. Aliquots of the diluted homogenates containing 10 µg proteins were incubated with a mixture of cold and radioactive cGMP (100 μM total cGMP concentration) containing16.5 nCi of radioactivity in a reaction buffer (pH 7.5) consisting of: TES (150 mM), soybean trypsin inhibitor (300 μg/ml), ovalbumin (600 μg/ml), $MgCl_2$ (6 mM), $CaCl_2$ (150 μM). The incubation lasted for 60 min at 37°C in a shaking water bath. Six concentrations of PDE5 inhibitor II ranging from 3 nM to 1 μM separated by half log units were added to the reaction mixture prior to the addition of the tissue homogenates. Homogentes from three different $cav1^{+/+}$ and three different $cav1^{-/-}$ were used for the reaction. Following the incubation, the reaction was stopped by the addition of 100 μl of 0.25 M HCl. The acid was neutralized by 100 μl NaOH (0.25 M) containing Tris (0.1 M, pH 8.2). 50 μl of rattle snake venom (1 mg/ml) was then added and the mixture was incubated once more at 37°C for 10 min to breakdown the radiolabelled GMP produced from the phosphodiesterase reaction into guanosine. The produced guanosine was then separated from any remaining cGMP on DEAE-sephacel ion exchange columns. The radioactivity of the solution drained out of the columns was measured using a Beckman LS6500 scintillation counter (Beckman Coulter Inc., Fullerton, CA). The measured disintegrations per minute value was used as an indication of the PDE activity. Background, blank (containing radioactive cGMP and no tissue), and total radioactivity controls were counted alongside with the samples.

4.2.6 *Materials:*

PDE5 inhibitor II was purchased from Calbiochem (San Diego, CA). The mouse anti-caveolin-1 and mouse anti-caveolin-3 were from BD Biosciences (Mississauga, ON). The rabbit anti-rat nNOS with NH_2-terminal epitope was from Euro-Diagnostica (Malmö, Sweden). The mouse anti-HuC/HuD neural protein and Alexa Fluor® 488 goat anti-rabbit IgG were from Molecular Probes (Burlington, ON). The rabbit anti-vimentin and rabbit anti-subunit α_2 of soluble guanylate cyclase were from Abcam, Inc. (Cambridge, MA). Cy3 conjugated donkey anti-mouse IgG was from Jackson ImmunoResearch Laboratories, Inc. (West Grove, PA). Rabbit anti-PDE5 and its antigenic peptide were from Fabgennix, Inc. (Frisco, TX). Rabbit anti-actin was from Santa Cruz Biotechnology, Inc. (Santa Cruz, CA). [^{3}H]-labelled cGMP was purchased from GE Healthcare (Piscataway, NJ). cGMP, TES, ovalbumin, soybean trypsin inhibitor, Tris, rattle snake venom, and DEAE-sephacel were purchased from Sigma (Oakville, ON).

PDE5 inhibitor II was dissolved in dimethyl sulfoxide to prepare a stock solution. Fresh dilutions were prepared before the experiment by tenfold dilution of the dimethyl sulfoxide stock with double distilled water. Dimethyl sulfoxide, in the amounts equivalent to that of the maximum drug concentration used (1 μl in a 10 ml bath), did not affect the functional activity of the tissue.

4.3 Results:

4.3.1 Electron microscopy:

In contrast to control mice, where smooth muscle cells and ICC showed abundant caveolae, electron micrographs of CM and LM layers from cav1$^{-/-}$ mice showed that caveolae were completely absent in LM (Fig 4.1a). In CM, the number of caveolae

Fig 4.1 Electron microscope images of LM (a) and CM (b) of cav1$^{+/+}$ and cav1$^{-/-}$ small intestine. a. Note the total absence of the flask-shaped caveolae on the plasma membrane of the LM cells of Cav1$^{-/-}$. Caveolae are indicated by solid arrow-heads. b. Note the total absence of caveolae in the inner circular muscle layer (ICM) in cav1$^{-/-}$, while a smaller number of caveolae appear in outer circular muscle (OCM) labeled by arrowheads. Small endoplasmic reticulum profiles (marked with thick arrows) and sarcoplasmic reticulum (marked with thin arrows) remain. ICC of the deep muscular plexus are labeled as ICC, mitochondria as M, nerves as N, fibroblasts as Fib, large granular vesicles as lgv, and small granular vesicles as sgv. Scale bar is 1 μm except for cav1$^{+/+}$ CM scale bar is 2 μm (electron microscopy was done by Woo Jung Cho).

Fig 4.1

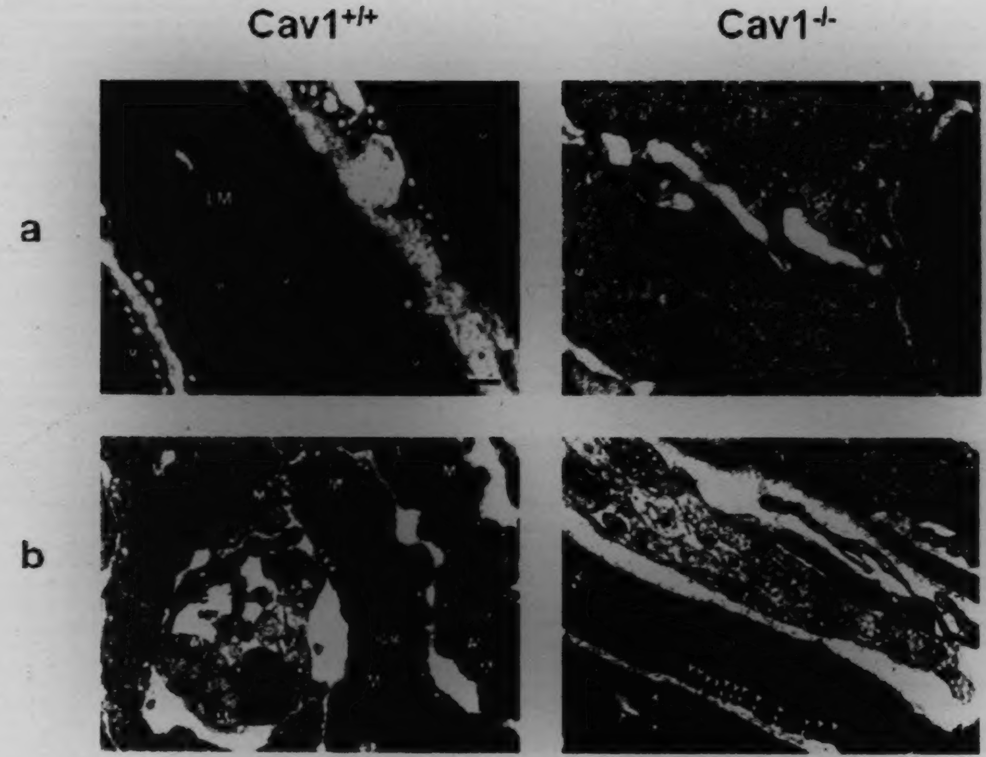
Cav1+/+
Cav1-/-
a
LM
b

was much reduced compared to the control tissue. Caveolae were confined to the outer CM and was absent in the inner CM (Fig 4.1b).

4.3.2 Immunohistochemical studies:

4.3.2.1 Immunohistochemical staining in cryosections:

Cryosections stained with caveolin-1 antibody showed lack of caveolin-1 immunoreactivity in smooth muscle cells and ICC of cav1$^{-/-}$ mice (Fig. 4.2a). Caveolin-1 immunoreactivity in cav1$^{+/+}$ tissues appeared as punctate staining in the periphery of smooth muscle cells and ICC (Fig 4.2a). Similarly, in cryosections stained with anti-caveolin-3, caveolin-3 immunoreactivity appeared in punctate sites in the periphery of smooth muscle cells in CM from cav1$^{+/+}$ mice (Fig 4.2b). In cav1$^{-/-}$ tissue, caveolin-3 immunoreactivity appeared in the outer CM layer (Fig 4.2b).

Cryosections with double immunostaining for caveolin-1 and soluble guanylate cyclase showed no colocalization of the two proteins in the cav1$^{+/+}$ tissue. While caveolin-1 appeared in punctate sites in the plasma membrane, soluble guanylate cyclase appeared mainly in the cytoplasm. Soluble guanylate cyclase was also in the cytoplasm in cryosections from cav1$^{-/-}$ tissues (Fig 4.2c).

4.3.2.2 Single immunohistochemical staining in whole mount preparations:

To examine the presence and distribution of myenteric plexus ICC, single staining with anti-vimentin, which recognizes vimentin filaments characteristically present in ICC[25], of whole mount preparations of jejunal tissue from cav1$^{+/+}$ and cav1$^{-/-}$ mice

Fig 4.2 Cryosections from cav1$^{+/+}$ and cav1$^{-/-}$ small intestine stained for caveolin-1 (a), caveolin-3 (b), and doubly stained for caveolin-1 and soluble guanylate cyclase (c). a. Note the total absence of caveolin-1 immunoreactivity in the cav1$^{-/-}$ tissue. b. Caveolin-3 immunoreactivity persists in the outer circular muscle layer of cav1$^{-/-}$ tissue. c. Immunostaining of caveolin-1 (red) and soluble guanylate cyclase (green) shows that they are not colocalized (no yellow colour in the merged image. cm, circular muscle layer; lm, longitudinal muscle layer. Scale bars are 5 µm (immunostaining and confocal imaging were done by Woo Jung Cho).

Fig 4.2

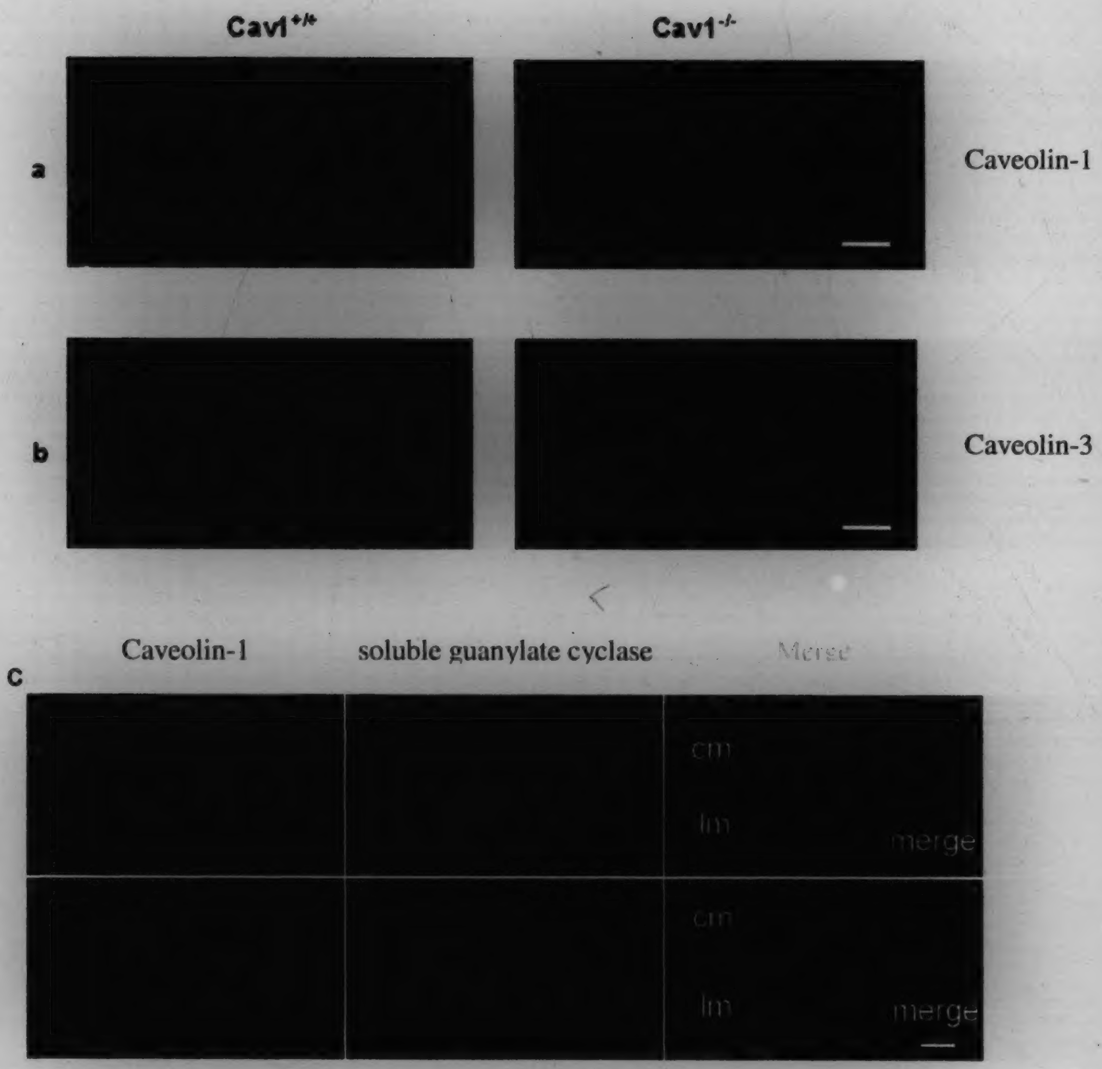
Cav1$^{+/+}$
Cav1$^{-/-}$
a
Caveolin-1
b
Caveolin-3
c
Caveolin-1
soluble guanylate cyclase
Merge
cm
lm
merge
cm
lm
merge

was done. It showed that the myenteric plexus ICC were equally present and similarly distributed in the small intestine of $cav1^{+/+}$ and $cav1^{-/-}$ strains (Fig 4.3a and 4.3b).

4.3.2.3 Double immunohistochemical staining in whole mount preparations:

This technique was used to quantify the differences in the expression of nNOS in the myenteric neurons of $cav1^{-/-}$ and $cav1^{+/+}$ mice (Fig 4.4). The number of cells showing specific staining with human neuronal protein HuC/D antibody, which recognizes the cytoplasm and the nucleus of myenteric neurons[26, 27], was considered to be the total number of myenteric neurons. The percentage of myenteric neurons expressing nNOS was determined separately by two individuals in the myenteric ganglia of $cav1^{+/+}$ and $cav1^{-/-}$ mice. Only cells with immunostaining in their cytoplasm brighter than glial cells and background staining were counted. The numbers of myenteric plexus ganglia examined were 8 in $cav1^{+/+}$ and 13 in $cav1^{-/-}$. Out of a total of 123 nerve cells examined in $cav1^{-/-}$, 78.9% showed nNOS immunoreactivity. While only 63.1% of 84 nerve cells showed nNOS immunoreactivity in $Cav1^{+/+}$ myenteric ganglia. The results indicate an increase in the percentage of myenteric neurons expressing nNOS in $cav1^{-/-}$ (*two-sided P-value = 0.0172 in contingency analysis*).

4.3.3 Functional studies:

4.3.3.1 Spontaneous activity:

The amplitudes of the spontaneous muscle contractions in LM and CM in $cav1^{+/+}$ and $cav1^{-/-}$ were measured at the end of the equilibration period. For LM, the values

Fig 4.3 Myenteric ganglia (MG) in whole mount preparations from cav1$^{+/+}$ (a) and cav1$^{-/-}$ (b) stained for vimentin (green). Myenteric ICC stained by anti-vimentin are marked by asterisks. Note the similar distribution of ICC in cav1$^{+/+}$ and cav1$^{-/-}$ preparations. Scale bar is 20 µm (immunostaining and confocal imaging were done by Woo Jung Cho).

Fig 4.3

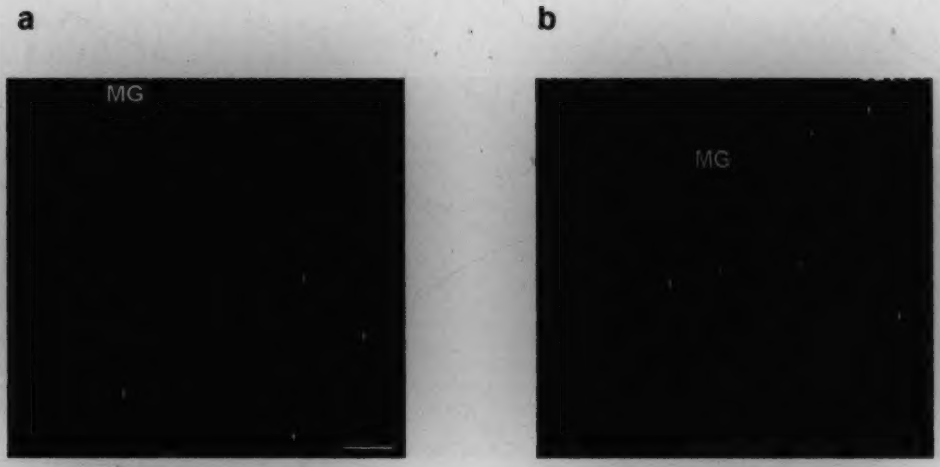

Fig 4.4 Myenteric ganglia in whole mount preparations from cav1$^{+/+}$ (a) and cav1$^{-/-}$ (b) stained for HuC/D protein (red) and nNOS (green). The cell bodies and cytosol of nNOS expressing neurons appear in yellow. Scale bar is 20 µm (immunostaining and confocal imaging were done by Woo Jung Cho).

Fig 4.4

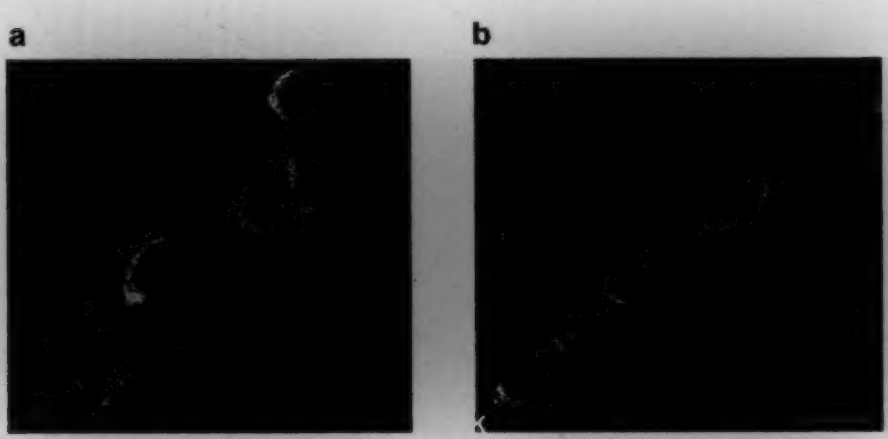

in mg tension were 129.3±17.9 for Cav1$^{+/+}$ (*n*=11), and 130.2±11.6 for Cav1$^{-/-}$ (*n*=18). For CM, the values in mg tension were 237.7±29.6 for cav1$^{+/+}$ (*n*=10) and 216.0±33.2 for cav1$^{-/-}$ (*n*=10). Statistical analysis (*t*-test) showed that there were no significant differences between the amplitudes of the spontaneous contractions in the two mice strains.

On the other hand, the spontaneous frequency of pacing was higher in CM of cav1$^{-/-}$ jejunum compared to cav1$^{+/+}$ (Fig 4.5a). Since there is a gradient in the frequency of pacing along the mouse small intestine[19], the frequency measurements were all done in the mid-jejunum in both strains. The frequency of pacing significantly increased in cav1$^{+/+}$ tissues treated with LNNA (100 μM) or ODQ (1 μM) but not in those from cav1$^{-/-}$ mice (Fig 4.5b). After blockade of NO production or action, all frequencies became the same. In LM, the frequency of pacing was similar in both strains and was neither affected by LNNA nor ODQ.

4.3.3.2 Effects of LNNA and ODQ on EFS-induced relaxation:

In LM, EFS elicited a transient relaxation in both strains, which increased in magnitude as the stimulation frequency was increased to reach a maximum at 10 Hz. Both strains showed relaxations of comparable magnitudes (no significant differences). In cav1$^{+/+}$, inhibiting NOS function with 100 μM LNNA abolished EFS-evoked relaxations at all stimulation frequencies (Fig 4.6b). On the contrary, in cav1$^{-/-}$ LNNA only reduced the relaxations at 1 and 3 Hz stimulations and had no significant effect on the relaxations at 10 and 30 Hz (Fig 4.6b).

Fig 4.5 Frequency of the spontaneously-paced contractions in CM of $cav1^{+/+}$ and $cav1^{-/-}$ small intestine. a. The frequency of pacing is higher in $cav1^{-/-}$ CM. b. The frequency of pacing increases after treatment with LNNA (100 µM) or ODQ (1 µM) in $cav1^{+/+}$ but not in $cav1^{-/-}$. Statistical significance was determined by *t*-test for (a) and ANOVA followed by Bonferroni *post hoc* test for (b) and denoted by $*P<0.05$ and $**P<0.01$. *n* values were 9 for control $cav1^{+/+}$ and $cav1^{-/-}$ tissues and 7 for LNNA- and ODQ-treated tissues.

Fig 4.5

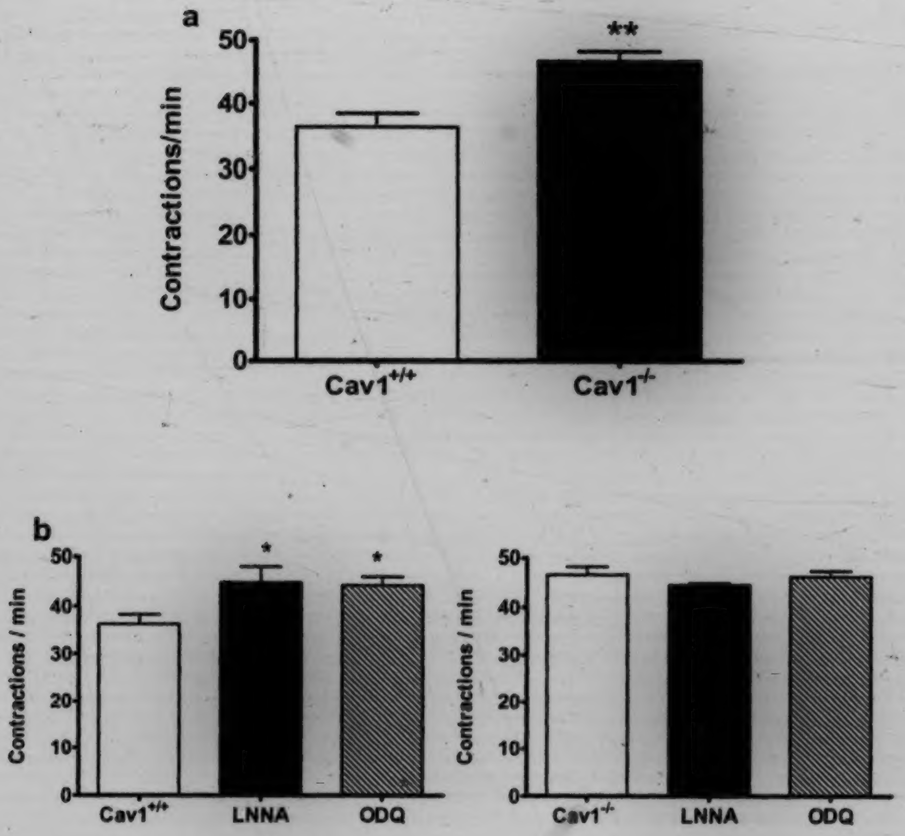
a
Contractions/min
0
10
20
30
40
50
**
Cav1$^{+/+}$
Cav1$^{-/-}$
b
Contractions / min
0
10
20
30
40
50
*
*
Cav1$^{+/+}$
LNNA
ODQ
Contractions / min
0
10
20
30
40
50
Cav1$^{-/-}$
LNNA
ODQ

Fig 4.6 Effect of LNNA (100 μM) on EFS-induced relaxation in the presence of atropine (10^{-7} M), prazosin (10^{-6} M), and timolol (10^{-6} M) in LM (a and b) and CM (c) of cav1$^{+/+}$ and cav1$^{-/-}$ small intestine. a. Representative tracings of the effect of LNNA (100 μM) on EFS-induced relaxation in LM at 10 Hz. b. The effect at all stimulation frequencies in LM on EFS-induced relaxation before and after adding LNNA to the same tissue. c. The effect at all stimulation frequencies in CM demonstrated as the difference in EFS-induced relaxation between LNNA-treated and control tissues. Statistical significance was measured by ANOVA followed by Bonferroni test and is denoted by *$P<0.05$, **$P<0.01$, and ***$P<0.001$. *n* values were 11 and 9 for cav1$^{-/-}$ LM and CM, and 6 for cav1$^{+/+}$ LM and CM.

Fig 4.6

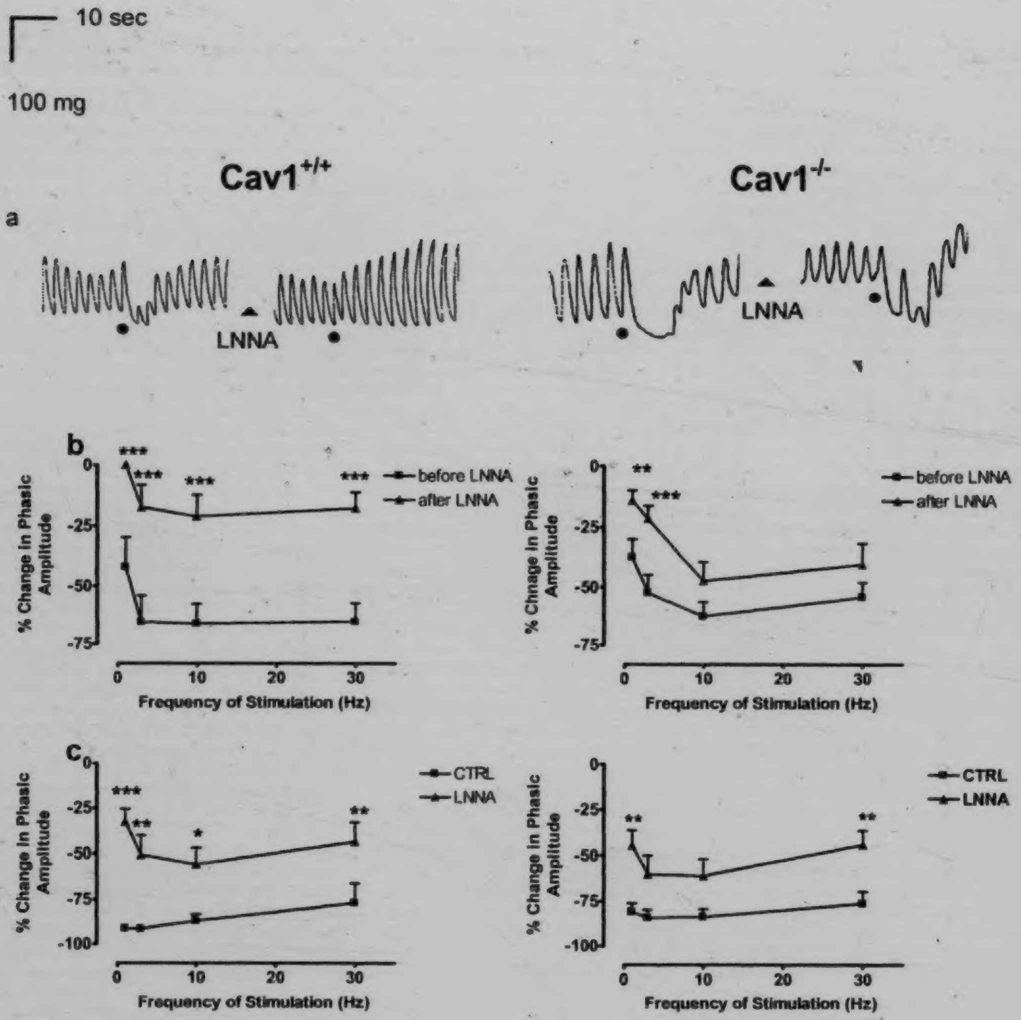
10 sec
100 mg
Cav1+/+
Cav1-/-
a
LNNA
LNNA
b
% Change in Phasic Amplitude
0
-25
-50
-75
***
***
***
***
before LNNA
after LNNA
**
***
Frequency of Stimulation (Hz)
0
10
20
30
c
0
-25
-50
-75
-100
***
**
*
**
CTRL
LNNA
**
**
Frequency of Stimulation (Hz)

In CM, EFS produced muscle relaxation that lasted for as long as the stimulus continued in most experiments. The relaxation was maximal at 3 Hz (Fig 4.6c). There were no significant differences in the extent of relaxation exhibited by both strains. The relaxation due to EFS was followed by a rebound contraction (or an "off-effect") in cav1$^{+/+}$ at higher frequencies. Cav1$^{-/-}$ CM segments did not show this "off-effect" at any frequency. This difference, measured at 30 Hz, was significant (data not shown). Inhibiting NOS activity by 100 μM LNNA significantly reduced the extent of EFS-induced relaxation in the Cav1$^{+/+}$ control strain at all stimulation frequencies (Fig 4.6c). In Cav1$^{-/-}$, the effect of LNNA was inconsistent and was only significant at 1 and 30 Hz (Fig 4.6c). Inhibition of soluble guanylate cyclase with ODQ (1 μM) had a similar effect to LNNA in LM and CM in both strains (data not shown).

4.3.3.3 Response to SNP:

In LM, the exogenous NO donor, SNP (100 μM), produced a reduction in the amplitude of the phasic contractions. The magnitude of SNP-induced inhibition was greater in cav1$^{+/+}$ compared to cav1$^{-/-}$ tissues. Both ODQ (1 μM) and apamin (1 μM) abolished the relaxant phase in the response to SNP in both strains (Fig 4.7a).

In CM, SNP produced a reduction in the amplitude of phasic contractions. The reduction was also higher in cav1$^{+/+}$ compared to cav1$^{-/-}$. ODQ (1 μM) reduced the inhibition due to SNP only in cav1$^{+/+}$ tissues, while apamin (1 μM) did not have any effect on the inhibition due to SNP in CM (Fig 4.7b).

Fig 4.7 Relaxation due to SNP (100 µM) in LM (a) and CM (b) of cav1$^{+/+}$ and cav1$^{-/-}$ and the effects of ODQ (1 µM) and apamin (1 µM) on this relaxation. Statistical significance is denoted by ****P*<0.001(ANOVA followed by Bonferroni for comparison of the different treatments), ##*P*<0.01, and ###*P*<0.001 (*t*-test comparison to the corresponding cav1$^{+/+}$). *n* values were 12 for control cav1$^{-/-}$ LM tissues and 6 for all other experiments.

Fig 4.7

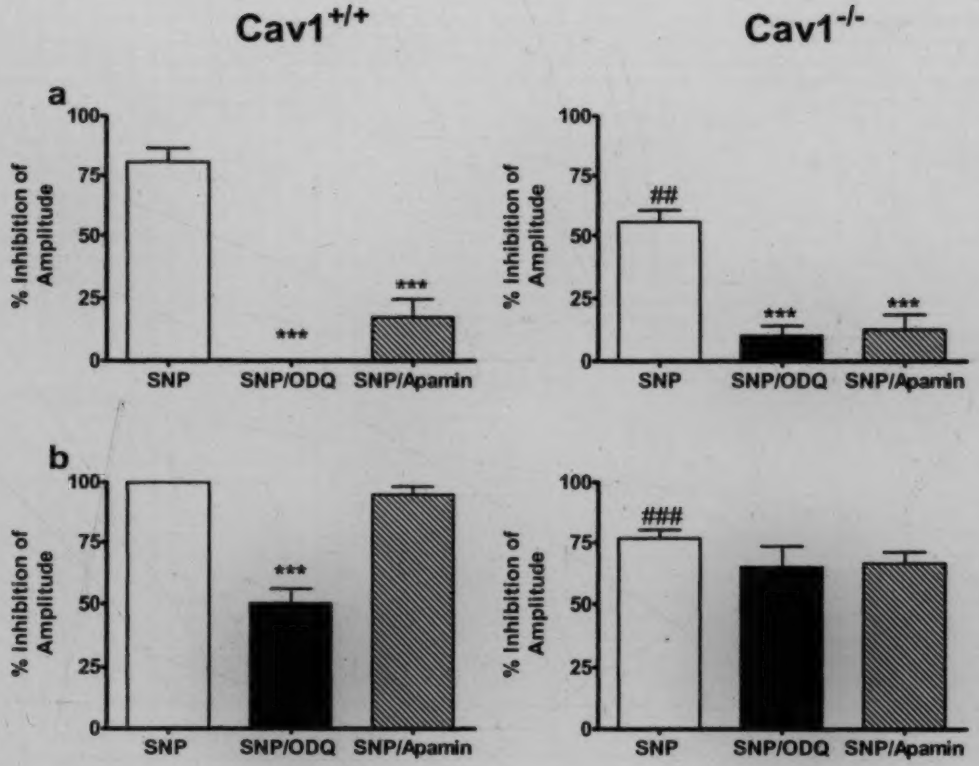
Cav1+/+
Cav1-/-
a
b
% Inhibition of Amplitude
100
75
50
25
0
SNP
SNP/ODQ
SNP/Apamin
***
##
###

4.3.3.4 Response to 8-br cGMP in LM:

8-br cGMP (100 µM), a plasma-membrane permeable analogue of the second messenger cGMP, produced a reduction in the amplitude of contraction of the muscle. There were no significant differences among the magnitudes of 8-br cGMP-induced inhibitions in cav1$^{-/-}$ mice and the cav1$^{+/+}$ tissues (data not shown).

4.3.3.5 Effects of LNNA on EFS-induced relaxation and response to SNP in LM in presence of PDE5 inhibitor II:

In presence of PDE5 inhibitor II (1 µM), LNNA significantly decreased the EFS-evoked relaxation in cav1$^{-/-}$ (Fig 4.8a) as the extent of inhibition of amplitude in response to EFS increased before the addition of LNNA. In addition, only in cav1$^{-/-}$ tissues were the responses to SNP in presence of PDE5 inhibitor II significantly higher than the responses obtained with SNP alone (Fig 4.8b).

4.3.3.6 Effects of apamin and apamin/LNNA combination on EFS-induced relaxations:

In LM, apamin (1 µM), caused a significant reduction in the magnitudes of EFS-induced relaxations at all stimulation frequencies in cav1$^{-/-}$ mice (Fig 4.9a). In cav1$^{+/+}$ control mice, the effect of apamin on the magnitude of EFS-induced relaxation was smaller and more variable resulting in it to be statistically insignificant except at the stimulation frequency of 30 Hz (Fig 4.9a). In cav1$^{-/-}$, a combination of LNNA and apamin abolished the EFS-evoked relaxation at 1 and 3 Hz. However, residual

Fig 4.8 Effect of PDE5 inhibitor II (1 µM) on LNNA (100 µM) blockade of EFS-evoked relaxation (effect before and after LNNA in the same tissue) (a) and SNP (100 µM)-produced relaxation (b) in $cav1^{+/+}$ and $cav1^{-/-}$ LM. Statistical significance was determined by ANOVA followed by Bonferroni test for (a) and t-test for (b) and is denoted by $^{***}P<0.001$. *n*-values were 12 for SNP-treated $cav1^{-/-}$ tissue and 6 for all other experiments.

Fig 4.8

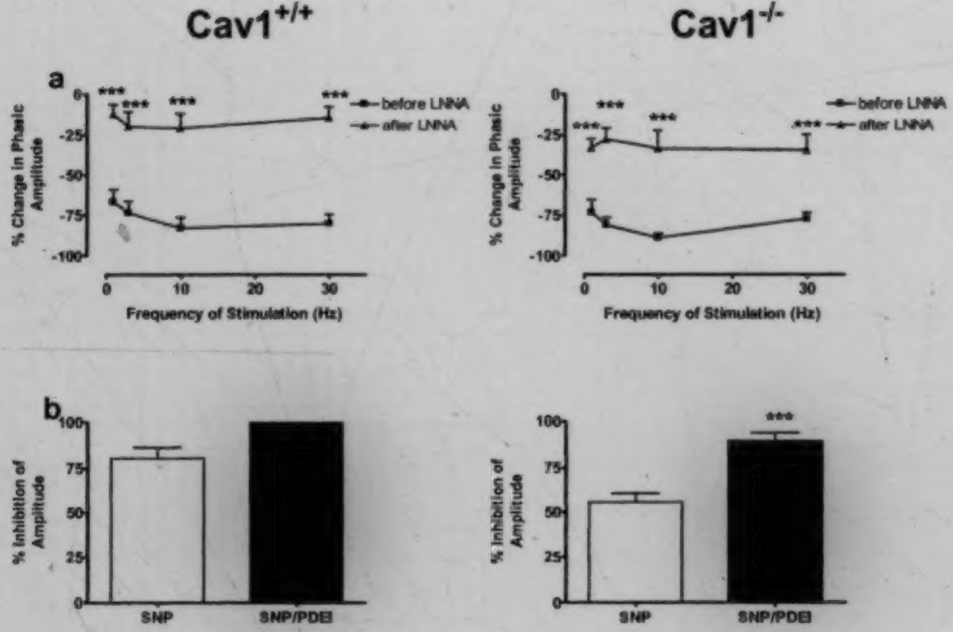
Cav1$^{+/+}$
Cav1$^{-/-}$
a
b
% Change in Phasic Amplitude
Frequency of Stimulation (Hz)
before LNNA
after LNNA
***
0
-25
-50
-75
-100
0
10
20
30
% Inhibition of Amplitude
100
75
50
25
0
SNP
SNP/PDEI

Fig 4.9 Effect of apamin (1 μM) on EFS-induced relaxation in LM (a) and CM (b) of cav1$^{+/+}$ and cav1$^{-/-}$ small intestine. The effect is compared between apamin-treated and control tissues. Statistical significance was measured by ANOVA followed by Bonferroni test and is denoted by **P*<0.05, ***P*<0.01, and ****P*<0.001. *n* values were 6 for experiments on LM and 7 for experiments on CM.

Fig 4.9

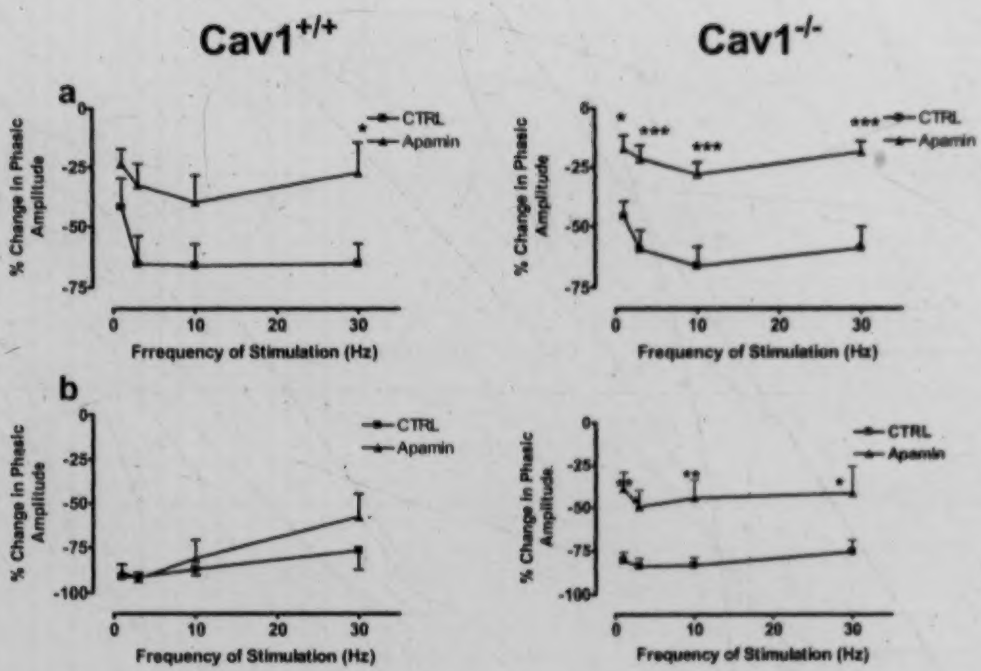
Cav1+/+
Cav1-/-
a
b
% Change in Phasic Amplitude
0
-25
-50
-75
-100
Frrequency of Stimulation (Hz)
Frequency of Stimulation (Hz)
0
10
20
30
CTRL
Apamin
*
***
**

inhibitions of -16.0% ± 3.0 and –22.3% ± 4.1 persisted at 10 and 30 Hz, respectively (*n*=6).

In CM, 1 μM apamin led to a significant reduction of the extent of EFS-evoked relaxation at all frequencies in cav1$^{-/-}$ (Fig 4.9b). In cav1$^{+/+}$, apamin did not affect the extent of relaxation (Fig 4.9b). A combination of LNNA (100 μM) and apamin (1 μM) almost abolished the EFS-induced relaxation in cav1$^{+/+}$ and cav1$^{-/-}$.

4.3.4 Western blotting:

The expression of soluble guanylate cyclase and PDE5 was examined by Western blotting in the caveolae/lipid raft-enriched membrane fraction of the small intestinal tissue in cav1$^{+/+}$ and cav1$^{-/-}$. Soluble guanylate cyclase was not present in this fraction in either strain (data not shown). However, the amount of PDE5 detected in this fraction was higher in cav1$^{+/+}$ tissues than in cav1$^{-/-}$ (Fig 4.10a). The total amount of PDE5 expressed in the whole tissue homogenate was examined, and was found to be similar in both strains when compared to actin as a loading control (Fig 4.10b). Membranes treated with the saturated PDE5 antibody did not show any bands (data not shown).

4.3.5 Measurement of PDE activity:

The total cGMP degradation was not found to be different in cav1$^{+/+}$ and cav1$^{-/-}$ tissue homogenates. There was a concentration dependent inhibition of the cGMP breakdown activity when the PDE5 inhibitor II was added that leveled off in the range between 300 nM and 1 μM inhibitor concentration (data not shown). There was

Fig 4.10 Expression of PDE5 in caveolae/lipid raft-enriched membrane fraction (a) and whole tissue homogenate (b) from $cav1^{+/+}$ and $cav1^{-/-}$ small intestine. PDE5 band densities were quantified by ImageJ software. Statistical significance was determined by *t*-test and denoted by $^{**}P<0.01$. *n* values were 3 for $cav1^{+/+}$ and $cav1^{-/-}$ in both experiments.

Fig 4.10

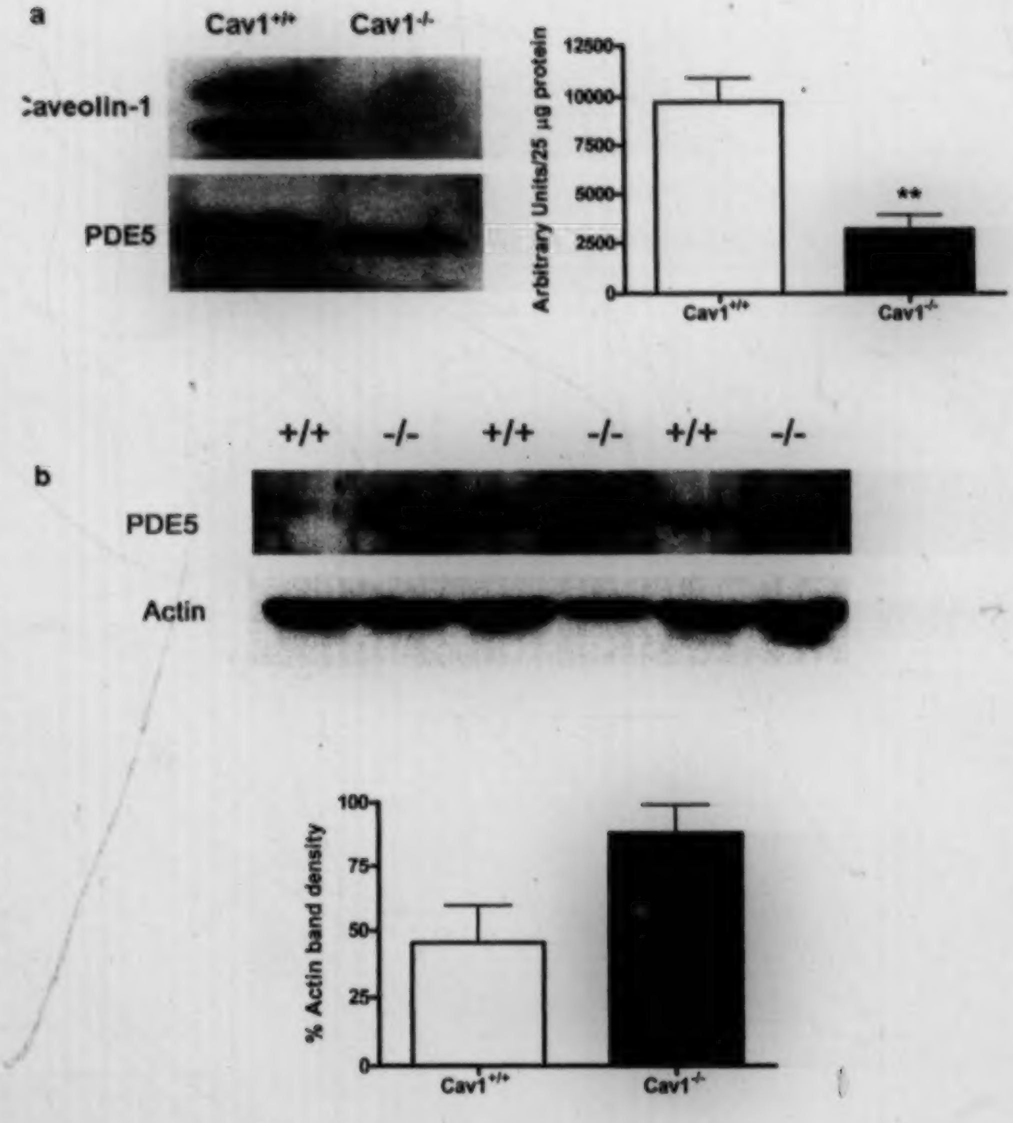
a
Cav1+/+
Cav1-/-
Caveolin-1
PDE5
Arbitrary Units/25 µg protein
12500
10000
7500
5000
2500
0
**
Cav1+/+
Cav1-/-
b
+/+
-/-
+/+
-/-
+/+
-/-
PDE5
Actin
% Actin band density
100
75
50
25
0
Cav1+/+
Cav1-/-

a trend for the cGMP degradation activity to be more susceptible to inhibition by PDE5 inhibitior II in cav1$^{-/-}$ than in cav1$^{+/+}$ but no statistical significance was achieved due to the relatively high residual activity remaining even after the highest inhibitor concentration used (data not shown).

4.4 Discussion:

Caveolin-1 is known to exert regulatory effects on a number of signaling molecules including NOS isoforms[17,28,29]. The present study examined the possible role of caveolin-1 in the regulation of NO function in the mouse small intestine. To this end, we examined the different aspects of NO function in cav1$^{-/-}$ mouse small intestinal tissue and compared them to cav1$^{+/+}$ tissue to avoid strain variations when comparing to BALB/c mice. Ultrastructural examination of LM and CM of cav1$^{-/-}$ small intestine confirmed the absence of caveolae in LM and their reduced abundance in the outer circular smooth muscle. The electron microscope findings coincided with the patterns of expression of caveolin-1 and -3 where caveolin-3 persisted only in the outer circular muscle of cav1$^{-/-}$. Based on protein sequence homology, caveolin-1 and caveolin-3 are about 65% identical and 85% similar[30]. Caveolin-3 also has the ability to drive caveolae formation and bind to and regulate signaling molecules[31]. The persistence of caveolin-3 in CM might explain some of the differences in the effect of caveolin-1 knockout between LM and CM.

The first finding to support our hypothesis of an altered response to NO in cav1$^{-/-}$ was in an increased frequency of pacing in CM of cav1$^{-/-}$ mice. As indicated in Chapter III, the CM pacing is controlled by an inhibitory input from myenteric nerves. Treatment with agents that block LNNA synthesis or action significantly increased the spontaneous pacing frequency. This was true only in the case of cav1$^{+/+}$ but not in cav1$^{-/-}$ tissues, supporting our hypothesis of a defective response to NO especially that examination of the myenteric plexus showed a similar distribution of ICC in cav1$^{+/+}$ and cav1$^{-/-}$.

To further test this hypothesis, the effect of blockade of NO synthesis by LNNA on EFS-induced relaxations in small intestinal smooth muscles was studied. We showed in Chapter III that NO is the main inhibitory mediator in LM of mouse small intestine. The effect of LNNA on the EFS-evoked relaxation was attenuated in cav1$^{-/-}$ LM tissue segments compared to cav1$^{+/+}$ where it almost abolished all the relaxation, suggesting that NO played a lesser functional role in these tissues. However, although the effect of LNNA on EFS-evoked relaxation in CM in cav1$^{-/-}$ was less than in cav1$^{+/+}$, it was not as great as in the case of LM. This might be due to the expression of caveolin-3 in this layer.

EFS-induced relaxation in CM of cav1$^{+/+}$ was followed by rebound contractions "off-effects" that was reported to be due to depolarization brought about by the activation of chloride[32] and non-selective cation conductance[33] reset during the hyperpolarization phase[34]. The lack of this "off-effect" in cav1$^{-/-}$ could possibly suggest that they do not have sufficient hyperpolarization to reset these channels. This hypothesis is consistent with the observation of reduced NO effects.

Similar to LNNA, inhibiting guanylate cyclase, the main intracellular target of NO action[35], abolished the EFS-evoked relaxation in cav1$^{+/+}$ LM but had no effect on cav1$^{-/-}$ LM. To rule out the possibility of a reduced abundance of nitrergic neurons in the myenteric plexus or a reduced expression of nNOS, we examined the number of nNOS-expressing neurons in cav1$^{+/+}$ and cav1$^{-/-}$ myenteric plexuses. nNOS-expressing neurons were present and even more abundant in the examined cav1$^{-/-}$ myenteric ganglia. This finding indicates that the defect in NO function is more likely to be post-junctional. Moreover, the increase in the number of myenteric nerve cells expressing nNOS in cav1$^{-/-}$ mice might be a possible compensatory outcome of the reduced smooth muscle and ICC NO responsiveness.

To confirm that the defect in NO function in the cav1$^{-/-}$ was post-junctional, we examined the effects of SNP on smooth muscle contraction. Both cav1$^{-/-}$ LM and CM preparations showed reduced responsiveness to SNP compared to control cav1$^{+/+}$ preparations. To determine the site of the deficiency down-stream of the NO signal, the inhibitory responses to 8-br cGMP were compared in LM preparations in both strains. The absence of significant differences indicates that the deficiency lies before the level of cGMP-controlled effectors. This might be due to a decrease in the activity of soluble guanylate cyclase. Yet this hypothesis cannot explain the ability of ODQ to abolish the relaxation due to SNP in LM preparations from cav1$^{-/-}$ mice. Moreover, Western blotting of membrane fractions showed that soluble guanylate cyclase was not present in the plasma membrane and also immunohistochemistry showed that it was not colocalized with caveolin-1. Therefore it is unlikely that soluble guanylate cyclase function will be affected by the absence of caveolin-1.

Another possible target that could be affected by caveolin-1 knockout is PDE5. PDE5 is the main regulator of NO effects in conditions of relaxation[36]. It was reported that PDE5 activity was higher in cav1$^{-/-}$ pulmonary artery smooth muscles and was the underlying cause for the pulmonary hypertension seen in this model[37]. A negative regulation of PDE5 by caveolin-1 might occur and thus in absence of caveolin-1 the activity of PDE5 might be higher. To test this hypothesis we used a PDE5 inhibitor. In presence of this inhibitor the effect of LNNA on EFS-evoked relaxation became significant in cav1$^{-/-}$ LM and the relaxation to SNP increased significantly, indicating that PDE5 activity might be higher in cav1$^{-/-}$ tissues contributing to the reduction of the response to NO. This hypothesis is further supported by the higher expression of PDE5 in caveolae-rich membrane fraction in cav1$^{+/+}$ compared to cav1$^{-/-}$ despite the observation that PDE5 is at least equally expressed in the whole tissue homogenates if not higher in cav1$^{-/-}$ homogenates. Thus we speculate that in absence of caveolin-1, PDE5 is no longer sequestered in the caveolae domain under the inhibitory clamp of caveolin-1 and retains higher activity. These findings are similar to what we showed for matrix metalloproteinase-2[38].

Despite reduced responses to NO, EFS produced relaxations in the cav1$^{-/-}$ small intestine that were comparable in magnitude to those obtained in cav1$^{+/+}$. This suggests that the relaxing function of NO in cav1$^{-/-}$ small intestine was substituted by other mediators. ATP and pituitary adenylate cyclase-activating peptide are inhibitory neurotransmitters that elicit inhibitory responses due to the activation of small conductance Ca^{2+}-dependant K^{+}-channels[39,40]. Therefore, addition of apamin may have affected both ATP and pituitary adenylate cyclase-activating peptide functions in the cav1$^{-/-}$ and cav1$^{+/+}$ small intestine. The apamin-induced reduction in EFS-evoked relaxation was significant only in cav1$^{-/-}$ intestine. This finding points out the fact that the contribution of apamin-sensitive inhibitory mediators in the regulation of cav1$^{-/-}$ small intestine motility increases in importance, possibly to compensate for the reduced NO function. However, these might not be the only possible mechanisms involved in the inhibitory neurotransmission in the cav1$^{-/-}$ small intestine. This was evident when a combination of apamin and LNNA was used, since residual inhibition of the amplitude of the contractions persisted at 10 and 30 Hz in LM. Here it is worth noting that strain variations play an important role in the mediators in play. As shown in Chapter III, a significant proportion of the EFS-evoked relaxation in CM from BALB/c persisted with a combination of LNNA and apamin, which did not occur in either cav1$^{+/+}$ or cav1$^{-/-}$ tissues.

In conclusion, the current study shows that caveolin-1 is necessary for normal NO function in the mouse intestine. Caveolin-1 gene knockout causes abnormalities in the ICC and smooth muscles of the mouse intestine leading to a reduced responsiveness to endogenous and exogenous NO. The impairment of NO function in cav1$^{-/-}$ mouse intestine may be compensated by the apamin-sensitive inhibitory mediators.

4.5 References

1. Sanders KM and Ward SM. Nitric oxide as a mediator of nonadrenergic noncholinergic neurotransmission. *Am J Physiol* 262: G379-G392, 1992.
2. Stark ME and Szurszewski JH. Role of nitric oxide in gastrointestinal and hepatic function and disease. *Gastroenterology* 103: 1928-1949, 1992.
3. Burnstock G, Campbell G, Satchell D, and Smythe A. Evidence that adenosine triphosphate or a related nucleotide is the transmitter substance released by non-adrenergic inhibitory neurons in the gut. *Br J Pharmacol* 40: 668-688, 1970.
4. Xue L, Farrugia G, Sarr MG, and Szuszewski JH. ATP is a mediator of the fast inhibitory junction potential in human jejunal circular smooth muscles. *Am J Physiol* 276: G1373-G1376, 1999.
5. Goyal RK and Rattan RS. VIP as a possible neurotransmitter in the non-cholinergic non-adrenergic inhibitory neurons. *Nature* 288: 378-380, 1980.
6. Schworer H, Katsoulis H, Creutzfeldt W, and Schmidt WE. Pituitary adenylate cyclase activiating peptide, a novel VIP-like gut-brain paptide, relaxes guinea-pig taenia caeci via apamin-sensitive potassium channels. *Naunyn Schmiedebergs Arch Pharmacol* 346: 511-514, 1992.
7. Rattan S and Chakder S. Inhibitory effects of CO on internal anal sphincter: heme-oxygenase inhibitor inhibits NANC relaxation. *Am J Physiol* 265: G799-G804, 1993.

8. Thornburg KD, Ward SM, Dalziel HH, Carl A, Westfall DP, and Sanders KM. Nitric oxide and nitrocysteine mimic nonadrenergic, noncholinergic hyperpolarization in canine proximal colon. *Am J Physiol* 261: G553-G557, 1991.

9. Jury J, Boev K, and Daniel EE. Nitric oxide mediates outward potassium currents in opossum esophageal circular smooth muscle. *Am J Physiol* 270: G932-G938, 1996.

10. Sanders KM. Post-junctional electrical mechanisms of neurotransmission. *Gut* 47: 23-25, 2000.

11. Crist JR, He XD, and Goyal RK. Chloride-mediated junction potentials in circular muscle of guinea pig ileum. *Am J Physiol* 261: G742-G751, 1991.

12. Barnette TJ, Torphy M, Grous M, Fine C, and Ormsbee HS III. Cyclic GMP: a potential mediator of neurally- and drug-induced relaxation of opossum lower esophageal sphincter. *J Pharmacol Exp Ther* 249: 524-528, 1989.

13. Sanders KM. G-protein couple receptors in gastrointestinal physiology. Neural regulation of gastrointestinal smooth muscle. *Am J Physiol* 275: G1-G7, 1998.

14. Sanders KM. Signal transduction in smooth muscle. Invited review: mechanism of calcium handling in smooth muscle. *J Appl Physiol* 91: 1438-1439, 2001.

15. Engelman JA, Zhang XL, Galbiati F, Volonte D, Sotgia F, Pestell RG, Minetti C, Scherer PE, Okamoto T, and Lisanti MP. Molecular genetics of caveolin gene family: implications for human cancer, diabetes, Alzheimer's disease and muscle dystrophy. *Am J Hum Genet* 63: 1578-1587, 1998.

16. Smart EG, Graf GA, McNiven MA, Sessa WC, Engelman GA, Scherer PE, Okamoto T, and Lisanti MP. Caveolins: liquid-ordered domains and signal transduction. *Mol Cell Biol* 19: 7289-7304, 1999.

17. Felly-Bosco E, Bender FC, Courjault-Gautier F, Bron C, and Quest A. Caveolin-1 down-regulates inducible nitric oxide synthase via the proteasome pathway in human colon carcinoma cells. *Proc Natl Acad Sci USA* 97: 14334-14339, 2000.

18. Sato Y, Ikuko S, and Shimizu T. Identification of caveolin-1-interacting site in neuronal nitric-oxide synthase. *J Biol Chem* 279: 8827-8836, 2004.

19. Daniel EE, Boddy G, Bong A, and Cho WJ. A new model of pacing in the mouse intestine. *Am J Physiol* 286: G253-G262, 2004.

20. Sotgia F, Lee JK, Das K, Bedford M, Petrucci TC, Macioce P, Sargiacomo M, Bricarelli FD, Minetti C, Sudol M, and Lisanti MP. Caveolin-3 directly interacts with the C-terminal tail of beta -dystroglycan. Identification of a central WW-like domain within caveolin family members. *J Biol Chem* 275:38048-38058, 2000.

21. Zizzo MG, Mule F, and Serio R. Duodenal contractile activity in dystrophic (*mdx*) mice: reduction of nitric oxide influence. *Neurogastroenterol Motil* 15: 559-565, 2003

22. Okasora T, Bywater RA, and Taylor GS. Projections of enteric motor neurons in the mouse distal colon. *Gastroenterology* 90: 1964-1971, 1986.

23. Satoh Y, Takeuchi T, and Yamazaki Y. Mediators of nonadrenergic, noncholinergic relaxation in longitudinal muscle of the ICR mice. *J Smooth Muscle Res* 35: 65-75, 1999.

24. Kincaid RL and Manganiello VC. Assay of cyclic nucleotide phosphodiesterase using radiolabelled and fluorescent substrates. In: Corbin J, Johnson R, Abelson J, and Simon M (Eds.) Methods in Enzymology, Academic Press, New York, NY, pp.457-470, 1988.

25. Komuro t, Seki K, and Horiguchi K. Ultrastructural characterization of the interstitial cells of Cajal. *Arch Histol Cytol* 62: 295-316, 1999.

26. Chicchetti R, Grandis A, Bombardi C, Clavenzani P, Costerbosa GL, Lucchi ML, and Furness JB. Characterisation of neurons expressing calbindin immunoreactivity in the ileum of the unweaned and mature sheep. *Cell Tissue Res* 318:289-303, 2004.

27. Lin Z, Gao N, Hu H-Z, Liu S, Gao C, Kim G, Ren J, Xia Y, Peck OC, and Wood JD. Immunoreactivity of Hu proteins facilitates the identification of myenteric neurones in guinea pig small intestine. *Neurogastroenterol Motil* 14: 197-204, 2002.

28. Venema VJ, Ju H, Zou R, and Venema RC. Interaction of neuronal nitric oxide synthase with caveolin-3 in skeletal muscle. Identification of a novel caveolin scaffolding/inhibitory domain. *J Biol Chem* 272: 28187-28190, 1997.

29. Feron O, Belhassen L, Kobzik L, Smith TW, Kelly RA, and Michel T. Endothelial nitric oxide synthase targeting to caveolae. Specific interaction with caveolin isoforms in cardiac myocytes and endothelial cells. *J Biol Chem* 271: 22810-22814, 1996.

30. Tang Z, Scherer PE, Okamoto T, Song K, Song K, Chu C, Kohtz DS, Nishimoto L, Lodish HF, and Lisanti MP. Molecular cloning of caveolin-3, a novel member

of caveolin gene family expressed predominantly in muscle. *J Biol Chem* 271: 2255-2261, 1996.

31. Okamoto T, Schlegel A, Scherer PE, and Lisanti MP. Caveolins, a family of scaffolding proteins for organizing "pre-assembled signaling complexes" at the plasma membrane. *J Biol Chem* 273: 5419-5422, 1998.
32. Crist JR, He XD, and Goyal RK. Chloride-mediated inhibitory junction potentials in opossum esophageal circular smooth muscle. *Am J Physiol* 261: G752-G792, 1991.
33. Inoue R. Effects of external Cd^{2+} and other divalent cations on carbachol activated non-selective cation channels in guinea pig ileum. *J Physiol (Lond.)* 442: 447-463, 1991.
34. Baker SA, Mutafova-Yambolieva V, Monaghan K, Horowitz B, Sanders KM, and Koh SD. Mechanism of active repolarization of inhibitory junction potential in murine colon. *Am J Physiol* 285: G813-G821, 2003.
35. Waldman SA and Murad F. Cyclic GMP synthesis and function. *Pharmacol Rev* 39: 163-196, 1987.
36. Rybalkin SD, Yan C, Bornfeldt KE, and Beavo JA. Cyclic GMP phosphodiesterases and regulation of smooth muscle function. *Circ Res* 93: 280-291, 2003.
37. Murray F, Patel HH, Suda RYS, Thistlethwaite PA, Yuan JXY, and Insel PA. Caveolar localization and caveolin-1 regulation of PDE5 in human pulmonary artery smooth muscle cells. *FASEB J* 20:A543, 2006 (abstract).

38. Chow AK, Cena J, El-Yazbi AF, Crawford BD, Holt A, Cho WJ, Daniel EE, and Schulz R. Caveolin-1 inhibits matrix metalloproteinase-2 activity in the heart. *J Mol Cell Cardiol* 42:896-901, 2007.

39. Ohno N, Xue L, Yamamoto Y, and Suzuki H. Properties of the inhibitory junction potential in smooth muscle of the guinea pig gastric fundus. *Br J Pharmacol* 117: 974-978, 1996.

40. Pluja L, Fernandez E, and Jiménez M. Electrical and mechanical effects of vasoactive intestinal peptide and pituitary adenylate cyclase-activating peptide in the rat colon involve different mechanisms. *Eur J Pharmacol* 389: 217-224, 2000.

CHAPTER V

CAVEOLIN-1 KNOCKOUT ALTERS β-ADRENOCEPTOR FUNCTION IN MOUSE SMALL INTESTINE

A version of this chapter has been published. El-Yazbi AF, Cho WJ, Schulz R, and Daniel EE. Caveolin-1 knockout alters β-adrenoceptor function in mouse small intestine. *Am J Physiol* 291: G1020-G1030, 2006.

5.1 Introduction:

Following an abdominal surgery or injury, the motility of the GIT is transiently impaired. Among the pathologic mechanisms underlying the paralytic state is the sympathetic inhibitory reflex[1]. The sympathetic hyperactivity in the postoperative period is the result of increased adrenergic neuronal hyperactivity or high circulating epinephrine released from the adrenal gland in response to surgical trauma[2,3]. Thus adrenergic receptors play a role in gut pathophysiology and modification of their function may alter these responses.

The inhibitory sympathetic effects in the GIT are mediated by α-[4] and β-adrenoceptors[5]. Sympathetic innervation to the GIT comes from extrinsic nerves, which mostly end on and modulate enteric nerves[6]. However, some adrenergically-mediated inhibitory actions occur at the level of receptors expressed on smooth muscle cells[7,8]. A recent study[9] showed that most of the β-adrenoceptor-mediated inhibition in response to β-adrenergic agonists, was independent of the enteric nervous system. Among the β-adrenoceptors, the β_3 subtype is of a special interest in gastrointestinal motility because it is abundantly present in the GIT[10].

β-adrenoceptors are G protein-coupled receptors, which upon activation by an agonist stimulate adenylyl cyclase to produce the second messenger, cAMP. The end effect of this process is the activation of PKA[11]. The receptor/G-protein/PKA interaction is not due to a random collision of freely moving proteins in the plasma membrane, but is rather due to a compartmentalized membrane process[12]. For β-adrenoceptors, this compartmentalization has been shown to occur in caveolae in cardiac myocytes[13,14] and cultured cell lines[15].

Caveolae are non-clathrin-coated plasma membrane invaginations that are abundant in terminally differentiated cells such as endothelial cells, adipocytes, fibroblasts, and myocytes[16]. Caveolae and their marker proteins, caveolins, are thought to be involved in signal transduction. Caveolin-1, through the caveolin scaffolding domain, binds to and regulates the activity of several distinct classes of signaling molecules[17]. Among these are the heterotrimeric G-proteins[18] and adenylate cyclase[19] that are essential for signal transduction downstream of β-adrenoceptors.

In the mouse small intestine, we showed that caveolin-1 is present in smooth muscle cells and ICC and is required for the normal pacing activity of the small intestine[20]. In the present study, we investigated alterations of GIT motility in small intestine from cav1$^{-/-}$ mice associated with β-adrenoceptor function. We hypothesize that the β-adrenoceptor function would be altered in the cav1$^{-/-}$ small intestine owing to the close relationship between caveolin-1 and β-adrenoceptor signaling. We also examined the underlying mechanism of alteration in the signaling cascade downstream of β-adrenoceptors.

5.2 Materials and methods:

5.2.1 Functional Studies:

5.2.1.1 Preparation of the tissue:

Mouse small intestinal tissue from cav1$^{+/+}$ and cav1$^{-/-}$mice was isolated and set up to record LM activity as described in Chapter II.

5.2.1.2 Experimental protocols:

Tissue segments were equilibrated in Krebs-Ringer solution for 15 min at the beginning of the experiments. 1 μM tetrodotoxin (TTX) was added to the solution at the beginning of the equilibration period to block enteric nerve activity. In preliminary experiments, this concentration was found to be sufficient to block responses to nerve activity elicited by electric field stimulation. In experiments to study the effects of β-adrenoceptor antagonists or H-89 on the (-)-isoprenaline-induced relaxation, the compounds were added at the beginning of the equilibration period and left in contact with the tissue throughout the experiment. CGP20712A (0.1 μM) was used to block β_1-adrenoceptors, ICI118551 (0.1 μM) was used to block β_2-adrenoceptors, and SR59230A (0.1 μM) was used to block β_3-adrenoceptors. H-89 (1 μM) was used to study the effect of PKA block on the response to (-)-isoprenaline. After the equilibration period, the tissues were contracted by Carbachol (CCh, 1 μM). A period of 15 min was allowed after the addition of CCh for the stabilization of the induced tone. In control experiments, the CCh-induced tone came to plateau after 10 min. Cumulative concentration-response curves (CRC) for (-)-isoprenaline were constructed using nine doses separated by half log units (10^{-9}-10^{-5} M). Similar CRCs were constructed for the selective β_3-agonist, BRL37344. At the end of a CRC, the tissue was brought to a state of maximum relaxation by washing twice with calcium-free Krebs-Ringer solution containing 1 mM EGTA at 37°C.

In other experiments H-89 (0.5 µM) was added to some tissues at the beginning of the equilibration period together with tetrodotoxin (1 µM). All tissues were contracted with 1 µM CCh. After 15 min, a single dose of N^6,2'-O-dibutyryladenosine 3':5'-cyclic monophosphate (di-bu cAMP, 100 µM) or forskolin (1 µM) was added.

5.2.1.3 Data analysis:

In the CRCs, the relaxing effect of each dose was calculated by normalizing the amount of relaxation brought about by (-)-isoprenaline addition to the CCh-induced tone prior to the first addition of (-)-isoprenaline. Sigmoid dose response curves with constant Hill-slope were estimated with GraphPad Prism 4.0. pEC_{50} values were calculated and expressed as mean±SEM. Statistical significance among pEC_{50} values was determined by unpaired *t*-test. A *P*-value < 0.05 was considered significant. In case of comparison of more than two pEC_{50} values, ANOVA was used followed by Bonferroni *post hoc* test. The relaxing effects of di-bu cAMP and forskolin were measured after five minutes following the addition of the drug and represented as a percentage of the relaxation brought about by calcium-free Krebs-Ringer solution with 1 mM EGTA added at the end of the experiment. The results are expressed as mean±SEM. In all cases *n* represents the number of animals whose small intestine provided segments for the study. The statistical significance of the H-89 effect was determined by comparison to controls run side-by side using unpaired *t*-test. A *P*-value < 0.05 was considered significant.

5.2.2 Immunohistochemistry:

Tissue preparation, cryosection, immunolabeling, and confocal imaging were done as described in Chapter II. Sources and concentrations of primary and secondary antibodies are summarized in Table 5.1. Double immunolabeling with primary antibodies from the same host was done by the conversion of one of them to be recognized as an antibody in a different host as previously described[21].

5.2.3 Western blotting of membrane fractions:

Full-length small intestinal tissues from 3 $cav1^{+/+}$ and 3 $cav1^{-/-}$ mice were collected, pooled, and used to prepare membrane fractions as described in Chapter II. Western blotting was done as described in Chapter II using mouse anti-caveolin-1 (1:1000) and mouse anti-catalytic subunit of PKA (1:1000) as primary antibodies. HRP-conjugated goat anti-mouse IgG (1:4000) was used as secondary antibody.

5.2.4 Materials:

(-)-isoprenaline, CCh, ICI118551, CGP20712A, SR59230A, BRL37344, forskolin, and di-bu cAMP were purchased from Sigma Canada (Oakville, ON). H-89 was purchased from Calbiochem (San Diego, CA). TTX was purchased from the

Table 5.1 Antibodies and normal sera used in Chapter V

Antibody	Host	Dilution	Peptide	Source
			Primary	
Cav1	Mouse	1:200	yes	BD Transduction Labs.
PKAc	Mouse	1:200	yes	BD Transduction Labs.
β1AR	Rabbit	1:100	no	Abcam Inc.
β2AR	Rabbit	1:100	no	Abcam Inc.
β3AR	Rabbit	1:100	yes	Alpha Diagnostic Intl.
			Secondary	
Fab fragment rabbit anti-mouse IgG				Jackson ImmunoResearch
Cy3-conjugated donkey anti-mouse IgG				Jackson ImmunoResearch
Alexa488-conjugated goat anti-rabbit IgG				Molecular Probes
Horse raddish peroxidase-conjugated goat anti-mouse				BD Transduction Labs.
			Sera	
Normal donkey serum				Calbiochem
Normal goat serum				Caltag Labs.

Cav1, caveolin-1; PKAc, cAMP-dependent protein kinase; β1AR, beta 1 adrenergic receptor; β2AR, beta 2 adrenergic receptor; β3AR, beta 3 adrenergic receptor; Peptide, antigenic peptide used to saturate the corresponding primary antibody.

Alomone Labs. (Jerusalem, Israel). Anti-fading agent was from Biomeda (Foster, CA). Cover glass slips were from Electron Microscopy Sciences (Washington, PA).

All the drugs used for functional experiments except SR59230A, forskolin, and TTX were dissolved as stock solutions in distilled water and frozen at -20°C until used. Fresh dilutions were prepared in distilled water on the day of the experiment. SR59230A and forskolin were dissolved in dimethylsulfoxide and TTX was dissolved in 0.1 M acetic acid. These solvents in the quantities added (10 μl in 10 ml) did not alter the tissue function in preliminary experiments.

5.3 Results:

5.3.1 Immunohistochemistry:

5.3.1.1 Double immunostaining for caveolin-1 and β-adrenoceptors:

Cav1$^{-/-}$ cryosections lacked caveolin-1 immunoreactivity and thus showed immunoreactivity only for β-adrenoceptors (Fig 5.1). In cav1$^{+/+}$, immunoreactivities of all three β-adrenoceptor subtypes were diffusely distributed in smooth muscles (circular and longitudinal) and myenteric plexus cells with only a limited co-localization with caveolin-1 in possible ICC in the deep muscular plexus, interstitial cells of Cajal in the myenteric plexus and some epithelial cells in the serosal layer (Fig 5.1c, 5.1i, and 5.1o). In cav1$^{-/-}$, the receptors had a distribution similar to that in cav1$^{+/+}$ and the immunofluorescence showed a comparable intensity (Fig 5.1e, 5.1k, and 5.1q).

Fig 5.1 Double immunohistochemical staining of caveolin-1 (red) and β-adrenoceptors (green) in cryosections from cav1$^{+/+}$ and cav1$^{-/-}$ small intestine. Panels a-f: immunohistochemical staining for caveolin-1 and β_1-adrenoceptors in cav1$^{+/+}$ (a-c) and cav1$^{-/-}$ (d-f). Panels g-l: immunohistochemical staining for caveolin-1 and β_2-adrenoceptors in cav1$^{+/+}$ (g-i) and cav1$^{-/-}$ (j-l). Panels m-r: immunohistochemical staining for caveolin-1 and β_3-adrenoceptors in cav1$^{+/+}$ (m-o) and cav1$^{-/-}$ (p-r). Co-localization is indicated in figures c, f, i, l, o, and r by yellow colour. Arrowheads indicate co-localization in possible ICC in the deep muscular plexus, thin arrows indicate co-localization in the myenteric plexus interstitial cells of Cajal, and thick arrows indicate co-localization in epithelial cells in the serosal layer. The scale bar is 20 μm. icm, inner circular muscle; ocm, outer circular muscle; lm, longitudinal muscle; mp; myenteric plexus (immunostaining and confocal imaging were done by Woo Jung Cho).

Fig 5.1

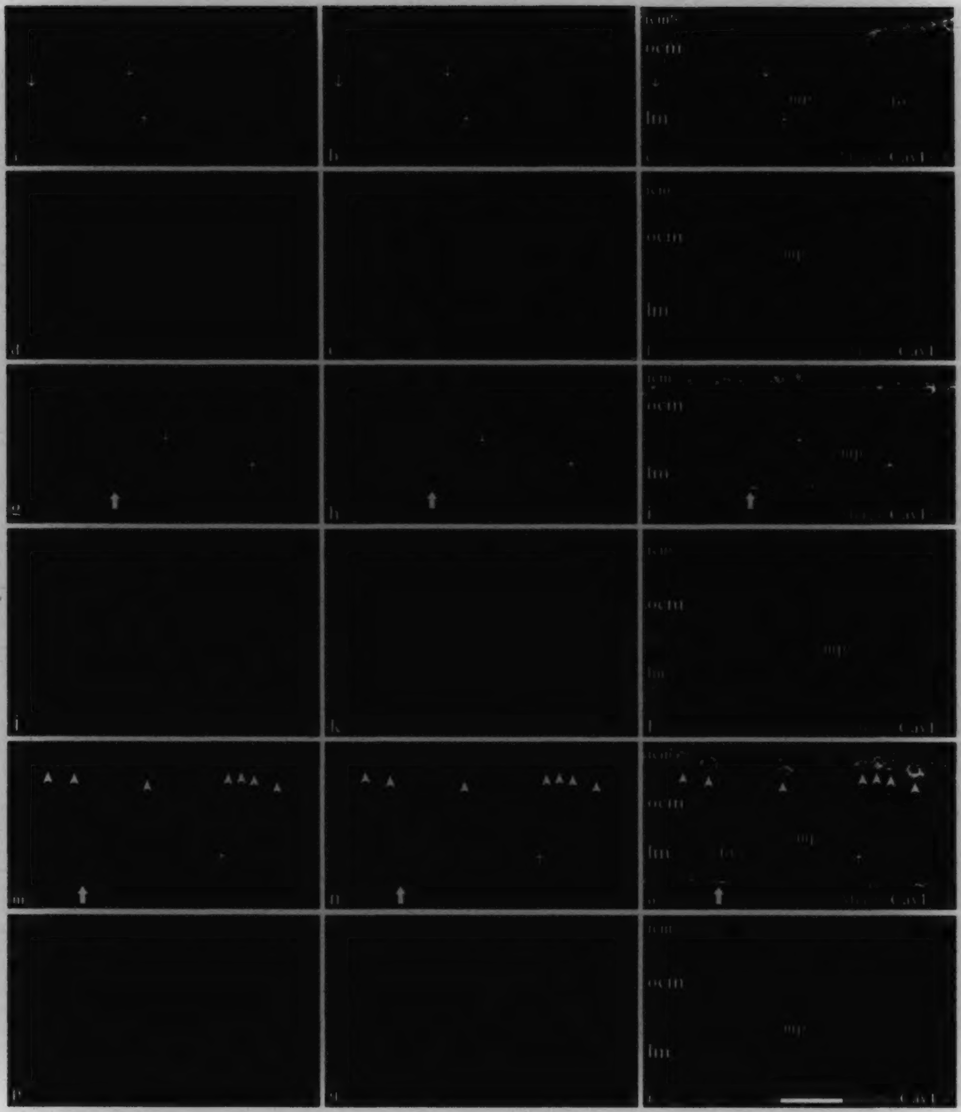
a
b
c
ocm
mp
lm
CavI
d
e
f
ocm
mp
lm
CavI
g
h
i
ocm
mp
lm
CavI
j
k
l
ocm
mp
lm
CavI
m
n
o
ocm
mp
lm
CavI
p
q
r
ocm
mp
lm
CavI

5.3.1.2 Double immunostaining for caveolin-1 and PKA:

In cav1$^{+/+}$, the PKA catalytic sub-unit immunoreactivity was mainly localized to the cell membrane of smooth muscles (Fig 5.2b). It showed a close colocalization with caveolin-1 in the cell membrane (Fig 5.2c). In cav1$^{-/-}$, no immunoreactivity to caveolin-1 was detected (Fig 5.2d), however, the immunoreactivity to the PKA catalytic subunit persisted in the cell membrane (Fig 5.2e). The immunofluorescence due to PKA catalytic subunit immunoreactivity was of a comparable intensity in cav1$^{-/-}$ and cav1$^{+/+}$.

5.3.2 Functional experiments:

5.3.2.1 Contractile response to CCh:

Upon treatment with CCh (1 μM), mouse small intestinal tissue segments responded with a sustained tonic contraction i.e. the phasic contractions persisted but at a higher tone. The tonic contraction level (after relaxation of a phasic contraction) came to a plateau within 10 min. The tonic response to 1 μM CCh was similar in cav1$^{+/+}$ and cav1$^{-/-}$ and was sub-maximal in both strains (Fig 5.3)

5.3.2.2 Effect of (-)-isoprenaline:

The non-selective β-agonist (-)-isoprenaline produced a concentration-dependent relaxation of the tissue segments contracted with CCh from both cav1$^{+/+}$ and cav1$^{-/-}$ mice. However, the response to (-)-isoprenaline in cav1$^{+/+}$ segments started at lower

Fig 5.2 Double immunohistochemical staining for caveolin-1 and catalytic sub-unit of PKA (PKAc) in cryosections from cav1$^{+/+}$ and cav1$^{-/-}$ small intestine. Panels a-c show immunostaining for caveolin-1 and PKAc in cav1$^{+/+}$ tissue. Panel c shows the colocalization as a yellow colour in the membrane of smooth muscle cells, possible ICC in the deep muscular plexus (indicated by arrowheads), ICC in the myenteric plexus (indicated by thin arrows), and epithelial cells in the serosal layer (indicated by thick arrows). Panels d-f show immunostaining for caveolin-1 and PKAc in cav1$^{-/-}$ tissue. The scale bar is 10 µm. icm, inner circular muscle; ocm, outer circular muscle; lm, longitudinal muscle; mp; myenteric plexus (immunostaining and confocal imaging were done by Woo Jung Cho).

Fig 5.2

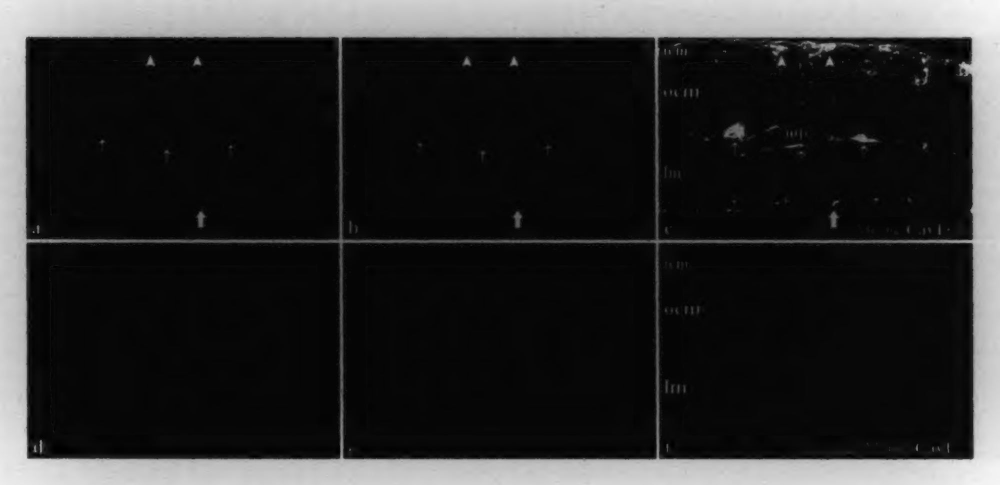
a
b
c
ocm
lm
d
e
f
ocm
lm

Fig 5.3 Tonic amplitude following CCh (1, 3, and 10 μM) addition to cav1$^{+/+}$ and cav1$^{-/-}$ LM preparations. The tonic amplitude after different CCh doses is represented as mean±SEM of mg tension developed. *n* values were six in all experiments.

Fig 5.3

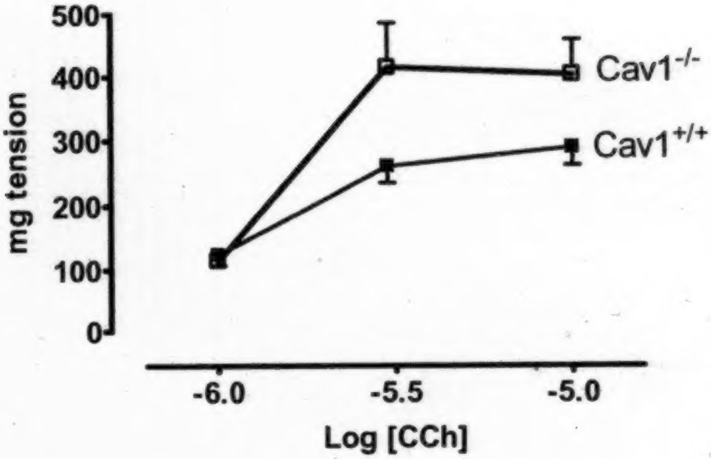

concentration than in cav1$^{-/-}$ segments (Fig 5.4a). The CRC of (-)-isoprenaline in the cav1$^{-/-}$ (pEC$_{50}$: 6.97±0.10) was shifted significantly (P<0.01) to the right with respect to the cav1$^{+/+}$ CRC (pEC$_{50}$: 7.60±0.15) (Fig 5.4b).

5.3.2.3 Effects of selective β-antagonists on relaxation due to (-)-isoprenaline:

We examined the effects of selective β-adrenoceptor antagonists on (-)-isporenaline-induced relaxation. The concentrations of the antagonists used were based on those reported in previous work on mouse intestine[22]. In cav1$^{+/+}$ tissues, 0.1 μM CGP20712A, a selective β_1-antagonist, significantly shifted the CRC of isoprenaline to the right (pEC$_{50}$: control, 7.60±0.15; CGP20712A, 7.08±0.14; $P<0.05$) (Fig 5.5a). However, in cav1$^{-/-}$, CGP20712A did not significantly shift the CRC of (-)-isoprenaline (pEC$_{50}$: control, 6.97±0.10; CGP20712A, 7.27±0.09) (Fig 5.5a). The selective β_2-adrenoceptor antagonist, ICI118551 (0.1 μM), had the same effect as the β_1-antagonist. It shifted slightly the CRC of (-)-isoprenaline in cav1$^{+/+}$ (pEC$_{50}$: control, 7.60±0.15; ICI118551, 6.95±0.15; $P<0.05$) and had no significant effect on the CRC in cav1$^{-/-}$ (pEC$_{50}$: control, 6.97±0.10; ICI118551, 6.72±0.13) (Fig 5.5b). The greatest shift in the CRC of (-)-isoprenaline in cav1$^{+/+}$ small intestinal tissue was obtained with the selective β_3-adrenoceptor antagonist, SR59230A (0.1 μM) (pEC$_{50}$: control, 7.60±0.15; SR59230A, 6.39±0.13; $P<0.001$) (Fig 5.5c). SR59230A (0.1 μM) did not affect the CRC in cav1$^{-/-}$ (pEC$_{50}$: control, 6.94±0.09; SR59230A, 6.71±0.09) (Fig 5.5c). The shift in the CRC in cav1$^{+/+}$ caused by SR59230A was higher than that due to CGP20712A ($P<0.01$) and ICI118551 ($P<0.05$) when measured in terms of pEC$_{50}$.

Fig 5.4 Concentration-response curves of (-)-isoprenaline in small intestinal tissue segments from cav1$^{+/+}$ and cav1$^{-/-}$ mice contracted with 1 µM CCh. a. Representative tracings of the effect of (-)-isoprenaline in cav1$^{+/+}$ and cav1$^{-/-}$. b. Concentration response curve of (-)-isoprenaline in cav1$^{+/+}$ compared to cav1$^{-/-}$ (n=6). The relaxing effect was measured at the tonic amplitude.

Fig 5.4

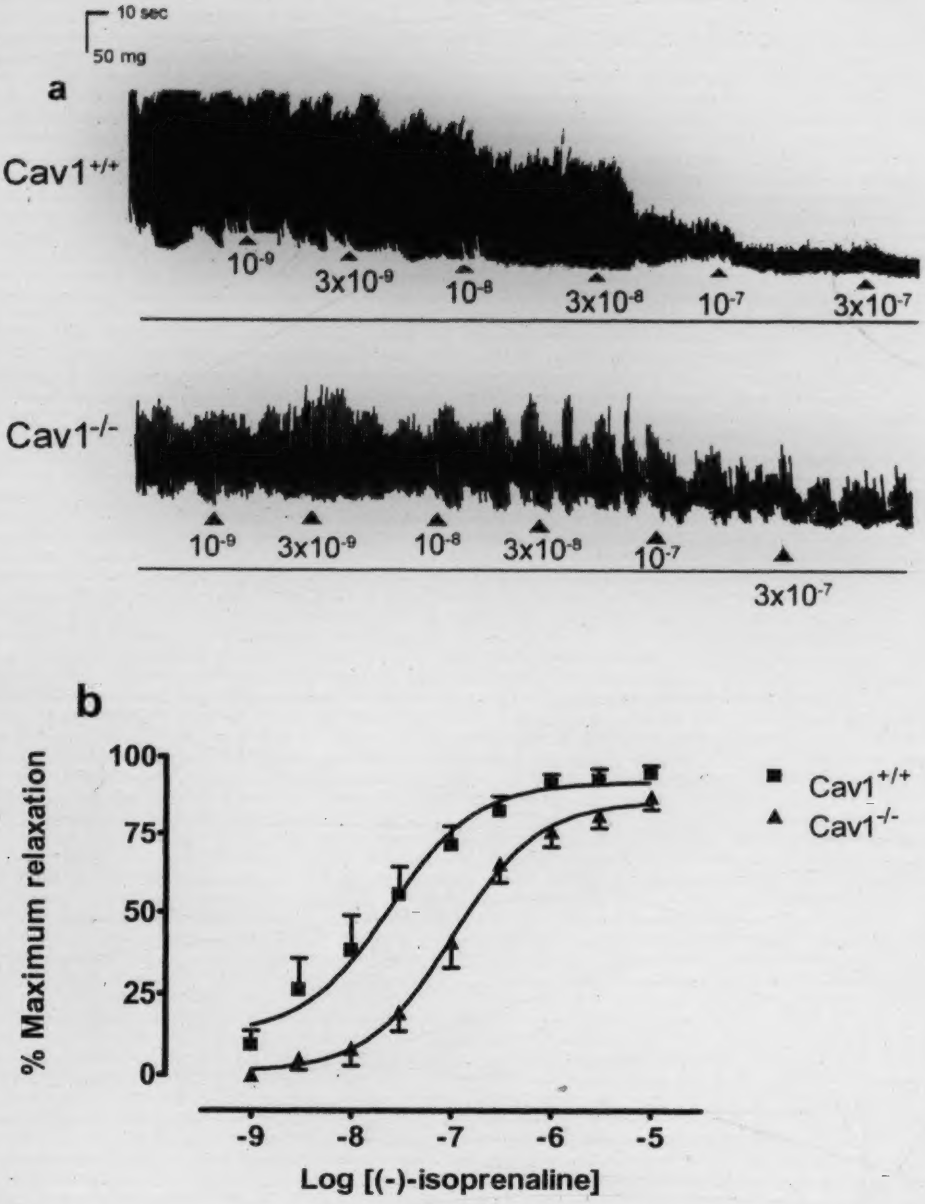
10 sec
50 mg
a
Cav1+/+
10-9
3x10-9
10-8
3x10-8
10-7
3x10-7
Cav1-/-
10-9
3x10-9
10-8
3x10-8
10-7
3x10-7
b
% Maximum relaxation
100
75
50
25
0
-9
-8
-7
-6
-5
Log [(-)-isoprenaline]
Cav1+/+
Cav1-/-

Fig 5.5 Effect of selective β-adrenoceptor antagonists (0.1 μM) on (-)-isoprenaline-induced relaxation in small intestinal tissue segments from cav1$^{+/+}$ and cav1$^{-/-}$ mice contracted with 1 μM CCh. a. The effect of the selective β_1-adrenoceptor antagonist, CGP20712A. b. The effect of the selective β_2-adrenoceptor antagonist, ICI118551. c. The effect of the selective β_3-adrenoceptor antagonist SR59230A (*n* values are 6 for all experiments).

Fig 5.5

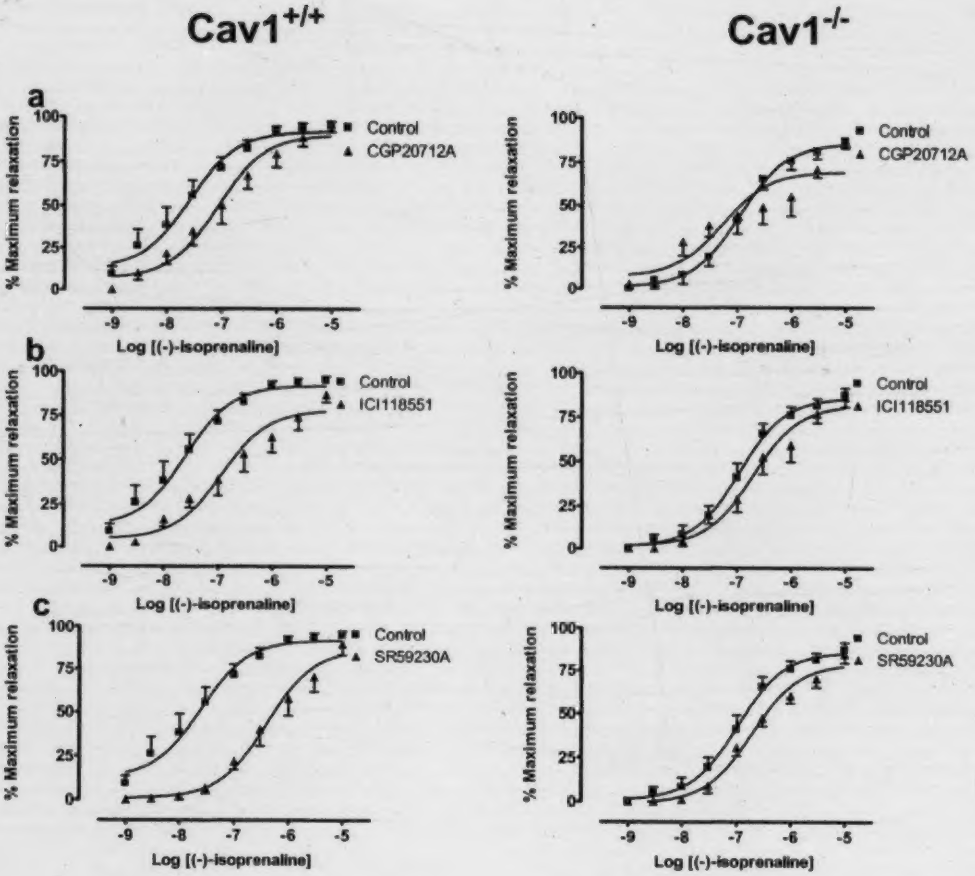
Cav1$^{+/+}$
Cav1$^{-/-}$
a
b
c
% Maximum relaxation
0
25
50
75
100
-9
-8
-7
-6
-5
Log [(-)-isoprenaline]
■ Control
▲ CGP20712A
▲ ICI118551
▲ SR59230A

5.3.2.4 Effect of a non-selective β-antagonist on the relaxation due to (-)-isoprenaline:

1 μM concentration of the non-selective β-antagonist, timolol, shifted the (-)-isporenaline CRC to the right significantly in cav1$^{+/+}$ (pEC$_{50}$: control, 7.60±0.15; timolol, 5.92±0.19; $P<0.001$) and cav1$^{-/-}$ (pEC$_{50}$: control, 6.97±0.10; timolol, 5.80±0.13; $P<0.001$) (Fig 5.6).

5.3.2.5 Responses to BRL37344:

BRL37344 caused a concentration-dependent relaxation of CCh-induced tone in cav1$^{+/+}$ tissue (pEC$_{50}$: 6.49±0.12) (Fig 5.7). In cav1$^{-/-}$ tissue the CRC of BRL37344 was shifted to the right (pEC$_{50}$: 5.55±0.19, $P<0.01$) (Fig 5.7) with respect to the CRC in cav1$^{+/+}$.

5.3.2.6 Effect of H-89 on (-)-isoprenaline-induced relaxation:

In cav1$^{+/+}$ tissue H-89 markedly shifted the CRC of (-)-isoprenaline to the right (pEC$_{50}$: control, 7.60±0.15; H-89, 6.02±0.22; $P<0.001$) (Fig 5.8). However, treatment of cav1$^{-/-}$ tissues with H-89 did not significantly affect the CRC of (-)-isoprenaline (pEC$_{50}$: control, 6.94±0.09; H-89, 6.75±0.19) (Fig 5.8).

5.3.2.7 Effect of H-89 on relaxation due to forskolin or di-bu cAMP:

The direct activator of adenylate cyclase, forskolin, produced a relaxation of CCh-induced tone in both cav1$^{+/+}$ and cav1$^{-/-}$ tissues (Fig 5.9a). In cav1$^{+/+}$, the relaxation

Fig 5.6 Effect of timolol (1 μM) on (-)-isoprenaline-induced relaxation in cav1$^{+/+}$ and cav1$^{-/-}$ tissue segments contracted with 1 μM CCh. *n* values are 6 for all experiments.

Fig 5.6

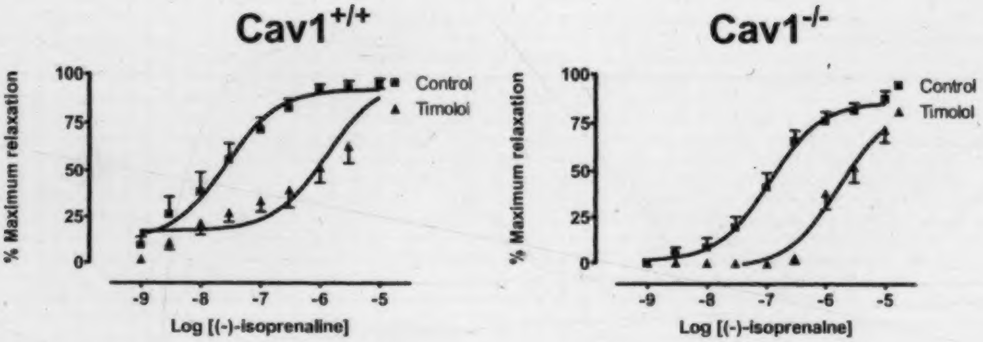
Cav1$^{+/+}$
Cav1$^{-/-}$
% Maximum relaxation
100
75
50
25
0
-9
-8
-7
-6
-5
Log [(-)-isoprenaline]
■ Control
▲ Timolol
% Maximum relaxation
100
75
50
25
0
-9
-8
-7
-6
-5
Log [(-)-isoprenalne]
■ Control
▲ Timolol

Fig 5.7 Concentration-response curves of BRL37344 in small intestinal tissue segments from cav1$^{+/+}$ and cav1$^{-/-}$ mice contracted with 1 µM CCh (*n*=6).

Fig 5.7

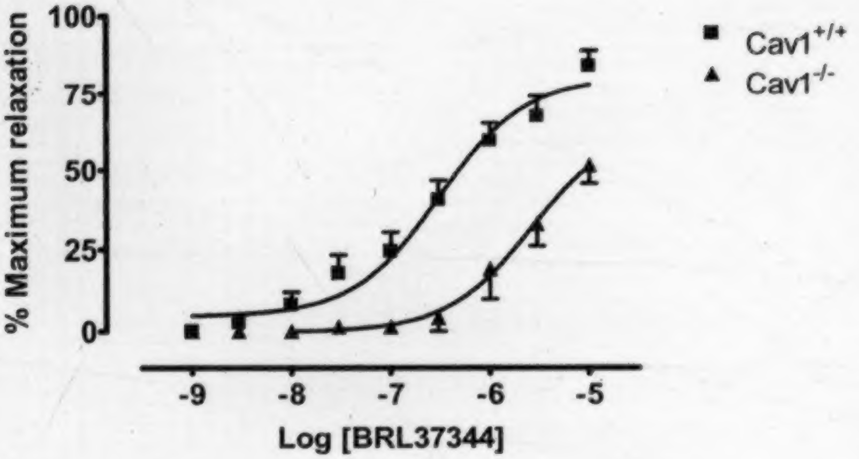

100
75
50
25
0
% Maximum relaxation
-9
-8
-7
-6
-5
Log [BRL37344]
■ Cav1$^{+/+}$
▲ Cav1$^{-/-}$

Fig 5.8 Effect of the PKA inhibitor, H-89 (1 μM), on the (-)-isoprenaline-induced relaxation in small intestinal tissue segments from cav1$^{+/+}$ and cav1$^{-/-}$ mice contracted with 1 μM CCh (*n*=6).

Fig 5.8

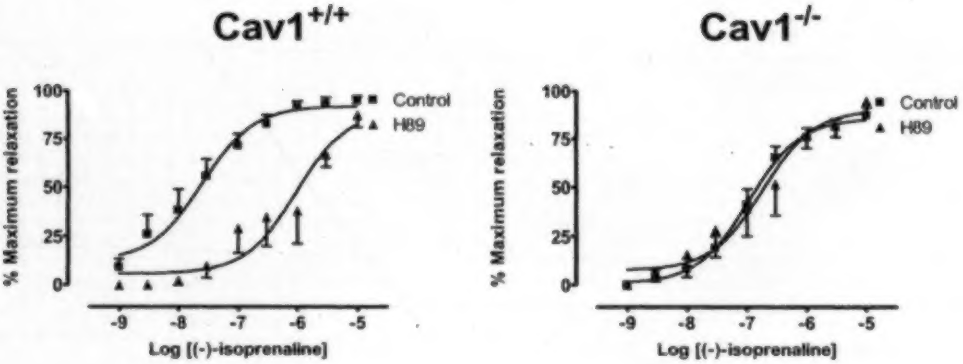
Cav1$^{+/+}$

Cav1$^{-/-}$

Fig 5.9 PKA inhibitor H-89 (0.5 µM) reduces the (a) forskolin (1 µM)- and (b) di-bu cAMP (100 µM)-induced relaxation in small intestinal tissue segments from cav1$^{+/+}$ but not from cav1$^{-/-}$ mice (*n*=6). Statistical significance was measured by the unpaired *t*-test and denoted by ***P*<0.01 and ****P*<0.001.

Fig 5.9

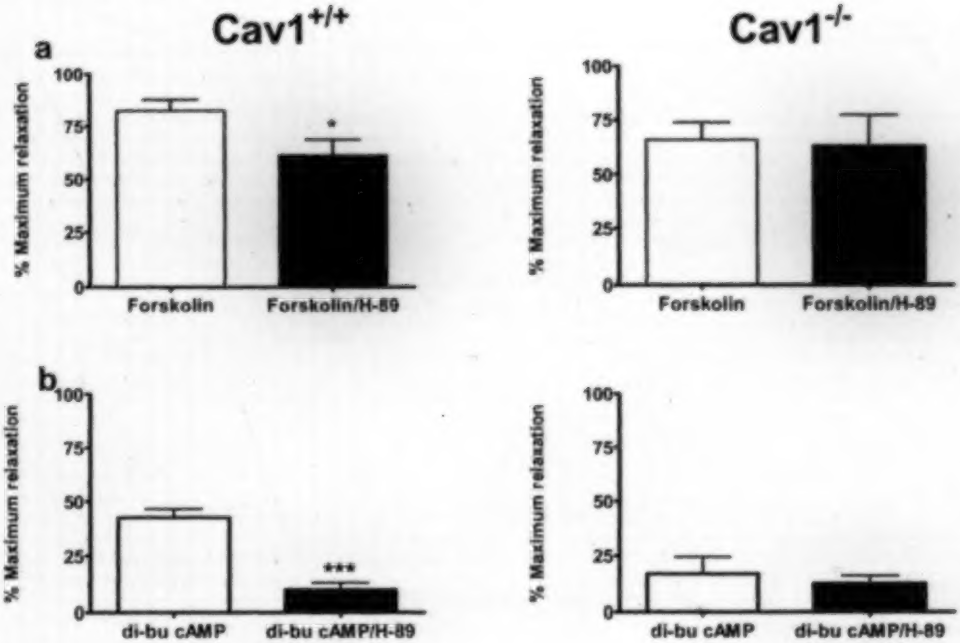
Cav1$^{+/+}$
Cav1$^{-/-}$
a
b
% Maximum relaxation
100
75
50
25
0
*
***
Forskolin
Forskolin/H-89
di-bu cAMP
di-bu cAMP/H-89

was reduced when the tissue was pretreated with H-89. On the other hand, H-89 pretreatment did not affect the relaxation due to forskolin in cav1$^{-/-}$ tissue.

5.3.2.8 Effect of H-89 on relaxation due to di-bu cAMP:

We studied the effect of di-bu cAMP on CCh-induced tone in intestinal tissue. Di-bu cAMP produced a greater relaxation in cav1$^{+/+}$ tissue than in cav1$^{-/-}$ (*P*<0.05). H-89 almost abolished the relaxation due to di-bu cAMP in cav1$^{+/+}$ tissues but had no significant effect in cav1$^{-/-}$. In addition, the response of the H-89 pretreated cav1$^{+/+}$ tissue to di-bu cAMP was similar to the control response in cav1$^{-/-}$ (Fig 5.9b).

5.3.3 Western Blotting:

Probing for the catalytic subunit of PKA showed that it was expressed in the lipid raft-rich membrane fractions in cav1$^{+/+}$ smooth muscles and in the heavy (non-raft) membrane fraction of both strains (Fig 5.10). In cav1$^{-/-}$, PKA catalytic subunit expression was greatly reduced in the lipid raft fraction compared to cav1$^{+/+}$. Caveolin-1 expression was observed only in the lipid raft-rich membrane fraction of cav1$^{+/+}$ (Fig 5.10).

5.4 Discussion:

To assess the alteration of the cAMP-mediated relaxation in cav1$^{-/-}$ small intestine, we examined the changes in β-adrenoceptor function. Initially, we found that the

Fig 5.10 Expression of PKA catalytic subunit in the lipid raft-rich membrane fraction of cav1$^{+/+}$ and cav1$^{-/-}$ (lanes a and b, respectively) and the heavy (non-raft) membrane fraction in cav1$^{+/+}$ and cav1$^{-/-}$ (lanes c and d, respectively) mice small intestinal tissue (done with the help of Jonathan Cena).

Fig 5.10

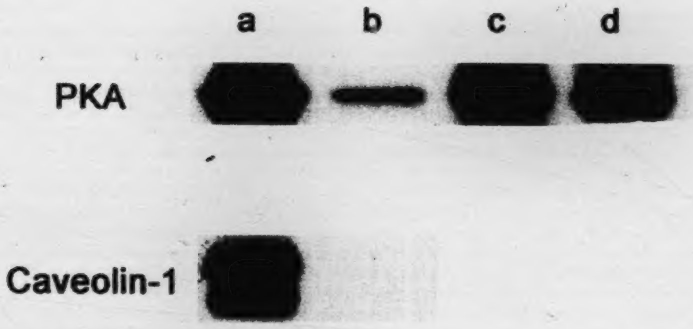
a
b
c
d
PKA
Caveolin-1

CRC representing the relaxation induced by (-)-isoprenaline in tissues contracted with CCh was shifted to the right in cav1$^{-/-}$ tissues compared to cav1$^{+/+}$. We considered this result to be related to the function of β-adrenoceptors expressed on smooth muscle cells since our experiments were conducted after nerve blockade with tetrodotoxin. Considering that β-adrenoceptors were reported to be localized in caveolae[14,15,23] , a possible explanation could have been a reduction in the expression of β-adrenoceptors on smooth muscle cells in cav1$^{-/-}$ due to the absence of caveolae. However, using immunohistochemistry, we found that the different sub-types of β-adrenoceptors were not colocalized with caveolin-1 and were similarly present in cav1$^{-/-}$ and cav1$^{+/+}$ tissues. The localization of a particular G-protein-coupled receptor to caveolae is cell-type dependent[24] and a previous study on cav1$^{-/-}$ mice[25] showed that they retained the β-adrenoceptors in adipocytes.

Consequently, we concluded that the defect in β-adrenoceptor function in cav1$^{-/-}$ small intestine lay in the signal transduction pathway downstream of these receptors. We examined the roles of the different β-adrenoceptor sub-types in the (-)-isoprenaline-induced relaxation and whether the functional defect was in all or some of them. In cav1$^{+/+}$, both β_1- and β_2-antagonists shifted the CRC of (-)-isoprenaline to the right slightly but significantly suggesting that they might have a role in the relaxation due to (-)-isoprenaline. However, similar to previous observations in mouse intestine[22], β_3-adrenoceptors play a major role in the relaxation due to (-)-isoprenaline. On the other hand, none of the selective β-adrenoceptor blockers appeared to have a significant effect on the relaxation due to (-)-isoprenaline in cav1$^{-/-}$ small intestine. This suggests that the lower relaxing effect of (-)-isoprenaline observed in cav1$^{-/-}$ might be due to an altered response of all three β-adrenoceptor subtypes. A failure of the three β-adrenoceptor antagonists to shift the CRC of (-)-isoprenaline in cav1$^{-/-}$ muscle at the concentration used (0.1 μM), despite the persistence of a response to (-)-isoprenaline, might be due to the requirement for a higher concentration of antagonist in the cav1$^{-/-}$ muscle. Note that higher concentrations of (-)-isoprenaline were required to show responses in the cav1$^{-/-}$ tissues. This suggestion is supported by the observation that in the cav1$^{+/+}$ tissues in presence of the selective antagonists, the same high concentrations of (-)-isoprenaline produced responses similar to those of cav1$^{-/-}$. Moreover, the (-)-isoprenaline responses in cav1$^{-/-}$ were still sensitive to higher concentrations of the non-selective antagonist timolol.

Furthermore, to specifically examine the function of β_3-adrenoceptor, being the sub-type that is mainly responsible for relaxation due to (-)-isoprenaline in mouse small intestine, we used a selective β_3-agonist, BRL37344. Relaxation to BRL37344 was reduced in cav1$^{-/-}$ segments in comparison to cav1$^{+/+}$, again indicating a reduction in the β_3-adrenoceptor activity.

To examine further the defect in β-adrenoceptor signaling in the cav1$^{-/-}$ small intestinal tissue, we studied the effect of the PKA inhibitor H-89 on (-)-isoprenaline-induced relaxation. In the GIT β_3-adrenoceptors were shown to effect relaxation by a mechanism involving an increase in cAMP[26]. In cav1$^{+/+}$ tissues, H-89 caused about a 40-fold increase in the EC_{50} of (-)-isoprenaline indicating that the relaxation observed is due to the activation of PKA downstream of β-adrenoceptors. Conversely, in cav1$^{-/-}$ H-89 had no significant effect on the CRC of (-)-isoprenaline indicating that the reduced response to (-)-isoprenaline might be due to a decreased function of PKA. To investigate this possibility further, we examined the effect of H-89 on the relaxation of CCh-contracted tissues due to forskolin, a direct activator of adenylate cyclase, and di-bu cAMP, a membrane permeable analogue of cAMP. Only in cav1$^{+/+}$ tissue did H-89 reduce the relaxation due to forskolin and di-bu cAMP. The relaxation due to di-bu cAMP in cav1$^{-/-}$ tissues was very small in tissues not treated with H-89; in fact, it was similar to the response of cav1$^{+/+}$ control tissues treated with H-89. Taken together these results suggest a reduced functionof PKA in the small intestinal tissue of cav1$^{-/-}$ mice.

The relaxation elicited by forskolin and di-bu cAMP in cav1$^{-/-}$ could be attributed to PKA-independent effects. These have also been shown to exist in cav1$^{+/+}$ mice as a relaxation equivalent to that seen in the knockout mice persisted in cav1$^{+/+}$ tissues treated with H89. cAMP production by non-selective activation of adenylate cyclase i.e. through the use of forskolin, is not expected to be compromised in cav1$^{-/-}$ as many adenylate cyclase isoforms are known to exist mainly outside of caveolae[25]. Forskolin and cAMP were shown to elicit smooth muscle relaxation by opening of calcium-activated potassium channels through mechanisms that are not dependent on PKA activation[27,28]. In addition, cAMP was postulated to produce relaxation in the intestinal smooth muscles by PKA independent mechanisms such as the activation of uncoupling protein-1[29] or cross activation of PKG[30].

Immunohistochemical staining of the catalytic unit of PKA showed that it was colocalized with caveolin-1 in the cell membrane of smooth muscles in cav1$^{+/+}$ small intestine. This was similar to other results[31] where PKA was shown to be colocalized with caveolin-1 in aortic rings. Caveolin-1 interacted directly with PKA[32] and this interaction was necessary for the modulation of cAMP-mediated signal transduction[32]. In cav1$^{-/-}$, PKA immunoreactivity persisted despite the absence of caveolae. However, further examination of the expression of PKA showed that the distribution of PKA within the membrane domains is not identical in cav1$^{+/+}$ and cav1$^{-/-}$. In the presence of caveolin-1, PKA is concentrated in the lipid raft membrane fraction i.e. in close association with caveolin-1 and caveolae. In contrast, in the absence of caveolin-1, very little PKA is expressed in these domains providing more evidence to support a role of caveolin-1 in the regulation of PKA in small intestinal tissue. The persistence of PKA in cav1$^{-/-}$ in general is in agreement with previous findings in these mice[25] where PKA expression was maintained in adipocytes. In that study, it was shown that the main role of caveolin-1 was to recruit the target proteins to be phosphorylated by PKA downstream of β_3-adrenoceptor activation. This might be the case in the present study where the absence of caveolin-1 did not alter the expression of PKA but clearly reduced its activity in relaxing smooth muscle as shown in functional experiments. Potential target proteins that may be recruited by caveolin-1 for phosphorylation by PKA to produce smooth muscle relaxation include the inositol triphosphate receptor, plasma membrane calcium pumps, myosin light chain kinase, phospholamban[33], and ATP-dependent K^+ channels[34].

Nevertheless, the PKA-mediated phosphorylation of intracellular targets is not the only signal transduction mechanism downstream of β-adrenoceptors. In addition to the previously mentioned mechanisms by which cAMP can elicit PKA-independent relaxation, several other mechanisms have been suggested to be associated with β-adrenoceptor activation. Among these mechanisms are activation of extracellular signal-related kinases 1 and 2 (ERK 1 and 2)[35], activation of cytosolic phospholipase A_2[36], and the activation of calcium-activated potassium channels by Gs_α that occurs independent of cAMP and PKA in a membrane delimited manner[37]. Any of these mechanisms could be active in $cav1^{-/-}$ tissues to cause relaxation despite the reduced PKA activity and account for the residual response to β-adrenoceptor agonists. These assumptions must be tested by future studies of the nature of (-)-isoprenaline-induced relaxation in $cav1^{-/-}$.

To conclude, our present results suggest that the β-adrenoceptor function in the mouse small intestine is reduced due to caveolin-1 knockout. The absence of caveolae might have reduced the relaxation response seen as a result of β_3-adrenoceptor activation. This could be due to the reduced activity of PKA that requires the recruitment of target proteins by caveolin-1 to elicit full activity.

5.5 References

1. Kehlet H. Postoperative ileus. *Gut* 47: 85-86, 2000.
2. Kasparek MS, Kreis ME, Jehle EC, Zittel TT. Postoperative ileus: part I (Experimental results). *Zentralbl Chir* 128: 313-319, 2003.
3. Perry LB, Van Dyker A, and Theye RA. Sympathoadrenal and hemodynamic effect of isoflurane, halothane, and cyclopropane in dogs. *Anaesthesiol* 40: 465-470, 1974.
4. Stebbing JM, Johnson PJ, Vremec MA, and Bornstein JC. Role of the α_2-adrenoceptors in the sympathetic inhibition of motility reflexes in guinea pig ileum. *J Physiol* 534: 465-478, 2001.
5. Taneja DT and Clarke DE. Evidence for a noradrenergic innervation to "atypical" beta adrenoceptors (or putative beta-3 adrenoceptors) in the ileum of guinea pig. *J Pharmacol Exp Ther* 260: 192-200, 1992.
6. Johnson LR, Alpers DH, Christensen J, Jacobson ED, and Walsh JH. Physiology of the gastrointestinal tract (3rd ed.), pp 751-794, Raven Press, New York, 1994.
7. Shibata C, Balsiger BM, Anding WJ, and Sarr MG. Adrenergic denervation hypersensitivity in ileal circular smooth muscle after small bowel transplantation in rats. *Dig Dis Sci* 42: 2213-2221, 1997.
8. Ohtani N, Balsiger BM, Anding WJ, Duenes JA, and Sarr MG. Small bowel transplantation induces adrenergic hypersensitivity in ileal longitudinal smooth muscles in rats. *J Gastrointest Surg* 4:77-85, 2000.

9. Seiler R, Rickenbacher A, Shaw S, and Balsiger B. α- and β-adrenergic mechanisms in spontaneous contractile activity of rat ileal longitudinal smooth muscle. *J Gastrointest Surg* 9:227-235, 2005.

10. Anthony A, Schepelmann S, Guillaume JL, Strosberg AD, Dhillon AP, Pounder RE, and Wakefield AJ. Localization of the beta (beta)3-adrenoceptor in the human gastrointestinal tract: An iimmunohistochemical study. *Aliment Pharmacol Ther* 12: 519-525, 1998.

11. Scott JD. Cyclic nucleotide-dependent protein kinases. *Pharmac Ther* 50: 123-145, 1991.

12. Neubig RR. Membrane organization in G-protein mechanisms. *FASEB J* 8: 939-946, 1994.

13. Head BP, Patel HH, Roth DM, Chin Lai N, Niesman I, Farquhar MG, and Insel PA. G-protein-coupled receptor signaling components localize in both sarcolemmal and intracellular caveolin-3-associated domains in adult cardiac myocytes. *J Biol Chem* 280: 31036-31044, 2005.

14. Rybin VO, Xu X, Lisanti MP, and Steinberg SF. Differential targeting of β-adrenergic receptor sub-types and adenylate cyclase to cardiomyocyte caveolae. *J Biol Chem* 275: 41447-41457, 2000.

15. Schwencke C, Okamura S, Yamamoto M, Geng YG, and Ishikawa Y. Colocalization of β-adrenergic receptors and caveolin within plasma membrane. *J Cell Biochem* 75: 64-72, 1999.

16. Couet J, Li S, Okamoto T, Scherer PE, and Lisanti MP. Molecular and cellular biology of caveolae: Paradoxes and plasticities. *Trends Cardiovasc Med* 7: 103-110, 1997.

17. Krajewska WM and Maslowska I. Caveolins: structure and function in signal transduction. *Cell Mol Biol Lett* 9: 195-220, 2004.

18. Li S, Okamoto T, Chun M, Sargiacomo M, Casanova JE, Hansen SH, Nishimoto I, and Lisanti MP. Evidence for a regulated interaction between heterotrimeric G proteins and caveolin. *J Biol Chem* 270: 15693-15701, 1995.

19. Toya Y, Schwencke C, Couet J, Lisanti MP, and Ishikawa Y. Inhibition of adenylyl cyclase by caveolin peptides. *Endocrinology* 139: 2025-2031, 1998.

20. Daniel EE, Bodie G, Mannarino M, Boddy G, and Cho WJ. Changes in membrane cholesterol affect caveolin-1 localization and ICC pacing in the mouse jejunum. *Am J Physiol* 287: G202-G210, 2004.

21. Cho WJ and Daniel EE. Colocalization between caveolin isoforms in the intestinal smooth muscle and the interstitial cells of Cajal in Cav1(+/+) and Cav1(-/-) mouse. *Histochem Cell Biol* 126: 9-16, 2006.

22. Hutchinson DS, Evans BA, and Summers R. β_1-Adrenoceptors compensate for β_3-adrenoceptors in ileum from β_3-adrenoceptor knockout mice. *Br J Pharmacol* 132: 433-442, 2001.

23. Ostrom RS, Violin JD, Coleman S, and Insel PA. Selective enhancement of β-adrenergic receptor signaling by over-expression of adenylyl cyclase type 6: Colocalization of receptor and adenylyl cyclase in caveolae of cardiac myocytes. *Mol Pharmacol* 57: 1075-1079, 2000.

24. Ostrom RS and Insel PA. The evolving role of lipid rafts and caveolae in G protein-coupled receptor signaling: Implications for molecular pharmacology. *Br J Pharmacol* 143: 235-245, 2004.

25. Cohen AW, Razani B, Schubert W, Williams TM, Wang XB, Iyengar P, Brasaemle DL, Scherer PE, and Lisanti MP. Role of caveolin-1 in the modification of lipolysis and lipid droplet formation. *Diabetes* 53: 1261-1270, 2004.

26. Koike K, Horinouchi T, and Takayanagi I. Signal transduction pathway involved in beta-3-adrenoceptor-mediated relaxation in guinea pig taenia caecum. *Jpn J Pharmacol* 68: 41-46, 1995.

27. Zhu S, White RE, and Barman SA. Effect of PKC isozyme inhibition on forskolin-induced activation of BKCa channels in rat pulmonary arterial smooth muscle. *Lung* 184: 89-97.

28. Barman SA, Zhu S, Han G, and White RE. cAMP activates BKCa channels in pulmonary arterial smooth muscle via cGMP-dependent protein kinase. *Am J Physiol* 284: L1004-L1011, 2003.

29. Shabalina I, Wiklund C, Bengtsson T, Jacobsson A, Cannon B, and Nedergaard J. Uncoupling protein-1: involvement in a novel pathway for β-adrenergic, cAMP-mediated intestinal relaxation. *Am J Physiol* 283: G1107-G1116, 2002.

30. Murthy KS. Signaling for contraction and relaxation in smooth muscle of the gut. *Annu Rev Physiol* 68: 345-374, 2006.

31. Linder AE, McCluskey LP, Cole KR 3rd, Lanning KM, and Webb RC. Dynamic association of nitric oxide downstream signaling molecules with endothelial caveolin-1 in rat aorta. *J Pharmacol Exp Ther* 514:9-15, 2005.

32. Razani B, Rubin CS, and Lisanti MP. Regulation of cAMP-mediated signal transduction via interaction of caveolins with the catalytic subunit of protein kinase A. *J Biol Chem* 274: 26353-26360, 1999.

33. Viard P, Macrez N, Mironneau C, Mirroneau J. Involvement of both G protein αs and βγ subunits in β-adrenergic stimulation of vascular L-type Ca^{2+}-channels. *Br J Pharmacol* 132: 669-676, 2001.

34. Kravtsov GM, Hwang IS, and Tang F. The inhibitory effect of adrenomedullin in the rat ileum: cross-talk with beta 3-adrenoceptor in the serotonin-induced muscle contraction. *J Pharmacol Exp Ther* 308: 241-248, 2004.

35. Hutchinson DS, Bengtsson T, Evans BA, and Summers RJ. Mouse β_{3a}- and β_{3b}-adrenoceptors expressed in Chinese hamster ovary cells display identical pharmacology but utilize distinct signaling pathways. *Br J Pharmacol* 135: 1903-1914, 2002.

36. Ait-Mamar B, Cailleret M, Rucker-Martin C, Bouabdallah A, Canadiani G, Adami C, Duvaldestin P, Pecker F, Defer N, and Pavoine C. The cytosolic phospholipase A_2 pathway, a safeguard for β_2-adrenergic cardiac effects in rat. *J Biol Chem* 280: 18881-18890, 2005.

37. Kume H, Hall IP, Washabau RJ, Takagi K, and Kotlikoff MI. β-adrenergic agonists regulate K_{Ca} channels in airway smooth muscle by cAMP-dependent and independent mechanisms. *J Clin Invest* 93: 371-379, 1994.

CHAPTER VI

LOSS OF SMOOTH MUSCLE NITRIC OXIDE SYNTHASE FUNCTION IN CAVEOLIN-1 KNOCKOUT MOUSE SMALL INTESTINE

A version of this chapter is currently under review in the *American Journal of Physiology-Gastrointestinal and Liver Physiology*. El-Yazbi AF, Cho WJ, Cena J, Schulz R, and Daniel EE. Smooth muscle nitric oxide synthase, colocalized with caveolin-1, modulates depolarization-induced contraction in mouse small intestine.

6.1 Introduction:

Nitric oxide is a key regulator of multiple biological processes in different organs and systems in the body. It is synthesized by the reaction of L-arginine and oxygen catalyzed by a group of enzymes called nitric oxide synthases to produce NO and citrulline. At least three distinct isoforms of NOS exist in mammalian cells: endothelial NOS (eNOS), neuronal NOS (nNOS), and inducible NOS (iNOS)[1]. Ca^{2+}-dependent NOS activity was first localized in neurons by Bredt *et al.*[2] where it releases NO to act as a neurotransmitter or retrograde messenger, and was later named neuronal NOS. However, following its identification in neurons, further examination of nNOS distribution showed that it existed in several other tissues including skeletal muscle[3], vascular smooth muscle[4], and in the cell membrane of intestinal smooth muscle in both dogs[5] and mice[6].

The earliest examination of the function of nNOS expressed outside nerve cells was in skeletal muscle tissue[7]. There the NO produced was shown to modulate the contractile activity of skeletal muscle through the activation of soluble guanylate cyclase. In vascular smooth muscle, NO produced by nNOS was shown to be responsible for reduced vascular contractility in hypoxia[8]. In dog lower oesophageal sphincter, smooth muscle nNOS activity was shown to be important in the modulation of the generated tone through the regulation of potassium channel activity[5].

Similar to eNOS, nNOS activity was shown to be regulated *in vitro* by its interaction with caveolin-1[9]. Caveolin-1 was shown to inhibit nNOS activity by interfering with calcium/calmodulin binding[9,10]. Moreover, examination of the *in vivo* distribution of nNOS and caveolin proteins showed that they were colocalized in skeletal muscle plasma membrane[9] and cell membranes of vascular smooth muscle[11], canine lower esophageal sphincter muscle[12], mouse small intestinal smooth muscle, and interstitial cells of Cajal[13].

Caveolin-1 knockout mice were shown to lack morphologically identifiable caveolae in tissues expressing caveolin-1. They show a number of abnormalities including defects in caveolar endocytosis, lung hypercellularity, decreased vascular tone, and atrophic fat pads[14]. Since nNOS is colocalized with caveolin-1 in mouse small intestine, we hypothesize that its function will be altered or lost in caveolin-1 knockout tissue. In the present study, we compared contractile responses as a result of NOS inhibition following an increase in intracellular Ca^{2+} concentration in caveolin-1 knockout and wild type small intestine to address the possible function of NOS expressed in small intestinal smooth muscle.

6.2 Materials and methods:

6.2.1 Functional experiments:

6.2.1.1 Tissue preparation:

CM from small intestinal tissue from BALB/c, $cav1^{+/+}$, and $cav1^{-/-}$ mice was isolated and set up to record contraction as described in Chapter II.

6.2.1.2 Experimental protocols:

Neuronal activity in intact tissue segments was blocked by 1 μM TTX and ω-conotoxin GVIA (1 μM). The blockade was ascertained by examining the response to electric field stimulation after TTX. Tissues were equilibrated for 25 min. After the equilibration period, tissues were contracted using 60 mM KCl and the contractions were allowed to reach a plateau. In some experiments, cyclopiazonic acid (1 μM), or CCh (10 μM) was added instead of KCl. Following the plateau of tissue tension or after 5 min following the addition of any of the previous drugs, the tissues were treated with 100 μM LNNA, 1 μM ODQ, 1 μM apamin, or 0.1 μM iberiotoxin (IBTx). In some of the KCl and CCh experiments, the tissues were pre-treated with nicardipine (1 μM).

In some experiments membrane cholesterol was presumably depleted by incubating the control mouse tissue for 1 hour at 37°C in Krebs-Ringer solution containing 40 mM methyl-β-cyclodextrin (Me-β-CDX) and continuously bubbled with carbogen. In some of these tissues 2.54 mM water soluble cholesterol in Krebs-Ringer was incubated for 1 hour at 37°C to replete the membrane cholesterol. KCl and LNNA were added to cholesterol depleted tissues and tissues treated with Me-β-CDX and water soluble cholesterol.

6.2.1.3 Data analysis and statistics:

The increase in tissue contractile tone was measured 5 min following the addition of LNNA at which time any additional contraction of the tissue reached a plateau. The increase in the tone of contraction following LNNA addition was normalized to the amplitude of the tone prior to the addition of KCl. Statistical comparisons were done as described in Chapter II.

6.2.2 Immunohistochemistry:

Tissue preparation, cryosections, whole mount preparations, immunostaining, and confocal imaging were done as described in Chapter II. The primary and secondary antibodies used are summarized in Table 6.1.

6.2.3 Co-immunoprecipitation and Western blotting:

A whole tissue homogenate was prepared from BALB/c mouse small intestine as described in Chapter II. The homogenate was divided into 500 µl aliquots. In some aliquots calcium chloride was added so that the final calcium concentration was 2 mM and calmodulin was added so that the final concentration was 5 µM. The aliquots were incubated with 5 µg/ml mouse anti-caveolin-1 or mouse IgG negative control overnight at 4°C. 50 µl aliquots of 50% slurry of protein G-coated sepharose beads were incubated with the mixture overnight at 4°C. The beads were separated from the homogenate by centrifugation at 12,000 *g*. The beads were separated and then washed three times in a high stringency buffer containing 500 mM NaCl, 1% IGEPAL CA-630, 50 mM Tris pH 8.0, and 1 mM phenylmethanesulfonylfluoride. This was followed by one wash in washing buffer (50 mM Tris, pH 8.0). The beads were then suspended in an elution buffer containing 1% sodium dodecyl sulphate, 100 mM dithiothreitol, 3% β-mercaptoethanol, 50 mM Tris pH 7.5. The mixture was heated at 95°C for 3 minutes followed by centrifugation to separate the beads. 1 µl of 0.1% bromophenol blue was added to the supernatant which was then loaded on a polyacrylamide gel and blotted as described in Chapter II using a 1:1000 mouse anti-nNOS (primary antibody) concentration.

Table 6.1 Antibodies and normal sera used in Chapter VI.

Antibody	Host	Dilution	Peptide	Source
			Primary	
Cav-1	Mouse	1:100	yes	BD Transduction Labs.
nNOS-C	Guinea Pig	1:100	no	Euro-Diagnostica
nNOS-N	Rabbit	1:100	no	Euro-Diagnostica
HuC/D	Mouse	1:100	no	Molecular Probes
			Secondary	
Cy3-conjugated donkey anti-mouse IgG				Jackson ImmunoResearch Labs.
FITC-conjugated donkey anti-guinea pig IgG				Research Diagnostics
Alexa488-conjugated donkey anti-rabbit IgG				Molecular Probes
			Sera	
Normal donkey serum		566460 / Calbiochem		

Cav-1, caveolin-1; nNOS-C, neuronal nitric oxide synthase, COOH- epitope; nNOS-N, neuroal nitric oxide synthase, NH_2-epitope; HuC/D, HuC/HuD neuronal protein (human); Peptide, antigenic peptide used to saturate the corresponding primary antibody.

1:4000 HRP-conjugated goat anti-mouse IgG was used as secondary antibody.

6.2.4 Measurement of NOS activity:

NOS activity was measured in whole homogenates and lipid-raft rich membrane fractions of small intestinal tissues from BALB/c mice using a method previously described[15]. The conversion of L-[^{14}C]arginine to [^{14}C]-citrulline was measured and used to estimate NOS activity. 20 µl aliquots of the samples were incubated with radioactive arginine (0.66 µCi/ml) in a reaction mixture containing: L-valine (7 mg/ml), KH_2PO_4 (50 mM), $MgCl_2$ (1.2 mM), $CaCl_2$ (0.24 mM), NADPH (119.5 µM), dithiothreitol (1.2 mM), L-citrulline (1.2 mM), cold L-arginine (22 µM), and tetrahydrobiopterin (12 µM). The incubation lasted for 120 min at 37ºC. The NOS inhibitor N^G-monomethyl-L-arginine (1 mM) was added to some samples to determine the reduction in counts due to NOS activity. EGTA (1 mM) was added to some samples to measure the calcium-independent NOS activity. Following the incubation the reaction was stopped by the addition of 1 ml 30% slurry of the activated ion exchange resin 50W-X8. After centrifugation at 16,000 *g* the supernatant was removed and its radioactivity was measured in a Beckman LS6500 scintillation counter. Background, total activity, and rat brain homogenate controls were measured alongside with the samples. The number of counts was normalized to the protein content of the sample and used as an indication of NOS activity.

6.2.5 Materials:

IBTx, cyclopiazonic acid, nicardipine, Me-β-CDX, water soluble cholesterol, phenylmethanesulfonylfluoride, L-valine, NADPH, dithiothreitol, L-citrulline, L-arginine, tetrahydrobiopterin, N^G-monomethyl-L-arginine and protease inhibitor cocktail were purchased from Sigma (Oakville, ON). ω-conotoxin GVIA was purchased from the Alomone Labs (Jerusalem, Israel). Monoclonal mouse anti-nNOS was purchased from BD Transduction Laboratories (Mississauga, ON). Mouse IgG control was purchased from Chemicon (Temecula, CA). Calmodulin was purchased from Biogenesis (Kingston, NH). 50W-X8 resin was from Bio-Rad Laboratories (Hercules, CA). L-[^{14}C]-arginine was from GE Healthcare (Piscataway, NJ).

6.3 Results:

6.3.1 Immunohistochemical staining of cryosections and whole mount preparations:

In experiments where primary or secondary antibodies were omitted, no immunoreactivity was seen (data not shown). Similar to BALB/c mice[13], cav1$^{+/+}$ small intestine cryosections showed nNOS C-terminal and caveolin-1 immunoreactivity colocalized in the smooth muscle plasma membrane (Fig 6.1a-c). The cav1$^{-/-}$ cryosections lacked immunoreactivity for both proteins (Fig 6.1d). On the other hand, examination of myenteric ganglia in whole mount preparations from both cav1$^{+/+}$ and cav1$^{-/-}$ showed that nNOS N-terminal immunoreactivity is expressed in neuronal cells of both mice strains (Fig 6.1e-j). An antibody to HuC/D protein was used to localize cell bodies of myenteric nerves (Fig 1e,h).

6.3.2 Co-immunoprecipitation and Western blotting:

Immunoprecipitation of caveolin-1 from BALB/c mouse small intestine homogenate followed by probing for nNOS showed a nNOS band at 150 kD (Fig 6.2). Immunoprecipitation in the presence of high calcium and calmodulin greatly reduced the nNOS band intensity. Tissue homogenates were also immunoprecipitated with the control mouse IgG under the regular low calcium conditions. No nNOS band was detected in the lanes corresponding to these treatments.

6.3.3 Functional experiments:

6.3.3.1 Spontaneous tone:

The spontaneous tone developed in each of the tissues was measured (relative to tone in calcium-free solution) before the addition of KCl and used as the 100% value to normalize the increase in tone that follows the addition of LNNA after KCl. The values of spontaneous tone developed were not different in BALB/c, $cav1^{+/+}$, and $cav1^{-/-}$ and were (in mg tension) 43.7±7.5 (*n*=13), 40.4±6.3 (*n*=6), and 40.5±4.8 (*n*=8), respectively.

6.3.3.2 Effect of LNNA on tissues contracted with KCl:

Mouse small intestinal tissues responded to 60 mM KCl by a transient phasic contraction that decayed gradually into a sustained increase in contractile tone (Fig 6.3).

Fig 6.1 Cryosections (a-d) and whole mount preparations (e-j) of $cav1^{+/+}$ and $cav1^{-/-}$ mice small intestine immunostained for caveolin-1 and nNOS. Panels (a-c) show caveolin-1 (a, red) and nNOS (b, green) immunoreactivity and their colocalization in the merged image (c, yellow) in the smooth muscle cell membrane of $cav1^{+/+}$ mice. Panel d is a merged image showing the absence of both caveolin-1 and nNOS immunoreactivity in $cav1^{-/-}$ mice. The scale bar is 10 µm. icm, inner circular muscle layer; ocm, outer circular muscle layer; and lm, longitudinal muscle layer. Arrows point to interstitial cells of Cajal in the myenteric plexus layer. Panels (e-j) show immunostained myenteric ganglia in $cav1^{+/+}$ (e-g) and $cav1^{-/-}$ (h-j) mice. Myenteric neuron cell bodies were localized by staining with HuC/D antibodies (e and h, red). Panels f and i show nNOS in myenteric ganglia (green). Panels g and j are merged images showing the colcalization of staining in the cytoplasm of cell bodies (yellow). Scale bar is 5 µm (immunostaining and confocal imaging were done by Woo Jung Cho).

Fig 6.1

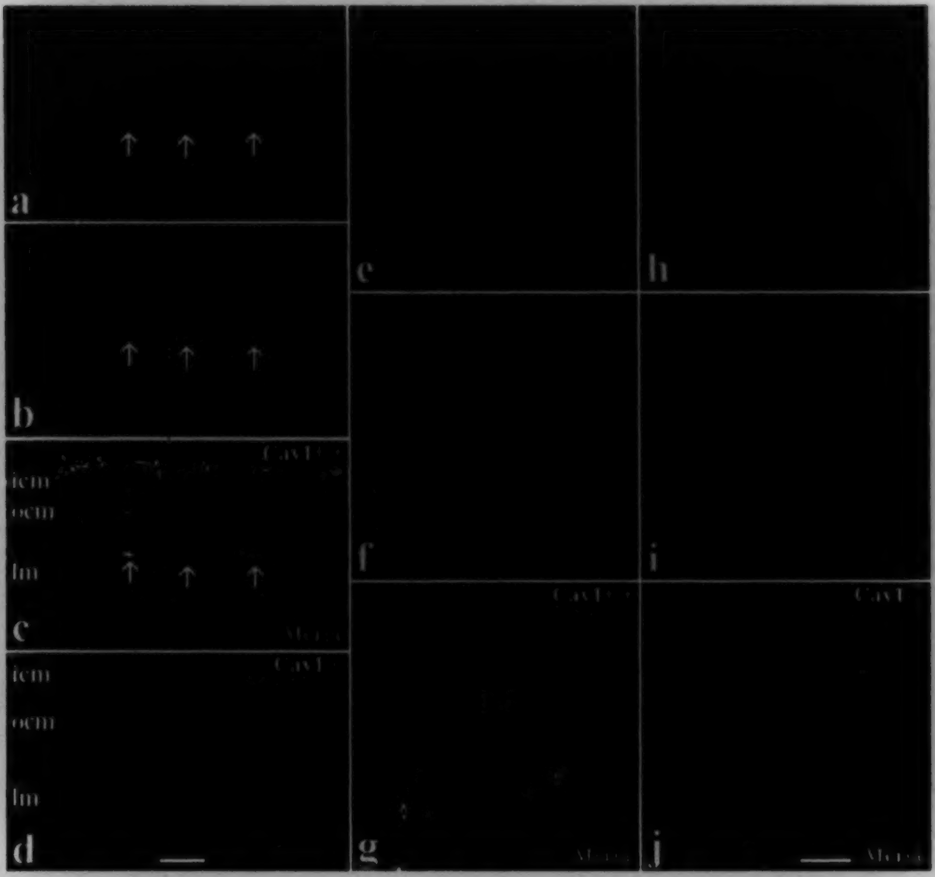
a
b
icm
ocm
lm
c
icm
ocm
lm
d
e
f
g
h
i
j
Cav1

Fig 6.2 Representative blot of nNOS immunoprecipitated from BALB/c mouse small intestinal homogenate with anti-caveolin-1 antibody. The amount of nNOS pulled down in high calcium (2 mM) and calmodulin (5 μM) is very much reduced compared to the amount pulled down when no exogenous calcium and calmodulin were added. Control mouse IgG was used to show the selectivity of the co-immunoprecipitation. Control IgG was added in conditions where no exogenous calcium and calmodulin were added. The blot is representative of four experiments with similar results (Jonathan Cena helped in doing this experiment).

Fig 6.2

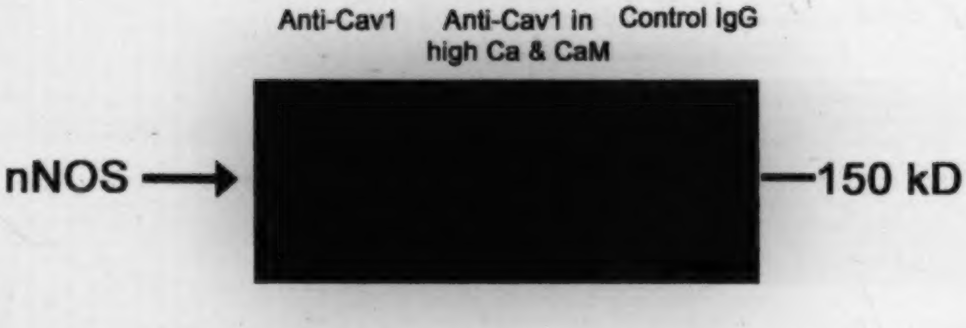
Anti-Cav1
Anti-Cav1 in high Ca & CaM
Control IgG
nNOS
150 kD

Addition of 100 μM LNNA after the KCl contraction plateaued caused an increase in the tone of contraction in BALB/c and cav1$^{+/+}$ tissue segments (Fig 6.3a). The increase in tonic contraction was very much reduced in the cav1$^{-/-}$ tissues when compared to the controls (Fig 6.3b).

6.3.3.3 Effect of cholesterol depletion on nNOS immunoreactivity and tissue response to LNNA:

Plasma membrane cholesterol was presumably depleted by incubating the tissue preparations for 1 hour in 40 mM Me-β-CDX. In these tissues the immunoreactivities of both nNOS C-terminal and caveolin-1 in smooth muscle cell membrane were reduced (Fig 6.4a). Although these tissues maintained their phasic activity and responded to KCl by contraction, they showed very little increase in contractile tone when LNNA was added following KCl (representative tracing in Fig 6.4b). However, when 2.54 mM water soluble cholesterol was used to replete the membrane cholesterol following depletion, the immunoreactivities of nNOS C-terminal and caveolin-1 in the smooth muscle plasma membrane were restored and the response to LNNA became similar to control levels (Fig 6.4c).

6.3.3.4 Effects of agents altering intracellular calcium levels:

The response to LNNA added after tissue preparations from BALB/C mice were incubated with compounds presumed to increase the intracellular cytosolic calcium level in ways other than by the opening of L-type calcium channel was studied. The SERCA inhibitor, cyclopiazonic acid (10 μM), was incubated with the tissue to block the reuptake

Fig 6.3 Effect of LNNA (100 µM) on contractile tone of BALB/c, cav1$^{+/+}$, and cav1$^{-/-}$ intestinal tissue preparations following depolarization by KCl (60 mM). a. Representative tracings showing the increase in tone after LNNA treatment only in BALB/c and cav1$^{+/+}$ but not in cav1$^{-/-}$ tissue. b. The increase in contractile tone, shown as mg tension increase after LNNA and the same value normalized to the initial tone developed by the tissue, is much reduced in cav1$^{-/-}$ in comparison to the control mice. *n* values are 13 for BALB/c, 6 for cav1$^{+/+}$, and 8 for cav1$^{-/-}$. Statistical analysis was done by ANOVA followed by Bonferroni *post hoc* test and significance is denoted by *$P<0.05$, **$P<0.01$, and ***$P<0.001$.

Fig 6.3

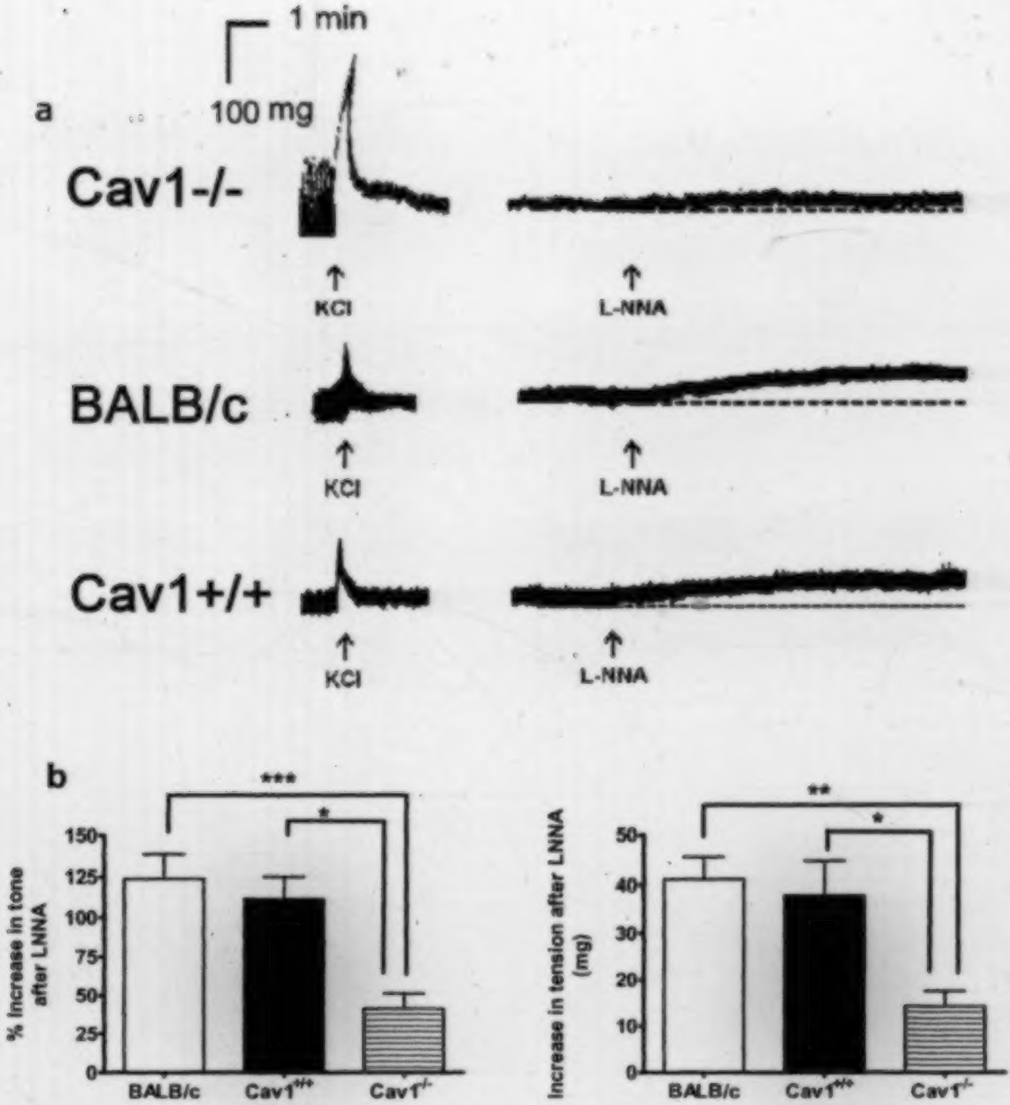
a
1 min
100 mg
Cav1-/-
KCl
L-NNA
BALB/c
KCl
L-NNA
Cav1+/+
KCl
L-NNA
b
***
*
% Increase in tone after LNNA
0
25
50
75
100
125
150
BALB/c
Cav1+/+
Cav1-/-
**
*
Increase in tension after LNNA (mg)
0
10
20
30
40
50
BALB/c
Cav1+/+
Cav1-/-

Fig 6.4 Effect of caveolae disruption by cholesterol depletion on the immunoreactivities of caveolin-1 and nNOS in smooth muscle cell membrane and the response to LNNA (100 µM) following tissue depolarization by KCl (60 mM) in BALB/c mouse small intestine. a. Immunostained cryosections of BALB/c mice small intestinal tissues showing the effects of Me-β-CDX treatment (a-c) and Me-β-CDX followed by water soluble cholesterol panels (d-f) on caveolin-1 (red) and nNOS (green) immunoreactivities and their colocalization (yellow). Scale bar is 10 µm. b. Representative tracings. c. Increase in tone after LNNA is added. *n* values are 13 for control and 5 for Me-β-CDX and Me-β-CDX/water soluble cholesterol treated tissues. Statistical analysis was done by ANOVA followed by Bonferroni *post-hoc* test and significance is denoted by $^{**}P<0.01$ and $^{***}P<0.001$.

Fig 6.4

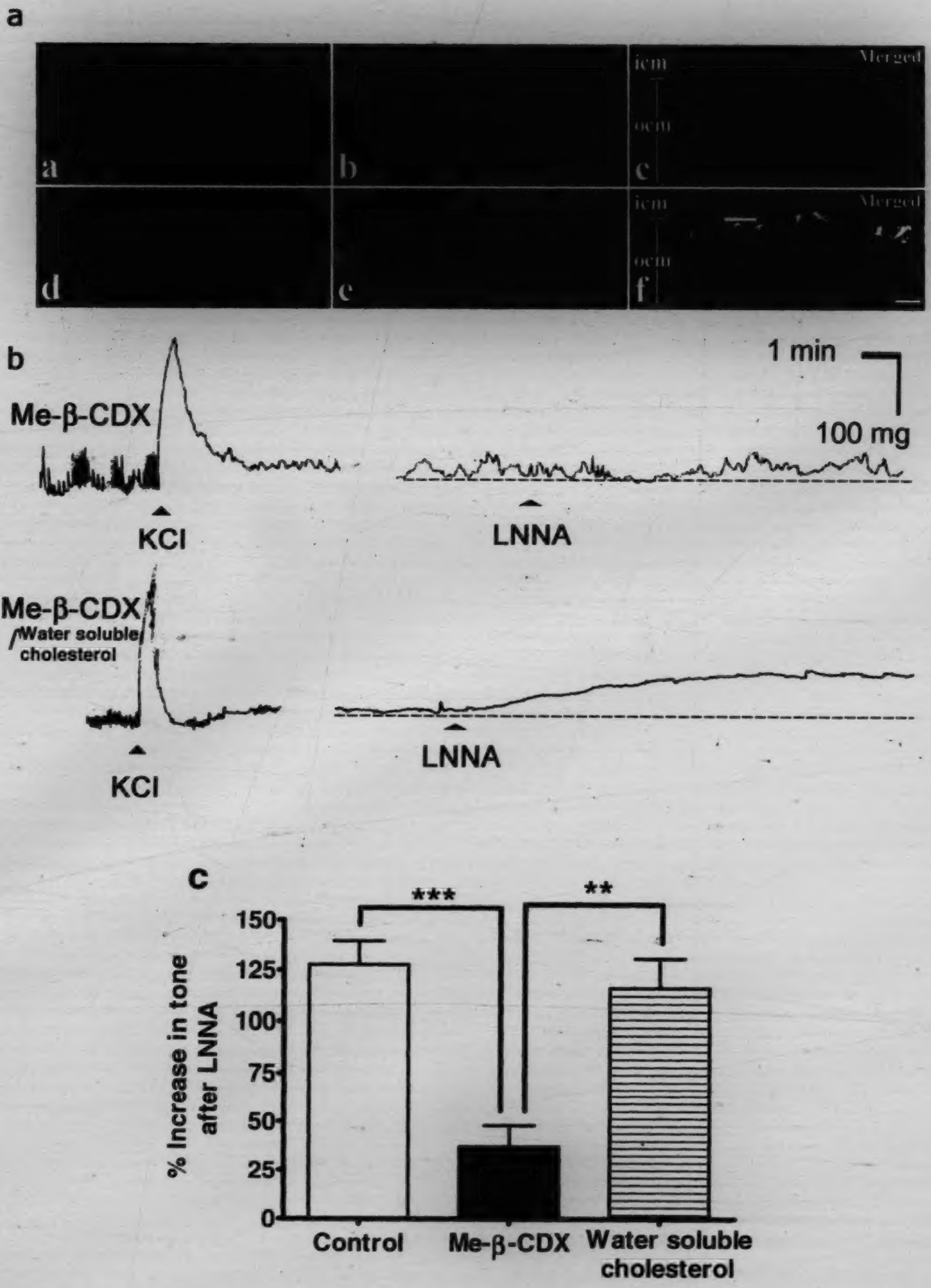
a
a
b
c
d
e
f
icm
ocm
Merged
icm
ocm
Merged
b
Me-β-CDX
1 min
100 mg
KCl
LNNA
Me-β-CDX /Water soluble cholesterol
KCl
LNNA
c
***
**
% Increase in tone after LNNA
150
125
100
75
50
25
0
Control
Me-β-CDX
Water soluble cholesterol

of the cytosolic calcium into the sarcoplasmic reticulum. In other tissues 10 µM CCh was used to increase intracellular calcium by both release from the sarcoplasmic reticulum and activation of L-type calcium channels. Addition of 100 µM LNNA five min after cyclopiazonic acid did not result in an increase in the tone of contraction while LNNA after CCh resulted in a small, significant increase in contractile tone (Fig 6.5a). On the other hand, pretreatment of the tissues with the L-type calcium channel blocker, nicardipine (1 µM), during the equilibration period abolished the tissue response to KCl and greatly reduced the response to LNNA added afterwards (Fig 6.5b). In addition, nicardipine partially reduced the contractile response to CCh. However, it abolished the response to LNNA added afterwards (Fig 6.5c and d). Adding LNNA to cav1$^{-/-}$ tissues treated with either cyclopiazonic acid or CCh did not result in an increase in tone (data not shown).

6.3.3.5 Effect of blocking NO action:

The effects of some pharmacological agents that block the action of NO on intracellular targets added after tissue depolarization with KCl were studied. The soluble guanylate cyclase inhibitor ODQ (1 µM), added after the KCl contraction plateaued, increased the tone of the contraction similar to LNNA. However, small and large calcium-activated potassium channel blockers, apamin (1 µM) and iberiotoxin (0.1 µM), did not produce a further increase in the contractile tone (Fig 6.6).

Fig 6.5 Increase in contractile tone by LNNA (100 µM) following different agents affecting intracellular calcium in BALB/c mice intestinal tissue. a. CCh only showed a partial increase in tone when LNNA was added. Cyclopiazonic acid did not cause an increase in the contractile tone when LNNA was added. *n* values are 13 for KCl, and 6 for CCh and cyclopiazonic acid. Statistical analysis was done by ANOVA followed by Bonferroni *post-hoc* test and significant difference from KCl is denoted by $^{***}P<0.001$. b. Blocking L-type calcium channels with nicardipine prior to tissue depolarization by KCl markedly reduced the increase in contractile tone when LNNA was added to the tissues. c. Representative tracings showing the tissue response to CCh and the increase in tone after the addition of LNNA. Nicardipine-treated tissues still responded with a contraction to CCh, however, they showed no further response to LNNA afterwards. d. Blocking L-type calcium channels with nicardipine prior to the addition of CCh abolished the increase in contractile tone when LNNA was added to the tissues. *n* values are 5 for the nicardipine treated tissues. Statistical analysis was done by *t*-test and significance is denoted by $^{**}P<0.01$ and $^{***}P<0.001$.

Fig 6.5

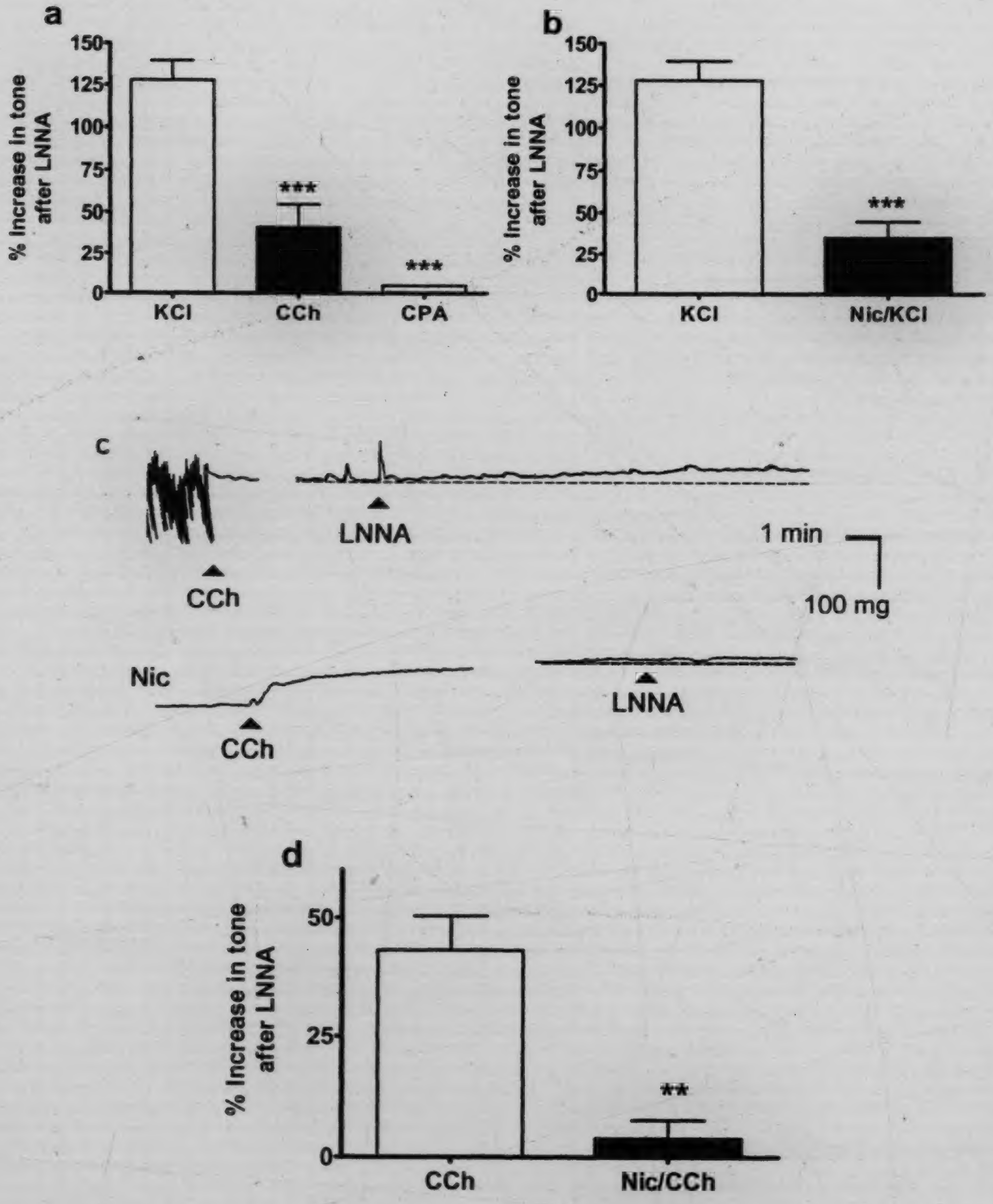
a
% Increase in tone after LNNA
150
125
100
75
50
25
0
***
***
KCl
CCh
CPA
b
% Increase in tone after LNNA
150
125
100
75
50
25
0
***
KCl
Nic/KCl
c
CCh
LNNA
1 min
100 mg
Nic
CCh
LNNA
d
% Increase in tone after LNNA
50
25
0
**
CCh
Nic/CCh

Fig 6.6 Effects of different agents acting on the signal transduction mechanisms downstream of NO on BALB/c intestinal tissue following depolarization by KCl (60 mM). *n* values are 13 for LNNA, 6 for ODQ and apamin, and 5 for IBTx. Statistical analysis was done by ANOVA followed by Bonferoni *post hoc* test and a significant difference from KCl/LNNA is denoted by ***$P<0.001$.

Fig 6.6

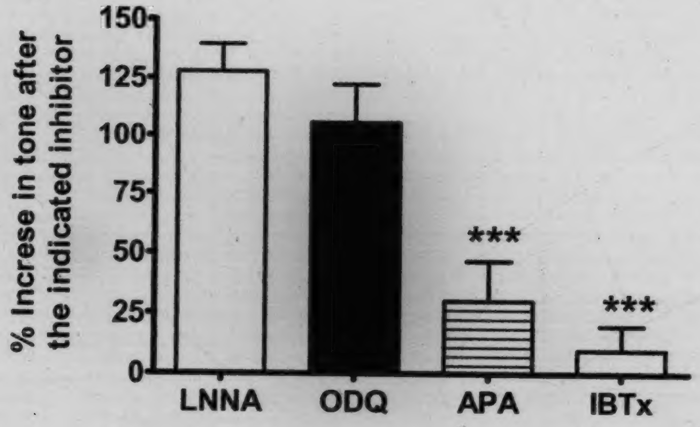

% Increse in tone after the indicated inhibitor
150
125
100
75
50
25
0
***
***
LNNA
ODQ
APA
IBTx

6.3.4 *Measurement of NOS activity:*

No calcium-dependent or calcium-independent NOS activity was detected in any of the samples derived from mouse small intestine. There was no reduction in the number of counts measured after the addition of EGTA and/or N^G-monomethyl-L-arginine in all of the samples tested.

6.4 Discussion:

In the present study we used immunohistochemistry and co-immunoprecipitation to show the association of caveolin-1 and nNOS in the small intestine of BALB/c mice. Previous studies showed that nNOS and caveolin-1 can interact directly *in vitro*[9] or indirectly through binding to the dystrophin complex[16] that interacts directly with the caveolin proteins[17]. Here we also showed that the interaction between caveolin-1 and nNOS is weakened in presence of calmodulin and a high calcium concentration. This provides evidence in an *ex vivo* model that nNOS is regulated by caveolin-1 in a manner similar to eNOS by interference with calcium and calmodulin binding.

Immunohistochemical examination of $cav1^{-/-}$ mice and their $cav1^{+/+}$ controls showed that small intestinal tissues from $cav1^{-/-}$ lacked, besides caveolin-1, the nNOS splice variant expressed in the smooth muscle plasma membrane (recognized by the antibody raised against the C-terminal epitope) but not the nNOS splice variant expressed in the myenteric plexus nerves (recognized by the antibody raised against the N-terminal epitope). This alteration further supports the association between caveolin-1 and nNOS in smooth muscle plasma membrane in the small intestine. Moreover, since they lack only nNOS in smooth muscle cells but not in myenteric neurons, cav1$^{-/-}$ mice offer a convenient model to act as a negative control in the study of the smooth muscle nNOS function. Since the activity of nNOS is calcium-dependent[18], we tested the function of the smooth muscle NOS using agents that increase intracellular calcium concentration. To avoid the activation of nNOS present in enteric neurons, our experiments were conducted after blocking the activity of the enteric neurons using TTX and ω-conotoxin GVIA. In BALB/c and cav1$^{+/+}$ tissues, activating the smooth muscle L-type calcium channels by depolarization with 60 mM KCl caused a phasic contraction that decayed into a sustained plateau phase. At this stage LNNA was added to block the smooth muscle nNOS activity. The resultant increase in the tone of contraction indicates that this enzyme was active in producing NO which modulated smooth muscle contraction in response to KCl. On the other hand, cav1$^{-/-}$ tissues that lack nNOS in smooth muscle, showed a very small increase in the tone of contraction when LNNA was added after KCl, indicating that the modulatory role of nNOS on the contraction is absent. In these experiments, we used cav1$^{+/+}$ controls in addition to BALB/c mice to show that the absence of the LNNA response in cav1$^{-/-}$ mice is linked to the absence of nNOS from smooth muscle cells, rather than because of a strain variation.

Further evidence to the role of activated smooth muscle nNOS in the modulation of the KCl contraction was provided by experiments using BALB/c mouse tissue that was incubated with Me-β-CDX that is known to disrupt caveolae by depletion of plasma membrane cholesterol. We previously showed that treatment of mouse small intestinal tissues with Me-β-CDX resulted in the loss of caveolin-1 immunoreactivity from the cell membrane and the loss of caveolae structures as shown using electron microscopy[19]. In the present study, we showed that disruption of caveolae by membrane cholesterol depletion reduced both nNOS and caveolin-1 immunoreactivity in the smooth muscle membrane. This was expected as we showed that nNOS is associated with caveolin-1. Me-β-CDX-treated tissues maintained their phasic activity and responded normally to KCl. However, these tissues responded very weakly to the addition of LNNA after KCl. Incubation of the Me-β-CDX-treated tissues with water soluble cholesterol to replete membrane cholesterol restored the response to LNNA and also the plasma membrane caveolin-1 and nNOS immunoreactivities. These results provide further evidence to the proposed function of nNOS i.e., that it requires the presence of nNOS presence in intact caveolae structures in the plasma membrane.

In addition to KCl, which activates L-type Ca^{2+} channels, we examined the effects of other agents which alter the level of cytosolic calcium. Addition of LNNA after the SERCA pump inhibitor cyclopiazonic acid did not produce an increase in contractile tone. On the other hand, CCh being a non-selective cholinergic agonist, is reported to induce smooth muscle contraction in mouse small intestine via two pathways[20]. The first pathway is the activation of M_3 receptors and the release of intracellular calcium and the second one is the activation of M_2 receptors which involves calcium entry through L-type calcium channels. The addition of LNNA to tissues treated with CCh resulted in an increase in the tone of contraction that was less than that seen in the case of KCl stimulation. This agrees with the partial dependence of the contractile effect of CCh on activation of L-type calcium channels in mouse small intestine. The importance of the activation of L-type calcium channels to obtain a response to LNNA was further shown by the absence of a response to LNNA after either KCl or CCh in tissues pre-treated with the L-type calcium channel blocker, nicardipine. We previously showed[13] that, although L-type calcium channels are not exclusively found in caveolae in mouse small intestine, they are co-localized with caveolin-1 to some degree. This makes the increase in cytosolic calcium concentration due to L-type calcium channel activation higher in the caveolar domains very near to the smooth muscle nNOS (see Fig 6.7) rather than a diffuse increase or accumulation of calcium brought about by the release of intracellular calcium or blockade of its uptake.

Following NOS activation the biosynthesized NO relaxes (or reduces the contraction of) smooth muscle through a number of mechanisms. The main intracellular receptor for NO is soluble guanylate cyclase[21]. Blocking soluble guanylate cyclase activity with ODQ following smooth muscle depolarization with KCl led to an increase in contractile tone that was similar to the use of LNNA. This indicates that NO produced by the smooth muscle nNOS activates soluble guanylate cyclase that produces cGMP. The latter in turn causes smooth muscle relaxation through different mechanisms (reviewed in[22]). The activation of calcium-activated potassium channels by NO in smooth muscle cells can occur independent of cGMP[23], leading to relaxation. In the present study we examined the role of both large conductance and small conductance calcium-activated potassium channels in the proposed action of smooth muscle nNOS using the selective blockers iberiotoxin and apamin, respectively. However, neither agent had an effect on contractile tone when added after KCl.

The results of the present study suggest that nNOS expressed in the caveolae of mouse small intestinal smooth muscle is involved in the modulation of contraction resulting from L-type calcium channels activation by NO and cGMP-dependent mechanism. L-type calcium channel activation is essential for the rhythmic contraction of smooth muscle in mouse small intestine[24]. The rhythmic contractions of smooth muscle occurring in almost all mammalian gut tissues are an important part of the normal physiological function of the intestine. Disruption of this function leads to serious effects on the overall intestinal function such as that observed in Hirschsprung's disease[25]. However, the implications of the results of the present study on the pathophysiological changes in the intestine remain yet to be determined.

Fig 6.7 Hypothesized role of smooth muscle nNOS in the regulation of contraction induced by depolarization. Activation of L-type calcium channels and calcium influx triggers contraction as well as the activation of nNOS through calmodulin and dissociation form caveolin-1. The activated NOS produces NO that in turn activates soluble guanylate cyclase to produce cGMP which triggers a number of mechanisms to counteract the contraction.

Fig 6.7

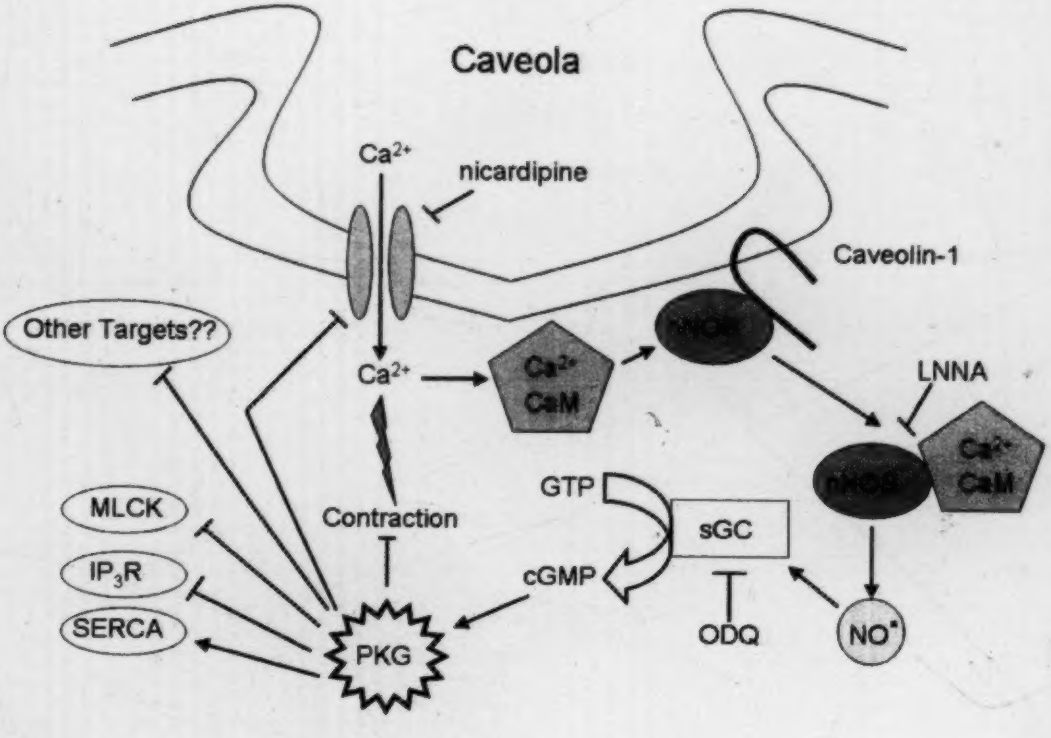
Caveola
Ca^{2+}
nicardipine
Caveolin-1
Other Targets??
Ca^{2+}
Ca^{2+} CaM
LNNA
nNOS
Ca^{2+} CaM
GTP
sGC
MLCK
Contraction
IP_3R
cGMP
SERCA
ODQ
NO$^\bullet$
PKG

6.5 References

1. Moncada S and Higgs EA. The discovery of nitric oxide and its role in vascular biology. *Br J Pharmacol* 147: S193-S201, 2006.
2. Bredt DS, Hwang PM, and Snyder SH. Localization of nitric oxide synthase indicating a neural role of nitric oxide. *Nature* 347: 768-770, 1990.
3. Nakane M, Schmidt HHHW, Pollock JS, Forstemann U, and Murad F. Cloned human brain nitric oxide synthase is highly expressed in skeletal muscle. *FEBS Lett* 316: 175-180, 1993.
4. Boulanger CM, Heymes C, Benessiano J, Geske RS, Levy BI, and Vanhoutte PM. Neuronal nitric oxide synthase is expressed in rat vascular smooth muscle cells: activation by angiotensin II in hypertension. *Circ Res* 83: 1271-1278, 1998.
5. Salapatek AM, Wang YF, Mao YK, Mori M, and Daniel EE. Myogenic NOS in canine lower esophageal sphincter: enzyme activation, substrate recycling, and product actions. *Am J Physiol* 43: C1145-C1157, 1998.
6. Mule F, Vannuchi MG, Corsani L, Serio R, and Faussone-Pellegrini MS. Myogenic NOS and endogenous NO production are defective in colon from dystrophic (*mdx*) mice. *Am J Physiol*, 281, G1264-G1270, 2001.
7. Kobzik L, Reid MB, Bredt DS, and Stamler JS. Nitric oxide in skeletal muscle. *Nature* 372: 546-548, 1994.
8. Ward ME, Toporsian M, Scott JA, Teoh H, Govindaraju V, Quan A, Wener AD, Wang G, Bevan SC, Newton DC, and Marsden PA. Hypoxia induces a functionally

significant and translationally efficient neuronal NO synthase mRNA variant. *J Clin Invest* 115: 3128-3139, 2005.

9. Venema VJ, Ju H, Zou R, and Venema RC. Interaction of neuronal nitric-oxide synthase with caveolin-3 in skeletal muscle. *J Biol Chem* 272: 28187-28190, 1997.
10. Sato Y, Sagami I, and Shimizu T. Identification of caveolin-1 interacting sites in neuronal nitric oxide synthase. Molecular mechanism for inhibition of NO formation. *J Biol Chem* 279: 8827-8836, 2004.
11. Segal SS, Brett SE, and Sessa WC. Codistribution of NOS and caveolin throughout the peripheral vasculature and skeletal muscle of hamsters. *Am J Physiol* 277: H1167-H1177, 1999.
12. Daniel E, Jury J, and Wang WF. nNOS in canine lower esophageal sphincter: co-localized with caveolin-1 and Ca^{2+}-handling proteins? *Am J Physiol* 281: G1101-G1114, 2001.
13. Cho WJ and Daniel EE. Proteins of the interstitial cells of Cajal and intestinal smooth muscle, colocalized with caveolin-1. *Am J Physiol* 288: G571-G585, 2005.
14. Razani B, Woodman S, and Lisanti M. Caveolae: from cell biology to animal physiology. *Pharmacol Rev* 54: 431-467, 2002.
15. Khadour, FH, Kao RH, Park S, Armstrong PW, Holycross BJ, and Schulz R. Age-dependent augmentation of cardiac endothelial nitric oxide synthase in a genetic rat model of heart failure. *Am J Physiol* 273: H1223-H1230, 1997.
16. Brenmann JE, Chao DS, Xia H, Aldabe K, and Bredt DS. Nitric oxide synthase complexed with dystrophin and absent from skeletal muscle sarcolemma in Duchene muscular dystrophy. *Cell* 82: 743-752, 1995.

17. Sotgia F, Lee JK, Das K, Bedford M, Petrucci TC, Macioce P, Sargiacomo M, Bricarelli FD, Mintti C, Sudol M, and Lisanti MP. Caveolin-3 directly interferes with the terminal tail of β-dystroglycan. *J Biol Chem* 275: 38048-38058, 2000.

18. Bredt DS and Snyder SH. Isolation of nitric oxide synthase, a calmodulin-requiring enzyme. *Proc Natl Acad Sci USA* 87: 682-685, 1990.

19. Daniel EE, Bodie G, Mannarino M, Boddy G, and Cho WJ. Changes in membrane cholesterol affects caveolin-1 localization and ICC-pacing in mouse jejunum. *Am J Physiol* 287: G202-G210, 2004.

20. Unno T, Matsuyama H, Sakamoto T, Uchiyama M, Izumi Y, Okamoto H, Yamada M, Wess J, and Komori S. M_2 and M_3 muscarinic receptor-mediated contractions in longitudinal smooth muscle of the ileum studied with receptor knockout mice. *Br J Pharmacol* 146: 98-108, 2005.

21. Waldman SA and Murad F. Cyclic GMP synthesis and function. *Pharmacol Rev* 39: 163-196, 1987.

22. Murthy KS. Signaling for contraction and relaxation in smooth muscle of the gut. *Annu Rev Physiol* 68: 345-374, 2006.

23. Bolotina VM, Najibi S, Palacino JJ, Pagamo PJ, and Cohen RA. Nitric oxide directly activates calcium-dependent potassium channels in vascular smooth muscle. *Nature* 368: 850-853, 1994.

24. Wegener JW, Schulla V, Koller A, Klugbauer N, Feil R, and Hoffmann E. Control of intestinal motility by $Ca_v1.2$ L-type calcium channels in mice. *FASEB J* 20: 1260-1262, 2006.

25. Kubota M, Ito Y, and Ikeda K. Membrane properties and innervation of smooth muscle cells in Hirschsprung's disease. *Am J Physiol* 244: G406-G415, 1983.

CHAPTER VII

CALCIUM EXTRUSION BY PLASMA MEMBRANE CALCIUM PUMP IS IMPAIRED IN CAVEOLIN-1 KNOCKOUT MOUSE SMALL INTESTINAL TISSUE

7.1 Introduction:

Smooth muscle contraction is usually triggered by a regulated rise in the intracellular calcium concentration occurring on the background of low basal calcium levels. This rise can be counteracted by several mechanisms located in different compartments within the cell to restore the low basal level of calcium and end the contractile phase[1]. An early study[2] of the distribution of calcium in smooth muscle cells found calcium, besides in the expected locations; i.e., the sarcoplasmic reticulum, the mitochondria, and the nucleus, in "surface microvesicles" or what is now commonly known as caveolae, indicating their possible involvement in the calcium handling process.

Caveolae are sarcolemmal invaginations that are present in smooth muscles along with many other cell types[3]. They occur in areas of the plasma membrane rich in cholesterol and sphingolipids called "lipid rafts" and their formation is triggered by the presence of the marker protein caveolin[3]. The caveolin protein family members are products of three genes coding for three members; caveolin-1, -2, and -3[3]. In smooth muscle cells, caveolae formation is mainly triggered by the insertion of caveolin-1 oligomers into the inner leaflet of plasma membrane[4]. Caveolae domains play a crucial role in the regulation of various signal transduction pathways within the cell[5]. Among these pathways are those involved in the regulation of calcium signals and excitation-contraction coupling within smooth muscle cells[6,7].

Among the calcium handling molecules in smooth muscle cells that have been shown by immunogold electron microscopy to localize in caveolae of smooth muscle cells is the plasma membrane calcium ATPase (PMCA)[8]. PMCA is a P-type calcium ATPase that utilizes ATP to extrude calcium across the plasma membrane against a very high chemical gradient[9]. PMCA has 4 isoforms (PMCA 1-4) with a number of splice variants[10] of which only PMCA1 and 4 are reported to be expressed in smooth muscle cells[11]. PMCA1 is thought to have a role in the regulation of the basal calcium level while PMCA4 has a low basal activity but is activated by calcium and calmodulin and is thought to be involved primarily in regulating the magnitude of calcium signals[12]. Genetic targeting of PMCA4 in smooth muscle cells of the uterus showed that it can account for up to 70% of the calcium efflux mechanisms[13].

The pharmacological study of PMCA function has been hindered by the absence of sufficiently selective inhibitors. Orthovanadate has sometimes been used to inhibit PMCA function, but it has limited specificity and inhibits all P-type ATPases including the other calcium removal mechanism, the SERCA[14]. However, a series of recently developed synthetic peptides, caloxins, have been shown to have an improved selectivity to PMCA[15]. Caloxins are non-competitive peptide inhibitors that bind to and inhibit the extracellular domains of the PMCA[16]. Several members of this series, 1A1, 2A1, 3A1, and 1B1, have been used successfully as PMCA inhibitors[17,18,19,20,21,22]. In the present study we used another member of this series, caloxin 1C2, that is selective for PMCA4 (K_i=2.35 μM; the K_i values for PMCA 1, 2, and 3 are tenfold higher)[23] to study the role of caveolae in calcium removal by PMCA in smooth muscle cells. To this end we compared PMCA function in small intestinal smooth muscle from caveolin-1 knockout and control mice. In addition, owing to the low expression level of PMCA[9] to studying the effects of cholesterol depletion on

PMCA function in bovine airway smooth muscle which have a larger smooth muscle mass that facilitated the study of PMCA exprssion.

7.2 Materials and methods:

7.2.1 Functional experiments:

7.2.1.1 Tissue preparation:

Small intestinal tissue from cav1$^{+/+}$ and cav1$^{-/-}$ mice was isolated and set up to record LM contractile activity as described in Chapter II. Bovine tracheae were obtained from the slaughterhouse on the morning of the day of experiments and kept in ice-cold Krebs' buffer. The smooth muscle was dissected from cartilage and freed from connective tissue and mucosa. Individual smooth muscle bundles (0.5 x 1 cm) were dissected and tied at both ends with silk suture. The individual bundles were tied to a holder, put in a tissue bath, and connected to an isometric force-displacement transducer to record their contraction. The Krebs' buffer used for bovine tissue contained (in mM): NaCl (117.9), $NaHCO_3$ (25), KCl (4.6), KH_2PO_4 (1.2), $MgSO_4.7H_2O$ (1.2), glucose (11), and $CaCl_2.2H_2O$ (2).

7.2.1.2 Experimental protocols:

The intestinal tissue segments were equilibrated for 30 min. TTX (1 μM) was added to intestinal tissue at the beginning of the equilibration period to block nerve activity. Intestinal tissue was either given CCh directly after the equilibration period or incubated for an additional 10 min with 5 μM caloxin 1C2

(TAWSEVLDLLRRGGGSK-amide)[23] or 5 μM of a peptide (GAETLSHGLRLGSVW-amide) used to control for caloxin 1C2 before the addition of 10 μM CCh. The control peptide has a control sequence of the amino acids of the parent peptide caloxin 1B1 that was used to generate the phagedisplay library from which caloxin 1C2 was cloned[34]. Some experiments on intestinal tissue were carried out in calcium-free Krebs-Ringer with 0.1 mM EGTA which was added after the equilibration period.

Following the equilibration period, bovine tracheal smooth muscle tissue was contracted several times with 60 mM KCl for five min separated by two washes with Krebs' buffer until a stable contraction level was reached. In preliminary experiments, 1 μM CCh was found to elicit maximal response and this concentration was added to all tissues after the KCl contraction stabilized to produce the maximal tissue response to CCh. After washout of the maximal concentration, a submaximal concentration of CCh (0.1 μM) was added to the tissues. After washing, tissues were incubated for 10 min with either 5 μM caloxin 1C2 or 5 μM of the control peptide followed by addition of 0.1 μM CCh. Similar experiments were also done in tissues in which caveolae were disrupted by the presumable cholesterol depletion by incubation with 40 mM Me-β-CDX for 3 hours at 37°C.

7.2.1.3 Data Analysis:

In mouse small intestinal tissue the response to CCh was measured as the increase in tonic amplitude normalized to the spontaneous tone of the tissue before the addition of caloxin 1C2 or the control peptide (dissolved in 1% ethanol-see

Materials). The values of spontaneous tone developed were not different in cav1$^{+/+}$ (65.2±6.0 mg tension) and cav1$^{-/-}$(71.6±6.2 mg tension). In experiments done on bovine tissue the response to 0.1 μM CCh was measured as the rise in tissue tone and was normalized to the rise in tone obtained by the maximal dose of CCh (1 μM). The normalized responses to CCh were compared by the unpaired *t*-test between caloxin 1C2-treated tissues and the control peptide-treated tissues in experiments done on mouse small intestinal tissues. In experiments done on bovine tracheal smooth muscle tissues, paired *t*-tests were used to compare the normalized responses to CCh before and after treatment with caloxin 1C2 or the control peptide.

7.2.2 Immunohistochemistry:

Mouse small intestinal tissue was prepared and fixed as described in Chapter II. Individual bundles of bovine tracheal smooth muscle were fixed as described in Chapter II. Tissue sectioning, immunostaining, tests for specificity of antibody binding and confocal microscopy were done as described in Chapter II. Mouse anti-caveolin-1 (1:100), mouse anti-PMCA (1:100), and mouse anti-PMCA4b (1:100) were used as primary antibodies. As primary antibodies were raised in the same host, one of either antibody used in double staining was converted to be recognized as rabbit by pre-incubation with Fab fragment rabbit anti-mouse IgG. Cy3-conjugated donkey anti-mouse IgG and Alexa488-conjugated goat anti-rabbit IgG were used as secondary antibodies.

7.2.3 Membrane fractionation and Western blotting:

Membrane fractions enriched in lipid rafts were prepared from mouse small intestinal tissues and bovine tracheal smooth muscle tissue as described in Chapter II. Western blotting for caveolin-1 and PMCA4 was done as described in Chapter II. Mouse anti-caveolin-1 (1:1000), mouse anti PMCA 4 (1:1000, for mouse tissue fractions), and mouse anti PMCA4b (1:1000, for bovine tissue fractions) were used as primary antibodies. HRP-conjugated goat anti-mouse IgG was used as secondary antibody.

7.2.4 Materials:

Caloxin 1C2 and the control peptide were synthesized by Dalton Chemical Laboratories Inc. (Toronto, ON). Mouse anti-PMCA was from Affinity Bioreagents Inc. (Golden, CO). Mouse anti-PMCA4 was from Abcam Inc. (Cambridge, MA). Mouse anti-PMCA4b was from Sigma (Oakville, ON).

Caloxin 1C2 and the control peptide were dissolved in 1% ethanol which tended to reduce the basal tone of contraction in mouse small intestinal tissues. Statistical comparisons were done in this case between tissues treated with similar amounts of ethanol.

7.3 Results:

7.3.1 Immunohistochemistry:

Cryosections of small intestine from cav1$^{+/+}$ and cav1$^{-/-}$ were examined for caveolin-1 and PMCA immunoreactivity. Caveolin-1 and PMCA immunoreactivities were co-localized in punctate sites in the plasma membrane of smooth muscle cells in cav1$^{+/+}$ tissues (Fig 7.1). Cav1$^{-/-}$ tissues lacked caveolin-1 immunoreactivity but retained PMCA immunoreactivity in smooth muscle membranes.

In cryosections from bovine tracheal smooth muscle, caveolin-1 and PMCA4b were co-localized in control tissues. On the other hand, in cryosections from tissues pretreated with Me-β-CDX immunoreactivities for both caveolin-1 and PMCA were much reduced (Fig 7.1).

7.3.2 Western blotting:

Both PMCA4a and b splice variant proteins appeared in the caveolin-rich membrane fractions from cav1$^{+/+}$ small intestinal tissue. Only PMCA4a protein appeared in cav1$^{-/-}$ lipid raft-rich fractions. PMCA4 was not detected in the heavy (non-raft) fraction in either strain under the experimental conditions used (data not shown). In fractions from bovine tracheal smooth muscle tissues, PMCA4b appeared in the caveolin-rich fractions and the heavy (non-raft) membrane fractions. In fractions from Me-β-CDX treated tissues, the distribution of both caveolin-1 and PMCA4b was reduced in the lipid raft-rich fractions (Fig 7.2).

Fig 7.1 Immunohistochemical staining of caveolin-1 and PMCA in cryosections from mouse small intestine and bovine tracheal smooth muscle. a. Cav1$^{+/+}$ tissue shows caveolin-1 (green) and PMCA (red) immunoreactivities that are co-localized (yellow) in smooth muscle membrane. b. Cav1$^{-/-}$ tissue shows only PMCA immunoreactivity (red). Scale bar is 10 μM for a and b. c. Control bovine tracheal smooth muscle tissue show caveolin-1 (green) and PMCA4b (red) immunoreactivities co-localized (yellow) in the cell membrane. d. Both caveolin-1 and PMCA immunoreactivities are almost abolished in the Me-β-CDX-treated bovine tracheal smooth muscle tissue. Scale bar is 5 μM for c and d (immunostaining and confocal microscopy were done by Woo Jung Cho).

Fig 7.1

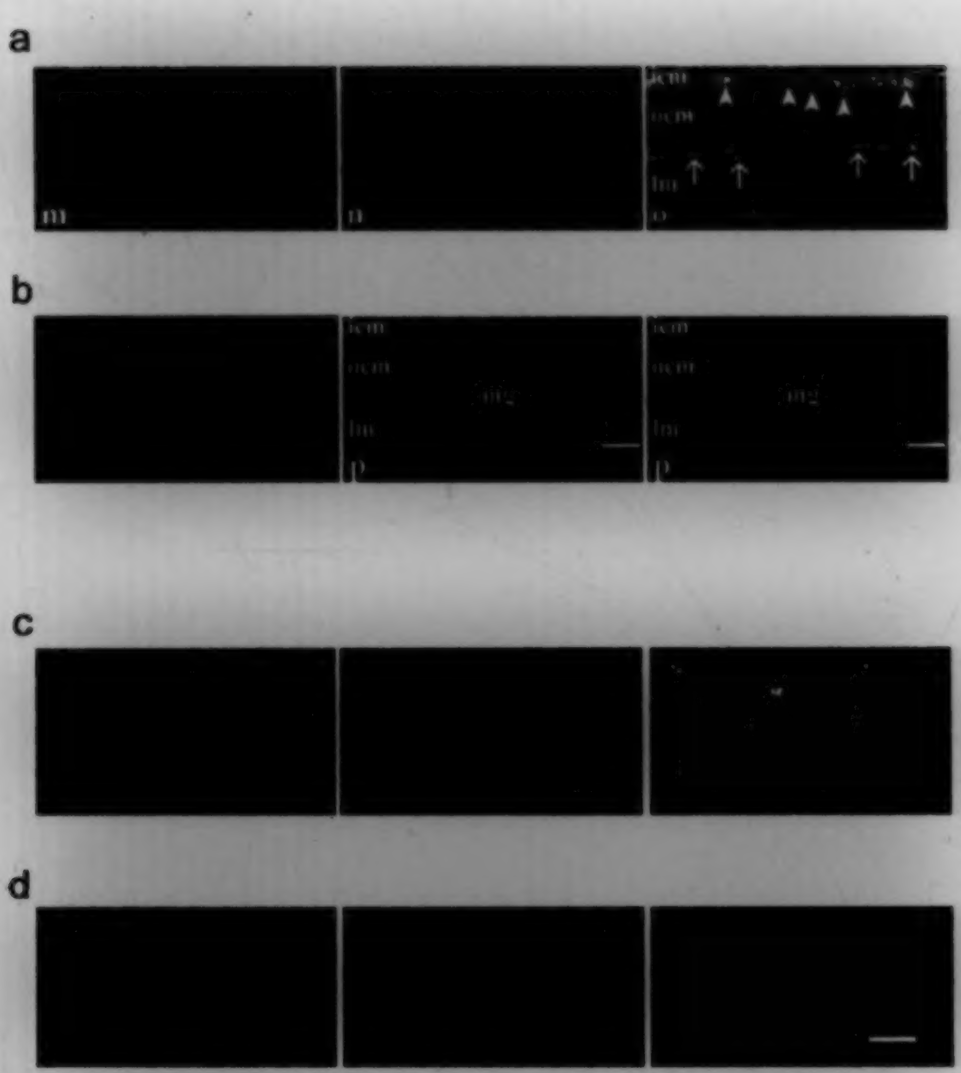
a
m
n
icm
ocm
lm
o
b
icm
ocm
mg
lm
p
icm
ocm
mg
lm
p
c
d

Fig 7.2 Distribution of PMCA4 in lipid raft-rich membrane fractions of mouse small intestinal and raft and non-raft membrane fractions from bovine tracheal smooth muscle. a. PMCA4 appears in the lipid raft-rich fraction in cav1$^{+/+}$ and cav1$^{-/-}$, however only PMCA4a is present in the cav1$^{-/-}$ fraction. b. PMCA4b distributes in lipid raft-rich fractions and heavy (non-raft) membrane fractions in control tissue. The numbers indicates the fraction in the sucrose density gradient. Fractions 1 and 2 were isolated from the 5% layer, fractions 3, 4, and 5 were isolated from the 35% layer, and fractions 6, 7, 8, 9 were isolated from the 45% layer. PMCA4b was almost removed from the lipid raft-rich fractions from Me-β-CDX-treated tissues.

Fig 7.2

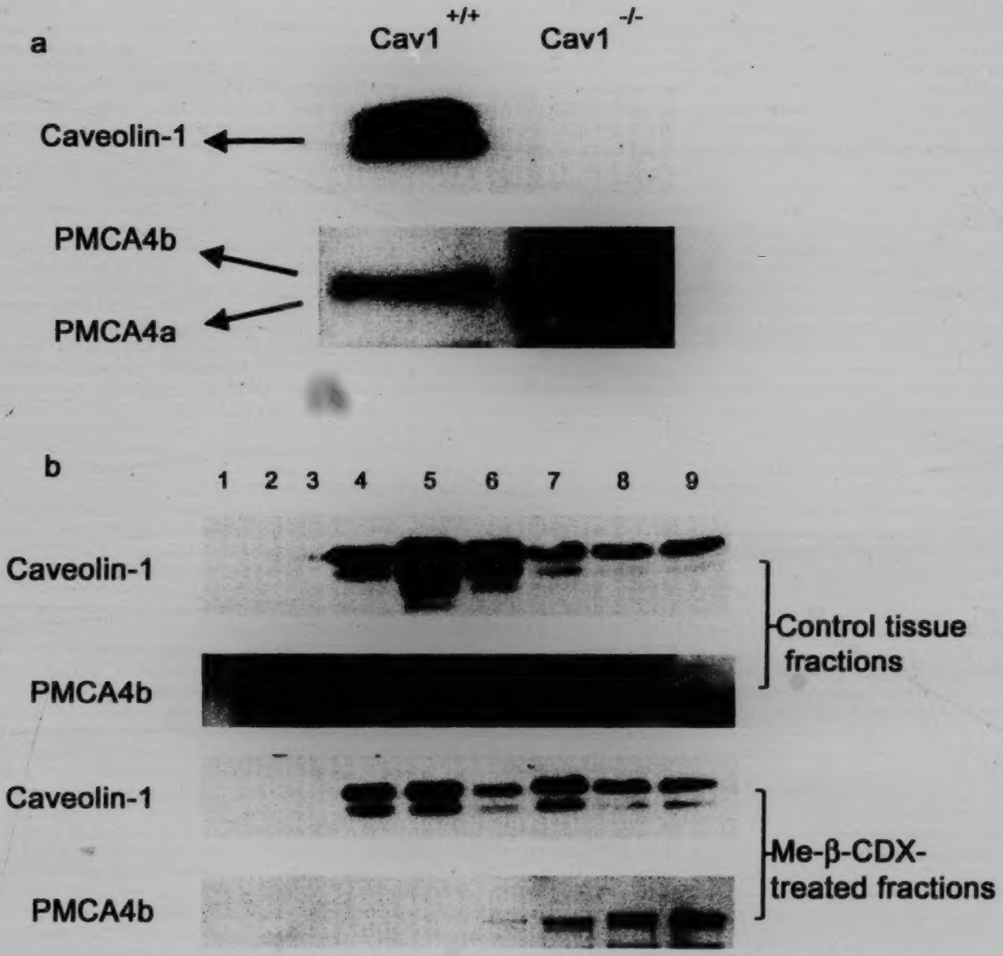
a
Cav1 +/+
Cav1 -/-
Caveolin-1
PMCA4b
PMCA4a
b
1
2
3
4
5
6
7
8
9
Caveolin-1
PMCA4b
Control tissue fractions
Caveolin-1
PMCA4b
Me-β-CDX-treated fractions

7.3.3 Functional experiments:

7.3.3.1 Responses to CCh in mouse small intestine:

The response to CCh in mouse small intestine had 2 phases: a rapid phasic contraction followed by a sustained tonic contraction (Fig 7.3). The tonic phase was compared in cav1$^{+/+}$ and cav1$^{-/-}$ at 3 CCh concentrations (1, 3, and 10 µM). At 10 µM the contraction was significantly higher in cav1$^{-/-}$ tissue segments (Fig 7.3).

7.3.3.2 Respose to CCh following the addition of caloxin or the control peptide in mouse small intestine:

To examine the role of PMCA4 in calcium extrusion in mouse small intestinal tissue, the tonic response to 10 µM CCh after treatment with 5 µM caloxin 1C2 or 5 µM control peptide was examined in cav1$^{+/+}$ and cav1$^{-/-}$ small intestinal segments. At this concentration, caloxin 1c2 would inhibit PMCA4 (Ki = 2.3 µM) for which it has greater than 10-fold higher affinity than for PMCA1, 2 or 3[23]. The response to CCh in cav1$^{+/+}$ tissue segments treated with caloxin was significantly higher than the response to CCh in the cav1$^{+/+}$ segments treated with the control peptide and also higher than the response to CCh in caloxin-treated cav1$^{-/-}$ segments. There was no difference between the response to CCh in caloxin-treated and control peptide-treated cav1$^{-/-}$ tissues (Fig 7.4a and b).

In calcium-free medium, caloxin-treatment increased the tonic response to CCh only in cav1$^{+/+}$ compared to responses of tissues treated with the control peptide. There was no difference between the responses to CCh in cav1$^{-/-}$ between the two

Fig 7.3 Response of small intestinal segments from cav1$^{+/+}$ and cav1$^{-/-}$ to CCh (1, 3, and 10 μM). a. The typical reponse to CCh consisted of a rapid phasic component and a sustained tonic component. The dot represents the time point at which CCh was added. b. The tonic response is significantly higher in cav1$^{-/-}$ tissue segments only at 10 μM. *n* values were at least six for all experiments. Statistical significance was determined using ANOVA followed by Bonferroni *post hoc* test and denoted by **P*<0.05.

Fig 7.3

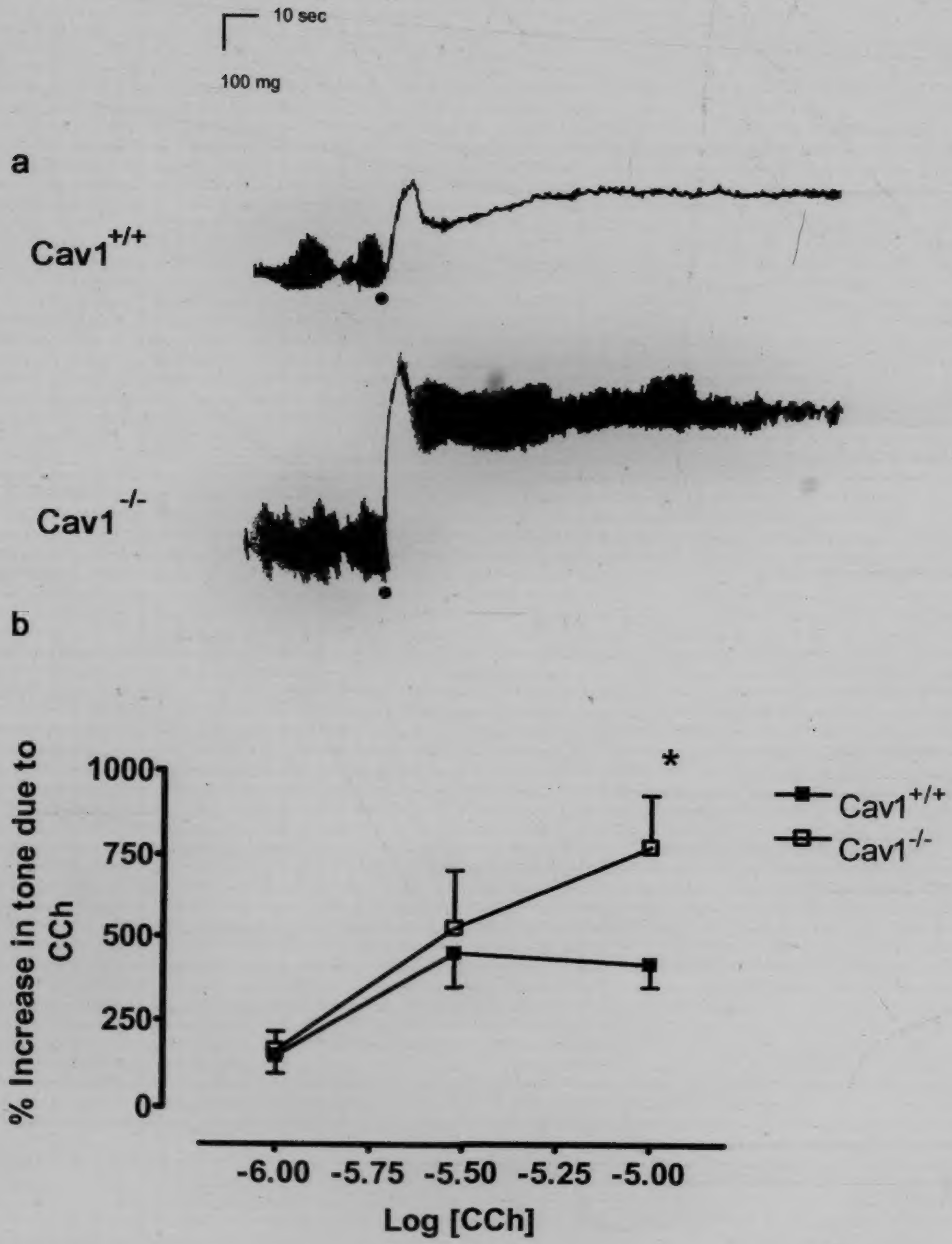
10 sec
100 mg
a
Cav1+/+
Cav1-/-
b
% Increase in tone due to CCh
1000
750
500
250
0
*
Cav1+/+
Cav1-/-
-6.00
-5.75
-5.50
-5.25
-5.00
Log [CCh]

Fig 7.4 Effect of caloxin 1C2 (5 µM) on tissue response to 10 µM CCh in $cav1^{+/+}$ and $cav1^{-/-}$ small intestinal tissue. a. Only $cav1^{+/+}$ segments treated with caloxin 1C2 maintained a high tonic response to CCh. The dot represents the time point when CCh was added. b. The response to CCh is higher in $cav1^{+/+}$ tissue segments treated with caloxin than in control tissues and $cav1^{-/-}$ tissues. *n* values are 7 for $cav1^{+/+}$ segments and 6 for $cav1^{-/-}$. c. In calcium-free medium, caloxin 1C2 produces a higher tonic response to CCh only in $cav1^{+/+}$ tissue. *n* values are 7 for $cav1^{+/+}$ segments and 6 for $cav1^{-/-}$ segments. Statistical significance was measured by ANOVA followed by the Bonferroni *post hoc* test and denoted by $^{*}P<0.05$ and $^{**}P<0.01$.

Fig 7.4

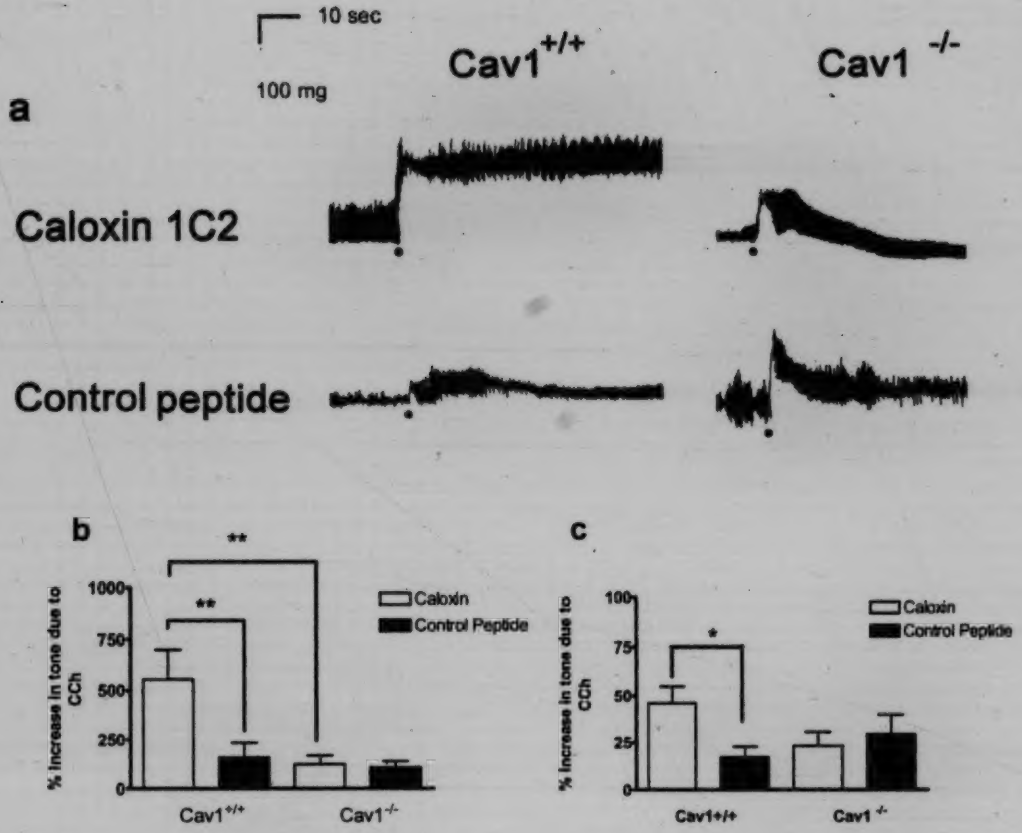
10 sec
100 mg
Cav1+/+
Cav1 -/-
a
Caloxin 1C2
Control peptide
b
**
**
1000
750
500
250
0
% Increase in tone due to CCh
Caloxin
Control Peptide
Cav1+/+
Cav1-/-
c
*
100
75
50
25
0
% Increase in tone due to CCh
Caloxin
Control Peptide
Cav1+/+
Cav1 -/-

treatments. Responses to CCh in calcium-free medium tended to be higher in cav1$^{-/-}$ than in cav1$^{+/+}$ (Fig 7.4c).

7.3.3.3 The effect of caloxin on CCh response in control and cholesterol-depleted bovine tracheal smooth muscle:

The response to 0.1 μM CCh was compared before and after the addition of 5 μM caloxin 1C2 or 5 μM of the control peptide to assess the role of PMCA4 in calcium extrusion in bovine tracheal smooth muscle. The contractile response to CCh increased only in the caloxin-treated tissue (Fig 7.5) indicating a role of PMCA4 in calcium extrusion. Caveolae disruption by depletion of membrane cholesterol led to the loss of the effect of caloxin 1C2 on the CCh response (Fig 7.5).

7.4 Discussion:

In this study, using a selective inhibitor of PMCA 4, we examined the importance of caveolin 1 and caveolae in calcium extrusion from smooth muscle cells by PMCA. The termination of the contractile signal in smooth muscle involves calcium extrusion from the cell as well as sequestration into the sarcoplasmic reticulum in order to reduce cytosolic calcium levels[24]. A study in uterine smooth muscle suggested that the SERCA and the plasma membrane calcium removal mechanisms (PMCA and Na^+/Ca^{2+} exchanger) act in series to reduce the cytosolic calcim level [25]. In addition, the presence of the sarcoplasmic reticulum in superficial regions in the smooth muscle cells[26] led to the proposal that calcium is removed from the contractile machinery primarily by the SERCA. In this proposal, calcium gets routed through the

Fig 7.5 Effect of caloxin 1C2 (5 µM) on the response to 0.1 µM CCh in bovine tracheal smooth muscle. a. Representative tracings showing the effect of caloxin 1C2 and the control control peptide on CCh contraction. The dot represents the time point when CCh was added b. The response to CCh only increases significantly after treatment with caloxin 1C2 and not the control peptide. The effect of caloxin is lost following cholesterol depletion by Me-β-CDX. *n* value is 7 for all experiments.

Fig 7.5

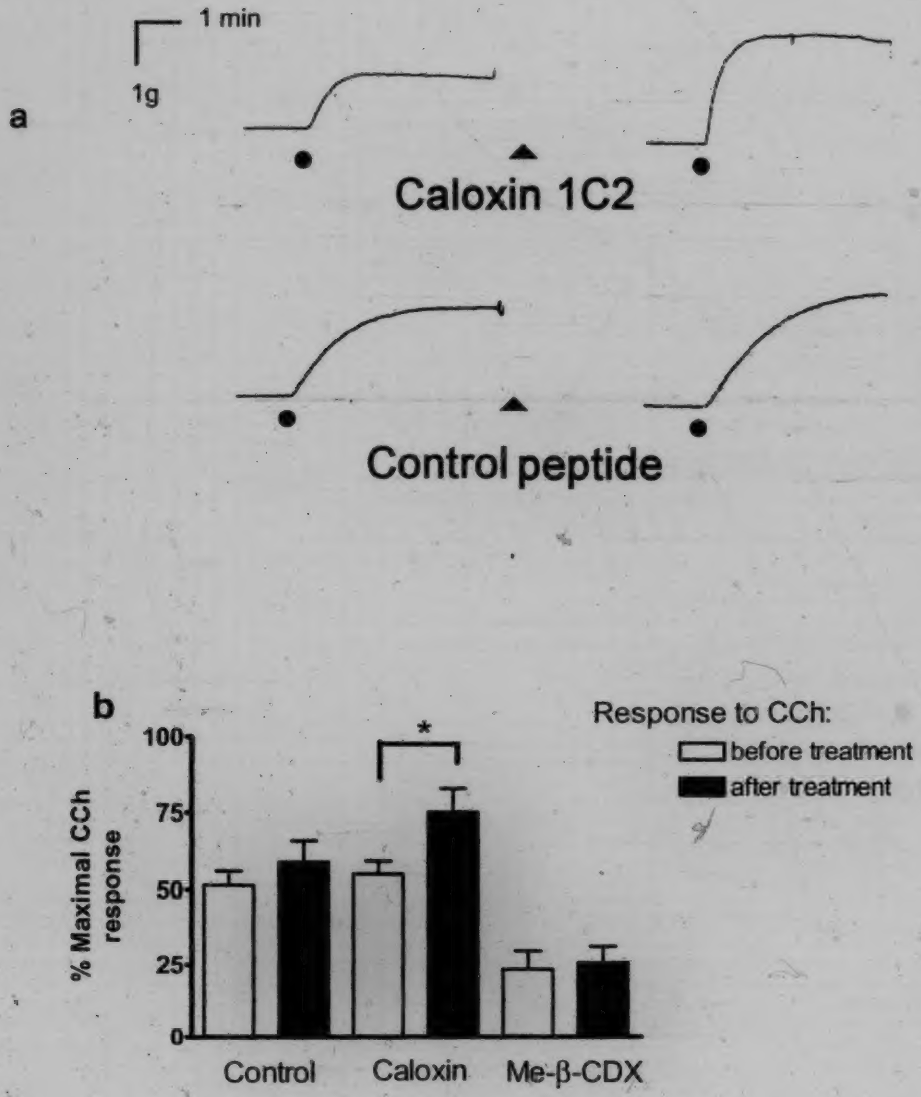
a
1 min
1g
Caloxin 1C2
Control peptide
b
Response to CCh:
before treatment
after treatment
% Maximal CCh response
100
75
50
25
0
*
Control
Caloxin
Me-β-CDX

sarcoplasmic reticulum, and is then released at a privileged cytosolic space between the sarcoplasmic reticulum and the plasma membrane where it gets extruded to the extracellular space[27]. This dynamic process is only achieved by a close association between the sarcoplasic reticulum and the plasma membrane allowing the delivery of calcium to calcium extrusion mechanisms[28]. A recent study[29] showed that 87% of the smooth muscle plasma membrane caveolae established very close contacts with the sarcoplasmic reticulum. This indicated a possible role for caveoale as a specialized plasma membrane domain for calcium removal in smooth muscle cells.

In the present study we used intestinal tissue from cav1$^{-/-}$ and cav1$^{+/+}$ mice to examine the role of caveolae in calcium removal from tissues contracted with CCh. Earlier we showed that cav1$^{-/-}$ mice lack significant caveolae expression in smooth muscle layers in small intestine[30]. Thus we hypothesized that the close contacts between the plasma membrane caveolae and the sarcoplasmic reticulum are lost and that the dynamic association required for the normal calcium extrusion is affected.

In order to test this hypothesis, we examined the CCh contraction in mouse small intestine. In this experimental model, CCh is known to induce contraction by increasing intracellular calcium from different sources, both release from sarcoplasmic reticulum and calcium entrance[31]. The tonic response to 10 μM CCh was higher in cav1$^{-/-}$ tissue which might be related to a decrease in calcium clearance. Indeed, a decrease in the rate of calcium clearance was observed in single smooth muscles from cerebral resistance arteries after interference with caveolin-1 by blocking antibodies or a peptide corresponding to the caveolin-1 scaffolding domain[32].

Since previous reports indicated that PMCA4 is present in lipid raft domains[33], we examined the expression of PMCA in mouse intestinal tissue in relation to caveolin-1. PMCA was colocalized with caveolin-1 in intestinal smooth muscle cells as shown by immunohistochemistry in $cav1^{+/+}$ tissue. PMCA4 was present only in the caveolae/lipid raft-enriched membrane domains. However, its immunoreactivity was not lost in $cav1^{-/-}$ tissues. This was a consequence of the presence of both splice variants PMCA4a and b in $cav1^{+/+}$, while only PMCA4a was present in the $cav1^{-/-}$ lipid raft fractions.

We deduced that in the presence of the selective inhibitor caloxin 1C2, calcium clearance by PMCA4 was reduced in $cav1^{+/+}$ tissues. In our experiments this was shown as an increase in the tone of CCh contractions in tissues treated with caloxin 1C2, but not with a control peptide. On the other hand, caloxin 1C2 had no effect on the CCh-induced tone in $cav1^{-/-}$ tissues. Even in calcium-free media, although the overall response to CCh was reduced, caloxin 1C2 treatment increased the response to CCh only in the $cav1^{+/+}$ tissues.

Since PMCA4b was missing from lipid rafts in $cav^{-/-}$ tissues and present in $cav1^{+/+}$ tissues, one explanation may be that this enzyme plays a more important role than PMCA4a in calcium extrusion from mouse intestinal smooth muscle. Alternatively, the failure of a response to caloxin 1C2 in $cav1^{-/-}$ tissues could be explained by the loss of proximity between caveolae and sarcoplasmic reticulum. So far there have been no measurements of the extent of changes in the structural relationships between the plasma membrane and sarcoplasmic reticulum in cav1$^{-/-}$ tissues. The fact that the effects of caloxin 1C2 were still present only in cav1$^{+/+}$ and not cav$^{-/-}$ tissues when calcium was absent from the extracellular medium suggests that it was calcium located either inside the caveolae or in an intracellular space dependent on caveolae which was the substrate for PMCA pumping.

To confirm the generality of our observations, we used another model to study the effect of caloxin 1C2 in relation to caveolae. Bovine tracheal smooth muscle responded to CCh by a sustained contraction due to the activation of M_3 muscarinic receptor and the production of IP_3 and release of calcium from the intracellular stores[34]. The magnitude of the response to CCh was increased in tissues treated with caloxin 1C2 but not in tissues treated with the control peptide, indicating that PMCA4 is involved in calcium extrusion in this tissue. Immunohistochemical examination indicated that PMCA4b was present in this tissue colocalized with caveolin-1. PMCA4b appeared in membrane fractions enriched in caveolin-1 as well. Caveolae disruption by the presumed membrane cholesterol depletion using Me-β-CDX led to the reduction of PMCA4b immunoreactivity in the plasma membrane and also to its displacement from the lipid raft enriched fractions toward the heavier membrane fractions. This was accompanied by a loss of the increase in the response to CCh following caloxin 1C2 treatment in functional experiments.

To conclude, our results indicate that PMCA4, likely PMCA4b, is involved in calcium extrusion following contractions in smooth muscle and its function is dependent on the presence of intact caveoale. In conditions where caveolae formation is prevented or caveoale are disrupted in smooth muscle cells, calcium extrusion by

PMCA4 is hindered. This might be due to the special role of PMCA 4b or to disruption of the close association of the plasma membrane and sarcoplasmic reticulum through caveolae.

7.5 References

1. Sanders KM. Invited review: Mechanisms of calcium handling in smooth muscles. *J Appl Physiol* 91: 1438-1449, 2007.
2. Popescu LM, Diculescu I, Zeick U, and Ionescu N. Ultrastructural distribution of calcium in smooth muscle cells of guinea-pig taenia coli. *Cell Tissue Res* 184: 357-378, 1974.
3. Razani B, Woodman SE, and Lisanti MP. Caveolae: from cell biology to animal physiology. *Pharmacol Rev* 54: 431-467, 2002.
4. Williams TM and Lisanti MP. The caveolin genes: from cell biology to medicine. *Ann Med* 36: 584-595, 2004.
5. Krajewska WM and Maslowska R. Caveolins: structure and function in signal transduction. *Cell Mol Biol Lett* 9: 195-220, 2004.
6. Taggart MJ. Smooth muscle excitation-contraction coupling: a role for caveolae and caveolins. *News Physiol Sci* 16: 61-65, 2001.
7. Darby PJ, Kwan CY, and Daniel EE. Caveoale from canine airway smooth muscle contain the necessary components for a role in Ca^{2+} handling. *Am J Physiol* 279: L1226-L1235, 2000.
8. Fujimoto T. calcium pump of plasma membrane is localized to caveolae. *J Cell Biol* 120: 1147-1157, 1993.
9. Floyd R and Wray S. Calcium transporters and signaling in smooth muscles. *Cell Calcium* In Press.

10. Strehler EE and Zacharias DA. Role of alternative splicing in generating isoform diversity among plasma membrane calcium pumps. *Physiol Rev* 81: 21-50, 2005.

11. Ishida Y and Paul RJ. Ca^{2+} clearance in smooth muscle: lessons from gene-ablated mice. *J Smooth Muscle Res* 41: 235- 245, 2005.

12. Padanyi R, Paszty K, Penheiter AR, Filoteo AG, Penniston JT, and Enyedi A. Intramolecular interaction of the regulatory region with the catalytic core in the plasma membrane calcium pump. *J Biol Chem* 278: 35798-35804, 2003.

13. Mathew A, Cartwright EJ, Burdyga T, Neyses L, and Wray S. The effect of knocking out isoform 4 of the plasma membrane Ca-ATPase (PMCA) on force in mouse myometrium. *J Physiol Proc Glasgow Meet Physiol Soc* 557P: p.C31, 2004.

14. Tiffert T and Lew VL. Kinetics of inhibition of the plasma membrane calcium pump by vanadate in intact human red cells. *Cell Calcium* 30: 337-342, 2001.

15. Pande J and Grover AK. Plasma membrane calcium pumps in smooth muscle: from fictional molecules to novel inhibitors. *Can J Physiol Pharmacol* 83: 743-754, 2005.

16. Holmes ME, Chaudhary J, and Grover AK. Mechanism of action of the novel plasma membrane Ca^{2+} pump inhibitor caloxin. *Cell Calcium* 33: 241-245, 2003.

17. De Luisi A and Hoffer AM. Evidence that calcium cycling by the plasma membrane calcium ATPase increases the "excitability" of the extracellular Ca^{2+}-sensing receptor. *J Cell Sci* 116: 1527-1538, 2003.

18. Kawano S, Otsu K, Shoji S, Yamagata K, and HiraokaM. Ca^{2+} oscillations regulated by the Na^{+}-Ca^{2+} exchanger and plasma membrane Ca^{2+} pump induce

fluctuations of membrane currents and potential in human mesenchymal stem cells. *Cell Calcium* 34: 145-156, 2003.

19. Vale-Gonzalez C, Alfonso A, Unol C, Vieytes MR, and Botana LM. Role of plasma membrane calcium adenosine triphosphatase on domoate-induced intracellular acidification in primary culture of cerebral granule cell. *J Neurosci Res* 84: 326-337, 2006.
20. Pande J, Mallhi KK, and Grover AK. Role of third extracellular domain of plasma membrane Ca^{2+}-Mg^{2+} ATPase based on the novel inhibitor caloxin 3A1. *Cell Calcium* 37: 245-250, 2005.
21. Pande J, Mallhi KK, and Grover AK. A novel plasma membrane Ca^{2+}-pump inhibitor: caloxin 1A1. *Eur J Pharmacol* 508: 1-6, 2005.
22. Pande J, Mallhi KK, Sawh A, Szewczyk MM, Simpson F, and Grover AK. Aortic smooth muscle and endothelial plasma membrane Ca^{2+} pump isoforms are inhibited differently by the extracellular inhibitor caloxin 1b1. *Am J Physiol* 290: C1341-C1349, 2006.
23. Pande J, Szewczyk MM, Kuszczak I, Grover S, Escher E, and Grover AK. Functional effects of caloxin 1c2, a novel engineered selective inhibitor of plasma membrane Ca^{2+}-pump isoform 4, on coronary artery. *J Cell Mol Med* (Submitted).
24. Thornloe KS and Nelson MT. Ion channels in smooth muscle: regulators of intracellular calcium and contractility. *Can J Physiol Pharmcol* 83: 215-242, 2005.

25. Shmigol AV, Eisner DA, and Wray S. The role of sarcoplasmic reticulum as a Ca^{2+} sink in rat uterine smooth muscle cells. *J Physiol* 520: 153-163, 1999.

26. Nixon GF, Mignery GA, and Somlyo AV. Immunogold localization of inositol 1,4,5-triphosphte receptors and characterization of ultrastructural features of the sarcoplasmic reticulum in phasic and tonic smooth muscle. *J Muscle Res Cell Motil* 15: 682-700, 1994.

27. Poburko D, Kuo KH, Lee CH, and Breemen C. Organellar junctions promote targeted Ca^{2+} signaling in smooth muscle: why two membranes are better than one. *Trends Pharmacol Sci* 25: 8-15, 2004.

28. Lee C-H, Poburko D, Kuo K-H, Seow CY, and van Breeemen C. Ca^{2+} oscillations, gradients, and homeostasis in vascular smooth muscle. *Am J Physiol* 282: H1571-H1583, 2002.

29. Popescu LM, Gherghiceanu M, Mandache E, and Cretoiu D. Caveolae in smooth muscles: nanocontacts. *J Cell Mol Med* 10: 960-990, 2006.

30. El-Yazbi AF, Cho WJ, Boddy G, Schulz R, and Daniel EE. Impact of caveolin-1 knockout on NANC relaxation in circular muscles of mouse small intestine compared with longitudinal muscles. *Am J Physiol* 290: G394-G403, 2006.

31. Unno T, Matsuyama H, Sakamoto T, Uchiyama M, Izumi Y, Okamoto H, Yamada M, Wess J, and Komori S. M_2 and M_3 muscarinic receptor-mediated contractions in longitudinal smooth muscle of the ileum studied with receptor knockout mice. *Br J Pharmacol* 146: 98-108, 2005.

32. Kamishima T, Burdyga T, Gallagher JA, Quayle JM. Caveolin-1 and caveolin-3 regulate Ca^{2+} homeostasis of single smooth muscle cells from rat cerebral resistance arteries. *Am J Physiol* 293: H204-H214, 2007.

33. Sepulveda MR, Berrocal-Carillo M, Gasset M, and Mata AM. The plasma membrane Ca^{2+}- ATPase isoform 4 is localized in lipid rafts of cerebellum synaptic plasma membranes. *J Biol Chem* 281: 447-453, 2006.

34. Gosens R, Zaagsma J, Grootte Bromhaar M, Nelemans A, and Meurs H. Acetylcholine: a novel regulator of airway smooth muscle remodeling? *Eur J Pharmacol* 500: 193-201, 2004.

CHAPTER VIII

GENERAL DISCUSSION, LIMITATIONS, AND FUTURE DIRECTIONS

8.1 General discussion:

In this thesis I examined the role of caveolin-1 in the organization of signaling events involved in the regulation of the motility of the small intestine of the mouse. I investigated the effects of caveolin-1 knockout on these processes. I showed that $cav1^{-/-}$ intestinal smooth muscle tissue had a reduced relaxation response to NO, relaxed less following β-adrenoceptor stimulation, lost the modulation of contraction provided by smooth muscle NOS, and had a diminished intracellular calcium clearance by PMCA. The results of my project emphasize the importance of the organization of signaling molecules in cellular microdomains. In most cases, caveolin-1 knockout had very little effect on the overall expression and/or function of individual signaling molecules. However, it appears that the defects in the overall function of the examined signaling pathways are due to an altered or defective organization of these molecules.

As mentioned in the Introduction, NO is considered to be the main inhibitory mediator in the GIT. Indeed, in Chapter III, I showed that this is the case in the longitudinal smooth muscle layer of mouse small intestine since an inhibitor of the synthesis of NO abolished the relaxation due to myenteric nerve stimulation. However, the inhibition of NO synthesis did not completely block the EFS-mediated relaxation in the circular smooth muscle layer, indicating that NO acted among other mediators there. The effect of NO on the circular smooth muscle layer was different in the two control mouse strains that I used, BALB/c and $cav1^{+/+}$. Blockade of NO synthesis had a more prominent effect on $cav1^{+/+}$ circular muscle. The reduced relaxation response to NO (produced endogenously by EFS) in $cav1^{-/-}$ tissue could not be explained on the basis of a lack of NO production since the number of NOS expressing neurons was higher in the $cav1^{-/-}$

myenteric plexus than in the cav1$^{+/+}$ myenteric plexus. This and the observation that exogenous NO donors also showed a reduced response in cav1$^{-/-}$ tissues indicate that there was a reduced responsiveness of the smooth muscle cells to NO effects. I used different tools to sort out the changes in function of the signaling components downstream of NO. I found that the most likely reason underlying the reduced responsiveness to NO in cav1$^{-/-}$ tissue is an increase in PDE5 activity. I showed that PDE5 is present in lipid raft-enriched membrane fractions, colocalized with caveolin-1 as observed in cav1$^{+/+}$ mice. Although the expression of PDE5 was not reduced in the whole homogenate of cav1$^{-/-}$ tissue, its presence in lipid rafts was reduced. Thus, I concluded that the sequestration of PDE5 in lipid rafts and its probable interaction with caveolin-1 could limit and regulate its effect on NO-induced cGMP production. I postulate that this regulation is lost in the absence of caveolin-1 and thus PDE5 will produce more hydrolysis of cGMP leading to a reduced relaxation in response to NO.

A similar situation existed in cAMP mediated relaxation downstream of β-adrenoceptor stimulation in mouse small intestine. The expression of β_1-, β_2-, and β_3-adrenoreceptors and PKA was not reduced in cav1$^{-/-}$ tissue yet the response to β-adrenoceptor agonists was reduced. Relaxation due to direct adenylate cyclase activation was less in cav1$^{-/-}$ tissue and the relaxation due to direct PKA activation was almost abolished there. Examination of the expression of PKA in different membrane domains revealed it to be much reduced in the lipid raft-enriched fractions from cav1$^{-/-}$ tissue, and in this case, located away from the different possible targets phosphorylated by PKA, which lead finally to relaxation.

I also showed that a nNOS variant expressed in smooth muscle plays an important role in the regulation of contraction. NOS is activated by calcium entering the cell through L-type calcium channels to release NO and counteract the contraction due to depolarization by KCl. Experimentally the smooth muscle NOS function was shown as an increase in the contractile tone following inhibition by LNNA after contraction had been stimulated by KCl. This nNOS variant was colocalized with caveolin-1 in mouse small intestinal smooth muscle plasma membrane. This variant was not present in the smooth muscle plasma membrane in cav1$^{-/-}$ tissues as examined by immunohistochemistry and the function I attributed to it was greatly reduced in cav1$^{-/-}$ preparations. Similarly, disruption of the caveolae of control mice by cholesterol depletion leads to the loss of nNOS immunoreactivity and its function. The localization of NOS in caveolae is important for its activation by calcium coming in through the nearby L-type calcium channels. Other sources of calcium did not produce the functional effect attributed to this NOS variant.

Another group reported a possible interaction between the smooth muscle nNOS variant and PMCA4 in vascular smooth muscle[1]. In this study, the contraction of vascular tissue preparations to KCl was examined in mice that lack PMCA4 or NOS. The contraction was less in preparations from mice lacking PMCA4 and more in tissues lacking NOS compared to control preparations. PMCA4 was also shown to bind NOS in smooth muscle cells by immunoprecipitation. The authors suggested that calcium removal by PMCA4 deprives the smooth muscle NOS from the necessary activation while in preparations lacking PMCA4, calcium accumulating in the cell produces more NOS activation and thus the contraction to KCl is less. On the other hand, vascular preparations lacking NOS did not have the feedback mechanism and thus had an increased contraction to KCl. In this thesis I also showed that PMCA4, the predominant

PMCA isoform in smooth muscle, was present in lipid raft-enriched membrane domains colocalized with caveolin-1.

A clear representation of the importance of microdomain organization is demonstrated in the function of PMCA4. As previously mentioned, I showed that PMCA4 was found in the lipid raft rich membrane domains. The function of PMCA4 in calcium clearance was demonstrated as a greater rise in CCh-induced contractile tone following PMCA inhibition using the selective extracellular inhibitor caloxin 1C2. This increase only occurred when the caveolae were intact. In cav1$^{-/-}$ tissue or when caveolae were disrupted by cholesterol depletion in bovine airway smooth muscle, the rise in tone was absent. PMCA expression persisted in cav1$^{-/-}$ tissue and in cholesterol depleted bovine airway smooth muscle tissue, though the membrane domain distribution differed in the latter case. However, the absence of caveolae in both cases led to the loss of PMCA function. I explained this on the basis of the loss of the close contact points between the plasma membrane and the sarcoplasmic reticulum offered by the caveolae or the special role of PMCA4b in caveolae.

Taken together, my results shed light on the arrangements of some of the processes involved in signaling in GIT smooth muscle, particularly those involved in relaxation. Caveolin-1 scaffolds the molecules involved in the different signaling events in a tight platform with their upstream modulators and their downstream targets. This arrangement offers a double-sided benefit. On the one hand, caveolin-1 brings together the different components of a signal transduction pathway for the rapid transduction of the extracellular signals. On the other hand, the negative regulatory effect that caveolin-1 exerts on most signaling molecules ensures that the pathway is only activated when triggered and not due a random interaction between molecules, being of high probability as they are spatially closer. In absence of caveolin-1, this organization is lost leading to a loss of coherent signaling. Some processes can become overactive as in case of the increased PDE5 activity, while others become less active, such as the phosphorylation of the PKA targets including PMCA, phospholamban, and ryanodine receptors, leading to relaxation. In addition, processes requiring close spatial arrangement will be affected as it is the case in the activation of nNOS in caveolae by calcium entering through L-type calcium channels and the extrusion of intracellular calcium that is thought to be released from the sarcoplasmic reticulum in the privileged space beneath the caveolae.

8.2 Limitations:

8.2.1 General limitations:

In this thesis, using the available resources and facilities, every effort was made to provide the best possible evidence to substantiate the conclusions reached. Although the provided data are compelling, a cautionary statement should be made when interpreting results obtained from whole body knockouts. $Cav1^{-/-}$ mice lack caveolin-1 throughout their whole life, including embyonic development. It is entirely possible, even likely, that several compensatory changes take place during their development[2]. One major compensatory change reported in these mice was the vascular hyperpermeability resulting from loss of tight junctions between endothelial cells[3]. This compensates for the loss of the normal transcytosis process mediated by caveolin-1[3]. A possible compensatory change that I reported was the increase in the relaxation response to the apamin-sensitive mediators in the longitudinal and circular smooth muscle layers of the cav1$^{-/-}$ mice. However, in the different studies presented in this thesis, I examined the function of pathways or molecules that I showed to be closely associated with caveolin-1 in control (BALB/c and cav1$^{+/+}$) mice. Thus the changes observed are more likely to be directly relevant to the lack of caveolin-1 rather than an indirect compensatory change that developed with time.

In addition, wherever possible, I confirmed the findings in cav1$^{-/-}$ tissues in control mouse tissue by experiments in which caveolae were disrupted by plasma membrane cholesterol depletion using Me-β-CDX. The latter model is not an ideal model to study functions associated specifically with caveolae and caveolin-1 in the sense that depletion of cholesterol from the plasma membrane will also affect the cholesterol-rich lipid raft domains that do not contain caveolin-1 and are hence not caveolae. In addition, removal of membrane cholesterol might result in significant plasma membrane damage reminiscent of the effects of polyene antibiotics (*e.g.* amphotericin B) and the consequent cell death. To avoid that I selected concentrations of Me-β-CDX that affected neither the spontaneous phasic contraction of the tissue nor the response to KCl. The results obtained from cav1$^{-/-}$ tissue and cholesterol depleted tissue agreed, supporting the proposed roles of caveolae and caveolin-1 in the specific processes studied.

An alternate and improved way to study caveolin-1 dependent processes is by the controlled downregulation of caveolin-1 expression in specific cells using small interfering RNA. This approach is commonly used in the literature for studies done in cultured cells[4,5,6]. Downregulating caveolin-1 in mature cells by-passes all the possible compensatory changes that might occur during the development of a caveolin-1 null cell.

However, using such an approach to produce the caveolin-1 deficient intact tissues required for our experiments is not directly feasible. Systemic administration of small interfering RNA to live animals to generate caveolin-1 defficient tissues is complicated by several factors. The amount of RNA administered, the frequency of its administration, the route of its administration and the optimal delivery system are all procedures that depend on the timing and rate of caveolin-1 expression in different tisues as well as on the accessibility to RNA of target tissues. Needless to say, developing and validating such a model is a huge undertaking that requires time and financial resources beyond those available to us at the time this project was underway.

8.2.2 Limitations to Chapter IV:

In Chapter IV, the main observation that led the way into the conclusion of a reduced smooth muscle response to NO, because of an increase in PDE activity, was that nNOS expression was increased in $cav1^{-/-}$ myenteric neurons. Although we supported this observation by showing that $cav1^{-/-}$ tissues had a reduced response to an exogenous NO donor, direct measurement of the NO released upon stimulation of myenteric neurons was not done. Previous trials to measure such a parameter in our laboratory in larger mammals were not successful and I am not currently aware of any other study that successfully measured this parameter in mouse small intestine.

I also attempted to measure the phosphodiesterase activity in the $cav1^{-/-}$ and $cav1^{+/+}$ tissue homogenates that was susceptible to inhibition by a selective PDE5 inhibitor, PDE inhibitor II. However, the high background signal that remained after adding several concentrations of the inhibitor within the selectivity range prevented isolation and measurement of the relevant signal.

8.2.3 Limitations to Chapter V:

In Chapter V evidence supportive of the conclusion that the changes downstream of β-adrenoceptor signaling in absence of caveolin-1 are due to changes of protein organization could have been provided by direct biochemical measurements of enzyme activities. Direct measurement of the cAMP produced by adenylate cyclase upon β-adrenoceptor stimulation could have demonstrated that the cAMP production is affected in $cav1^{-/-}$ tissue. Indeed, a study in cardiac myocytes[7] showed that β-adrenoceptors (β_1 and β_2) mainly activate the adenylate cyclase pool in caveolae. In addition, direct measurement of PKA-mediated phosphorylation would have elaborated on the conclusion that the deficiency in relaxation is mainly due to the loss of the close spatial placement of PKA and its downstream target rather than a loss of function of PKA.

8.2.4 Limitations to Chapter VI:

In the context of the experiments done in Chapter VI, I attempted to measure the conversion of radioactive arginine into radioactive citrulline by membrane fractions isolated from mouse small intestine to demonstrate the presence or absence of nitric oxide synthase activity in smooth muscle membrane. However, these measurements were unsuccessful in detecting NOS activity in either the membrane fractions or the whole homogenates. Several modifications of the method were used including the use of immunoprecipitation prior to the assay. The failure of detection of this activity may be due to the low signal level and small amounts of tissue in mouse small intestine. So far, I am not aware of any successful measurement of nitric oxide synthase activity in mouse small intestinal tissue using this technique.

Further, additional investigation of the exact splice variant of neuronal nitric oxide synthase expressed in smooth muscle cells using polymerase chain reaction would confirm and strengthen our results. We tried to isolate a layer of the small intestinal wall containing only circular smooth muscle during the preparation of whole mount preparations for immunohistochemistry. However, due to the minute thickness of the tissue, any attempts of microscopic dissection yielded very small amounts of smooth muscle tissue that had parts of the nerve tissue of the myenteric plexus attached to it. In the future, polymerase chain reactions on purified intestinal smooth muscle cell culture might offer a solution to this problem.

In this chapter I used an anti-caveolin-1 antibody to immunopreceipitate caveolin-1 and smooth muscle nNOS. In my experiments, I showed that NOS appeared with anti-caveolin-1 antibody but not with the IgG control antibody. Yet, it was not possible to show caveolin-1 on the Western blot as a loading control because its molecular weight interferred with one of the denatured chains of the antibodies used for immunoprecipitaion.

8.2.5 Limitations to ChapterVII:

In Chapter VII I used CCh to induce contraction and to elevate intracellular calcium levels. I used the CCh-induced tone as a measure of intracellular calcium level but did not measure it directly. Although it has been shown that in the models we used that CCh-induced contraction is mediated by an increase in intracellular calcium levels, smooth muscle contraction is a complicated process that involves the interaction between a number of signaling molecules and structural components, and also involves sensitization of contractile proteins to calcium. A more direct measurement of intracellular calcium concentration using calcium imaging techniques would provide further evidence to support our conclusions regarding the role of PMCA in relation to caveolae and caveolin-1. At the time when this project was underway, the available facility (in another laboratory in the department of Pharmacology) allowed for measuring calcium levels in isolated cells and not in intact tissue segments.

8.3 Future directions:

Understanding of the role of caveolin-1 and caveolae in the organization of signal transduction pathways in different tissues and organs depends on the availability of efficient and effective tools to conduct these studies. As mentioned in the previous sections each of the tools readily available to us had certain limitations that leave a measure of uncertainty about the results obtained using them. In my opinion, an ideal model for the study of the role of caveolin-1 is the development of a conditional knockout that allows for the control of caveolin-1 expression in certain organs or tissues at certain time points. Tetracycline-regulated gene expression was first described in 1992[8]. In this model, DNA recombination is used to produce mice where the gene of interest is expressed under the control of tetracycline-responsive promotor and a tetracycline regulator protein.The spatial control of protein expression is achieved by restricting the tetracycline regulator protein expression in certain cell types using tissue specific promotors. Temporal control of expression is achieved by treating the animals with tetracycline or doxycycline that binds to the tetracycline regulator protein and thus the expression of the protein of interest will be prevented or enhanced in a certain tissue. However, in my opinion, the major drawback of this model is the necessity for the use of tetracycline or doxycycline which might have effects that interfer with the normal physiology of the animals e.g. inhibition of matrix metalloproteinases[9]. An additional model for conditional knockout is available, the *Cre/lox* system[10]. Spatial control of gene expression can be obtained by the tissue-specific infection with *Cre* encoding adenovirus or by the production of double transgenics in which *Cre* expression is controlled by a tissue specific promotor[11].

In this thesis and elsewhere[12,13], I have shown that caveolin-1 is necessary for the effective organization of signaling molecules for the proper regulation of a number of intracellular processes in smooth muscle. Yet an unanswered question is whether any of the abnormalities detected in absence of caveolin-1 occur in pathophysiological situations due to an alteration in caveolin-1 expression. The roles of caveolae and caveolin-1 in smooth muscle-related pathologies have not been widely addressed. $\mathrm{Cav1}^{-/-}$ mice show pulmonary hypertension that was found to be due to an increase in PDE5 activity making the smooth muscle cells less sensitive to the relaxing effect of endothelial NO[14]. However a recent study on pulmonary artery smooth muscle cells isolated from patients with pulmonary hypertension showed that these cells had an overexpression of caveolin-1 and increased caveolae formation[15]. The authors suggested that the increase in caveolae formation led to an increase in capacitative calcium influx and hence an increased vascular smooth muscle contraction. Another study, related reduced colonic motility in aged rats to a decreased caveolin-1 association with signaling molecules[16]. In the former study, it was shown that the recruitment of Rho A and protein kinase C to the plasma membrane, which is a key step in the transduction of the contractile signal in smooth muscle cells, was altered and the association of these proteins with caveolin-1 was reduced. Overexpression of caveolin-1 in colonic smooth muscle cells from aged rats corrected the alteration in the signaling pathway and restored the contractile activity to the normal level. The outcome of these studies represents a potential explanation of pathological condition that is related to alterations in caveolin-1 expression and suggests that the manipulation of caveolin-1 expression might carry a possible therapeutic benefit in the future.

Further, smooth muscle-related pathologies are common in diabetes which is becoming one of the major medical concerns all over the world with a rapidly increasing prevalence and an increased mortality rate due to complications[17]. So far, there has been no study of the changes in caveolae/caveolin-1 expression in smooth muscle in diabetes if any. Studies showed that caveolin-1 and caveolae expression are altered in dibetes in endothelial cells[18], monocytes[19], and renal cortical cells[20]. A number of disorders common in diabetic patients involve changes of smooth muscle functions notably appearing as alterations in vascular responses especially of the resistance arteries[21]. The resultant poor control of organ-specific blood flow through these vessels increases the susceptibility of diabetic patients to damage of downstream structures in the eye, glomerulus, and cerebral circulation leading to the long-term complications of diabetes[22]. The mechanisms underlying the defective vascular response have not yet been completely adressed. In fact, the exact molecular mechanism leading to the vascular defects associated with diabetes is far from being understood. A change in smooth muscle response to normal signals might underlie these defects. These alterations could be related to a change in caveolin-1 and caveolae expression in smooth muscle cells. Significantly, when caveolae are disrupted or caveolin-1 is knocked out, vascular tissues show alterations in the vascular response response similar to those seen in diabetes[23,24]. A detailed study of the expression of caveolin-1 in smooth muscle in diabetes is required together with the effects on the function of the different possible targets leading to the pathological observations in these conditions. Such an understanding of the underlying changes leading to the defective vascular function in diabetes might help in the identification of novel therapeutic approaches, possibly involving a change in caveolin-1 and caveolae expression, that cease ot retard the progression of these alterations and thus reduce the incidence and mortality due to the complications of diabetes.

8.4 References

1. Schuh K, Quaschning T, Knauer S, Hu K, Kocak S, Roethlein N, and Nyses L. Regulation of vascular tone in animals overexpressing the sarcolemmal calcium pump. *J Biol Chem* 278: 41246-41252.
2. Insel PA and Patel HH. Do studies in caveolin-knockouts tell us about physiology and pharmacology or instead, the ways mice compensate for 'lost proteins'? *Br J Pharmacol* 150: 251-254, 2007.
3. Schubert W, Frank PG, Woodman SE, Hyogo H, Cohen DE, Chow CW, and Lisanti MP. Microvascular hyperpermeability in caveolin-1 -/- knock-out mice. Treatment with a specific nitric-oxide synthase inhibitor, L-NAME, restores normal microvascular permeability in Cav-1 null mice. *J Biol Chem* 277, 40091–40098, 2002.
4. Gonzalez E, Nagiel A, Lin AG, Nolan DE, and Michel T. Small interfering RNA-mediated down-regulation of caveolin-1 differentially modulates signaling pathways in endothelial cells. *J Biol Chem* 279: 40659-40669, 2004.
5. Zuo L, Ushio-Fukai M, Ikeda S, Hilenski L, Patrusha N, and Alexander RW. Caveolin-1 is essential for the activation of Rac 1 and NAD(P)H oxidase after angiotensisn II type 1 receptor stimulation in vascular smooth muscle cells: role in redox signaling and vascular hypertrophy. *Arterioscler Thromb Vasc Biol* 25: 1824-1830, 2005.

6. Swaney JS, Patel HH, Yokoyama U, Head BP, Roth DM, and Insel PA. Focal adhesion in (myo)fibroblasts scaffolds adenylyl cyclase with phosphorylated caveolin-1. *J Biol Chem* 281: 17173-17179, 2006.
7. Ostrom RS, Violin JD, Coleman S, and Insel PA. Selective enhancement of beta-adrenergic receptor signaling by overexpression of adenylyl cyclase type 6: colocalization of receptor and adenylyl cyclase in caveolae of cardiac myocytes. *Mol Pharmacol* 57: 1075-1079, 2000.
8. Gossen M and Bujard H. Tight control of gene expression in mammalian cells by tetracycline-responsive promotors. *Proc Natl Acad Sci USA* 89: 5547-5551, 1992.
9. Golub LM, Goodson JM, Lee HM, Vidal AM, McNamara TF, and Ramamurthy NS. Tetracyclines inhibit tissue collagenases. Effects of ingested low-dose and local delivery systems. *J Periodontol* 56: 93-97, 1985.
10. Nagy A. Cre recombinase: the universal reagent for gene tailoring. *Genesis* 26: 99-109, 2000.
11. Maltzman JS and Turka LA. Conditional gene expression, a new tool for the transplantologist. *Am J Transplant* 7: 773-740, 2007.
12. Chow AK, Cena J, El-Yazbi AF, Crawford BD, Holt A, Cho Wj, Daniel EE, and Schulz R. Caveolin-1 inhibitos matrix metalloproteinase-2 activity in the heart. *J Mol Cell Cardiol* 42: 896-901, 2007.
13. Sommer B, Montaño L, Bazan-Perkins B, El-Yazbi AF, Cho WJ, and Daniel EE. Caveolae disruption impairs serotoninergic (5-HT$_{2A}$) and histaminergic (H$_1$) responses in bovine airway smooth muscle: role of Rho-kinase signaling. *J Cell Mol Med* under review.

14. Murray F, Patel HH, Suda RYS, Thistlethwaite PA, Yuan JXY, and Insel PA. Caveolar localization and caveolin-1 regulation of PDE5 in human pulmonary artery smooth muscle cells. *FASEB J* 20:A543, 2006 (abstract).

15. Patel HH, Zhang S, Murray F, Suda RY, Head BP, Yokoyama U, Swaney JS, Niesman IR, Schermuly RT, Pullamsetti SS, Thistlethwaite PA, Miyanohara A, Farquhar MG, Yuan JX, and Insel PA. Increased smooth muscle expression of caveolin-1 and caveolae contribute to the pathophysiology of idiopathic pulmonary hypertension. *FASEB J* 21: 2970-2979, 2007.

16. Somara S, Gilmont RR, Martens JR, and Bitar KN. Ectopic expression of caveolin-1 restores physiological contractile response of aged colonic smooth muscle. *Am J Physiol* 293: G240-G249, 2007.

17. Larsen PR, Kronenberg HM, Melmed S, and Polonsky KS (eds.). Larsen: Williams textbook of endocrinology, 10th ed. Saunders, Philadelphia, Pennsylvania, 2003.

18. Jamieson HA, Cogger VC, Twigg SM, McLennan SV, Warren A, Cheluvappa R, Hilmer SN, Frase R, de Caba R, and Le Couteur DG. Alterations in liver sinusoidal endothelium in a baboon model of type I diabetes. *Diabetologia* In Press.

19. Hayashi T, Juliet PA, Miyazaki A, Ignarro LJ, and Iguchi A. High glucose down regulates the number of caveolae in monocytes through oxidative stress from NADPH oxidase: implications for atherosclerosis. *Biochem Biophys Acta* 1772: 364-372, 2007.

20. Komers R, Schutzer WE, Reed JF, Lindsley JN, Oyama TT, Buck DC, Mader SL, and Anderson S. Altered endothelial nitric oxide synthase targeting and conformation and caveolin-1 expression in the dibetic kidney. *Diabetes* 55: 1651-1659, 2006.

21. Schofield I, Malik R, Izzard A, Austin C, and Heagerty A. Vascular structural and functional changes in type 2 diabetes mellitus: evidence for the roles of abnormal myogenic responsiveness and dyslipidemia. *Circulation* 106: 3037-3043, 2002.

22. Loutzenhiser R, Griffin K, Williamson G, and Bidani A. Renal autoregulation: new perspectives regarding the protective and regulatory roles of the underlying mechanisms. *Am J Physiol* 290: R1153-R1167, 2006.

23. Adebiyi A, Zhao G, Cheranov SY, Ahmed A, and Jaggar JH. Caveolin-1 abolishment attenuates the myogenic response in murine cerebral arteries. *Am J Physiol* 292: H1584-H1592, 2007.

24. Potocnik SJ, Jenkins N, Murphy TV, and Hill MA. Membrane cholesterol depletion with beta-cyclodextrin impairs pressure-induced contraction and calcium signalling in isolated skeletal muscle arterioles. *J Vasc Res* 44: 292-302, 2007.